AUGUST 1976

Contract No. NAS 5-20812

SEVERE STORMS OBSERVING SATELLITE (STORMSAT) FINAL REPORT

Hughes Ref No. D1737 • SCG 60320R

HUGHES
HUGHES AIRCRAFT COMPANY
SPACE AND COMMUNICATIONS GROUP

PREPARED FOR
GODDARD SPACE FLIGHT CENTER
GREENBELT, MARYLAND 20771

NASA CR- 156735

TECHNICAL REPORT STANDARD TITLE PAGE

1. Report No. Final Report	2. Government Accession No.	3. Recipient's Catalog No.
4. Title and Subtitle SEVERE STORMS OBSERVING SPACECRAFT (STORMSAT) FINAL REPORT		5. Report Date August 1976 6. Performing Organization Code
7 Author(s) Brinkman, K.L.; Johansen, D.; Milliken, S.		8. Performing Organization Report No. SCG 60320R
9. Performing Organization Name and Address Hughes Aircraft Company Space and Communications Group P.O. Box 92919 Los Angeles, CA 90009		10. Work Unit No. 11. Contract or Grant No. NAS 5-20812
12. Sponsoring Agency Name and Address Goddard Space Flight Center Greenbelt, Maryland 20771 Technical Monitor: Mr. Seymour Kant		13. Type of Report and Period Covered Final Report (Type III) Aug. '75 - Aug. '76 14. Sponsoring Agency Code

15. Supplementary Notes

16. Abstract

The objective of this study was the establishment of conceptual spacecraft and systems designs for the Severe Storms Observing Spacecraft (SSOS), known as STORMSAT.

The primary payload for this satellite is the Advanced Atmospheric Sounding and Imaging Radiometer (AASIR), which will perform precise infrared temperature sounding and visible/infrared imaging from geostationary orbit. A secondary payload instrument which may be utilized on STORMSAT is the Microwave Atmospheric Sounding Radiometer (MASR), which provides an independent set of temperature and humidity soundings in cloudy, meteorologically active regions.

The study provides satellite designs and identifies mission-unique subsystems using the Multimission Modular Spacecraft (MMS), using a Shuttle/Interim Upper Stage launch vehicle.

17. Key Words (Selected by Author(s)) STORMSAT (SSOS) MASR Severe Storms Mesoscale AASIR

18. Distribution Statement

MAY 1978

RECEIVED NASA STI FACILITY

19. Security Classif. (of this report)	20. Security Classif. (of this page)	21. No. of Pages	22. Price*
UNCLASSIFIED	UNCLASSIFIED	194	

*For sale by the Clearinghouse for Federal Scientific and Technical Information, Springfield, Virginia 22151.

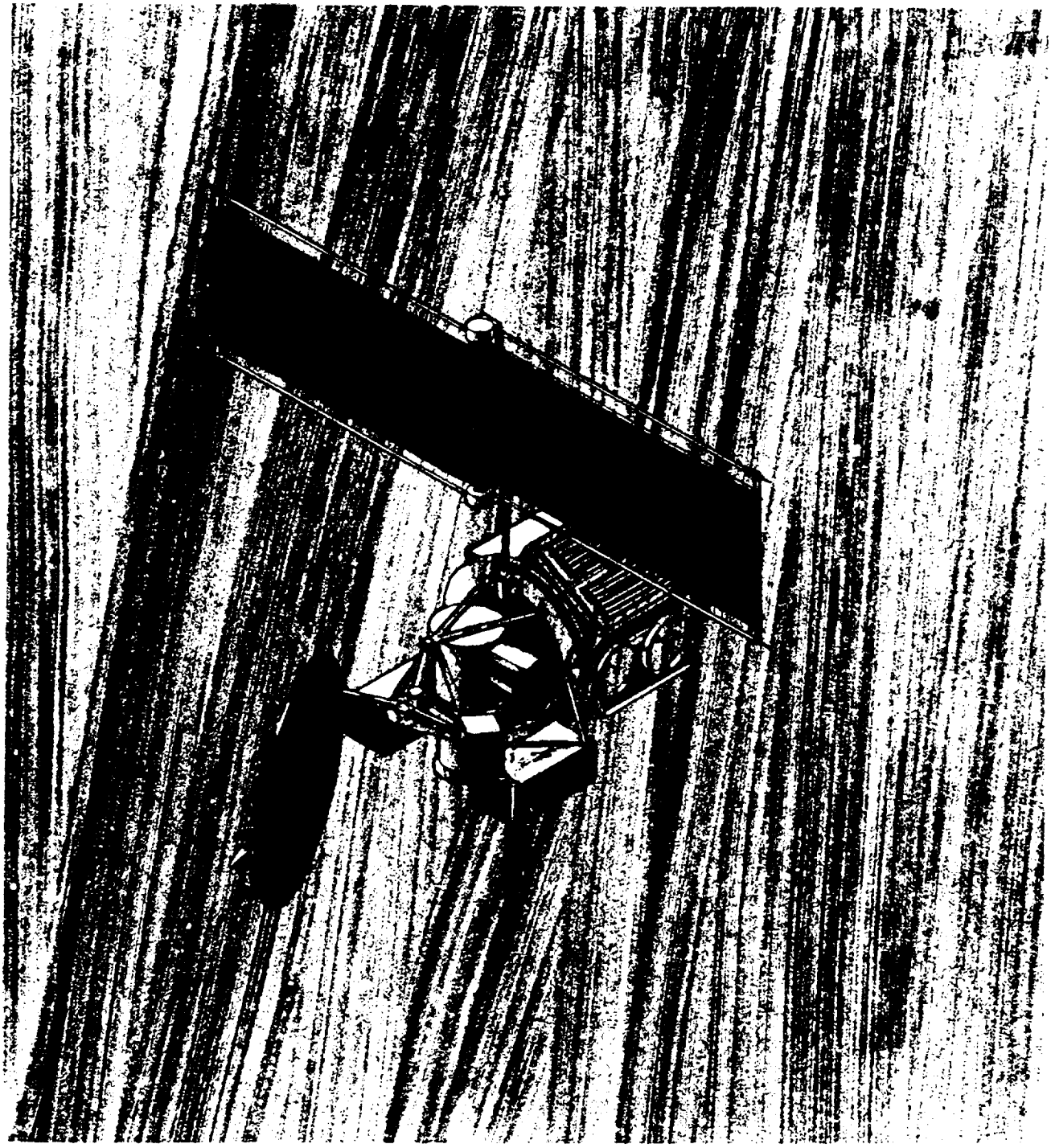

PREFACE

This report has been prepared under the direction of Seymore Kant of NASA/GSFC for the Severe Storms Observing Satellite conceptual design. It is based on the use of the Space Transportation System together with the Interim Upper Stage. The spacecraft consists of the Multimission Modular Spacecraft plus the mission-unique equipment.

Earlier study efforts were concentrated on attitude control and stability analysis. A report covering alternative attitude control approaches was submitted in April 1975. A preliminary analysis of the Multimission Modular Spacecraft attitude control subsystem as applied to the STORMSAT mission was submitted in July 1975. The current report supersedes these earlier analysis and design studies.

This effort at Hughes Aircraft Company was directed by K. L. Brinkman, NASA Systems Division, Space and Communications Group. He may be reached at (213) 648-3329 for further information. The study was performed under contract NAS 5-20812 and covered the period from February 1975 to July 1976.

CONTENTS

ILLUSTRATIONS

TABLES

ABBREVIATIONS

AASIR	Advanced Atmospheric Sounding and Imaging Radiometer
ACS	attitude control subsystem
A/D	analog-to-digital
ADC	anolog-to-digital converter
AOIPS	atmospheric and oceanographic information processing system
APT	automatic picture transmission
ATS	application technology satellite
CDAS	command and data acquisition station
C&DH	communications and data handling
C&DHM	communications and data handling module
CRT	cathode ray tube
CSS	coarse sun sensor
DCP	data collection platform
DUS	data utilization station
EIRP	effective isotropic radiated power
ETC	Engineering Training Center
EU	extender unit
FOB	federal office building
FOV	field of view
FRUSA	flexible rolled-up solar array
GFE	Government-furnished equipment
GMS	geostationary meteorological satellite
GOES	Geostationary Operational Environmental Satellite
GRARR	Goddard range and range rate
GSFC	Goddard Space Flight Center
HRDT	high rate data transmission
HRSP	high rate signal processor
IFOV	instantaneous field of view
IGFOV	instantaneous geometric field of view
IRU	inertial reference unit
IUS	interim upper stage
LCMS	low cost modular spacecraft

LOS	line of sight
LSB	least significant bit
MACS	MMS attitude control subsystem
MASR	Microwave Atmospheric Sounding Radiometer
MM	mission module
MMS	Multimission Modular Spacecraft
MPS	modular power subsystem
MTF	modulation transfer function
NEA	noise equivalent angle
NOAA	National Oceanic and Atmospheric Administration
OBC	on-board computer
PCM	pulse code modulation
PDSS	precision digital sun sensor
PMP	premodulation processor
PRU	power regulator unit
PSD	power spectral density
PSK	phase shift keying
RIU	remote interface unit
SEM	space environmental monitor
SMS	synchronous meteorological satellite
SOCC	Spacecraft Operations Control Center
SSOS	Severe Storms Observing Spacecraft (STORMSAT)
STACC	standard telemetry and command components
STACC-CU	STACC central unit
STDN	Spaceflight Tracking and Data Network
STINT	STACC interface unit
TARS	turnaround ranging station
TT&C	telemetry, tracking, and command
VAS	VISSR atmospheric sounder
VISSR	visible and infrared spin scan radiometer
WEFAX	weather facsimile
WMC	World Meteorological Center (Washington, D.C.)

1. INTRODUCTION AND SUMMARY

1.1 INTRODUCTION

The objective of this contract (NAS 5-20812) is the establishment of conceptual spacecraft and systems designs for the Severe Storms Observing Spacecraft (SSOS), known as STORMSAT. The primary payload for this satellite is the Advanced Atmospheric Sounding and Imaging Radiometer (AASIR), which will perform precise infrared temperature sounding and visible/infrared imaging from geostationary orbit. The performance requirements for this payload sensor are associated with the measurement of meteorological observables which permit the assessment of vertical temperature profiles to an accuracy of approximately 1°K ($\Delta T \leq 1°K$) and wind velocities to an accuracy of approximately 1 m/sec ($\Delta V \leq 1$ m/sec). The AASIR sensor, when mounted on the STORMSAT, is capable of positioning to anywhere within the earth's disk selected frame sizes which vary from full earth disk coverage to sectors of 750 km square. This capability should be of considerable value in mesoscale severe storms observations.

A secondary payload instrument which may be utilized on the STORMSAT is the Microwave Atmospheric Sounding Radiometer (MASR). In addition to providing an independent set of sounding data complementing the infrared sounding provided by the AASIR, this instrument can provide soundings in cloudy, meteorologically active regions not sampled by infrared sounding, as the quality of infrared soundings are significantly affected by a small fraction of clouds in the field of view of the AASIR.

The meteorological data which are collected serve several functions. Horizontal wind velocity field and vertical temperature and humidity profiles are inputs to larger numerical weather forecast models to enable mesoscale as well as synoptic weather effects to be studied. High quality imagery data, at visible and infrared wavelengths, allow the observation of detailed storm pattern development, and through correlation with other data, identify and evaluate the significant factors involved in storm evolution.

While this STORMSAT study emphasizes the experimental nature of the primary meteorological mission, called Mission A, design compatibility with the possible follow-on mission (Mission B) is considered as well. Follow-on mission requirements may differ from the primary mission

in that the follow-on STORMSAT may be additionally required to perform all of the functions currently provided by the operational Geostationary Operational Environmental Satellite (GOES) system. These additional functions consist of the following:

1) Collection and relay of data from ground-based remote data collection platforms (DCP)

2) Relay of weather facsimile (WEFAX) data

3) Space environmental monitor (SEM) data collection

The study was divided into three phases. The objective of the first phase was the establishment of the attitude control system (ACS) concepts that could be used with either a Type I (two degree of freedom) or a Type II (one degree of freedom) AASIR to fulfill the mission requirements. The results of the tradeoffs among the candidate concepts were presented in the first interim report, the ACS study report, submitted to NASA GSFC in April 1975.

The second interim report was the result of GSFC redirection with respect to subsequent phases of the study. The decision was made at the completion of the first phase to examine the application of a Shuttle-launched Low Cost Modular Spacecraft (LCMS)* concept to the STORMSAT mission. GSFC therefore decided to concentrate on a Type II AASIR mounted on a gimbal that is capable of scanning the entire AASIR in one axis. Since a stellar-inertial ACS was considered to be more compatible with the multimission (low orbit and geostationary orbit) objectives of the Multimission Modular Spacecraft (MMS) concept, the redirection included use of this type of attitude control system. In particular, the strapped-down star tracker/gyro system described in Low Cost Modular Spacecraft Description, NASA GSFC Document X-700-75-140 (May 1975), was examined in terms of its suitability for the STORMSAT mission. The results of this phase of the study were presented in the STORMSAT Phase II Interim Report (July 1975).

The third and final phase of the study is the subject of this report. It addresses the conceptual design of spacecraft and ground systems for the STORMSAT missions. The guideline established was to avoid, if possible, any modification of the MMS. The payload instruments, the AASIR, and MASR, were considered as Government-furnished equipment (GFE) to be integrated into the mission module with a minimum of instrument design impact. A description of the mission-unique equipment required to ensure successful completion of the STORMSAT mission objectives was desired, and any mission-peculiar interface requirements were to be delineated.

*The LCMS has subsequently been designated the Multimission Modular Spacecraft (MMS).

the on-board computers within the C&DH module for satisfying the STORMSAT attitude control requirements. The additional mission-unique equipment required is defined and system performance estimates made.

Section 6 discusses the STORMSAT telemetry, tracking, and command (TT&C) system and concentrates on the mission-unique equipment which must be provided to interface with the C&DH module to perform the STORMSAT missions. This high rate data transmission system is composed of the high rate signal processor, which processes the payload sensor (AASIR and MASR) and mission module telemetry data, the telecommunications RF group, which modulates and transmits these data, and the remote interface group, which interfaces with the C&DH module.

Section 7 treats the STORMSAT electrical power subsystem. The aspects of the power subsystem are delineated in terms of mission-unique equipment which must be provided to interface with the modular power subsystem (MPS), which is part of the MMS. Power requirements are established and MPS batteries are selected. The mission-unique solar cell array with its drive and deployment mechanism is selected and its mass properties estimated.

The STORMSAT propulsion system is discussed in Section 8. The MMS small propulsion module can be used, but if north-south stationkeeping is desired, a mission-unique propulsion system is necessary. This would represent the only major deviation from MMS philosophy. For this unique design, propellant budgets are established, tank size estimated, and a preliminary propulsion system design concept established. Structural integration and attachment to the MMS is discussed. Utilization of existing tooling for the tank is stressed. Maximum use is made of propulsion components being developed by the NASA Low Cost Systems Office.

Section 9 develops the STORMSAT spacecraft structure concept. Design loads for operation with the Space Shuttle/Interim Upper Stage are noted, as they may be critical for the MMS structure.

An initial thermal design concept is treated in Section 10. The approach taken was to treat the mission payload sensors and spacecraft modules as isolated thermal systems. Structural thermal control to avoid thermomechanical motion between the payload references and the ACS reference is discussed. The thermal design for mission-unique electronic components is similar to that used on the MMS.

The ground system is treated in the final section of the report. Since the real time processing requirements were still in the formulation stage, the associated real time ground data processing facilities are not treated here. In this phase of the study, emphasis was placed on the RF portion of the ground system only. The potential impact of the real time processing requirement on ground system network and the associated data flow are discussed. An RF link budget is established and link margins are developed for candidate NASA and NOAA data acquisition sites.

1.3 CONCLUSIONS AND RECOMMENDATIONS

The Multimission Modular Spacecraft (MMS) can be made compatible with the STORMSAT mission requirements with the addition of mission-unique equipment and subsystems. The mission-unique equipment is, for the most part, located with the Mission Module (MM). Utilization is made of the standard MMS modules in all areas, with the possible exception of the propulsion module. This exception results from the possibility of a requirement for orbit inclination control (north-south stationkeeping) and the desire to minimize overall IUS/spacecraft length. Existing standard propulsion modules with adequate propellant capacity to perform north-south inclination control for the STORMSAT mission are quite long and are not mechanically compatible with the IUS. As a result, a mission-unique propulsion system is described which provides the requisite capacity while minimizing length. The other MMS modules are adequate to meet the STORMSAT requirements within the limitations discussed below.

1.3.1 Attitude Control Subsystem

The gyro selected for the MACS must meet or exceed the capabilities specified in this report if the STORMSAT mission requirements are to be satisfied. Data from various vendors, such as Honeywell and Northrup, indicate that gyro performance at the required level is available.

The Ball Brothers fixed head star tracker, CT-401, can meet the requirements for the STORMSAT mission using gyros with the specified performance, provided that both trackers in the MMS are operating. Should one of these trackers fail, the performance of the system will be degraded below STORMSAT requirements. Should the reliability doctrine for STORMSAT require it, an additional star tracker can be easily added to the MM to provide increased reliability.

The reaction wheels of the MACS should be adequate to handle compensation of MASR/AASIR motion disturbances for instruments with the inertias and scan profiles for this study. Changes in these parameters, such as an increase in the diameter of the MASR to 4.4 meters, could significantly impact this conclusion.

Distortion of the MMS structure due to varying temperature gradients, if not suitably controlled, can produce attitude control drifts unacceptable for the STORMSAT mission. Aluminum structural elements will require precise temperature control by techniques such as insulation and thermostatically controlled heaters. Alternative structural materials would alleviate this problem for the STORMSAT mission.

1.3.2 Communications and Data Handling Subsystem

This module is well equipped for STORMSAT command and housekeeping telemetry requirements. Interface between mission-unique sensors and subsystems on the MM and MMS subsystems is accomplished through the use of remote interface units (RIUs) within the MM, in keeping with the

modular design philosophy. The higher rate sensor payload data transmission is accomplished by means of a mission-unique high rate data transmission system.

1.3.3 Electrical Power Subsystem

This subsystem, with the appropriate selection of modular battery complement and mission-unique solar panel and array drive mechanism, is adequate to handle power requirements for the STORMSAT mission. The flexible rolled-up solar array (FRUSA) has been space qualified on an earlier flight. The panel drive mechanism may be selected from developed drives which meet the STORMSAT stability and power handling requirements.

1.3.4 AASIR Integration

Precision east-west pointing of the AASIR requires the development of a rotary suspension system utilizing high gain servo controllers. Care must be exercised in this design to avoid low level instability and interaction with spacecraft structures. It is concluded that a geared servo drive will minimize these problems. The geared drive will require development to ensure the desired mission lifetime.

Equal angle data sampling for AASIR results in a nonuniform data rate because of the harmonic scan mirror drive. Some buffer storage will be necessary to provide a uniform data output stream. Close coordination between the AASIR and data processor designers will be required to achieve a system design that meets STORMSAT data accuracy requirements.

1.3.5 MASR Integration

The MASR is characterized by a large aperture antenna with an attendant large inertia. Motion of the MASR will require angular momentum compensation to avoid excessive distrubance to the AASIR line of sight. It is concluded that the reaction wheels in the ACS module are adequate for this function for a 2.5 meter MASR antenna. Larger instruments may require a mission-unique angular momentum compensation subsystem.

2. STORMSAT MISSION REQUIREMENTS

2.1 STORMSAT PRIMARY MISSION REQUIREMENTS (MISSION A)

The STORMSAT spacecraft and its primary sensors, the Advanced Atmospheric Sounding and Imaging Radiometer (AASIR) and Microwave Atmospheric Sounding Radiometer (MASR), will be used to provide the data base to enhance understanding of mesoscale weather phenomena. The primary data provided by STORMSAT will be visible images, infrared images, infrared temperature and humidity sounding, and microwave temperature and humidity sounding. These data will be processed into visible and infrared pictures, vertical temperature and humidity profiles, and possibly precipitation estimates. These data are currently being provided by a combination of polar orbiting and geostationary satellites, but not with the time and/or space resolution needed for mesoscale observation.

Mesoscale weather phenomena, including destructive events such as tornados, thunderstorms, and hail, have lifetimes from a few minutes to a few hours and space scales from a few hundred meters (e.g., tornados) to a few hundred kilometers (e.g., squall lines). Polar orbiting satellites get, at most, one look at a mesoscale event because they have periods of 12 hours between measurements over a given geographical location. The present Geostationary Operational Environmental Satellite (GOES) produces visible and infrared global images every 30 minutes, but it lacks temperature and humidity sounding capability provided by the next generation GOES sensor, the VISSR Atmospheric Sounder (VAS). STORMSAT has frame repetition rates for the AASIR from 20 minutes to 1 minute, and a frame repetition rate for the MASR of 30 minutes. The addition of the MASR to STORMSAT will provide temperature, humidity, and possibly precipitation information in the meteorologically active cloudy atmospheric regions. The first experimental STORMSAT mission will supply the information needed to define future operational mesoscale meteorological satellites. It could provide the satellite data base necessary for mesoscale weather prediction.

Table 2-1 contains the attitude and orbit control requirements as specified by NASA GSFC, together with an interpretation of these requirements in terms of the STORMSAT meteorology mission. More detailed explanations of the mission requirements will be found in the succeeding section of this report.

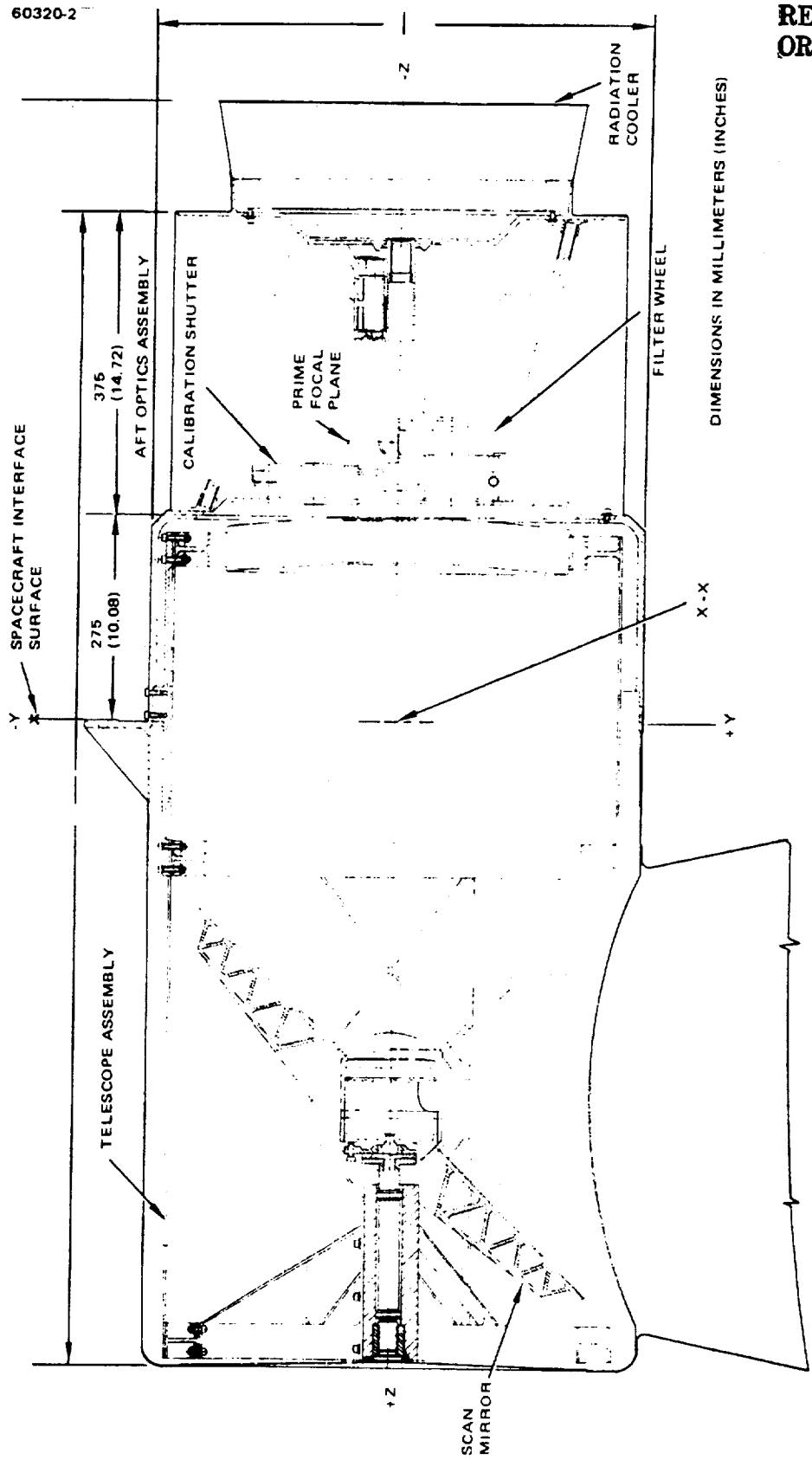

FIGURE 2-1. ADVANCED ATMOSPHERIC SOUNDING AND IMAGING RADIOMETER

TABLE 2-1. STORMSAT ATTITUDE AND ORBIT REQUIREMENTS AND MISSION IMPACT

Requirements	Specification (1σ)	Mission Impact
Real time attitude determination	Pitch = 0.03° Roll = 0.03° Yaw = 0.18°	Locates AASIR frame center to within about 25 km
Short term attitude stability (tens of seconds)	Pitch = 4.2 μrad Roll = 4.2 μrad Yaw = 87 μrad	Provides line to line stability for AASIR visible images of 1/5 instantaneous field of view (IFOV) = 4.2 μrad to limit cross-scan modulation transfer function (MTF) degradation to 5% Provides stability of about 1% of IR sounding IFOV (3.75 μrad) needed to spatially "register" sounding spectral channels collected over several scan lines
Long term attitude stability (20 minutes)	Pitch = 11 μrad Roll = 11 μrad Yaw = 87 μrad	Provides attitude stability required to register successive frames of imagery to determine cloud motion without the use of ground truth landmarks
Orbit inclination*	$\leq 0.025°$	Eliminates need to produce different perspective grids for imagery as function of time of day Eliminates need to correct for north-south spacecraft motion in wind velocity extraction algorithms

*Not yet a firm requirement

2.1.1 AASIR Description

Visible and infrared (IR) imaging, as well as IR sounding data will be provided by the AASIR in variable frame size square raster formats. The current AASIR configuration is shown in Figure 2-1. The scan function will be supplied by the sinusoidal resonant scan mirror oscillating about the x-axis in the figure, and will move the AASIR line of sight (LOS) north and south in object space. East-west motion of the LOS will be provided by stepping the entire sensor about the z-axis from the spacecraft interface surface. Spectral separation of the sounding channels will be achieved by stepping a filter wheel on repeated scans of the same raster line. Cooling of the IR detector will be provided by a two-stage radiation cooler.

A schematic of the AASIR focal plane projected onto the telescope prime focal plane is shown in Figure 2-2. The three rows of large detectors are for sounding, and the two sets of smaller detectors are for visible and IR imaging. Six repeated lines of sounding data are collected while the filter wheel is stepped to each of the six positions. Simultaneously a secondary optical system repositions the imaging detectors to a different scan

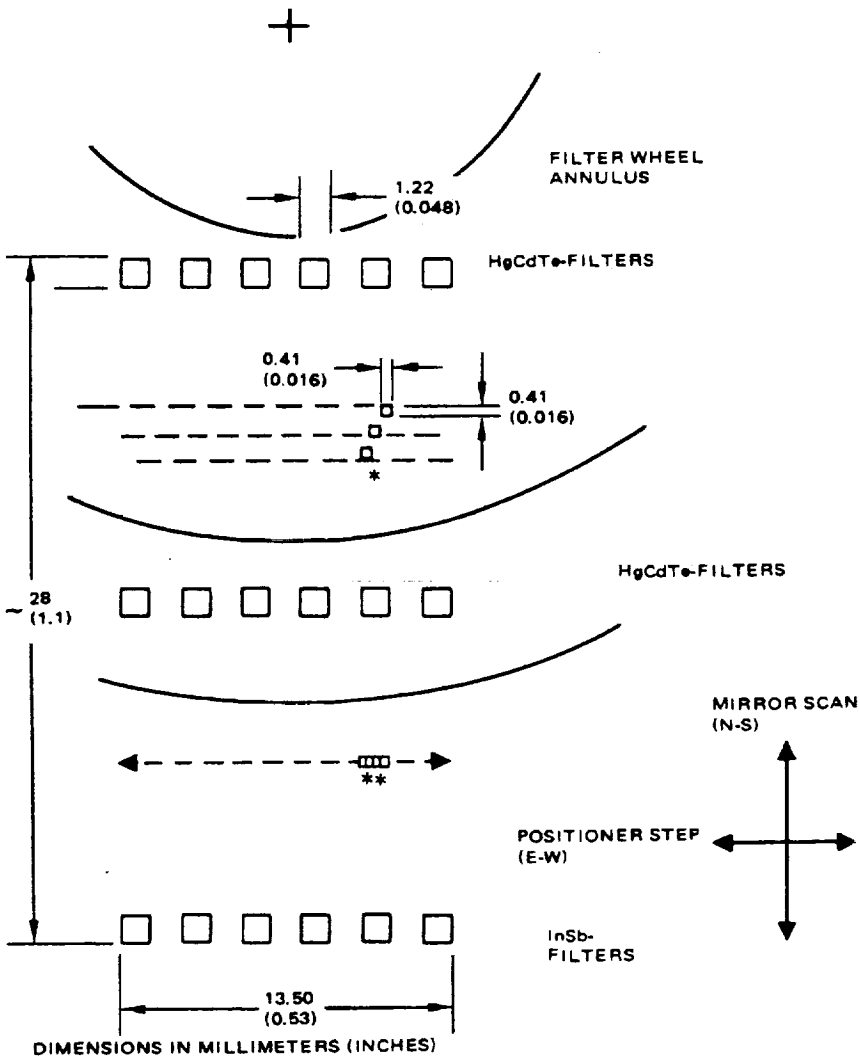

* 11-μm WINDOW IR IMAGING CHANNELS WITH FIXED FILTER VIEWING THROUGH HOLE IN FILTER WHEEL

** VISIBLE CHANNEL PRISM LOCATED AHEAD OF FILTER WHEEL

FIGURE 2-2. FOCAL PLANE LAYOUT (DIMENSIONS REFER TO TELESCOPE FOCAL PLANE)

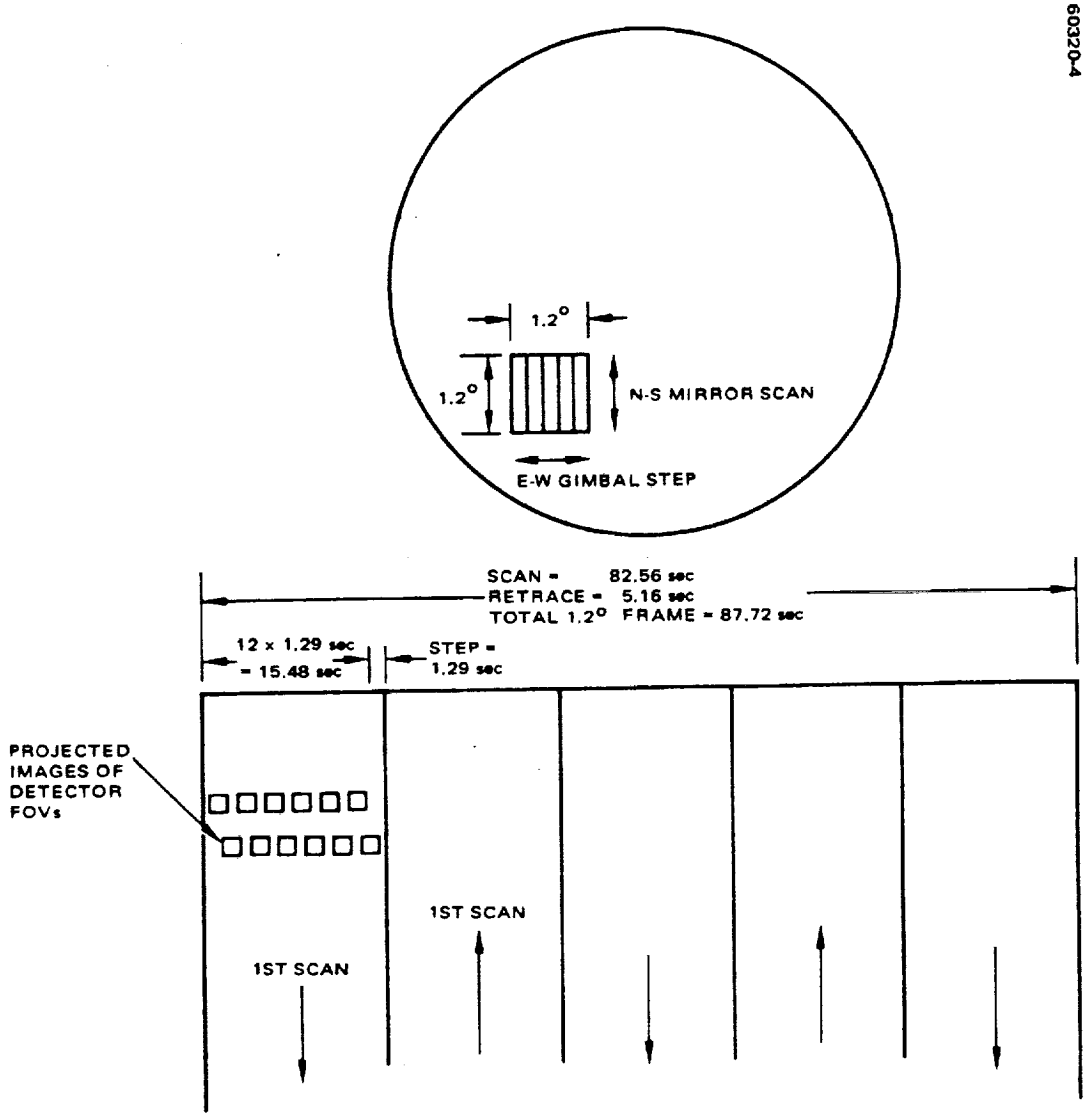

FIGURE 2-3. SCAN PATTERN FOR 1.2° BY 1.2° FRAME SIZE

line on each of the repeated scans. At the end of this sequence, the entire sensor is stepped east (or west) by one sounding field of view, and six more repeated scans of sounding data are collected, again stepping the imaging detectors to a new location on each repeated scan. The sensor is then stepped east (or west) by 11 sounding fields of view, and the whole process is repeated until the frame is completed. One half cycle of the scan mirror is allotted to complete the large AASIR step, whereas the small step is completed in the mirror turnaround time. The scanning sequence is illustrated in Figure 2-3 for a 1.2 by 1.2° frame size. Approximate frame sizes and corresponding frame times are shown in Table 2-2, together with limiting spatial resolutions of the various data types. The ranges of data rates due to the sinusoidad for the different data types and frame sizes are given in Table 2-3.

TABLE 2-2. AASIR DATA CHARACTERISTICS

Angular Frame Size, θ, deg	Linear Frame Size, $\theta_{rad} R_S$, km*	Frame Time, Min
20 by 20	Whole earth	23.7
4 by 4	2500 by 2500	4.73
1.2 by 1.2	750 by 750	1.42
Data Type	**IGFOV Angular, μrad****	**IGFOV Linear (Nadir), km**
Visible image	21 by 21	0.75 by 0.75
Infrared image	125 by 125	4.5 by 4.5
Infrared temperature sounding	375 by 375	13.4 by 13.4

*θ_{rad} = angular frame size radians; R_s

= Geostationary altitude to earth surface (3.58×10^4 km)

* IGFOV = instantaneous geometric field of view

TABLE 2-3. AASIR SENSOR CHANNEL BIT RATE GENERATION SUMMARY

Channel	Bit Rate, Mbps		
	20 by 20° Frame	4 by 4° Frame	1.2 by 1.2° Frame
Visible	$3.63 \leq B_v \leq 6.17$	$0.808 \leq B_v \leq 1.37$	$0.311 \leq B_v \leq 0.529$
IR	$0.152 \leq B_i \leq 0.259$	$0.0339 \leq B_i \leq 0.0557$	$0.0131 \leq B_i \leq 0.0222$
Sounding	$0.305 \leq B_s \leq 0.518$	$0.0678 \leq B_s \leq 0.115$	$0.0261 \leq B_s \leq 0.0444$
AASIR output	$4.09 \leq B_t \leq 6.95$	$0.910 \leq B_t \leq 1.55$	$0.350 \leq B_t \leq 0.596$

2.1.2 Imaging

2.1.2.1 Visible Imaging Requirements

STORMSAT visible image data will be used quantitatively and semi-quantitatively in following the evolution of cloud patterns. The quantitative function is the extraction of wind velocities from movement of cloud tracers. This function, currently operational over oceans with the GOES system, will be extended on STORMSAT to include tracers over land around regions of

severe storm activity. From this wind information it may be possible to identify and compute the strengths of mesoscale features, such as surface convergence, often associated with severe weather events. STORMSAT visible images will also provide the synoptic scale wind information needed to define the large scale flow pattern in which the mesoscale event is imbedded.

Perhaps more important than the quantitative information extracted from STORMSAT visible images will be the semiquantitative information derived from the images themselves. The resolution (0.75 km) and rapid frame repetition rates (between 1 and ≈20 minutes) of STORMSAT images will give the meteorological community the opportunity to observe the detailed evolution of mesoscale weather events. These observations will most probably lead to a set of empirical relationships between STORMSAT images and the characteristics of developing mesoscale weather. An example of such a relationship, identified from Applications Technology Satellite 3 images, is J. Purdom's observation that regions along the boundary between clear and cloudy atmospheric regions in the early morning are likely candidates for severe afternoon convective activity because of differential surface heating (Reference 1).

The most stringent requirement on the spacecraft implied by the visible imaging data is a 20 minute stability requirement on the attitude control system resulting from the wind velocity extraction process. The size of allowable ACS error is driven by a user requirement to resolve cloud speed with an error less than 1 m/sec, an uncertainty comparable to the inherent accuracy of clouds as wind tracers. The operational wind extraction unit of NOAA uses ground landmarks to align successive GOES images prior to extracting cloud motion information, thus reducing the dependence on spacecraft attitude information. Since the STORMSAT imaging sensor, AASIR, can operate for extended periods in less than full earth frame size in regions devoid of landmarks, there is a requirement to have independent spacecraft attitude information to use in the wind extraction algorithms. The resulting stringent line of sight (LOS) stability requirements are discussed below.

Clouds can serve as tracers of local wind velocity fields. This is especially true for clouds that maintain a sufficient degree of pattern structure to permit the comparison of the cloud's position is subsequent viewing frames. The accuracy with which the wind velocity can be deduced from an observation of cloud motion depends on several factors, some of which are the following:

1) The correlation between the local wind structure and the motion of observable properties of the cloud

2) The degree to which the cloud features remain intact or have local regions of identification

3) The resolution to which a cloud feature can be established within a frame, determined by the IGFOV of the viewing

instrument (AASIR), as well as the nature of the cloud development

4) The stability of the instrument (LOS) in establishing the vector position of corresponding picture elements (pixels) within successive frames

A cloud which translates without growing or changing in size can serve as a good tracer of average wind velocity, within the degree of correlation permitted by cloud dynamics and wind field structure interaction. Clouds with small turbulent eddy structure may tend to break up or radically change shape over time, so that detailed features within the cloud will have to be observed in order to extract the local wind patterns. This phenomenon tends to limit the wind velocity measuring accuracy when tracking rapidly changing and diffusing clouds.

The first two factors listed above tend to obscure the desired wind velocity during the observing process, but are factors beyond the control of the system designer. These factors serve to limit the accuracy to which it is reasonable to design the LOS stability of the AASIR/STORMSAT for additional mission benefit.

The latter two factors, however, are within the control of the AASIR/STORMSAT system designer and can be optimized to permit maximum utility of the data collected. The spacecraft ACS specification does not account for errors of the AASIR LOS with respect to the AASIR mounting ring. These errors are assumed to be the subject of a separate instrument (AASIR) specification. This approach provides a clean interface between the instrument (AASIR) contractor and the spacecraft contractor, and can ensure that the meteorological mission objectives will be met if a total error budget is established, including both the AASIR instrument and spacecraft ACS errors. Plotted in Figure 2-4 are cloud velocity tracking errors $|\Delta\bar{V}|$ versus pitch and roll error (assumed equal) in the AASIR LOS. A worst case yaw error of 87 μrad between two frames of data separated in time by 22 minutes is assumed. The four curves shown are for different great circle offset angles, Φ, from satellite nadir. As indicated in the figure, for spacecraft ACS errors of 11 μrad in pitch and roll as specified in the STORMSAT RFP, the cloud velocity errors $|\Delta\bar{V}| \leq 1$ m/sec is satisfied, even when an equal error is allocated to the the AASIR SENSOR.

STORMSAT north-south stationkeeping can be designed to maintain an orbit inclination of $\leq 0.025°$. Maintenance of a tight orbit position will simplify the ground processing functions of the payload data; but is by no means required to extract all usable information from STORMSAT data. Orbit inclination, if uncorrected in ground processing, would have two adverse effects on STORMSAT imagery. First, as the spacecraft nadir point moves about, the viewing perspective of the earth's surface changes. In terms of superimposing grids of the earth's land features onto the picture, this means that different sets of grids could be required as a function of north-south position. To estimate the magnitude of the gridding error, a

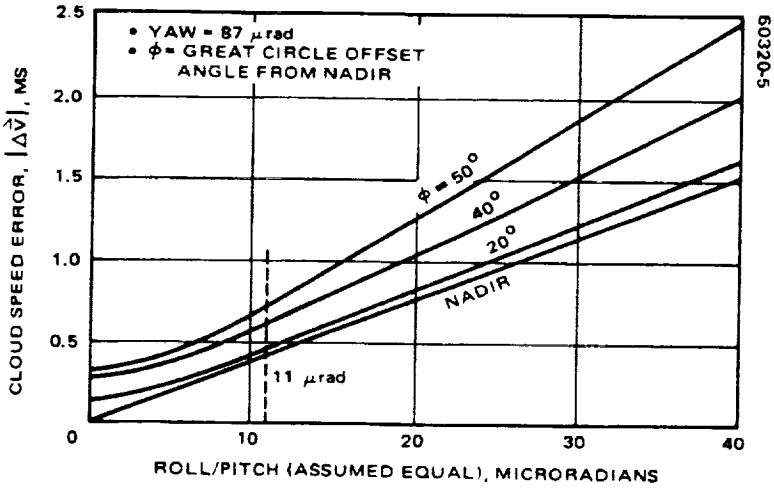

FIGURE 2-4. CLOUD SPEED ERRORS AS FUNCTION OF ACS ERRORS (22 MINUTES)

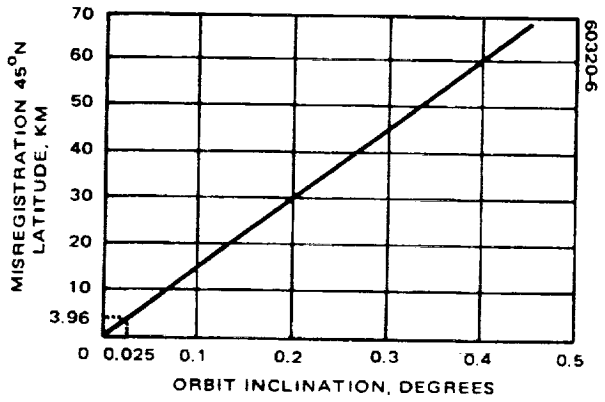

FIGURE 2-5. WORST CASE GRID ERROR DUE TO ORBIT INCLINATION WITH EARTH CENTER POINTING REFERENCE

worst-case calculation of its value was made as a function of orbital inclination. A perfectly fitted grid was assumed with the spacecraft at its southern orbit extreme. Twelve hours later the same grid was overlaid on another image that was registered to the first one at the original satellite nadir position. The misregistration of the grid at t = 12 hours computed at 45° N latitude as a function of orbit inclination is shown in Figure 2-5. With the specified value of orbit inclination (0.025°), a worst-case gridding error of 3.96 km, or ≈ 5 visible resolution elements results at 45° N latitude. This error should be acceptable to the user community with no further correction.

The second effect of orbit inclination is to cause movement of the satellite nadir between frames of imagery. Assuming that the ACS system will stabilize an axis pointing at earth center rather than an axis pointing at

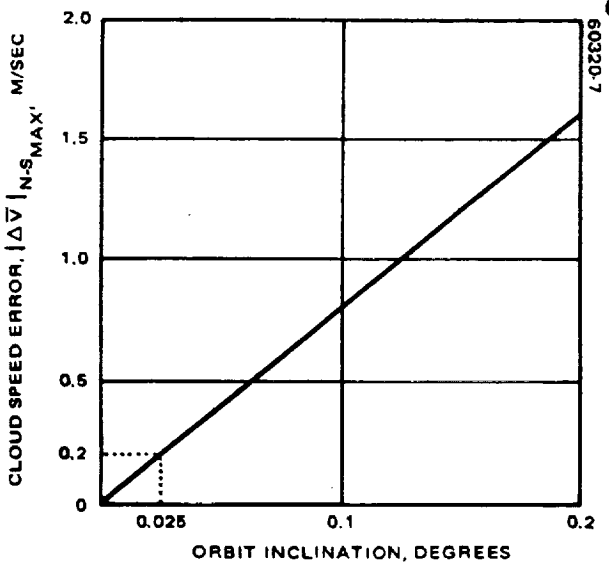

FIGURE 2-6. WORST CASE CLOUD VELOCITY ERROR AS A FUNCTION OF ORBIT INCLINATION

some fixed point on the earth's surface, the changing satellite nadir position, if uncorrected in data processing, will appear directly as a north-south cloud velocity error. Plotted in Figure 2-6 is cloud velocity error on the earth meridian through satellite nadir as a function of orbit inclination at the worst case time of equatorial crossing. The error is given by

$$|\Delta V|_{N\text{-}S} \approx R_e\, i\omega \cos \omega t$$

$$|\Delta V|_{N\text{-}S_{max}} \approx R_e\, i\omega$$

where

i = orbit inclination, rad

R_e = earth radius = 6378 km

ω = orbital angular velocity = $2\pi/24$ hours

The design goal for orbit inclination control of 0.025°, even uncorrected, leads to a cloud velocity error of only 0.2 m/sec, well within the desired limit of cloud speed error of 1 m/sec. If a simple correction algorithm for north-south drift due to orbit inclination were included in the wind velocity extraction procedure, it would be possible to reduce the requirements for north-south orbit control by an order of magnitude. The only

other penalty to be paid would be the generation of several grids for different times of the day, but this function is already being performed for the GOES satellite series.

To meet the requirement for high quality imagery for detailed severe storm evaluation, the ACS system must satisfy two criteria: 1) the ACS motion from scan line to scan line must have a negligible effect on the modulation transfer function (MTF) of the image, and 2) the ACS drift over a full earth disk image should not contribute noticeably to overall frame distortion. The short term stability requirement of 1/5 IFOV or 4.2 μrad in any 8 second period results in less than a 5 percent degradation in MTF for a scene component of spatial frequency of 1 cycle/42 μrad. To meet the overall distortion requirement, a stability requirement of 1 IFOV per frame or 21 μrad in any 22 minute period was established. The real time attitude determination requirement was fixed by a desire to center the AASIR frames to an accuracy ≤25 km at earth surface.

2.1.2.2 Infrared Imaging Requirements

AASIR infrared images will be used to measure surface temperatures, cloud top temperatures, and values of clear column radiances for input to the sounding inversion algorithms. In addition, these images will be used to replace the visible images for cloud tracking during the night. At all times the IR images will be used to determine cloud top heights from measured cloud top temperatures and temperature profiles calculated from the IR and microwave sounding data. These cloud top heights will then be used in the wind velocity extraction algorithms to fix the heights of the horizontal wind velocities measured on visible images.

All the attitude and orbit requirements discussed in the previous section apply equally to the IR images. However, since the requirements were scaled on the basis of the visible IFOV (21 x 21 μrad) and the IR imaging IFOV (125 x 125 μrad) has a linear dimension six times as large, the attitude and orbit requirements generated previously will easily satisfy the requirements for IR imaging.

2.1.3 Atmospheric Sounding

2.1.3.1 Infrared Sounding Requirements

The infrared sounding capability on the AASIR will provide vertical temperature profiles and estimates of humidity in clear and partially cloudy atmospheric regions. Knowledge of the vertical temperature profile, coupled with humidity estimates, allows the meteorologist to calculate, for example, the vertical stability of the atmosphere to convective overturning associated with severe mesoscale weather phenomena. Knowledge of the total atmospheric water vapor content is also an indicator of the potential for severe weather, since the energy for severe mesoscale weather is supplied by the latent heat of water vapor condensation. The temperature and humidity information from STORMSAT could be used in mesoscale numerical models or in semiquantitative forecast procedures.

Radiance measurements made over a molecular absorption band of a uniformly mixed atmospheric constituent (e.g., CO_2 or O_2) can be processed to yield a vertical temperature profile. The temperature in the retrieved profile is a strong function of relative radiance errors across the absorption band. The sounding process in the AASIR involves the collection of radiance samples from a particular earth location in a small number of spectral intervals in the 15 and 4.3 μm CO_2 absorption bands. Additional radiance measurements in the 3.7 and 11 μm window regions are necessary to determine the nature of the earth boundary contribution to the radiance values measured in the absorption bands. Measurements of radiance in an H_2O absorption band are made at 6.7 and 7.25 μm, to estimate the water vapor content of the atmosphere.

An accurate estimate of the fraction and brightness temperatures of any clouds falling within the sounding field of view is necessary if a temperature profile with acceptable errors is to be deduced from the radiance data. Implicit in this requirement is the assumption that the set of radiance measurements collected in the $C0_2$ absorption bands and atmospheric windows are precisely from the same earth location. The radiance set is assumed to be spatially registered. In the presence of a partially cloudy field of view, misregistration between the window channel measurements and the absorption band measurements will result in an incorrect estimate of cloud cover in the field of view, whereas misregistration among the absorption band measurements contribute directly to interchannel radiance errors. Ultimately, both kinds of registration errors result in relative radiance errors. The user community has expressed the need to maintain relative radiance errors to less than 0.25 erg/sec-cm^2-sr-cm^1, or roughly 0.5 percent of the total radiance signal in the 15 w μm $C0_2$ absorption band as an essential requirement in achieving desired temperature profile accuracies.

There are several sources of registration errors in the AASIR sensor, but consideration here will be focused on the ACS and sampling contributions to the problem. To collect all the spectral samples used in a single temperature sounding takes several seconds in the present AASIR design. Any movement of the stable reference block during the collection interval will contribute to the registration error. In order to maintain radiance errors during the collection interval to $\approx$0.25 erg/sec-cm^2-sr-cm^{-1}, it is necessary to maintain the AASIR LOS stable to within 1 percent in area of a sounding field of view, or 3.75 μrad. This point is illustrated in Figure 2-7 for an absorption channel at 14.2m μm and the 11m μm window channel for both high and low level clouds. The data are based on a recent study for NASA by the University of Wisconsin and a worst-case assumption that a 1 percent registration error will cause a 1 percent change in cloud fraction within the field of view. For a 1 percent registration error, the radiance error is within the requirement for the 14.2 μm channel, but does not satisfy the requirement for the window channel.

In the AASIR design all the spectral information necessary to accurately estimate the fraction and brightness temperature of any clouds falling within the sounding field of view is collected independently by each sounding detector. Thus, the contribution of sampling to the registration error has

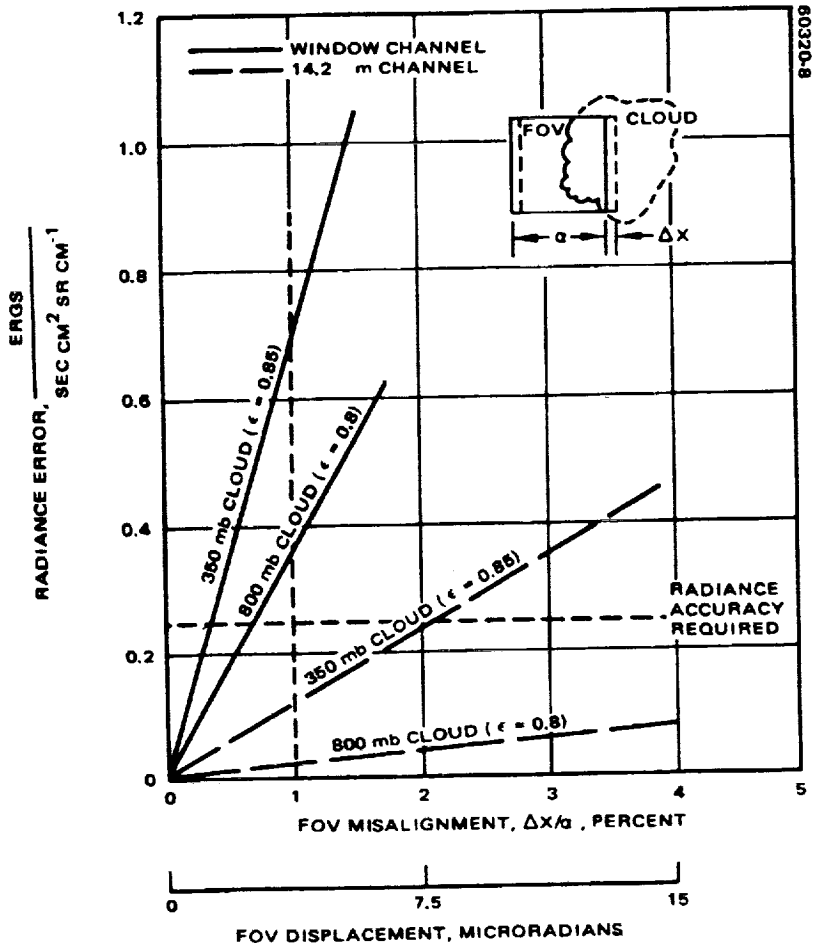

FIGURE 2-7. MEASURED RADIANCE ERROR VERSUS FIELD OF VIEW MISALIGNMENT FOR SCENE WITH CLOUDY EDGE

been reduced to a requirement of sampling individual detectors repeatably over the several scan lines required to collect a complete spectral set of temperature sounding data. To meet the 1 percent registration requirement, the sampler must be capable of sampling each detector repeatably over the several scan lines to ≤3.75 μrad.

2.1.3.2 Microwave Sounding Requirements

The results of microwave sounding experiments in Nimbus 5 and 6 have demonstrated that the addition of microwave channels to a sounding system will greatly improve the system performance by:

1) Providing the capability of sounding areas covered by clouds that cannot be penetrated by the infrared channels thus increasing the yield of useful soundings in cloudy, meteorologically active regions.

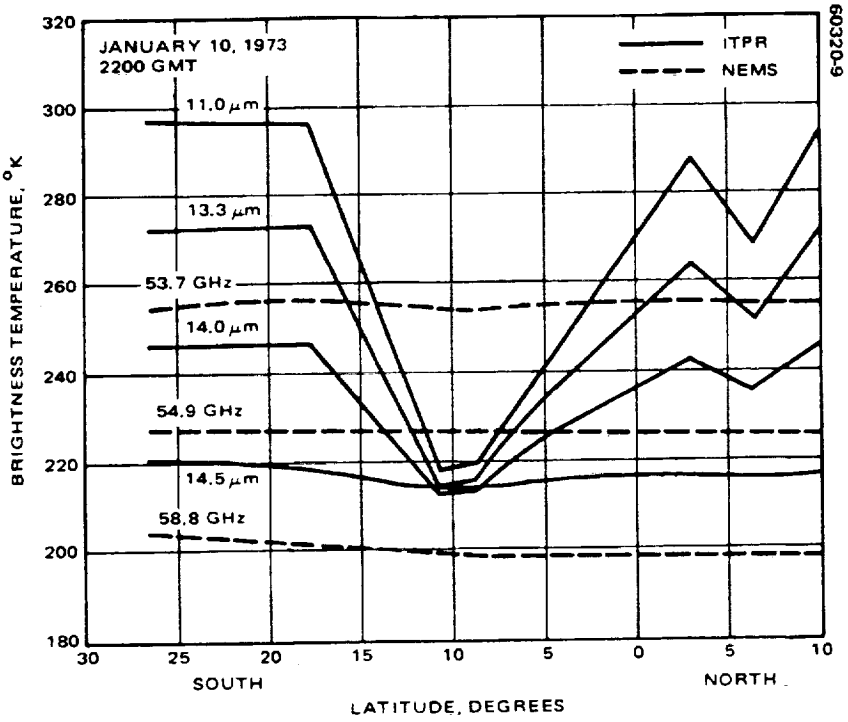

FIGURE 2-8. BRIGHTNESS TEMPERATURES OBSERVED BY NEMS (MICROWAVE) AND ITPR (INFRARED) CHANNELS ON NIMBUS OVER A TROPICAL STORM IN THE SOUTH PACIFIC

2) Providing sounding channels with sharper (altitude) weighting functions, particularly near the tropopause, which will improve the vertical resolution and accuracy of temperature profiling.

3) Complementing the infrared data with a set of independent microwave data; when the two sets are combined, synergistic improvements are obtained in the accuracy of the infrared temperature and humidity profiles.

The reduction of cloud errors in microwave sounding is due to the property that clouds are more transparent to microwave than to infrared radiation, particularly ice clouds. Figure 2-8 shows a comparison between the microwave and infrared sounding radiances (expressed as brightness temperatures) measured, respectively, by NEMS and ITPR on Nimbus 5, as their fields of view pass over a tropical storm at 9° S and 154.5° W. It shows clearly the difference in the sensitivity to cloud effects between the microwave and infrared channels.

Figure 2-9 shows the standard deviations between radiosonde and radiance derived temperatures from Nimbus 5 microwave and infrared data. It shows that better results are achieved from the combined set of infrared and microwave measurements than can be achieved by either set used individually.

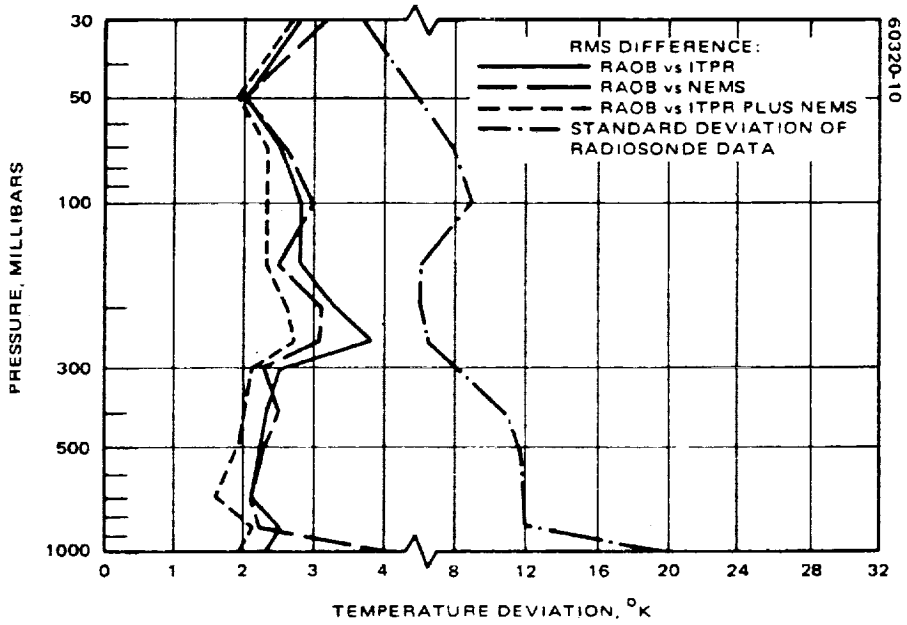

FIGURE 2-9. STANDARD DEVIATIONS BETWEEN RADIOSONDE AND RADIANCE SPECIFIED TEMPERATURES (ITPR ALONE, NEMS ALONE, AND ITPR AND NEMS COMBINED) FOR NIMBUS 5 SOUNDING SYSTEM

It is currently planned to add microwave sounding to STORMSAT. The MASR described in Reference 2 was used as a model for the purpose of this study; data that are lacking in Reference 2 were developed in consultation with the author of that document. The MASR is a multichannel Dicke radiometer for measuring the earth's brightness temperatures at several frequencies near the 118 GHz 0_2 line and the 183 GHz H_20 line. The brightness temperatures near the 118 GHz line will be used to derive temperature profiles, while those near the 183 GHz line will be used to derive water vapor profiles. Microwave images in the wings of the 183 GHz H_20 absorption line, formed by continuous scanning in a raster pattern, will yield water vapor maps of severe storms. Microwave images at other frequencies, such as 120 GHz, can be used for mapping the spatial distribution of rainfall.

Spatial Resolution and Beamwidth

A critical requirement imposed on a geosynchronous microwave sounder is that its antenna must have a very narrow beamwidth to achieve the ground resolutions required for sounding severe storms. Figure 2-10 (from Reference 2) shows the horizontal spatial resolution and observation frequency required for temperature and humidity sounding of severe storms. The ground resolutions required vary for different severe storms phenomena; they fall mostly in the 10 to 100 km range. For nadir observation this range corresponds to antenna beamwidths in the range 0.28 to 2.8 mrad.

A specific example of resolution requirement is illustrated by the 42 km grid (Figure 2-11) used in a numerical mesoscale model (Reference 3) to study the Palm Sunday tornados of 11 April 1965. (That outbreak of more

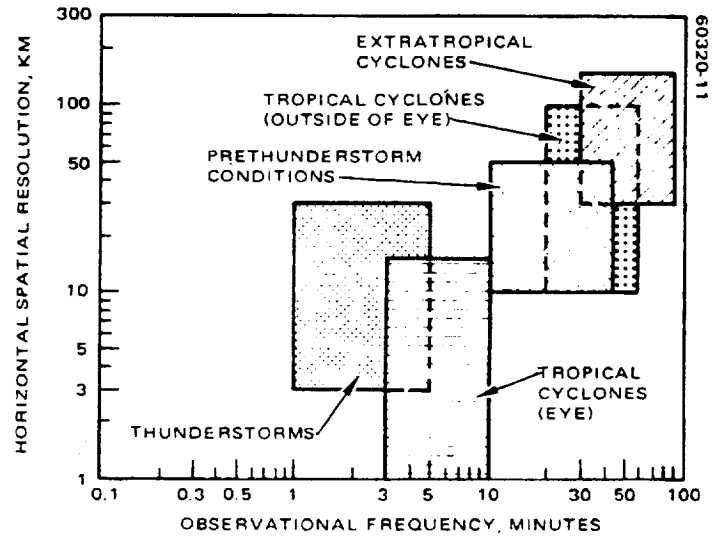

(ADAPTED FROM M. W. SHENK AND E. KREINS, 9TH CONF. ON SEVERE STORMS; NORMAN, OKLAHOMA, OCTOBER 1975)

FIGURE 2-10. HORIZONTAL SPATIAL RESOLUTION AND OBSERVATIONAL FREQUENCY REQUIREMENTS FOR TEMPERATURE AND HUMIDITY SOUNDING OF SEVERE STORMS

than 37 separate tornados occurring over six midwestern states killed 258 persons, injured 3148, and caused over 23M in property damage.) The model, initialized by radiosonde data gathered 6 hours earlier, was able to numerically generate the squall line originating the tornados. If the STORMSAT sounding data were used to initialize or update such a mesoscale forecast model in real time, ~42 km ground resolution for the sounder is adequate. The resolution sizes shown in Table 2-4 for a 2.5 m antenna satisfy this requirement nicely.

High Frequencies, Large Aperture, and Mechanical Scanning

Because of the fundamental limitation of diffraction, a typical radiometer antenna of diameter D can only give a beamwidth of the order $1.3\ \lambda/D$, where λ is wavelength. The frequencies of the microwave absorption resonances of 0_2 and H_20 which are available for the sounding of atmospheric temperature and water vapor, respectively, are shown in Figure 2-12. The 60 GHz 0_2 and 22 GHz H_20 resonances have been used in all microwave sounders flown or designed to date, since these sounders are for observing synoptic scale phenomena from low altitudes (~1000 km), where antenna beamwidths in the range of 7° to 10° are adequate. For geosynchronous sounding of severe storms, there is a need to use the higher frequency 0_2 resonance at 118 GHz (2.53mm) for temperature sounding, and the H_20 resonance at 183 GHz (1.64 mm) for water vapor sounding. These shorter

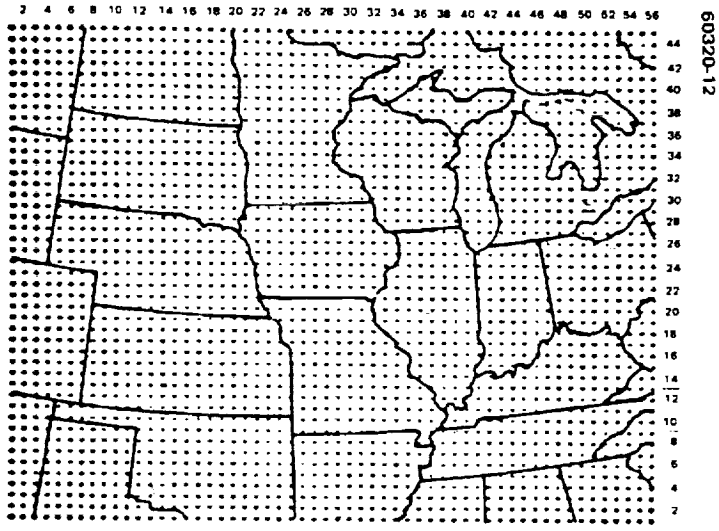

FIGURE 2-11. 42 KM GRID MATRIX EMPLOYED TO PREDICT PALM SUNDAY TORNADO OUTBREAK OVER IOWA, ILLINOIS, WISCONSIN, MICHIGAN, INDIANA, AND OHIO

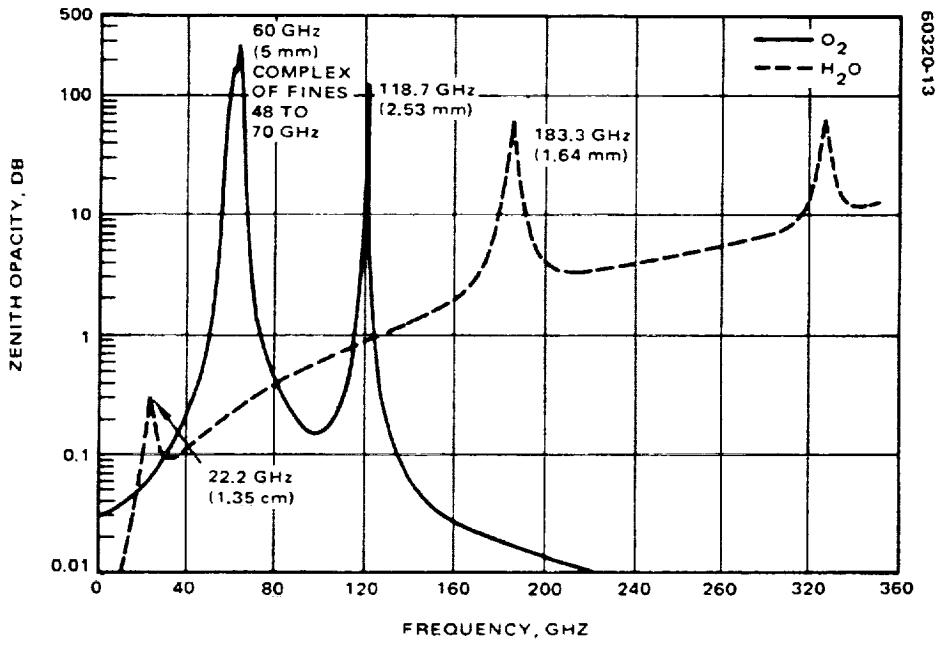

FIGURE 2-12. MICROWAVE ABSORPTION RESONANCES OF O_2 AND H_2O AVAILABLE FOR SOUNDING. QUANTITY PLOTTED IS SEA LEVEL ZENITH OPACITY IN U.S. STANDARD ATMOSPHERE. H_2O CURVE IS FOR ONE PRECIPITABLE CENTIMETER OF WATER VAPOR

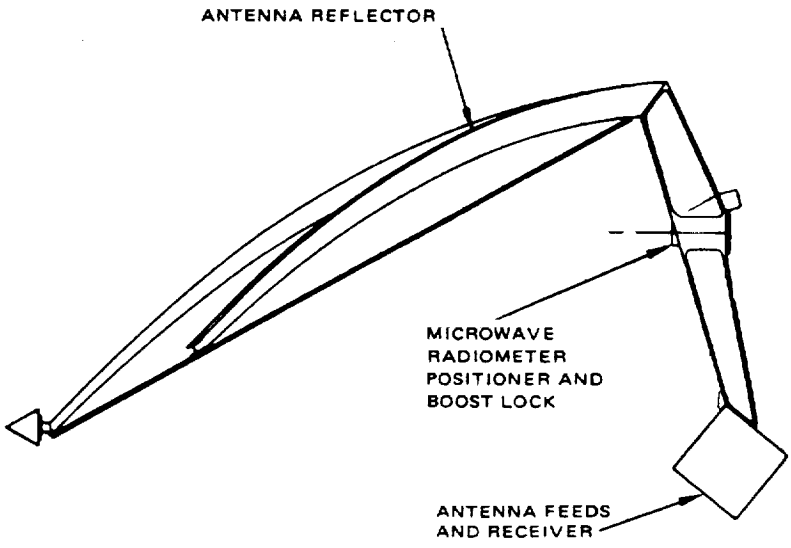

PHYSICAL CHARACTERISTICS

- APERTURE DIAMETER = ~ 2.5 m
- MASS (EXCLUDING GIMBAL) = ~ 72.5 kg (150 lb)

OPERATING WAVE LENGTHS

- TEMPERATURE SOUNDING = 118 GHz (0_2 ABSORPTION)
- HUMIDITY SOUNDING = 183 GHz (H_2O ABSORPTION)

FIGURE 2-13. MICROWAVE ATMOSPHERIC SOUNDING RADIOMETER

TABLE 2-4. IFOV SIZES FROM GEOSYNCHRONOUS ORBIT FOR 2.5M ANTENNA

Size	Subsatellite Point		45° Inclination	
	Frequency, GHz		Frequency, GHz	
	183*	118**	183*	118**
Major diameter, km	30	47	52	80
Minor diameter, km	30	47	32	50
Geometric mean, km	30	47	41	63

*Assumes 0.8 mrad beamwidth.
**Assumes 1.3 mrad beamwidth.

wavelengths allow the required narrow beamwidths to be achievable with practical antenna sizes (<4.5m) that can fit into the Shuttle payload bay without furling.

The need for a narrow antenna beam thus leads to two critical requirements for geosynchronous microwave sounding:

1) Large aperture reflector antenna, 2.5 m or more in diameter

2) Low noise radiometer operating between 118 and 183 GHz.

To map a finite area on earth, the antenna beam has to scan in two orthogonal dimensions. Because of the very high frequencies, electrical scanning becomes difficult to implement, so mechanical scanning is required. This leads to a third critical requirement:

3) Mechanical scanning of a large antenna in two orthogonal axes

This last requirement has a major impact on the spacecraft design. The spacecraft must provide a mechanical system to orient and scan a large antenna with the necessary accuracy and to compensate for the angular momentum perturbations caused by the antenna motion, so as not to violate the AASIR pointing requirements. The baseline MASR and its physical characteristics are shown in Figure 2-13. This offset parabolic configuration was established by a joint effort of NASA GSFC and Hughes. Functional requirements for this instrument are discussed in the follow section. The impact of these requirements on the two-axis gimbals are developed in Section 4.2.

Temporal Resolution and Frame Time

A primary driving factor for severe storm observation is that the same scene must be viewed repeatedly at 1 hour or shorter intervals. This is basically the raison d'etre of the geosynchronous STORMSAT mission. The required observation frequency determines a frame time within which an

area on earth is to be covered by the sounder. A frame time of 30 minutes for a 1000 by 1000 km frame is assumed for this study. This results in a scan rate of 0.29 mrad/sec with an associated dwell time of 2.75 seconds per 1 FOV. These assumptions are summarized in Table 2-5.

Area Coverage Sizes

The area coverage requirements for severe storm observation are shown in Table 2-6, taken from Reference 2. The area frame sizes considered for this study were $(1000\ km)^2$, $(1500\ km)^2$ and $(2000\ km)^2$. The 1000 km size was assumed as a design point, while the other two sizes were considered only to evaluate their impact on the system design.

TABLE 2-5. MASR BASELINE FUNCTIONAL REQUIREMENTS

Frame size	1000 by 1000 km
Frame time	30 minutes
Scan rate	0.29 mrad/sec
Dwell time	2.75 sec
Beam width	
f = 183 GHz	0.8 mrad
f = 118 GHz	1.3 mrad
Channels	16
Encoding	10 bits/sample
Data rate	Less than 500 bps

TABLE 2-6. SEVERE STORM OBSERVATION AREA REQUIREMENT

Phenomenon	Square Area Size, km^2
Thunderstorm outbreak	750
Tropical cyclone	1500
Extra tropical cyclone	3000

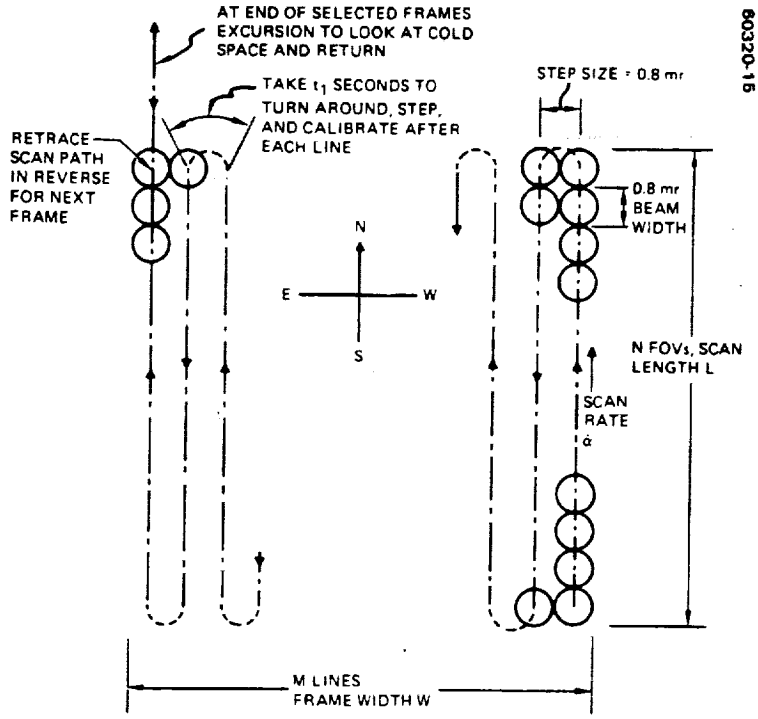

FIGURE 2-14. RASTER SCAN PATTERN FOR STORMSAT MICROWAVE RADIOMETER

Each frame is to be swept out with contiguous coverage of the 0.8 mrad (183 GHz) beam, allowing the 1.3 mrad (118 GHz) beam to overlap. The antenna is assumed to have only a single beam at each frequency.

Raster Scan Pattern

Figure 2-14 shows the raster scan pattern assumed. The scan lines are generated at the constant rate of 0.29 mrad/sec by continuous motion of the field of view in the north-south direction, the direction chosen for dynamical considerations. The lines are stepped in the east-west direction. At the end of each scan line the beam is stepped, turned around, and calibrated against a blackbody source. Periodically, at the completion of selected frames, the beam travels to a point 10° away from nadir to look at cold space for calibration. After returning to the frame location, the scan pattern may be retraced in reverse. If this technique is utilized, the scan motion alternates between forward and backward modes between cold space calibrations.

Table 2-7 shows the scan parameters calculated for the three frame sizes; these parameters are used for the spacecraft system study. The numbers in Table 2-7 are based on a scan rate of 0.29 mrad/sec, a calibration during turnaround at the end of each line of 2.75 sec duration, and 52 by 32 km resolution cell size, as given in the 45° column of Table 2-4.

TABLE 2-7. SCAN PARAMETERS FOR DIFFERENT CASES OF FRAME SIZES STUDIED

Parameter	Case		
	A*	B	C
Surface Coverage (at 45° N, Subsatellite Longitude), km	1000 x 1000	1500 x 1500	2000 x 2000
Number of FOVs per Scan Line, N	19	29	38
Number of Scan Lines, M	31	47	63
Length of Scan, L, deg	0.87	1.33	1.74
Frame Width, W, deg	1.42	2.15	2.89
FOV Dwell Time, sec	2.75	2.75	2.75
Scan Rate ($\dot{\alpha}$), mrad/sec	.29	.29	.29
Time per Scan, sec	52.2	79.8	104.4
Turnaround Time, t_1, sec**	2.75	2.75	2.75
Frame Time, min	28.4	64.6	112.5

*Design point

**t_1 is time to turnaround, step, and calibrate (with internal source) at end of each scan.

The parameters calculated are angular frame size, time per scan, and total frame time. The round trip excursion time for a space calibration must be added to the total frame time to determine the time between sets of frames. The time interval required between space calibrations has not yet been established.

The MASR will be capable of positioning the sounding frame at any point on the disk. However, for the purpose of this study, it was suggested by GSFC that a nominal location (45° N, subsatellite longitude) be taken as a design point, as illustrated in Figure 2-15. Table 2-7 is based on this frame location. At that location the 0.8 mrad beam subtends a 52 by 32 km quasiellipse on the surface and traces out the 1000 by 1000 km square area by scanning an angular frame 87° by 1.4°. At other locations on the disk, the size and orientation of the IGFOV cell ellipse are different, and to trace the same size square area will require different angular frame sizes. The system should be able to accommodate such flexibility.

Slew Mode for Space Calibration

At the end of selected frames the beam is slewed to 10° off nadir and returns in less than a certain specified time, say t_2 seconds. This time for space calibration must include acceleration to slew rate, slew time to 10°, turnaround, and deceleration to next frame start. The beam may travel from point A to B (Figure 2-15) and return via any path, as long as B is ~10° off nadir, and time required is less than t_2 seconds. The nominal location at 45° N latitude is already 6.8° off nadir and requires a

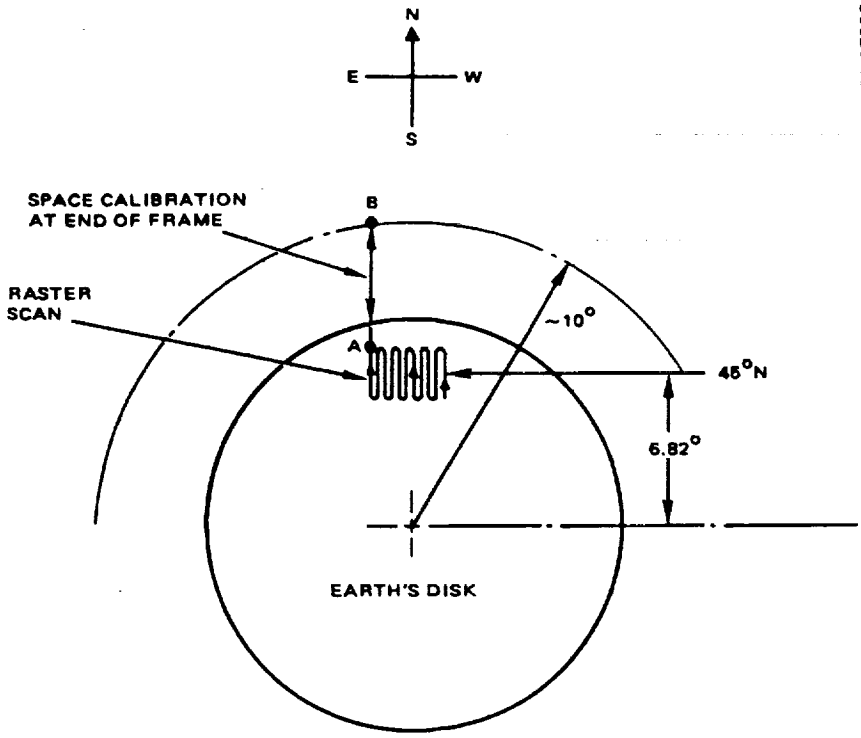

1) MAY GO FROM A TO B AND BACK VIA ANY PATH. B ON 10° CIRCLE.
2) SAME MODE OF OPERATION MUST BE POSSIBLE IF SPACECRAFT IS TURNED UPSIDE DOWN.

FIGURE 2-15. SLEW MODE FOR SPACE CALIBRATION

smaller travel rate to complete the space look excursion in a given time than from other points nearer to nadir.

The establishment of space calibration intervals between frames, the time allocated for space look are the associated slew rates involved, impact the instrument scan efficiency on the one hand and the momentum compensation of the spacecraft due to slew disturbances on the other. Travel status between instrument design and spacecraft momentum compensation will be required as these requirements become further delineated. This space calibration mode should not be confused with the internal calibration performed at the end of each scan during turnaround time, t_1.

Whole Disk Coverage

The whole disk coverage is not a primary mode for severe storm observation, but is used only occasionally when there are no severe storms to observe. The system is to be sized primarily by the $(1000\ km)^2$ coverage requirement. The system so designed will be evaluated for what it can do in the way of whole disk coverage.

2.1.3.3 Pointing Stability and Accuracy

The attitude of the microwave sounder and its supporting platform should remain stable while the antenna beam scans the raster pattern of Figure 2-14. The required stability is determined by the need to maintain fidelity in the 183 GHz microwave image for deriving water vapor maps. The attitude stability in either the east-west or north-south direction is required to be 10 percent of the 183 GHz beam, or 80 μrad (1σ) over the 30 minute frame time. The antenna line of sight jitter due to errors in the gimbal and scanning drive mechanisms is also required to be less than 80 μrad (1σ).

It is anticipated that the microwave and infrared sounding data will be combined in the sounding inversion to take advantage of synergistic benefits, as was done in References 4 and 5. This will require that the relative angular location between the microwave and infrared sounding field of view centers be determinable and not vary excessively. The relative location should not vary by more than 200 μrad (1σ) in either the east-west or north-south direction. This tolerance is determined by the leeway in locating the 375 μrad IR sounding IGFOV within the 800 μrad microwave IGFOV. The 80 μrad variability of the microwave radiometer line of sight relative to itself specified above is included as a contributor to the 200 μrad error. Since the fields of view of the AASIR are much smaller than those of the MASR, the requirements on absolute pointing accuracy and real time attitude determination for the AASIR, are also adequate for the MASR. Having specified the accuracy of determining the relative orientation of the microwave sounder with respect to the AASIR, it is permissible to leave the absolute pointing accuracy of the microwave sounder unspecified, as a tentative approach pending better definition of the microwave sounder requirements.

2.1.4 Real Time Sensor Data Processing Requirements

Due to the extremely transient character of mesoscale weather phenomena, STORMSAT data will have to processed with minimum time delays to be useful for operational prediction or warning of severe storm events. For example, thunderstorm and tornado producing squall lines have active lifetimes from a few minutes to a few hours. In a prethunderstorm condition, before the cumulonimbus clouds have formed, time delays of up to an hour may be tolerated in processing STORMSAT data. However, during active portions of a storm, STORMSAT data would have to flow through the ground processing system and out to the public with time delays on the order of 5 minutes, if action is to be taken to reduce loss of life and damage to property. This requirement will have significant impact on the ground data processing system design.

2.2 STORMSAT FOLLOW-ON MISSION REQUIREMENTS (MISSION B)

While emphasis in this study was on the primary STORMSAT mission, some consideration was given to the follow-on mission and the impact on system design due to extended mission requirements. The follow-on STORMSAT may be required to perform all of the functions currently provided by the operational GOES system, as illustrated in Figure 2-16 (Reference 6).

2.2.1 Data Collection

A large amount of useful meteorological data is derived from in situ sensors located on remote data collection platforms (DCPs) such as ships, aircraft, ocean buoys, and inland areas not conveniently connected by surface communications. The current GOES system is designed to collect these data by means of satellite interrogation of these DCPs and to relay these data via satellite to the command and data acquisition station (CDAS). The follow-on STORMSAT may be required to provide this data collection service.

These DCP report data will either be stored at the CDAS or transmitted via landline (or microwave link) to NESS, Suitland, for subsequent processing. A small minicomputer installation at NESS is dedicated to the handling and processing of DCP reporting data and DCP network control. Hydrological, meteorological, and atmospheric data will be observed and reported by this network.

2.2.1.1 DCP System Description

Two different schemes have been implemented for the SMS/GOES DCP; the first the self-timed, and the second the interrogated DCP. The former concept employs a clock which allows 1 to 12 hour synoptic reporting intervals, in 1 hour increments. When not transmitting, the DCP is in its "powered down" clocking mode. Transmission utilizes 30 seconds. The second concept appears to be most useful and requires half the report channel spacing. Either design utilizes UHF reception and transmission with transponding in the SMS/GOES for S band interface with the CDAS. Approximately 10,000 platforms are contemplated in eventual service.

The collection of data from the interrogated DCP begins with the preparation of a programmed sequence of interrogation commands which is recorded on magnetic tape. The interrogation command consists of a digital word, the first part of which is a preamble common to all DCPs, followed by an address unique to each DCP. These digital commands drive a PSK modulator at the CDAS. The interrogation signal transmitted from the CDAS is at an S band frequency such that it falls within a satellite channel that translates the command to an UHF downlink frequency. At the DCP it is received, demodulated, and decoded. If the decoded address agrees with the address stored in the DCP, the set is placed into an active mode for transmission of data. Transmissions are spaced at 1500 Hz

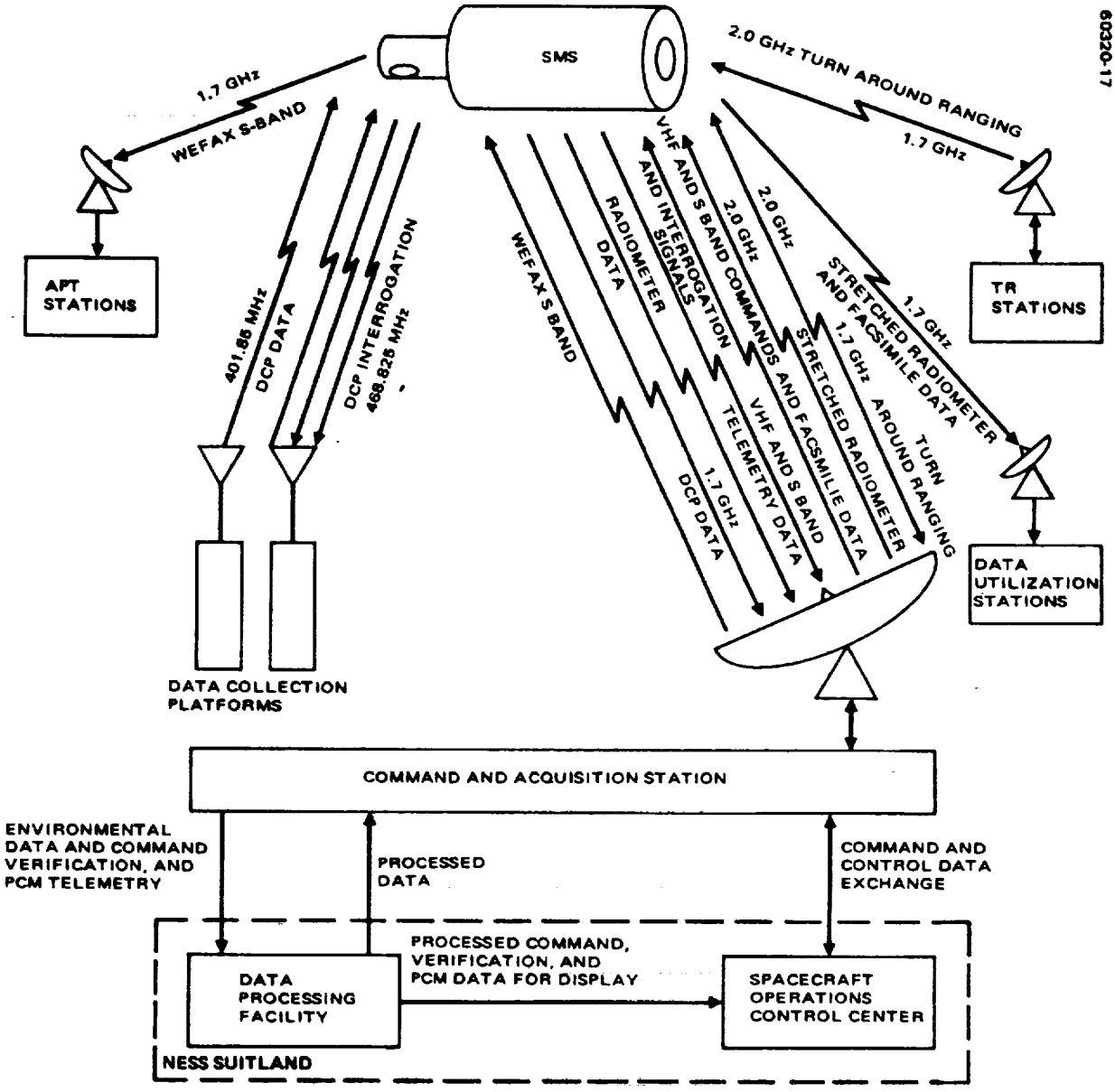

FIGURE 2-16. SMS/GOES SYSTEM CONCEPT

intervals in the band 401.849 588 to 401.998 095 MHz, and the received signals are at the assigned UHF interrogation frequency of 468.825 MHz. The DCP-to-spacecraft uplink at UHF is provided by a 5 watt transmitter driving a 10 dB gain antenna system.

2.2.1.2 Impact of DCP Requirements on STORMSAT

The baseline STORMSAT design for the primary mission has no UHF-to-S band and S band-to-UHF transponding capability. In fact, though provision for a receiving S band antenna has been made on the mission module, no such capability has been incorporated into the baseline. Therefore, interface with the current GOES DCPs will require addition of this transponding capability. Specifically:

1) Addition of an S band receive capability at ~2000 MHz (a parabolic antenna of ~2 feet diameter can be accommodated on the earth viewing module)

2) Addition of a UHF earth coverage receive and transmit capability is required. Ten to 40 watts of UHF RF mode switchable power is compatible with current GOES.

3) Addition of frequency translation and interface electronics is required for the CDAS-STORMSAT-DCP S band to UHF interrogation link downconversion and DCP-STORMSAT-CDAS reporting link upconversion

It should be noted that the addition of S band receive capability for the DCPS would allow further capabilities, such as redundant command link and WEFAX data relay.

2.2.2 Data Relay

Local weather forecasting depends on ready access to a large amount of data collected by the National Weather Service. Some of these data originate at the World Meteorological Center (WMC), Washington D. C. Weather facsimile (WEFAX) data consists of temperature profiles, weather maps, and other data products. Broadcasts are made at scheduled times. The geostationary metsats beginning with Application Technology Satellites (ATS) and continuing with SMS/GOES provide the capability to relay facsimile and other low bandwidth data via satellite to globally situated automatic picture transmission (APT) sites which have a front-end RF conversion capability that translates the SMS/GOES S band transmissions to VHF frequencies, compatible with APT terminals.

The GOES concept is designed to minimize user costs for this APT conversion. The signal baseband structure of the WEFAX is made compatible with the APT video formerly generated by the ATS. In this manner, the only major modification of the VHF APT equipment is the addition of an S band antenna, receiver, and downconverter. The basic

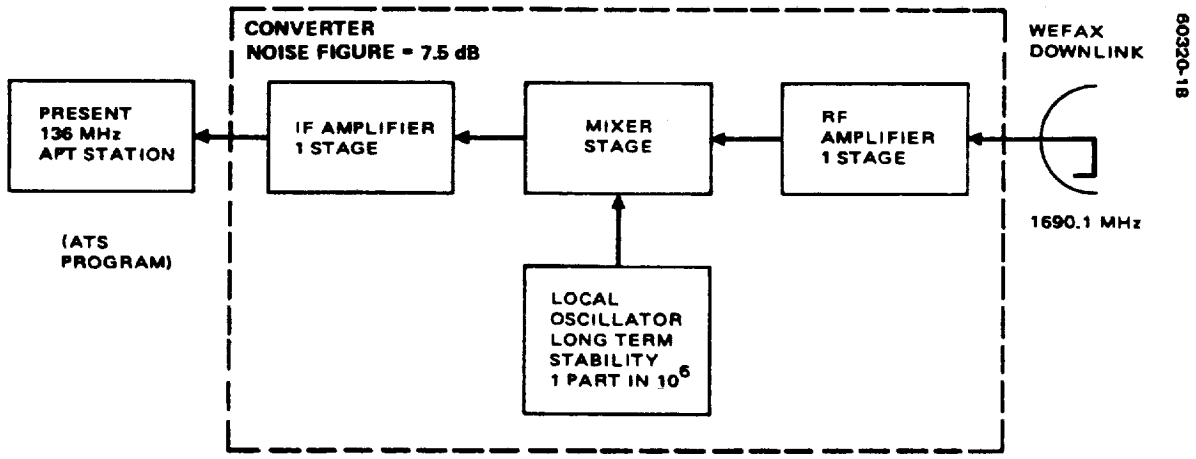

FIGURE 2-17. TYPICAL S BAND CONVERSION BLOCK DIAGRAM FOR WEFAX APT STATION

simple facsimile transmission concept is retained. A block diagram of the conversion equipment is given in Figure 2-17. The scheduling and ancillary operational data necessary for these terminals are provided via landlines (Telex).

2.2.2.1 Impact of WEFAX Relay on STORMSAT

The GOES provides a geostationary relay capability at S band for low rate facsimile and other forecast products generated by WMC. The STORMSAT could provide analogous service to these stations or, ultimately, to all digital stations of modest capability. In fact, if appropriate measures are taken on-board, mesoscale viewing (less than global digital) of the AASIR could be provided at these small stations. The impact of interfacing with current GOES compatible APT sites includes the following:

1) A STORMSAT S band receive capability must be provided, about 2033 MHz. Providing S band receive capability appropriate for remote data collection platform interrogation will also allow this capability.

2) Similarly, S band transmit capability about 1691 MHz, with EIRP ≥45 dBm, will allow transmission of narrowband facsimile data to a modest APT station (10 foot parabolic dish, transistor frontend).

3) Dual frequency S band capability at special classes of small receiving sites, more capable than the APT inferred above, would allow reception of limited field of view (4° by 4° or smaller) AASIR data directly from STORMSAT (if the spacecraft data rates were properly adjusted). Thus, relatively small stations, similar to the stretched VISSR data utilization station (DUS) at NOAA/NESS Federal Office Building No. 4, could receive both facsimile and realtime STORMSAT payload data.

2.2.3 Space Environmental Monitoring Requirements

NOAA has continuing interest in the collection of data related to the effect of solar disturbances on the near-earth environment. Space environments monitoring (SEM) sensors designed to measure important effects of solar activity for real time use in warning of radiation hazards in space are planned on satellites with available space and weight. These data are available for uses such as the study of the effect of certain solar activity on the earth's weather and climate. The SMS/GOES carries a SEM package and the follow-on operational STORMSAT may be required to do so as well.

2.2.3.1 SMS/GOES SEM Sensors

SEM sensors orbiting on the GOES satellites consist of a magnetic field monitor, an energetic particle monitor, and a solar X-ray monitor. The magnetometer measures three orthogonal components of magnetic field. The energetic particle monitor measures proton and alpha particles fluxes in several energy ranges up to 500 MeV foı protons and up to 400 MeV for alphas. The energetic particle monitor consists of a telescope spectrometer for the low energy range and a dome spectrometer for the high energy range. In addition, the dome spectrometer measures the flux of electrons with energies ≥ 0.5 MeV. The solar X-ray monitor measures solar X-ray flux in the wavelength ranges of 1 to 8°A and 0.5 to 3°A.

2.2.3.2 Impact of SEM Requirement on STORMSAT

The change from a spinning spacecraft (GOES) to a body stabilized spacecraft (STORMSAT) has a significant impact on the design of the SEM sensors. All three SEM instrument packages on GOES are designed to make use of GOES spacecraft spin motion to generate their scan function. Modification of the magnetometer to operate on STORMSAT would require the addition of a third magnetic sensor to measure a third axis of magnetic field. The current operational version has one sensor oriented along the spacecraft spin axis and a second in the plane perpendicular to the spin axis.

The solar X-ray monitor would have to be provided with an additional gimbal about the pitch axis, current GOES spin axis, to track the sun over the course of the day. A single gimbal is already present in existing equipment to track the annual change of solar elevation angle.

The energetic particle monitor poses a more difficult problem. Its function is to average particle flux over the 2π rotation of the satellite and over the acceptance angles of the instruments. The pointing direction of both the dome spectrometer and telescope spectrometer on the GOES is perpendicular to the spacecraft spin axis. To achieve the 2π averaging on STORMSAT would require the addition of more sensors or a spin table on which to mount existing sensors. A more reasonable approach to the problem may be to re-examine the basic requirements for particle flux monitoring to see if a simpler approach exists for satisfying the monitoring needs.

2.3 REFERENCES

1. J. F. W. Purdom, Satellite Imagery and the Mesoscale Convective Forecast Problem, Preprints of the 8th Conference on Severe Local Storms, Denver, Colorado, October 15-17, 1973, American Meteorological Society, pp 244-251.

2. J. C. Shiue, AAFE Proposal for Geosynchronous Sounding Microwave Radiometer, in response to A. O. OA-75-3, November 1975, Goddard Space Flight Center.

3. M. L. Kaplan, D. A. Paine, and N. J. Tetrick, The Results of a Mesoscale Numerical Prediction of the Squall Line Organizating the Palm Sunday Tornadoes, Reprints of the 8th Conference on Severe Local Storms, pp 320-327.

4. W. L. Smith, H. M. Woolf, P. G. Abel, C. M. Hayden, M. Chalfant, and N. Grody, Nimbus 5 Sounder Data Processing System, Part I Measurement Characteristics and Data Reduction Procedures, NOAA Technical Memorandum NESS 57, NOAA, NESS, Washington, D. C., June 1974.

5. W. L. Smith, H. M. Woolf, C. M. Hayden, W. C. Shen, Nimbus 5 Sounder Data Processing System, Part II: Results, NOAA Technical Memorandum NESS 71, NOAA, NESS, Washington, D. C., July 1975.

6. P. L. McKowan, "Data Processing Plan for Synchronous Meteorological and Geostationary Operational Environmental Satellites (SMS/GOES)", October 1975, Goddard Space Flight Center.

3. SPACECRAFT SYSTEM DESIGN

3.1 INTRODUCTION

This section, together with Sections 4 through 10, presents a spacecraft preliminary design assessment for performing the STORMSAT mission using the Multimission Modular Spacecraft (MMS) and mission-unique equipment. STORMSAT, together with the Interim Upper Stage (IUS), will be launched by the Space Shuttle System into low altitude earth orbit and be delivered to synchronous orbit by the IUS. The spacecraft configuration presented in this study provides for independent operation of the AASIR and MASR meteorological sensors. These payload sensors are incorporated into a mission module (MM) which is supported by the MMS and its subsystems. A detailed definition of the payload sensors, as with the MMS and its subsystems, has not been completed at this time. However, the functional requirements and preliminary configuration characteristics of the sensors and subsystems are well enough defined that a meaningful preliminary spacecraft configuration study could be performed.

The AASIR as incorporated into this study is defined functionally by the design review report issued by Santa Barbara Research Center in November 1975. Physical design characteristics of the AASIR have evolved since that time, and the characteristics known in January 1976 are assumed for this study. It is anticipated that some of the AASIR functional characteristics will be revised. In particular, this is expected to affect visible sensor resolution and data rate by requiring a fast imaging mode using smaller instantaneous fields of view for the imaging sensor channels. These changes are not considered for this report but may be examined in a subsequent phase of this program.

The MASR experiment as proposed by GSFC in November 1975 is also incorporated into this study of STORMSAT. The definition of this experiment has been initiated. Configuration mass and power requirements have been estimated for this study.

Characteristics of the MMS are based on the Low Cost Modular Spacecraft Definition Report dated May 1975, and also on the specifications for the communications and data handling module, attitude control subsystem module, and electric power subsystem module released in December 1975. The approach generally taken was to utilize the modules as defined by the above documents. Any additional equipment required to perform the STORMSAT

mission is properly a part of the mission-unique equipment assigned to the mission module. An exception is the mission-unique propulsion module that is incorporated into this configuration of STORMSAT to provide a more favorable installation for orbit inclination control.

The specifications for the IUS have recently been released. It is specified that the IUS will utilize solid propellant motors and deliver a payload of 2273 kg (5000 pounds) to synchronous orbit. The payload interface to the IUS is equivalent to that of the Titan IIIC. It is expected that a variety of adapters may eventually be designed and be available for various users. The Shuttle/IUS is expected to deliver the spacecraft near to its operational station in geosynchronous orbit and to provide a known attitude for initialization of the spacecraft attitude control subsystem. Separation may be achieved by either IUS or spacecraft commands.

This study has been principally directed toward identifying problem areas arising from the use of the MMS, IUS, and Space Shuttle System in the performance of the STORMSAT mission. Problem areas which have arisen during the study are identified in each section. It is suggested that some of these areas be investigated in greater technical depth in subsequent phases of the STORMSAT program.

3.2 GENERAL ARRANGEMENT

The baseline spacecraft configuration is arranged so that the orbital velocity vector nominally coincides with the spacecraft longitudinal axis. STORMSAT mission requirements appear to be achieved by this configuration. This approach results in rather large yaw-roll torques due to solar radiation pressure and a requirement to reorient the spacecraft for orbit adjust maneuvers. An alternative approach which would minimize these operational constraints is to orient the spacecraft longitudinal axis normal to the orbit plane. Detailed layouts are required to verify the design feasibility for this alternative configuration.

The general arrangement of the STORMSAT spacecraft baseline design is illustrated in Figure 3-1. The MASR is located at the forward end of the spacecraft, providing the instrument with an unobstructed view of earth. It is mounted on a gimbal attached to a truss structure built up from the mission payload adapter of the MMS. The AASIR is located within this truss. Earth viewing for the AASIR is accomplished by an internal mirror for the north-south direction of scan and by rotation of the entire instrument in the east-west direction of scan. A positioner assembly provides support for the AASIR, facilitating the east-west motion. The positioner assembly, in turn, is mounted to a frame structure attached to the mission payload adapter. A clear field of view is provided for the AASIR radiation cooler. It is oriented south in spring and summer and north in fall and winter to avoid direct viewing of the sun. Reorientation is accomplished by a yaw maneuver twice per year.

FOLDOUT FRAME 1

FOLDOUT FRAME 2

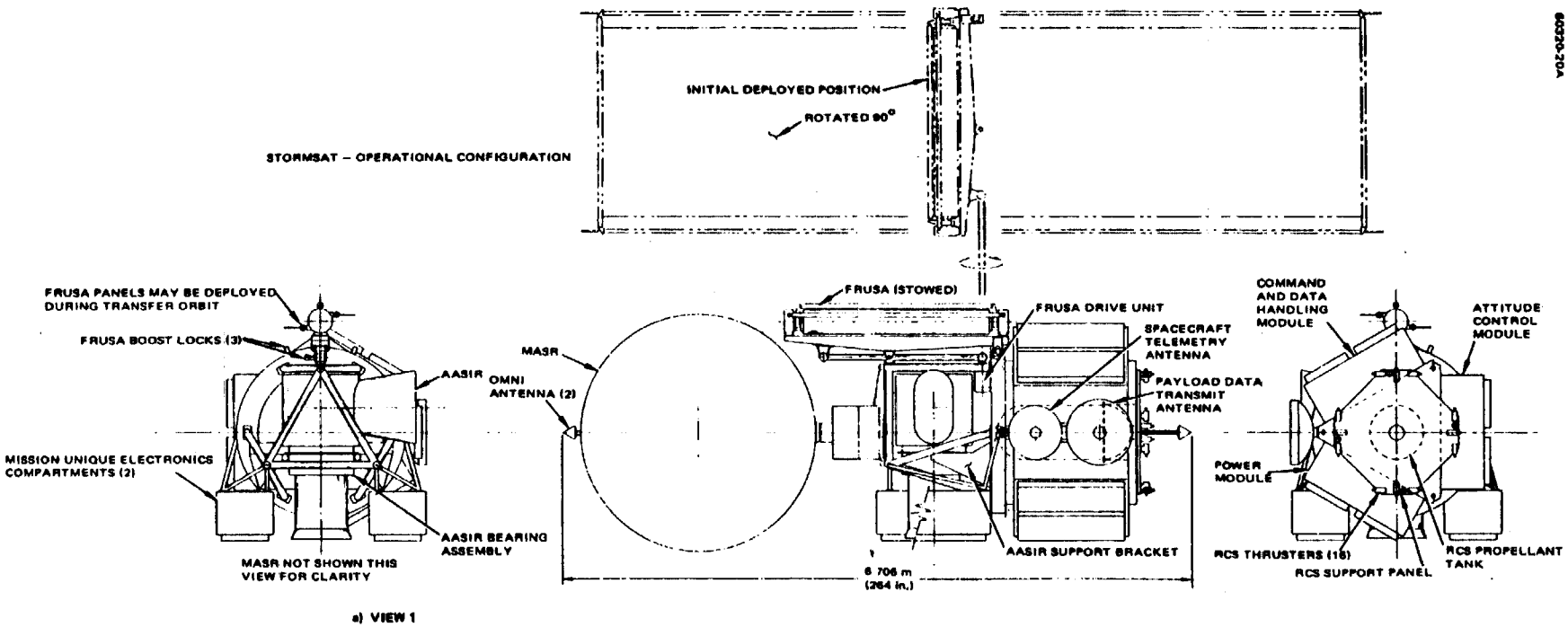

FIGURE 3-1. STORMSAT GENERAL ARRANGEMENT

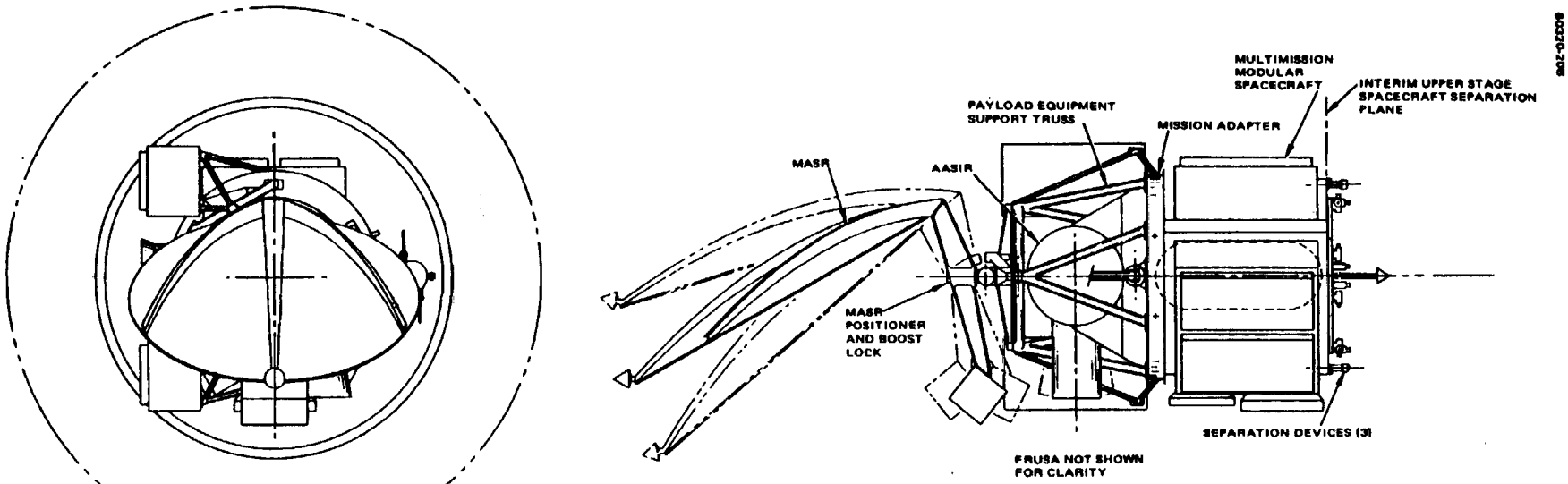

b) VIEW 2

FIGURE 3-1 (CONTINUED). STORMSAT GENERAL ARRANGEMENT

Mission-unique electronic equipment is mounted in two equipment modules supported by the payload truss structure. These modules are equipped with thermal control radiators facing in the same direction as the AASIR radiation cooler. Equipment associated with AASIR data handling may be mounted on the rotary side of the AASIR positioner to minimize cable wrap. Special provisions will be required to provide thermal control for these units. The solar cell array is located on the opposite side of the mission payload module. It is a sun oriented array and is provided with an unobstructed view of the sun. The array orientation mechanism is mounted on the transition adapter; it controls the solar cell array through a strut which also serves to deploy the solar array to its operational position.

The MMS spacecraft modules are aft of the transition adapter. The attitude control module is located in the anti-nadir position, the electrical power module is located on the side facing generally away from sunlight, and the communications and data handling module is mounted on the sunlit side. A mission peculiar propulsion module is installed at the base of the MMS. Its propellant tank nests within the triangular cavity of the MMS while providing acceptable room for cabling. This configuration minimizes overall length of STORMSAT and facilitates installation of an adapter to the IUS.

The integration of the STORMSAT spacecraft with the IUS is shown in Figure 3-2, installed in the payload bay of the orbiter vehicle of the Space Shuttle System. The spacecraft is cantilevered from the IUS by a conical adapter. The IUS is supported by cradles which pick up payload attachment points inside the orbiter payload bay. It is expected that other orbiter payloads may be located either forward or aft of the STORMSAT/IUS combination. Center of gravity restrictions on the orbiter limit forward installed payload to approximately 4545 kg (10, 000 pounds) to maintain the orbiter cg within specified limits. A combination of forward and aft fixed payloads which satisfy orbiter cg limits with or without the STORMSAT/IUS payload could also be selected. The 29, 545 kg (65, 000 pounds) maximum payload of the orbiter could be achieved with this configuration of payloads. An alternative to the forward or aft location of other payloads would be to offset the STORMSAT/IUS toward the bottom of the orbiter payload bay. This would allow other spacecraft to be located above the STORMSAT/IUS combination. Detail studies of the support equipment are required to establish realistic envelopes for this approach.

3.3 SPACECRAFT CHARACTERISTICS

STORMSAT is a large satellite for synchronous orbit operations. Its most demanding characteristic is precision attitude control stability for cloud velocity estimation and minimization of atmospheric sounding registration errors. A second characteristic is high data rates from mission sensors which require a separate data link. A third major characteristic is that STORMSAT is composed of spacecraft elements from many sources. The following subparagraphs provide data defining spacecraft characteristics. More detailed data is presented in the appropriate subsystem sections.

3.3.1 Dimensions

Spacecraft dimensions in the launch configuration (including the spacecraft/IUS adapter) are as follows:

	mm	Inches
Length	6858	270
Width	2235	88
Height	2540	100

The length of the IUS is estimated to be 4.572 m (180 inches). Thus, the overall length of the IUS and spacecraft is 11.430 m (450 inches).

Dimensions of the spacecraft after separation from the IUS and deployment of the solar cell array are as follows:

	mm	Inches
Length	6706	264
Width	2235	88
Height	5385	212

The solar cell array has an estimated width of 8.000 m (315 inches). Total projected area of the solar cell array is approximately 12.258 m^2 (19,000 square inches).

3.3.2 Spacecraft Estimated Power

Normal mode electrical power requirements are listed in Table 3-1. Mission sensor power includes sensor positioning mechanism power and mission data multiplexer power. The power requirements for the MMS modules are generally derived from their specifications. Battery charge power is based on conventional practice for earth synchronous satellites. Peak loads in attitide control and propulsion equipment may be handled while mission sensors are in a standby mode and battery charge is discontinued. As this occurs infrequently for momentum dumping and orbit adjust maneuvers, no significant loss of mission data is expected.

3.3.3 Spacecraft Propellant Budget

Propellant is allocated for a station acquisition maneuver of 5 deg/day, for stationkeeping, orbit inclination control, and attitude control subsystem momentum control. Propellant budgets for 3 and 5 year missions are listed in Table 3-2. Propellant mass is based on a spacecraft initial orbital mass of 1545 kg (3400 pounds) and rocket specific impulse expected for that type of service.

FOLDOUT FRAME

FOLDOUT FRAME

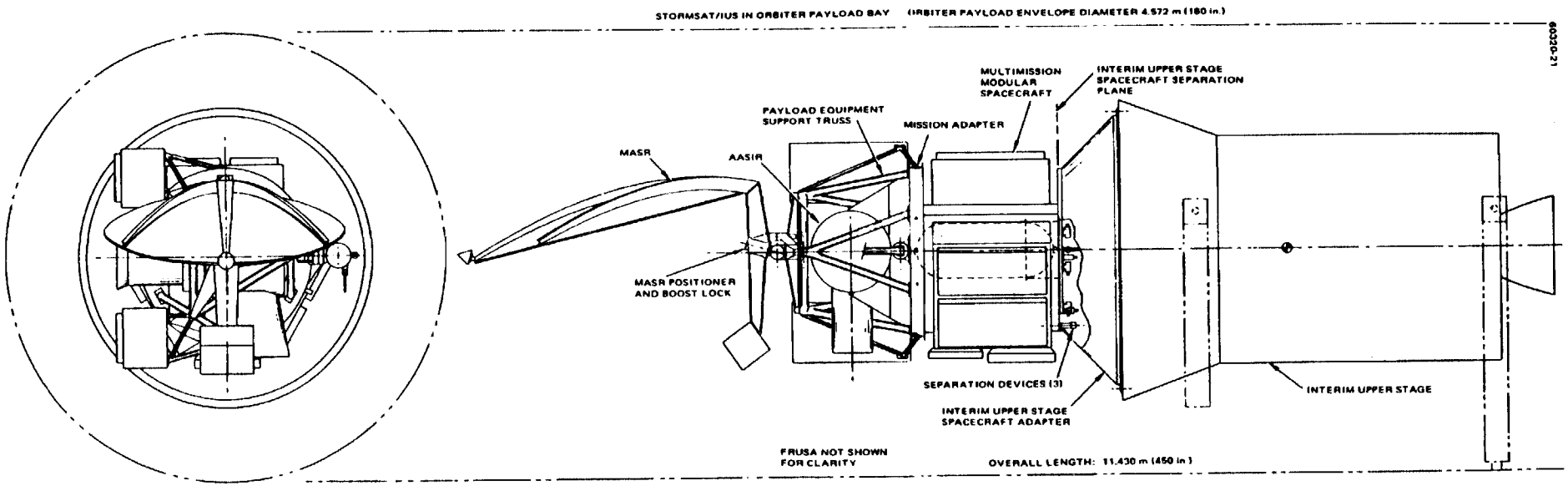

FIGURE 3-2. STORMSAT/IUS IN ORBITER PAYLOAD BAY

TABLE 3-1. STORMSAT NORMAL MODE POWER REQUIREMENTS

Subsystem	Power, W
AASIR and support equipment	151
MASR and support equipment	85
Mission data transmitter	90
Communications and data handling	115
Attitude control	170
Power subsystem	175
Battery charge	233
Thermal control	100
Contingency and miscellaneous	138
Solar cell array power	1,257

3.3.4 Spacecraft Estimated Mass

A preliminary estimate for the STORMSAT mass is presented in Tables 3-3 and 3-4. Subsystem mass estimates are based on component masses, which are derived from sources developing the equipment, from MMS module specifications, or estimated for this study if no other source is available. The spacecraft as separated from the IUS is constrained at 1545 kg (3400 pounds) for this study. Total mass, including the spacecraft/IUS adapter, is estimated to be 1623 kg (3570 pounds). The IUS System Specification, dated 15 January 1976, provides for a payload capability of 2273 kg (5000 pounds) for synchronous equatorial orbit; a payload reserve of 650 kg (1430 pounds) is accordingly available for spacecraft and launch vehicle development contingency, for mission growth, or for deployment of additional payload.

The AASIR utilizes a silica/invar optical subsystem design. A mass of 105 kg (230 pounds) is allocated for this instrument and its electronics. The mass of the MASR is not known with a high degree of precision, as only

TABLE 3-2. MISSION REQUIREMENTS AND PROPELLANT BUDGET

	3 Year Mission				5 Year Mission			
	Requirement		Propellant Required		Requirement		Propellant Required	
	m/sec	fps	kg	lb	m/sec	fps	kg	lb
Station acquisition	14.3	47	10.2	22.5	14.3	47	10.2	22.5
Stationkeeping	6.4	21	6.7	14.7	10.7	35	11.1	24.4
Inclination control	155.5	510	106.3	233.8	259.1	850	172.4	379.4
Attitude control	12,800 N-m/sec	9450 ft-lb-sec	6.5	14.4	21,400 N-m/sec	15,750 ft-lb-sec	20.9	24.0
Total		–	129.7	285.4		–	204.6	450.3

NOTE: Injection error corrections are assumed to be performed by the IUS.

TABLE 3-3. STORMSAT SUBSYSTEM MASS SUMMARY

Subsystem	Mass, kg	Mass, lb
Mission sensors and integration	270	594
Communications and data handling	138	303
Attitude control	182	400
Electrical power	270	595
Propulsion	68	150
Structure	256	563
Thermal control	32	70
Wire harness	67	148
Contingency	58	127
Spacecraft, end of life	1341	2,950
Propellant	205	450
Spacecraft, beginning of life	1546	3,400
Adapter	77	170
Required payload	1623	3,570
IUS specified payload	2273	5,000
Payload reserve	650	1,430

a conceptual design is currently identified; a mass of 68 kg (150 pounds) is allocated for this equipment. The mass estimate for the AASIR bearing and the microwave radiometer gimbal is also preliminary, since sufficient design studies have not been accomplished to select the best approach. It is expected that the baseline approach is conservative.

Mass estimates for the spacecraft subsystems are based principally on the MMS module specifications. Mass estimates for the auxiliary data transmission equipment of the communications and data handling (C&DH) subsystem are based on current development on the Japanese Geostationary Meteorological Satellite (GMS). A third star sensor may be included for the attitude control subsystem (ACS) to avoid degradation of performance if one of the star sensors in the ACS module were to fail. The third star sensor would be mounted on the mission payload adapter to avoid MACS design changes. Its mass has not been included in subsystem and component mass statement.

The propulsion subsystem is a mission-unique design utilizing the NASA standard thrusters, valves, and controls, and mission-unique propellant tank and integration hardware. It is mounted on a structural plate so that it can be mated with the spacecraft as an assembly. The mass of this integration structure is included in the propulsion subsystem mass estimate, as has been done for the electronic equipment modules.

A contingency mass of 58.5 kg (127 pounds) is included in the hardware mass estimate for STORMSAT. This will accommodate hardware mass

TABLE 3-4. STORMSAT SUBSYSTEM AND COMPONENT MASS

Subsystem/Component	Quantity	Mass		Reference
		kg	lb	
MISSION SENSOR AND INTEGRATION		270.0	594	
AASIR	1	104.5	230	SBRC
AASIR electronics	2	9.1	20	SBRC
AASIR bearing assembly	1	55.4	122	Hughes
AASIR bearing controller	2	4.5	10	Hughes
MASR	1	68.2	150	Hughes
MASR gimbal	1	19.1	42	Hughes
MASR gimbal controller	4	9.1	20	Hughes
COMMUNICATIONS AND DATA HANDLING		137.7	303	
AASIR data processor	2	15.5	34	Hughes
Mission data transmitter	2	6.4	14	GMS
Mission data antenna	1	2.3	5	Hughes
Remote interface units	6	13.6	30	S-714-11
C & DH module	1	90.9	200	S-700-15
C & DH omni antennas	2	2.3	5	Hughes
C & DH directive antenna	1	2.3	5	Hughes
Coaxial cables	1 set	4.5	10	Hughes
ATTITUDE CONTROL MODULE	1	181.8	400	S-700-17
ELECTRICAL POWER		270.4	595	
Power subsystem module	1	216.3	476	S-700-16
FRUSA	1	38.6	85	Calculated
Deployment mechanism	1	6.8	15	Hughes
FRUSA drive mechanism	1	6.8	15	Hughes
Drive controller	2	1.8	4	Hughes
PROPULSION		68.2	150	
Tank	1	20.5	45	Hughes
Valves and thrusters	16	6.8	15	NASA Std
Structure and integration	1	40.9	90	Hughes
STRUCTURE		255.9	563	
Payload truss	1	13.6	30	Hughes
Gimbal support	1	9.1	20	Hughes
AASIR bearing support	1	18.2	40	Hughes
FRUSA support	1	9.1	20	Hughes
Payload electronic compartments	2	72.7	160	Hughes
Electronic compartment support	2	4.5	10	Hughes
MMS structure	1	76.4	168	S-700-13
Transition adapter	2	52.3	115	S-700-13

Table 3-4 (continued)

Subsystem/Component	Quantity	Mass kg	Mass lb	Reference
THERMAL CONTROL*		31.8	70	
Exterior payload blanket	1	9.1	20	Hughes
AASIR blanket	1	2.3	5	Hughes
Propellant tank blanket	1	2.3	5	Hughes
Structural insulation	1 set	9.1	20	Hughes
Heaters	1 set	4.5	10	Hughes
Miscellaneous	1 set	4.5	10	Hughes
WIRING HARNESSES		67.3	148	
MMS wiring	1 set	44.5	98	S-700-13
Mission unique wiring	1 set	22.7	50	Hughes
MMS/IUS ADAPTER	1	77.3	170	Hughes

*Module thermal control mass is included in module mass estimate.

changes up to that amount without requiring a resizing of the propulsion subsystem. It is suggested that the propulsion subsystem be resized to match either the launch vehicle capability or the allocated mass for STORMSAT. This will allow orderly development of subsystem equipment and mission growth without impacting the propulsion subsystem.

3.3.5 Spacecraft Characteristics Summary

A summary of preliminary STORMSAT characteristics is given in Table 3-5 for the configuration defined in this report. The reader is cautioned that AASIR data acquisition characteristics are currently under review. Changes in that area will affect overall data rates, impacting spacecraft power requirements and mass.

3.4 SUBSYSTEM DESIGN APPROACH

A concerted effort has been made in this study to utilize the MMS and its subsystems without change. This has led to spacecraft system design approaches which minimize the impact of one subsystem or another. Mission requirements which exceed the capability of the MMS modules are handled by the specification of mission-unique equipment to be installed in the mission equipment module. In the case of the attitude control subsystem (ACS), detail performance specifications for mission critical components such as the inertial reference unit and the star sensors are not currently available. Performance requirements for these components have been established to perform the STORMSAT mission and are included in Section 5. A mission-unique propulsion module is defined for STORMSAT. Conceptual designs defined for the MMS program do not appear compatible for synchronous orbit missions using the IUS if orbit inclination control is required. A conceptual design

TABLE 3-5. SPACECRAFT CHARACTERISTICS SUMMARY

AASIR			
Functions	Visible and IR imaging radiometry Temperature and humidity sounding		
Frame size	20 by 20°, 4 by 4°, 1.2 by 1.2°		
Frame time (full earth)	~24 minutes with retrace		
Frame positioning	Anywhere within earth disk		
Spatial resolution	21 μrad visible 125 μrad IR imaging 375 μrad sounding		
Spectral band coverage	0.55 → 1.1 μm visible 3.72 → 14.96 μm IR		
NER (full earth)	0.0023 to 3.2 ergs/sec cm^2 ster cm^1		
Encoding	8 bits per sample visible, 10 bits IR		
MASR			
Function	Microwave atmospheric sounding radiometry		
Frame size	1000 by 1000 km to full earth		
Frame times	30 minutes for 1000 by 1000 km frame and 6 hours for full earth		
Frequencies	118 and 183 GHz		
Channels	16		
Encoding	10 bits per sample		
ATTITUDE STABILIZATION AND CONTROL			
Functions	Pointing and stabilization of spacecraft and sensors		
	Roll	Pitch	Yaw
Absolute pointing, μrad	183	182	181
20 minute stability, μrad	10.2	10.5	10.4
8 second stability, μrad	2.1	3.4	0.7
Settling time	~1 minute		
PROPULSION			
Functions	Initial station acquisition Stationkeeping and repositioning ACS momentum control		
Velocity capability	284 m/sec (932 fps)		
Momentum control	21,400 N-m/sec (15,750 ft-lb-sec)		
TELECOMMUNICATIONS			
Functions	Spacecraft command and control Spacecraft status telemetry Ranging Mission data transmission		
FREQUENCIES			
Command	2.0 to 2.1 GHz (STDN compatible)		
Status telemetry	2.2 to 2.3 GHz (STDN compatible)		
Ranging	STDN compatible		
Mission data	~1.7 GHz (metsat allocation)		

Table 3-5 (continued)

DATA RATES	
Command	0.125, 1 or 2 kbps
Status telemetry	1, 2, 4, 8, 16, 32, or 64 kbps
Mission data	~11 Mbps maximum
TRANSMIT POWER (RF)	
Status telemetry	1.75, 3.5, or 7.1 W
Mission data	30 W
ELECTRICAL POWER	
Functions	Provide electrical power to spacecraft equipment in operational configuration
Solar electric power	1257 W
Battery power	876 W
Battery capacity	100 A-hr
STRUCTURE	
Functions	Support spacecraft in launch environment. Provide stable mounting base for spacecraft systems in orbit of environment
Bending moment at spacecraft adapter	0.226 MN /m (2×10^6 in-lb)
Vertical shear at spacecraft adapter	0.143 MN (32,000 lb)
Stability, ACS module to AASIR	4 μrad in 20 minutes
THERMAL CONTROL	
Functions	Constrain equipment temperature
TEMPERATURE LIMITS AT MOUNTING INTERFACE	
AASIR	0 to 35°C (32 to 95°F)
MASR	0 to 35°C (32 to 95°F)
Electronics	0 to 40°C (32 to 104°F)
Propulsion	5 to 35°C (41 to 95°F)
GENERAL CHARACTERISTICS	
Lifetime	5 years maximum
Overall length	6.858 m (270 in.) (including adapter)
Overall mass	1623 kg (3570 lb) (including adapter)

approach for a propulsion module for synchronous orbit missions is included in this study and is described in Section 8.

3.4.1 Mission Sensor Integration

Integration of STORMSAT mission sensors presents significant spacecraft design constraints because of the sensors' size and field of view requirements, their movement, and its potential impact on spacecraft precision pointing, and the need to protect them from adverse solar radiation heating effects. Another consideration is that the AASIR and the MASR are to be operated independently. Thus, it is necessary to assure that operation of one sensor does not produce adverse effects on the other or on other spacecraft subsystems.

AASIR dimensions are 1650 by 1400 by 712 mm (65 by 55 by 28 inches). It requires an onobstructed view of full earth plus a few degrees over travel so that the AASIR detectors can be calibrated viewing cold space. A second requirement is that the AASIR radiation cooler have a clear field of view of the polar hemisphere in the direction away from the sun. It is thus necessary to invert the spacecraft at the vernal and autumnal equinoxes.

The AASIR is suspended in the spacecraft so that it can be rotated in an east-west direction relative to earth. The AASIR scan mirror assembly provides the north-south degree of freedom for the AASIR line of sight. The AASIR and its positioner have sufficient moment of inertia that momentum compensation is required to avoid excessive disturbance to the spacecraft ACS with correspondingly long settling times for major steps. Momentum compensation is planned to be accomplished by producing torque impulse doublets with the MACS reaction wheels. The torque impulse doublets may be adjusted in orbit to achieve more perfect compensation for the AASIR stepping motion.

The AASIR and its structural support must be protected from the effects of solar radiation heating. As this heating is applied around the spacecraft once per day, varying temperature gradients across the structure can cause motion of the AASIR mount relative to the MACS reference. It will be necessary to insulate the spacecraft structure and possibly to provide sensors and heaters to nullify the effects of diurnal heating of the sun. Graphite fiber reinforced plastic structures may be attractive for the MMS to alleviate the effects of temperature gradients. The AASIR itself must also be protected from the spacecraft and space environments. This is accomplished by insulation blankets around the AASIR and by constraining the AASIR suspension to be at the same bulk temperature as its mounting pads.

The MASR has the same type of insulation problems as the AASIR except that it presently does not require a field of view for a radiation cooler. Its dimensions are 3180 by 2440 by 2030 mm (125 by 96 by 80 inches). It is mounted on a gimbal to provide scan in both the east-west and north-south directions. Its moment of inertia is much larger than that of the AASIR and momentum compensation is required to avoid excessive attitude control

disturbance. Thermal protection will undoubtedly be required for the radiometer antenna structure and the receiver electronics. It is suggested that insulation blankets be placed over the back of the reflector and around the feed support structure. Insulation blankets will be constrained, as required, to avoid any interaction with spacecraft attitude control. The compartment housing the receiver will require both insulation blankets and thermal radiators. The gimbal also requires similar thermal control treatment.

3.4.2 Attitude Determination and Control

Spacecraft attitude control is accomplished by the equipment located in the MMS attitude control subsystem (MACS) module operating in conjunction with the spacecraft computer located in the communications and data handling (C&DH) module. Attitude control sensors are an inertial reference unit and fixed star trackers. The inertial reference unit provides the direct short term attitude reference. Star sighting provides information to the system to correct long term gyro drift. Geocentric spacecraft pointing is accomplished by slewing the pitch gyro so that actual star crossing times are correlated with predicted star crossing times.

The settling time for the ACS is of the order of a minute. It would be a severe loss in scan efficiency to require the system to settle between each movement of a payload sensor. Sensor disturbance effects can be reduced to acceptable levels by means of momentum compensation, or sensor pointing can be adjusted by means of spacecraft attitude control error signals. Preliminary investigation indicates that momentum compensation devices driven in conjunction with mission payload position actuators will cancel payload disturbance torque impulse sufficiently well to avoid the need for slaving payload sensors to the inertial reference unit error signals. A doublet of torque impulses is transmitted to the reaction wheel controller to produce an equal and opposite disturbance to the spacecraft to that caused by sensor motion. The reaction wheels in the ACS module are capable of correcting the disturbance caused by AASIR and MASR scanning.

It is also necessary to provide a stable structure between the attitude control module and the mission payload sensors. Permissible thermal-structural distortion is of the order of 4 μrad in 20 minutes. Allowable differential temperature drift across the spacecraft structure cannot exceed approximately 0.1°C (0.2°F) within any 20 minute period for the current aluminum MMS spacecraft structure. It is planned to provide this degree of structural temperature control in the MMS and mission-unique structural elements by means of temperature controlled heaters and insulation blankets. It is noted that information from both star trackers is required to meet STORMSAT mission requirements.

3.4.3 Communications and Data Handling

STORMSAT telemetry, tracking, and command may be accomplished by the communications and data handling (C&DH) subsystem of the MMS except for mission high data rate sensor telemetry. Mission wideband data

will be telemetered by a mission-unique high rate data transmission (HRDT) subsystem installed in the mission module.

Spacecraft communication frequencies are Spaceflight Tracking and Data Network (STDN) compatible, commands in the 2.0 to 2.1 GHz band, and telemetry in the 2.2 to 2.3 GHz band. Mission data are currently planned to be telemetered in the band for meteorological satellite to ground station at 1.7 GHz. It is noted that this band is being phased out, and in view of its limited bandwidth, consideration should be given to other space-to-ground frequency allocations.

Mission data telemetry is designed to be compatible with the NOAA 7 meter (24 foot) terminal currently utilized for stretched VISSR data from the GOES system. This station requires a spacecraft EIRP of approximately 33 dBW to receive data at a rate of approximately 7 Mbps. It may be achieved with a fixed antenna and a transmitter power of 30 watts. Mission data could also be telemetered in the 2.2 to 2.3 GHz band using the NASA standard S band transponder modified to accept wideband data. Maximum power for this transponder is 7 watts. A reduction in receive system noise temperature from 300 K to 150 K and the use of a 12 meter (40 foot) antenna is required for this approach. If AASIR options currently under consideration to increase the imaging data rate by a factor of 4 are accepted, then higher frequency space-to-ground telemetry bands should be considered for the STORMSAT mission.

Omnidirectional antennas are installed fore and aft on the spacecraft. The forward mounted omni antenna is exposed when the spacecraft is mated to the IUS. The aft mounted omni antenna is installed with the spacecraft/IUS adapter and is not exposed until after separation from the IUS and adapter. STORMSAT is nominally passive during transfer orbit and until separation from the IUS. It will be possible to receive spacecraft telemetry and ground commands during this period by properly orienting the IUS so that communications may be established via the spacecraft forward omni antenna.

Mission growth to an operational spacecraft configuration may require the addition of UHF communication links for the interrogation of remote in situ sensors. This will also require the addition of an S band receiver designed to operate in conjunction with the UHF downlink. The UHF uplink return could utilize the mission data transmitter during periods when data is not transmitted. These transponders may also be used for the distribution of meteorological information in the same manner as for the GOES system.

3.4.4 Electrical Power

STORMSAT electrical power is provided by a sun oriented solar cell array. This power is roughly regulated and stored in batteries by the power subsystem module of the MMS. Spacecraft power requirements have been estimated for mission-unique equipment and added to the specified power budgets for the MMS. A flexible roll-up solar array (FRUSA) is used for this configuration of STORMSAT. It is a developed and flight proven design which can be applied to MMS missions at minimum cost. It also is more

easily supported on the spacecraft during the launch and transfer orbit phase of flights than rigid folding solar cell arrays. Transfer orbit power requirements can be met by partially extending the FRUSA. It is then retracted prior to apogee injection by the IUS. After deployment of the boom it is extended to its full length to meet operational orbit power requirements.

Two 50 A-hr batteries have been selected for the STORMSAT mission. They will provide full power demand during solar eclipses so that all spacecraft subsystems and sensors may be operated at that time if required. These batteries are larger than required for this mission but are the next available capacity offered by the MMS power subsystem module. If mission power budgets are reduced as firm data accumulate, or it is decided not to operate mission sensors or data links during an eclipse, three 20 A-hour batteries are sufficient.

The solar cell array is controlled by a positioner nominally driven by clock signals of the spacecraft computer. It is planned to inhibit movement of the solar cell array while mission sensors are active. It is possible to inhibit its movement for periods of 1 or 2 hours without serious loss in available power. This will be critical only as the solar cells are degraded to their end of life design values. As the spacecraft is inverted every 6 months, the positioner will need to operate in both clockwise and counterclockwise directions.

3.4.5 Propulsion

Except for orbit inclination control, mission propulsion requirements could be handled by the small propulsion module. Data reduction is simplified if the spacecraft is constrained to an orbit inclination less than 0.025°. It is adapted for this spacecraft design and accordingly requires either the large propulsion module or a mission-unique propulsion module. A mission-unique propulsion module has been configured for this length of STORMSAT to minimize the overall length of the STORMSAT/IUS combination in the orbiter payload bay.

The propulsion equipment is mounted on a plate which is mated to the aft end of the MMS as an integrated subassembly. One tank and four clusters of four thrusters, together with plumbing, valves, and fittings are provided. The tank is 22 inches in diameter and occupies the triangular space between the modules of the MMS.

The spacecraft must be yawed 90° until the longitudinal axis is normal to the orbit plane for orbit inclination control maneuvers. This maneuver must be performed approximately every 10 days to maintain the orbit within the specified 0.025° allowable inclination. Stationkeeping maneuvers can be performed at the same time by inclining the vehicle so that an easterly or westerly impulse is delivered. It is estimated that these maneuvers, including time for spacecraft reorientation and ACS reacquisition, will require approximately 1 hour.

3.4.6 Structure

The spacecraft structure consists of the module support structure, the transition adapter, the mission-unique equipment support structure, and an MMS/IUS adapter. The module support structure is a triangular frame structure to which the MMS modules are attached and which also provides the load path between the MMS/IUS adapter and the transition adapter. The mission-unique equipment is supported by the transition adapter. Propulsion equipment is mounted to a structural plate attached to the aft end of the module support structure. Explosive separation nuts are used to secure the module support structure to the MMS/IUS adapter.

Critical design loads for spacecraft structure arise from orbiter landing load factors. These loads are currently estimated at +10, -8 g in pitch, ±4 g in yaw, and ±4.5 g longitudinally. Landing loads would be experienced only if the launch mission were aborted prior to separation of the IUS/STORMSAT from the orbiter. The IUS/spacecraft adapter is designed to a bending moment about the pitch axis of 3.4 MN/m (3×10^6 in-lb) with a combined vertical shear load of 0.16 MN (36,000 lb). These preliminary load estimates need to be upgraded by the results of dynamic loads analysis using Orbiter, IUS, and spacecraft dynamic models during the development phase.

The structure must also be stable with respect to orbital loads and thermal-structural distortions must be consistent with mission sensor pointing accuracy and drift requirements. A preliminary assessment of thermal distortion characteristics of the aluminum module support and mission sensor support structures leads to a requirement to restrict relative temperature changes across to the structure to less than 0.1°C (0.2°F) in any 20 minute period. This will require insulation of the structure and may necessitate active temperature control by means of heaters and temperature control sensors.

3.4.7 Thermal Control

Each subsystem of the MMS is designed to be thermally independent. This applies to payload sensors as well as electronic equipment. AASIR thermal control consists of isolating the instrument from the spacecraft and external space environment as much as possible and providing radiators for internally dissipated heat. The entire instrument assembly is blanketed except for the entrance aperture and the radiation cooler aperture; a sun shade surrounds the entrance aperture to minimize the amount of sunlight entering the telescope. The MASR consists of an antenna reflector assembly and an electronics box located at the focus of the reflector. Insulation blankets may be used to cover the backside of the reflector and supporting structure. The electronic equipment box will require the use of radiators and insulation blankets. Thermal control for this item is similar to that for the MMS equipment modules. Instrument suspension and positioning equipment require protection similar to that provided for the meteorological sensors, and payload electronic equipment will be thermally controlled by means of insulation blankets, louvers, and radiators, as is the case for MMS equipment modules.

Structure thermal control requires close control for the STORMSAT mission. Deviations in temperature gradients across the spacecraft structure are required to be less than 0.1°C (0.2°F) in any 20 minute period. Insulation of individual structural members is clearly required. Heat leaks into the structure from spacecraft equipment or the external environment must be minimized. As noted for the structure subsystem, alternative materials to aluminum should be considered for this mission to minimize structure temperature control requirements.

3.5 LAUNCH VEHICLE INTERFACE

The spacecraft is supported as a cantilever beam by the IUS. Eight spacecraft mounting holes are provided by the IUS structural interface as a bolt hole circle 2839 mm (111.77 inches) in diameter. An adapter provides the load path between the IUS structural interface and the MMS structural interface. Spacecraft separation is effected at the MMS/adapter interface by means of three electro-explosive nut release devices. Full redundancy is achieved by the use of releasable nuts on both sides of the interface.

Spacecraft interface loads are developed due to the Space Shuttle flight operations during liftoff and boost and also due to orbiter atmospheric entry and landing maneuvers in the event of an aborted launch attempt. Orbiter landing loads appear to be the most severe. These loads arise because of spacecraft, IUS, and orbiter dynamic interaction. A detailed dynamic analysis is required to establish final design loads; preliminary loads of ±4.5 g longitudinally, ±4.0 g laterally and +10, -8 g vertically have been specified for IUS spacecraft payloads.

The IUS/spacecraft interface is designed to minimize heat transfer. An insulation blanket is required across the cavity aperture to minimize radiative heat transfer, and conductive heat transfer must also be controlled at each attachment point by requiring a thermal resistance of at least 11°C (20°F) per watt. Heat transfer between the orbiter and the spacecraft is a potential problem area: preliminary analysis indicates that spacecraft temperatures may approach or exceed 38°C (100°F). The principal area of concern is the deleterious effect of these temperature levels on spacecraft batteries. This is an area requiring detailed investigation.

Critical flight safety commands may be sent to the spacecraft by means of hardwire transmission lines while it is in the orbiter payload bay. The commands are routed via the IUS and its support equipment in the orbiter. Telemetry of spacecraft status is transmitted to the orbiter via the IUS and its support equipment. It may also be transmitted to ground by the orbiter S band communication links. After separation from the orbiter, the spacecraft telemetry goes directly to ground by the spacecraft S band communication links. This may necessitate reorientation of the IUS to provide a favorable aspect for the exposed forward omnidirectional antenna.

The IUS provides electrical power to the spacecraft while it is in the orbiter payload bay and while it remains attached to the IUS during orbital transfer maneuvers. A total energy transfer of 5.2 kW-hr is required of

the IUS, with peak power demand of 1 kW. The FRUSA on the spacecraft may be extended during coast phases of the orbit transfer maneuvers and additional power generated for spacecraft loads and battery charging. The FRUSA would be retracted during the boost phases of the orbital transfer maneuvers.

Protection of optical and thermal control surfaces is required to avoid contamination from the orbiter payload compartment. Protection is also required for ground handling. A preliminary approach to this problem is to cover these surfaces with protective plastic covers and bags. It will, of course, be necessary to remove these protective devices after the IUS and spacecraft have been removed from the Orbiter payload compartment.

4. MISSION SENSOR INTEGRATION

The AASIR and MASR were the primary mission sensors considered in this study. Both meteorological sensors require two-axis scan capability. The AASIR is equipped with an oscillating mirror that provides north-south scan; spacecraft equipment must perform the east-west scan function. Both scan functions are performed by spacecraft equipment for the MASR. Space environment monitors (SEM) and various data collection and data relay radio services may also be required for follow-on missions. The SEM equipment may also require scanning mechanisms. No attempt has been made to integrate the SEM equipment into STORMSAT because of lack of detail definition.

Integration of the meteorological sensors into STORMSAT imposes special performance requirements on nearly all other spacecraft subsystems. The requirements identified for a specific subsystem are treated in the section of the report dealing with that subsystem. This section deals with the mission-unique equipment items required to install and operate the mission sensors and the interface requirements with the equipment of other subsystems.

4.1 AASIR INTEGRATION

Physical characteristics of the AASIR have changed recently to reflect changes in the AASIR optical design. The current AASIR mounting diameter, 610 mm (24 inches), is immediately below the mounting ring. Overall length is 1651 mm (65 inches). Allocated AASIR mass is (114 kg (250 pounds) including electronics. It is anticipated that AASIR characteristics will continue to change as the design effort proceeds. For example, consideration is being given to higher resolution visual imaging detectors and special imaging modes uncoupled from sounding that will provide visible images in approximately one-fourth the time required for the current AASIR design.

4.1.1 AASIR Positioner

The AASIR is mounted in a bearing assembly or suspension which will allow east-west or pitch pointing of its line of sight. A total travel of ± 10° from nadir is required. The positioner moves the AASIR line of sight either through a short step of 375 μrad or a long step of 4125 μrad with step-to-step positioning accuracy of ± 2 μrad relative to a stable base reference. Ideally, the positioning step should be accomplished during the AASIR scan mirror turnaround time, approximately 0.52 second. Longer times, if required to

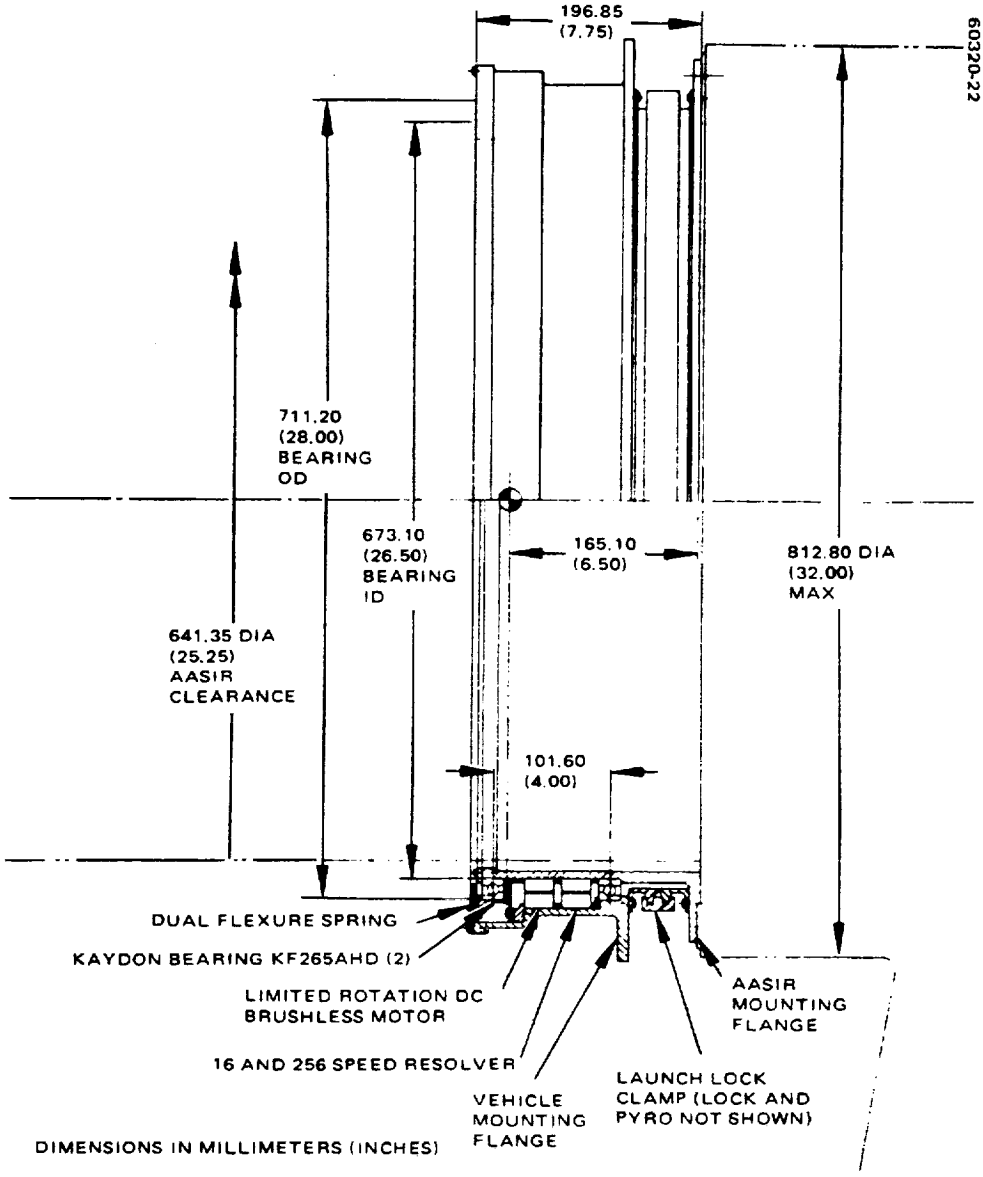

FIGURE 4-1. AASIR CENTRAL BEARING SUSPENSION AND POSITIONER CONCEPTUAL DESIGN

minimize spacecraft altitude control disturbance will decrease scan efficiency and should progress from a single turnaround to a double turnaround, etc. Allowable stepping time will therefore follow the progression 0.52 second, 1.81 seconds, 3.10 seconds, etc.

Stepping of the AASIR will produce angular momentum impulses on the spacecraft unless some means is established to accomplish angular momentum compensation. An uncompensated short step will result in a spacecraft pitch disturbance less than 1 μrad and is within the error budget. A large step would cause a reaction in pitch of approximately 10 μrad and is outside the allowable error budget. The spacecraft attitude control subsystem would counteract this disturbance but the settling time is of the order of 1 minute and this would degrade scan efficiency by suspending AASIR data acquisition while the system settles down. Compensation of this angular momentum disturbance will be accomplished by means of torque impulse doublet commands to the pitch reaction wheel and others if required.

Alignment of the AASIR body must also be stable about the roll axis to an accuracy of ±2 μrad for a short or long step relative to a stable base reference. This primarily affects the runout precision requirements of the bearings in the AASIR positioner.

4.1.1.1 Design Approach

The AASIR positioner required for east-west motion of the AASIR represents a new development item for STORMSAT. The required performance is comparable to that being achieved with precision rate and position tables and is considered to be within the state of the art. However, to achieve such performance under the weight constraints and environmental exposures of a spacecraft presents some very challenging problems. The principal elements of the AASIR positioner are the bearing assembly or suspension which provides for east-west rotation, the drive mechanism, and the angle resolver to provide precise control of AASIR pointing. The suspension must have stable mechanical properties over a reasonable range of temperatures and temperature gradients. The bearing must have a low and consistent stiction level under these same conditions. Furthermore, a method must be found to carry the dynamic loads of the AASIR through the boost phase without damaging the suspension.

4.1.1.2 AASIR Suspension

The most direct AASIR suspension design approach is to support the AASIR in a bearing assembly large enough to accommodate the AASIR at its mounting ring near its center of mass. This approach provides for east-west rotation of the AASIR about its centerline. A rotation step about this axis will induce the minimum reaction on the spacecraft. A central bearing support for the AASIR has been configured as shown in Figure 4-1. It requires the use of 660 mm (~26 inches), very slim type ball bearings. These bearings require a preload of approximately 900 N (200 pounds) to avoid gall skidding. Thin diaphragm springs, machined from steel plate, provide a very consistent axial preload over the temperature range while being very stiff in the radial direction. This axial compensation system eliminates radial free play and provides structural stiffness that is adequate for pointing stability requirements. The two bearings are spaced far enough apart to satisfy the runout error limit requirement.

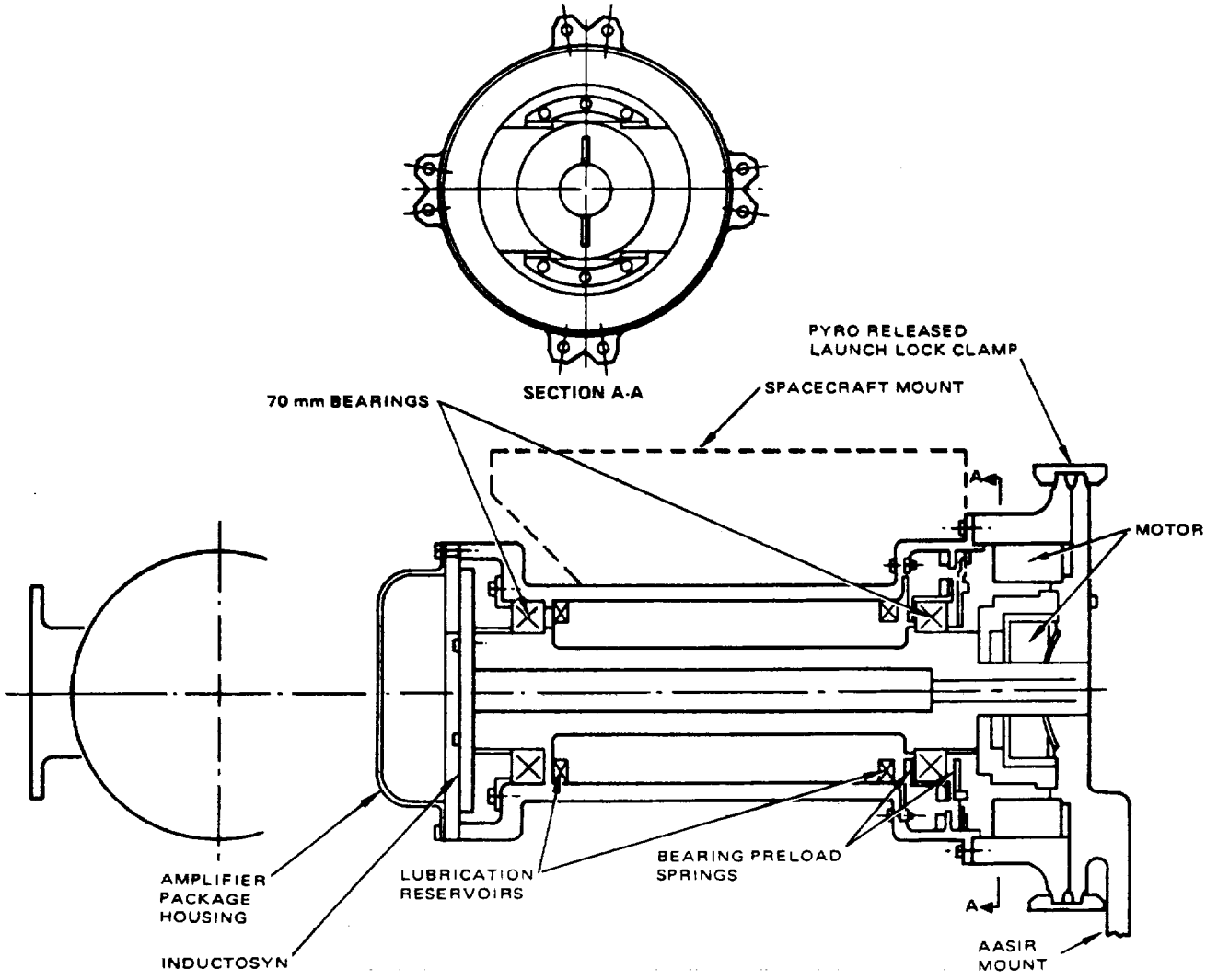

FIGURE 4-2. ALTERNATIVE AASIR OFFSET BEARING SUSPENSION AND POSITIONER CONCEPTUAL DESIGN

The bearings are lubricated by an RF sputtered application of dry molybdenum disulfide (MoS_2). This application process provides a uniform thin film of lubricant without the use of a binder. It adheres tightly to the balls and races and does not upset the internal geometry of the bearing. The resultant bearing is extremely smooth running with excellent wear life capabilities, and is compatible in a space environment for close proximity to optical surfaces. The ball separator in each bearing is segmented to eliminate force interactions between various balls around the bearing. The separator is fabricated from a sputtered bronze material that provides for a minute transfer of MoS_2 lubricant replenishment as the bearing operates. There is no sloughing off of particles that would cause debris buildup problems with this design approach. A launch lock clamp is provided to avoid bearing roughness due to launch levels that might affect overall pointing performance. This clamp provides a direct structural tie between the AASIR and the spacecraft and effectively removes the bearings from the main load path during launch. Based on extrapolation of test data from smaller bearings, bearing friction torque is estimated to be 0.7 N-m (0.5 ft-lb) for this AASIR bearing assembly design.

An alternative design approach that avoids the use of large diameter bearings is to suspend the AASIR on a bearing assembly located to the side of the AASIR. One point design that has been examined in some detail uses two 70 mm angular contact ball bearings located approximately 254 mm (10 inches) apart. Bearing friction for this design is estimated to be approximately 0.07 N-m (0.05 ft-lb), a significant difference from the 0.7 N-m of torque for the large bearing assembly. The moment of inertia of the AASIR about a pivot axis offset 406 mm (16 inches) from the AASIR centerline is 22 kg-m^2 (16 slug-ft^2). As this is approximately three times as great as the moment of inertia of the AASIR about its centerline, a larger component of angular momentum compensation is required. Estimated torque required to compensate large steps is 0.14 N-m (0.1 ft-lb). This is well within the capability of the reaction wheels in the ACS module. Figure 4-2 is a schematic of this alternative design.

4.1.1.3 Drive Mechanism

Direct drive torque motors have been considered for the AASIR positioner. The drive motor is required to produce a torque of 0.7 N-m (0.5 ft-lb) to achieve a static position error of 2.5 μrad. The high torque gain of 0.27 MN-m/rad (200,000 ft-lb/rad) required to reduce static errors to acceptable limits results in a servomechanism with a high frequency response because of the relatively low AASIR and positioner inertia. It is expected that it will be difficult to stabilize.

A piezoelectric driver provides a very stiff drive source that has positive lock capabilities to counter residual torques. One device, developed by J. H. Bruning of Bell Laboratories, Murray Hill, N. J., for lens alignment applications, consists of a piezoelectric ceramic sleeve with separate silver ring electrodes on the outer surface. The inside of the sleeve is carefully lapped so that there is a slight interference fit between the sleeve and the internal plug or shaft, holding the sleeve firmly in place. A flange is bonded to one end for support. When a negative voltage is applied between

one of the bands and an inner plug, that ceramic segment becomes slightly larger in diameter and elongates; its grip on the plug slackens and the segment expands. Driving circuitry excites the bands in pairs from one end of the device to the other, setting up a peristaltic wave that moves the plug relative to the sleeve.

A geared drive provides the high torque through the mechanical advantage of a gear train. Motor inertia adds to that of the AASIR and its bearing support, thereby reducing the high natural frequency of the servomechanism when operated at the same high torque gain. It is also easier to provide tachometric feedback around the motor with this approach, as motor velocities are increased by the gear ratio of the drive relative to the direct drive.

High gear ratio drives may be efficiently achieved by means of screw or worm drives. A micrometer screw with 1.57 turns/mm (40 turns/inch) mounted 406 mm (16 in) from the AASIR center of rotation provides a gear ratio of approximately 4000:1. The motor effective moment of inertia is equal to the product of the motor moment of inertia and the square of the gear ratio. For this case, with a small drive motor the effective moment of inertia is estimated to be 68 kg-m^2 (50 slug-ft^2). This compares to 7 kg-m^2 (5 slug-ft^2) for the case of the direct drive positioner. The frequency response of the servo will be reduced by a factor of 3.2, thereby alleviating structural mounting stiffness requirements. This type of actuator will require preload springs to minimize the effect of backlash.

Actuator lifetime may be a problem with this design. The AASIR is repositioned at an average rate of 1 deg/min while taking data, the screw accordingly turns 4000°, or 11 turns per minute. The retrace will nearly double this rate to approximately 20 turns per minute. If the AASIR is operated 2/3 of the time, the screw will be driven through 20×10^6 revolutions. This is an order of magnitude greater than the operating requirements for currently qualified space mechanisms, and a test program will be required to demonstrate the feasibility of achieving these functional requirements.

4.1.1.4 Angle Resolver

Knowledge of AASIR angular position is required to reorient the AASIR accurately so that adjacent imaging elements are aligned to an accuracy of 4.2 μrad. As the AASIR is alternately repositioned with a short step of 375 μrad and a long step of 4125 μrad, the system demands knowledge of AASIR angular position relative to the spacecraft to an accuracy of 2 μrad.

One technique for AASIR angle control is to employ a geared stepper or servo motor drive and calibrate the system. Steps of roughly 4 μrad are required to achieve the specified position accuracy. Accordingly, a short AASIR step of 375 μrad will require approximately 100 motor steps; a long step of 4125 μrad will require ~1100 motor steps. An encoded servo motor is required to achieve the AASIR long step in a reasonable time. Variations in mechanism linearity may be compensated by adjusting the specific number of steps for each position. The principal disadvantage of this approach is that it is partially open loop and variations in temperature and mechanism

wear may result in erroneous system calibration. A more positive approach is to employ an angle resolver mounted on the AASIR and to control the AASIR position by feedback control techniques.

Multipole resolvers or inductosyns are capable of measuring angles repeatedly to about 1 μrad with an absolute accuracy of 20 μrad. These devices require an electronic resolver to digital converter. The combination is required to have a resolution of ~1 μrad. System accuracy may possibly be improved by calibration so that AASIR steps could be made to the required accuracy. However, this is again an open loop technique subject to change in calibration.

The feasibility of using laser interferometric techniques in a precision angle resolver for space application was demonstrated in 1975 at the Space Sensors Laboratory, Electro-Optical Division of Hughes Aircraft Company. This laboratory demonstration was based on the approach suggested by J. W. Edgerton and K. L. Andres in an article in the Review of Scientific Instruments, Vol. 45, No. 2, dated February 1974. A HeNe laser was used in this development which had a demonstrated 5 year lifetime. The output of the device is a pair of electrical sine waves in quadrature so that the sense of direction may be detected. It is conservatively estimated that the absolute accuracy of this approach is 0.2 μrad. The demonstration was a laboratory setup and additional development is required to productize the equipment for the STORMSAT application. This approach offers sufficient accuracy to meet the AASIR positioner requirements. As it employs available technology, development could proceed in an orderly way for STORMSAT.

4.1.1.5 Servomechanism Analysis For Large Bearing Support With Direct Drive Torque Motor

Pointing control loop design is dominated by the need for reduction of bearing friction errors so that short-term stability requirements are met. The resulting high servo bandwidth introduces potential instabilities when spacecraft flexible interaction effects are considered. In addition, high noise transmission can cause significant pointing jitter and excessive motor power use unless the gimbal angle pickoff noise is adequately reduced. Preliminary servo design is based on the linear model shown in Figure 4-3. The dc torque gain constant is selected to maintain a standoff error of less than 2.5 μrad for friction torques of 0.68 N-m (0.5 ft-lb). Thus, torque gain, K_P, of 0.27 MN-m/rad (200,000 ft-lb/rad) is required. The lag-lead term with time constants τ_1 and τ_2 is included to implement a partial integral error shaping. The lead-lag-lag term implements derived rate shaping for stability. The nominal values for these time constants are selected to provide adequate stability margins and high frequency noise filtering.

Flexible interaction effects are included in the analysis based on the linear dynamics model shown in Figure 4-4. This model represents a greatly simplified version of the actual flexible coupling which will be present. Two dynamic modes are represented by the parameters $\sqrt{k_S/I_S}$ and $\sqrt{k_R/I_R}$, which are the natural frequencies of oscillation of AASIR bearing mount structure and the MASR mount structure, respectively, in radians per

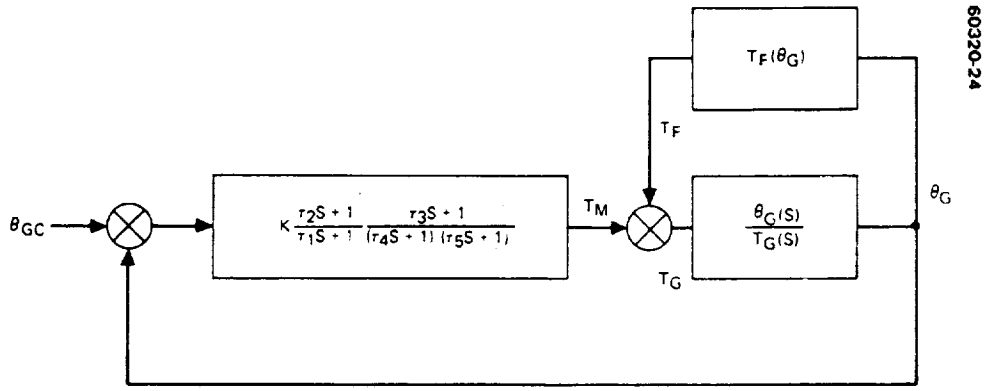

POINT DESIGN:
- K = 0.27 MN m/rad (200,000 ft lb/rad)
- τ_1 = 1.0 sec
- τ_2 = 0.2 sec
- τ_3 = 0.02 sec
- τ_4 = 0.0025 sec
- τ_5 = 0.002 sec

FIGURE 4-3. AASIR SERVO ANALYSIS MODEL

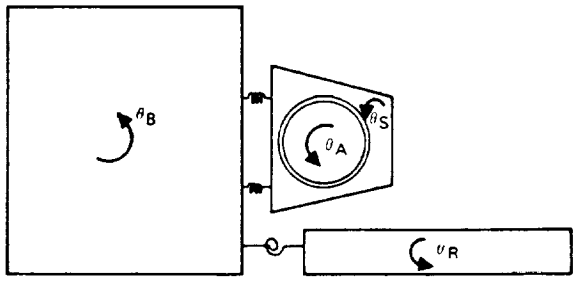

- θ_A = AASIR POINTING ANGLE
- θ_B = SPACECRAFT POINTING ANGLE
- θ_S = AASIR GIMBAL MOUNT POINTING ANGLE
- θ_R = RADIOMETER GIMBAL MOUNT POINTING ANGLE
- θ_G = θ_A θ_S = AASIR E W GIMBAL ANGLE

$$\frac{\theta_G(S)}{T_G(S)} = \frac{1}{I_A S^2}\,\frac{(I_S+I_A)\,I_B I_R S^4 + [(I_B+I_S+I_A)\,I_R k_S + (I_S+I_A)(I_B+I_R)\,k_R]\,S^2 + (I_B+I_R+I_S+I_A)\,k_R\,k_S}{I_B I_R I_S S^4 + [(I_B+I_S)\,I_R\,k_S + I_S(I_B+I_R)\,k_R]\,S^2 + (I_B+I_R+I_S)\,k_R\,k_S}$$

WHERE

I_A, I_B, I_S, I_R = MOMENTS OF INERTIA OF RESPECTIVE BODIES ABOUT PIVOT POINT
k_S, k_R = MODAL SPRING CONSTANT OF RESPECTIVE BODIES WRT SPACECRAFT

POINT DESIGN:

- I_A = 6.8 kg·m^2 (5.0 slug·ft^2)
- I_B = 2360 kg·m^2 (1750 slug ft^2)
- I_S = 13.5 kg·m^2 (10.0 slug·ft^2)
- I_R = 337 kg m^2 (250 slug ft^2)
- $k_S = (2\pi 40.0)^2\, I_S$
- $k_R = (2\pi 10.0)^2\, I_R$

FIGURE 4-4. FLEXIBLE INTERACTIONS MODEL

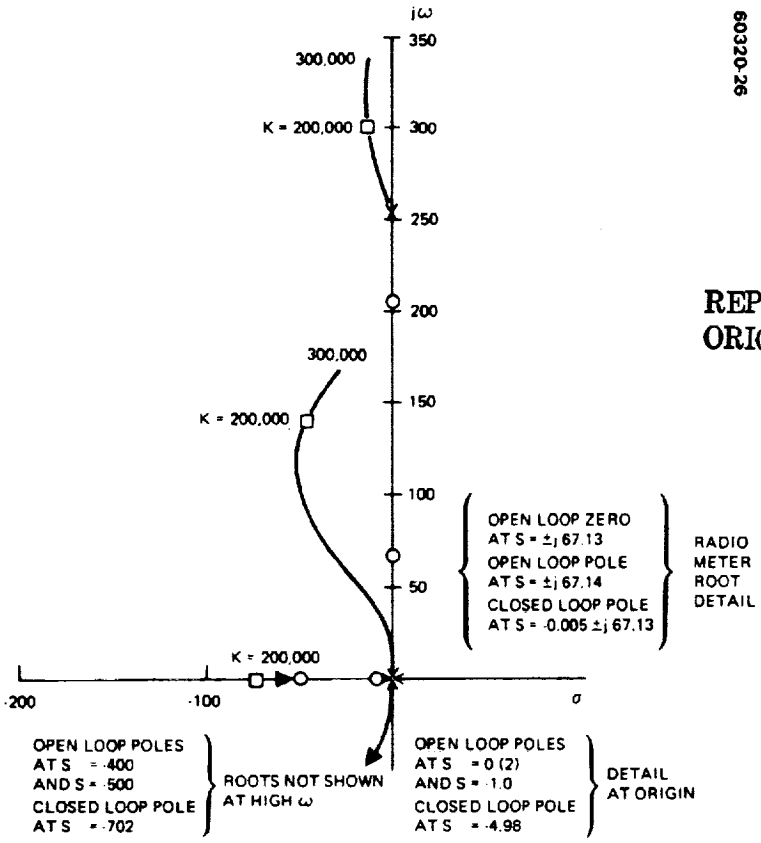

FIGURE 4-5. AASIR POSITION SERVOMECHANISM ROOT LOCUS ANALYSIS

second. Representative inertia properties for the four bodies are as given in Figure 4-4. Model spring constants were selected to give resonant frequencies of 40 Hz and 10 Hz for the ASSIR bearing mount and MASR attachment structure, respectively. Because of the relatively low attitude control loop bandwidth, the spacecraft control effects are negligible in the frequency range of interest and so have not been included.

A root locus plot illustrating closed loop stability is shown in Figure 4-5. The dominant closed loop poles indicate a bandwidth of 150 rad/sec (24 Hz) and a damping ratio of 0.31. The decay time constant, $1/\zeta\omega_N$, is equal to 0.02 second, so that transient effects are damped well within the minimum response interval of 0.5 second. The closed-loop poles associated with the AASIR mount have a frequency of 300 rad/sec (48 Hz) and damping ratio of 0.047. The decay time constant for these poles is 0.07 second, indicating that disturbances to this mode will also be well damped within the minimum response interval provided the excitation is low. The MASR modes are damped only slightly by the AASIR servo. It is anticipated that passive structural damping will be somewhat greater than the active damping due to the servo. Simulation results show that the radiometer structural resonance is only slightly excited by AASIR motion so that light damping is acceptable for these roots.

For the point design values given in Figure 4-3, gimbal measurement in the high frequency region is 0.65 MN-m/rad (480,000 ft-lb/rad), with first order filtering at 500 rad/sec (80 Hz). With 3.0 μrad sample noise uncorrelated at 2 kHz sample frequency, the rms motor torque due to pickoff noise will be 0.98 N-m $[(3.0 \times 10^{-6})(0.48 \times 10^{6})/\sqrt{(1000)/(2000)}(2) = 0.72$ ft-lb.] It is therefore desirable to maintain less than 3.0 μrad so that noise effects do not increase motor power beyond that required for friction torque.

A digital simulation based on the linear analysis models presented in Figures 4-3 and 4-4 was used to determine servo time response characteristics. A nonlinear bearing friction model proposed by Dahl (References 1 and 2) was used to simulate friction effects. This model is of the form

$$dT_F/d\theta_G = \tau[T \text{ sign } (\theta_G) - T_o]^2$$

where T_o is the steady state rolling friction equal to 0.5 ft-lb. The coefficient γ was assumed equal to 500,000 $(\text{ft-lb/rad})^{-1}$. With these values, the model closely approximates classic Coulomb friction for deflections greater than about 20 μrad.

Preliminary runs using a step command of 375 μrad indicated unsatisfactory response due to high excitation of structural resonances. Apart from these effects, the overshoot due to the lightly damped dominant servo poles produced friction reversal. This resulted in excessive errors at 0.5 second because of the time required for the integral shaping to "pull" the error back to null. These undesirable effects were removed by ramping the command at a rate of 1000 μrad/sec between the command limits. This resulted in negligible structural excitation and reduced overshoot to less than 5 μrad.

A typical settling transient is illustrated in Figure 4-6, where friction torque is plotted versus gimbal angle with time as a parameter. At 375 ms, motor torque is applied to reduce the AASIR rate to zero. This results in some excitation of the 40 Hz AASIR mount resonance which is damped by 500 ms. During the ramp interval, friction torque reaches the value of 0.7 N-m (0.5 ft-lb). This is reduced during settling by the gimbal rate reversals due to motion of the AASIR mount and reduction of the AASIR inertial rate. As may be seen, adequate response is obtained. Further improvements are anticipated using additional smoothing of the step command.

4.1.2 AASIR Data Conditioning and Timing Interface

AASIR data are categorized into visible and infrared imaging, atmospheric sounding, and AASIR status. Equiangle sampling of imaging and sounding channels is required to achieve efficient data transmission to the ground and to minimize data processing requirements in the ground system. Timing signals are required to be generated by the AASIR and transmitted to the AASIR data multiplexer for each equiangle data sample required. As the AASIR scan mirror is mounted on a spring restrained pivot suspension, the timing signals will not be uniform and should be generated as the scan mirror crosses each required data point.

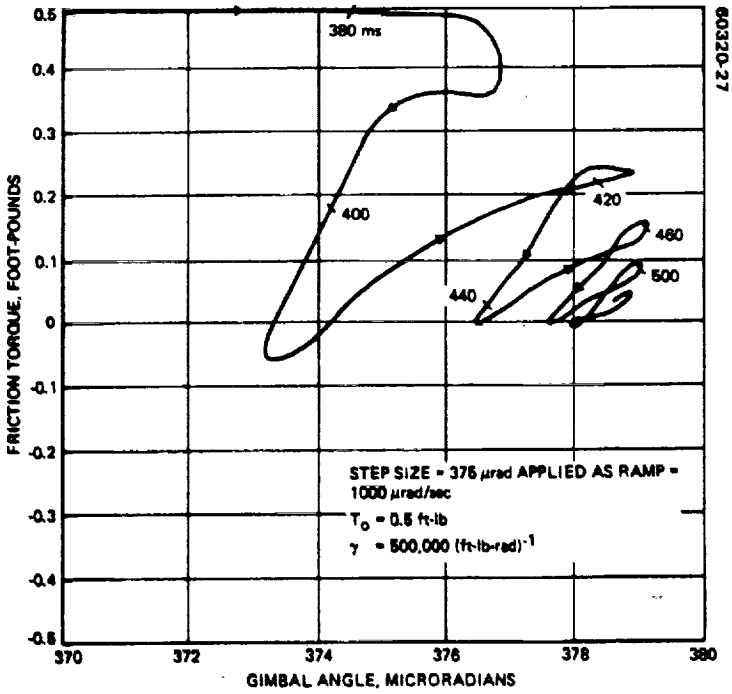

FIGURE 4-6. AASIR STEP SETTLING TRANSIENT

Data are sampled twice per IFOV for all functions. Visible imaging data are sampled each 10.4 μrad, infrared imaging data each 62.5 μrad, and infrared atmospheric sounding channels each 187.5 μrad. As peak data rate occurs when all channels must be sampled during one interval, a data buffer storage may be used to transmit data at a more uniform rate. Visible channels are sampled at 8 bit accuracy and all infrared channels are sampled with 10 bit accuracy. Table 4-1 summarizes this AASIR data channel characteristics.

TABLE 4-1. AASIR SENSOR CHANNEL CHARACTERIZATION

Channels	Number of Detectors	Sampling Rate	IFOV	PCM Encoding Level Required, bits
Visible imagery	15	2/IFOV	(21 μrad)^2	8
IR imagery	3	2/IFOV	(125 μrad)^2	10
Sounding	12	2/IFOV	(375 μrad)^2	10

4.1.2.1 AASIR Data Rate

The AASIR scan pattern is a resonant sinusoidal with a period of 1.72 seconds whose functional form is given by

$$\theta(t) = A \sin\left(\frac{2\pi}{2.58}\right) \cdot t \qquad (1)$$

Scan efficiency is specified at 60 percent for the 20° frame (including an overscan of 0.573° to accommodate AASIR detector spacing). The amplitude of the AASIR line of sight is 0.222 radian for the assumed sinusoidal scan pattern. Scan rate is given by the relation:

$$\dot{\theta} = \left(\frac{2\pi A}{2.58}\right) \cos\left[\frac{2\pi}{2.58}\ t\right]$$

At the frame edge, the scan rate is 0.477 rad/sec and at frame center, the scan rate is 0.540 rad/sec. The bit rate, R, for a given function is then given by

$$R = \frac{(\dot{\theta})\ (\text{encoding level})\ (\text{No. of detectors})\ (\text{sampling rate})}{(\text{IFOV})}$$

The maximum visible image data rate in the whole earth frame coverage mode is given by the following:

$$R_{max} = \frac{(0.540)\ (8)\ (15)\ (2)}{21 \times 10^{-6}\ \text{rad}} = 6.17 \times 10^{6}\ \text{bps}$$

with similar calculations for the remaining data channels. The maximum instantaneous AASIR sensor data rage is approximately 7 Mbps for global coverage, with progressively lower rates for smaller instrument frame sizes. AASIR data rates are itemized in Table 4-2.

TABLE 4-2. AASIR SENSOR CHANNEL BIT RATES GENERATION SUMMARY

Channels	Mbps		
	20 by 20° Frame	4 by 4° Frame	1.2 by 1.2° Frame
Visible	$3.63 \leq B_v \leq 6.17$	$0.808 \leq B_v \leq 1.37$	$0.311 \leq B_v \leq 0.529$
IR	$0.152 \leq B_i \leq 0.259$	$0.0339 \leq B_i \leq 0.0557$	$0.0131 \leq B_i \leq 0.0222$
Sounding	$0.305 \leq B_s \leq 0.518$	$0.0678 \leq B_s \leq 0.115$	$0.261 \leq B_s \leq 0.0444$
AASIR output	$4.09 \leq B_t \leq 6.95$	$0.910 \leq B_t \leq 1.55$	$0.350 \leq B_t \leq 0.596$

No ASSIR sensor data conditioning such as presample filtering or integrate-and-dump processing will be performed within the instrument itself. The only exception to this concept will be provisions for bandlimiting and buffering any of the imaging and sounding channels within the instrument so that the system specifications on modulation transfer function (MTF) and signal-to-noise ratio (SNR) can be met with downstream signal processing outside the AASIR instrument.

In addition to these analog channel outputs, the AASIR signal processor must be supplied with AASIR scan angle data of adequate resolution and bandwidth to provide multiplexer timing information. The AASIR sensor data is generated on an equal-scan angle basis, not on an equal-time interval basis. A 16-bit AASIR angle encoding signal will offer a LOS angle identification tag of ~100 μr resolution for subsequent fixed data rate reformatting. Presumably, the scan encoder angle versus time data is of interest to the AASIR data user, and should also be transmitted to ground. Line scan identification information must also be supplied by the AASIR to its signal processor. The physical location of the AASIR signal processing and transmission elements is shown in Figure 4-7.

4.1.3 AASIR Status Telemetry Data Characteristics

A preliminary AASIR telemetry function list is presented in Table 4-3. Clearly, these telemetry functions are all slowly varying parameters, and will be satisfactorily sampled by telemetry bit rates on the order of 2 to 3 kbps. The allocated capacity of the MMS C& DHM in terms of this rate requirement is adequate.

The MMS/C& DHM has a standardized signal interface with all potential user subsystems. This interface is provided by a remote interface unit (RIU), and its capacity-extension expander units. The RIU multiplexes and digitally encodes multiple channels of analog data, or accepts input digital data from user subsystems on request from the central unit of the MMS/C& DHM via the supervisory data bus. The serial digital data is then transmitted to the MMS/C& DHM central unit via the reply wire pair of the MMS/C& DHM multiplex data bus for subsequent buffering, reformatting, and transmission on the MMS/C& DHM S band transponder downlink.

4.1.4 AASIR Command Interface

At least three concepts can be considered for commanding the AASIR instrument. These are: 1) a straight-through real time command-by-command concept with no intervening on-board storage or processing, 2) a special purpose processor used for AASIR mode control, and 3) a general purpose computer for mode control. These concept options still apply, though modified by the presence of the MMS. The capabilities inherent in the MMS/C& DHM, such as stored commands and on-board computer (NSSC) processing, are essentially those involved in option (3).

The baseline STORMSAT concept requires that the MMS/C& DHM perform all on-board command processing for AASIR mode control. Clearly,

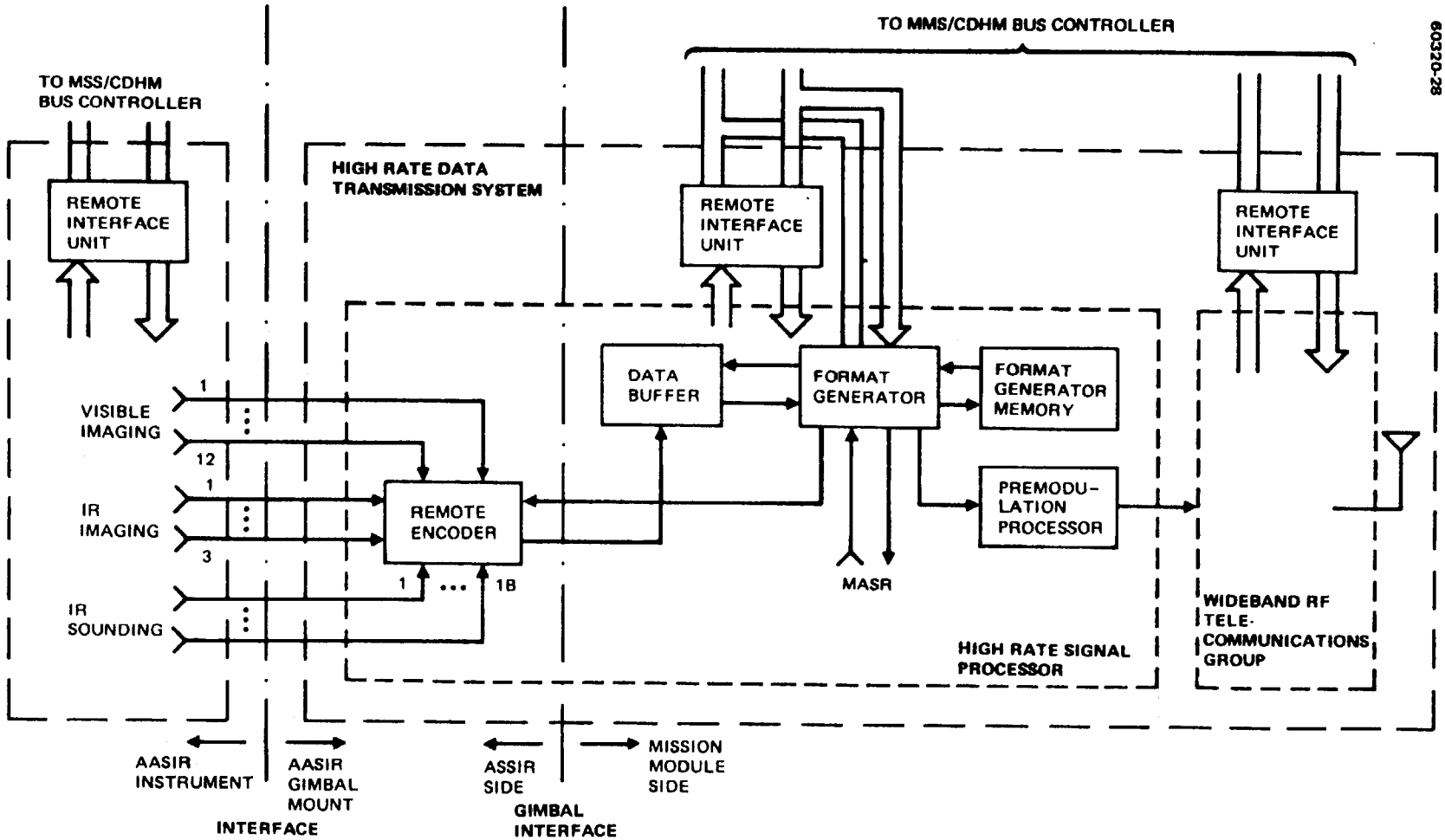

FIGURE 4-7. AASIR INTERFACE HARDWARE PHYSICAL DESCRIPTION

TABLE 4-3. PRELIMINARY AASIR TELEMETRY FUNCTIONS

ANALOG

1. +15 V signal power supply
* 2. +15 V auxiliary (telemetry reference) power supply
3. +5 V motor power supply
4. +5 V auxiliary power supply
* 5. Primary mirror temperature
* 6. Secondary mirror temperature
* 7. Primary encoder temperature
* 8. Redundant encoder temperature
* 9. Blackbody temperature 1
*10. Blackbody temperature 2
*11. Radiation cooler stage 1 temperature
*12. Radiation cooler stage 2 temperature
*13. Electronics module temperature
*14. Infrared detector temperature control voltage
*15. Scan mirror temperature
*16. Baffle tube forward end temperature
*17. Baffle tube aft end temperature
*18. Shutter cavity temperature
19. Infrared channel focus drive position
20. Visible channel focus drive position
21. 29 V dc current level
22. Primary scan drive torque
23. Redundant scan drive torque
*24. Radiation cooler sunshield temperature (earth shield)
*25. Radiation cooler ambient stage temperature
*26. Primary mirror aperture stop temperature
*27. Secondary mirror shield temperature
*28. Filter wheel heater temperature 1
*29. Filter wheel heater temperature 2
Plus spares

DIGITAL

1. Primary power supply, ON/OFF
2. Redundant power supply, ON/OFF
3. Visible channel electronics, ON/OFF
4. Infrared channel focus command, FORWARD
5. Infrared channel focus command, REVERSE
6. IR channel 1 gain line
7. IR channel 2 gain line
8. IR channel 3 gain line
9. IR channel 4 gain line
10. IR channel 5 gain line
11. IR channel 6 gain line
12. IR channel 7 gain line
13. IR channel 8 gain line
14. IR channel 9 gain line
15. IR channel 10 gain line
16. IR channel 11 gain line
17. IR channel 12 gain line
18. IR channel 13 gain line
19. IR channel 14 gain line
20. IR channel 15 gain line
21. IR channel 16 gain line
22. IR channel 17 gain line
23. IR channel 18 gain line
24. IR channel 19 gain line
25. IR channel 20 gain line
26. IR channel 21 gain line
27. IR channel 22 gain line
28. IR channel 23 gain line
29. IR channel 24 gain line
30. IR radiation cooler heater 1, ON/OFF
31. IR radiation cooler heater 2, ON/OFF
32. IR detector temperature control heater, ON/OFF
33. Scan drive, PRIMARY/REDUNDANT
34. Internal calibration command, ON/OFF
35. Scan mirror stow command, ON/OFF
36. Scan mirror stow position, UNLATCH/LATCH
37. Visible channel focus limit, FORWARD/OFF
38. Visible channel focus limit, REVERSE/OFF
39. Infrared channel focus limit, FORWARD/OFF
40. Infrared channel focus limit, REVERSE/OFF
41. Visible channel focus command, FORWARD
42. Visible channel focus command, REVERSE
43. Scan ON/OFF
44. Step scan, ON/OFF
45. Processor, ON/OFF
46. Filter wheel FWD STEP
47. Filter wheel REV STEP
48. Filter wheel position bit 1
49. Filter wheel position bit 2
50. Filter wheel position bit 3
51. Infrared channels gain
52. Calibration shutter phase and amplitude lock
53. Filter wheel heater ON/OFF
54. Blackbody heater ON/OFF
55. Frame size bit 1
56. Frame size bit 2
57. Frame center bit 1
58. Frame center bit 2
59. Frame center bit 3
60. Frame center bit 4
61. Frame center bit 5
62. Frame center bit 6
63. Frame center bit 7
Plus spares

*Telemetry signals shall be available when the instrument is OFF and the satellite ±15 Vdc secondary power is ON.

the capabilities of the MMS/C&DHM in automating certain AASIR operations, such as frame size sequences, imaging, and sounding and landmarking, and other preprogrammed operational sequences should be utilized. The interface between the AASIR instrument and the MMS/C&DHM is established by the decoding function of the remote interface unit (RIU). The channel capacity for each RIU compatible with the MMS/C&DHM is discussed in Section 6. A preliminary AASIR command list is presented in Table 4-4.

4.1.5 AASIR Instrument/Mission Module Interface

The bearing which provides one degree of freedom of AASIR scan motion presents an interface which affects the distribution and location of the

TABLE 4-4. PRELIMINARY AASIR COMMAND LIST

1. Scan mirror stow, LATCH
2. Scan mirror stow, UNLATCH
3. Radiation cooler heater 1, ON
4. Radiation cooler heater 2, ON
5. All heaters, OFF
6. Primary power supply, ON
7. Redundant power supply, ON
8. PPS/RPS, OFF
9. Detector temperature control heater, ON
10. Visible channel electronics, ON
11. Visible channel electronics, OFF
12. IR channel electronics, ON
13. IR channel electronics, OFF
14. IR channel 1 gain, STEP
15. IR channel 2 gain, STEP
16. IR channel 3 gain, STEP
17. IR channel 4 gain, STEP
18. IR channel 5 gain, STEP
19. IR channel 6 gain, STEP
20. IR channel 7 gain, STEP
21. IR channel 8 gain, STEP
22. IR channel 9 gain, STEP
23. IR channel 10 gain, STEP
24. IR channel 11 gain, STEP
25. IR channel 12 gain, STEP
26. IR channel 13 gain, STEP
27. IR channel 14 gain, STEP
28. IR channel 15 gain, STEP
29. IR channel 16 gain, STEP
30. IR channel 17 gain, STEP
31. IR channel 18 gain, STEP
32. IR channel 19 gain, STEP
33. IR channel 20 gain, STEP
34. IR channel 21 gain, STEP
35. IR channel 22 gain, STEP
36. IR channel 23 gain, STEP
37. IR channel 24 gain, STEP
38. Visible channel focus, FORWARD-blackbody heater, ON
39. Visible channel focus, REVERSE-blackbody heater, OFF
40. Infrared channel focus, FORWARD-electronic calibration waveform, INHIBIT
41. Infrared channel focus, REVERSE-electronic calibration waveform, ENABLE
42. Internal calibrate, ON
43. Scan drive primary, ON
44. Scan drive redundant, ON
45. Step scan, ON
46. Step scan, OFF
47. Processor, ON
48. Processor, OFF
49. Internal calibrate, OFF
50. Filter wheel, FORWARD STEP, FOCUS POSITION TM, ON
51. Filter wheel, REVERSE STEP, FOCUS POSITION TM, OFF
52. AASIR parameter dedicated line 1
53. AASIR parameter dedicated line 2 (redundant)
54. AASIR scan, ON (redundant)
55. Infrared channels gain, STEP
56. Filter wheel heater, ON
57. Frame size increase, STEP
58. Frame size decrease, STEP
59. Frame center-UP, STEP
60. Frame center-DOWN, STEP

Plus spares

AASIR sensor and telemetry data handling subsystem components. At least two concepts for component placement have been examined.

1) All major ASSIR sensor signal conditioning, multiplexing, encoding, and subsequent RF carrier modulation are performed on the MM side of the AASIR instrument/MM bearing. In addition, the MMS/C&DHM RIU is mounted on mission module side of the AASIR positioner. Only signal buffering adequate to drive the flexible cable lengths separating the scanning AASIR instrument and the fixed MM need be provided on the AASIR instrument itself. From the mechanical point-of-view, this configuration results in minimum rotational inertia for the AASIR instrument. On the other hand, greater potential exists for electrical noise pickup and stray capacitance in the signal leads with a larger burden on AASIR signal buffering. Further, the cable wrap for on-the-order of 150 AASIR telemetry and control leads will induce additional friction torque, degrading performance of the positioner.

2) All signal conditioning, multiplexing, and encoding are performed on the AASIR instrument side of the bearing, allowing transmission of perhaps two serial PCM bit streams (sensor plus telemetry) plus supervisory data across the bearing interface. The RIU telemetry PCM bit stream would be conducted across the MM/MMS interface for subsequent processing by the MMS/C&DHM; the AASIR sensor data PCM bit stream would be input to the remainder of the high-rate signal processor (HRSP) and high-rate data transmission subsystem (HRDTS) on the MM. This portion of the HRDTS consists of the HRSP elements such as buffer memories, format generator, format timing and control circuitry and the wideband RF group (angle modulator, RF upconverter, exciter, RF power amplifiers, and power supplies) necessary to transform the encoded AASIR signals to a modulated RF carrier. The use of microelectronics would minimize the contribution to rotational inertia of the ASSIR instrument; the small coaxial cable wrap would produce little disturbance torque. The design difficulties for adequate signal buffering within the AASIR instrument would be minimal in this concept.

The selection of the correct design approach is dependent on the design selected for positioning the AASIR. If a high torque drive mechanism such as the precision screw and nut is selected, then cable friction may not be of great importance in establishing AASIR positioning servo performance. The installation of electronic equipment on the AASIR positioning platform adds to its inertia and also produces a heat source which may couple with the AASIR. Detail design studies are required to resolve these design approaches.

4.2 MASR INTEGRATION

The MASR is characterized by a large aperture offset fed precision antenna 2.5 meters (98 inches) in diameter. It operates at the oxygen and water vapor resonances of 118 and 183 GHz. The diameter-to-wavelength ratio of this antenna is 1540:1, and it is an instrument with a small beamwidth (~800 μrad) requiring precision pointing and control. A receiver is mounted in an environmentally controlled compartment located behind the prime focus of the antenna reflector. Radiometer feeds extend from the compartment to the focus of the antenna. Transmission line losses are very low and temperature errors are thereby minimized. Data from the receiver is encoded at that location also minimizing errors due to noisy electrical transmission lines.

4.2.1 MASR Positioner Design Approach

The MASR is mounted on a gimbal. The inner gimbal axis (roll) provides for the north/south pointing and the outer gimbal axis (pitch) provides for the east/west pointing control. It is planned that the radiometer scan in the north/south direction and step in the east/west direction to minimize torque impulse disturbances to the spacecraft as the minimum moment of inertia for the MASR is about the roll axis. The basic positioner requirements are listed:

- Travel is $\pm 10^{\circ}$ about either axis
- Position readout, to 20 μrad accuracy
- Gimbal positionable within 40 μrad accuracy
- Scan rate of 0.29 mrad/sec (1000 km square frame)
- Slew rate of 2.9 mrad/sec for calibration excursions
- 55,000 radians life in 5 years (0.296 mrad/sec 100 percent duty cycle +20 percent for calibration slews)
- MASR movements to be compensated for angular momentum.

A conventional ball bearing gimbal design is considered adequate for this application. The bearings should be sized to accept loads due to ground test and checkout operations. As no RF energy needs to be transferred across the gimbal, and as motions are restricted to $\pm 10^{\circ}$, no slip rings or rotary RF joints are required. Power, command, and data transfer are accomplished by flexible wire transmission lines.

At one end of travel of the pitch axis the radiometer frame meets a rigid structure extending from the vehicle. Pyrotechnic device(s) provide a structural tie during launch; radiometer loads are then transferred mainly through the launch lock structure and only partially through the gimbal bearings.

Gimbal motion may be accomplished by either direct torque motor driver or geared motor drivers. Direct drive torque will require elaborate gravity compensation devices to allow for ground testing of the system. Geared drivers will ease this problem but probably not eliminate their need. Other factors affecting choice of a driver are bearing and cable friction and scan motion smoothness and accuracy. A geared servo motor drive will provide high output torque and allow the use of tachometric feedback to produce a smooth running servo with accurate velocity control.

Multipole angle resolver feedback is adequate for this application. It may be desirable to correlate MASR and AASIR sounding data so that an absolute pointing accuracy of the order of 40 mrad relative to the AASIR may be required. This is well within the capability of the multiple angle resolvers.

4.2.2 MASR Data Conditioning and Timing Interface

In a similar fashion to the AASIR data handling, the choices for MASR data transmission include: 1) encoding and transmission of MASR sensor and housekeeping data only through the MMS/CDHM via its standardized RIU interface, 2) encoding and transmission of this data only by the mission module via the wideband AASIR telecommunications link, or 3) a combination of both. The multiplexing and encoding of this data may be performed by the high-rate signal processor (HRSP) used for AASIR sensor processing, or by a dedicated unit. A combination of both modes defined above (Option 3), wherein MASR status telemetry and mission data is available both on the MMS/CDHM telemetry and mission unique high rate AASIR link has been chosen for the STORMSAT baseline. This will satisfy a reasonable mission requirement for collocation of MASR and AASIR data sinks as well as allowing separate MASR principal investigator data acquisition via the STDN. The implications of placing MASR data only on the high rate AASIR data link are that only data users at a relatively capable RF receiving site can then receive the MASR in realtime, since downlink bit rates of the order of 7 Mbps are anticipated. Alternatively, incorporating the MASR data only in the MMS/CDHM telemetry data stream will require an RF receive frequency capability different from that anticipated for the high rate AASIR data stream, and require transfer from the STDN sites to the MASR principal investigator and AASIR data user via landlines.

The most flexible approach is that chosen for the baseline with MASR data appearing in both the MMS/CDHM and AASIR data streams. The composite MASR housekeeping and sensor data rate is anticipated to be less than 1000 bps, entirely compatible with the MMS/CDHM telemetry capability. At least two approaches can be considered incorporating into the high rate AASIR data stream: 1) time multiplexing, or 2) by link multiplexing using a modification of orthogonal phase modulation techniques; i.e., modified quadraphase phase shift keying (QPSK). Frequency multiplexing of MASR data by means of a high frequency subcarrier does not appear hopeful due to the large occupied RF bandwidth of the AASIR data. If MASR and other payload housekeeping data is to be obtained during the AASIR active scan period, on-board data storage and reclocking at effectively high data rates for transmission during the AASIR turnaround time must be considered.

Since the MASR is in the very early stages of definition, this data rate estimate should be taken as a rough estimate. The estimate is based on two framing modes: 1) 1000 km)^2 coverage in 30 minutes, and 2) whole earth coverage in 6 hours to minimize the effect of diurnal variation in whole earth maps. An assumption will be made of 8 spectral channels of data in both the 118 GHz O_2 and 183 GHz H_2O absorption bands, a total of 16 analog sensor data channels. Following J. Schiue of NASA contiguous coverage of the 183 GHz band will be assumed for the limited frame mode and contiguous coverage of the 118 GHz band for the whole earth mode. Dwell time for the small frame mode will be calculated assuming nadir viewing and for earth coverage from solid angle arguments.

$$t_d = \frac{E\, T_F\, (\gamma\, L_A)^2}{L_F^{\,2}}$$

where

t_d = dwell time per IFOV, seconds

E = scan efficiency

T_F = frame time, seconds

L_A = distance to earth's surface, meters

L_F = size of frame, meters

γ = angle subtended by radiometer beams, radians

γ_{118} = 1.3 mrad

γ_{183} = 0.8 mrad

Therefore, for the 1000 by 1000 km frame mode,

$$t_d = \frac{0.9\,(1800)\,(3.58 \times 10^4 \times 0.8)^2}{(1000)^2} = 1.33 \text{ second}$$

The bit rate is computed for a quantization level Q of 10,

$$R = \frac{(\text{Number of channels})\,(Q)}{t_d}$$

$$= \frac{16 \times 10}{1.33} = 120 \text{ bps}$$

To determine the number of samples required to cover earth, compare the MASR beam solid angle with the earth solid angle subtended from synchronous altitude; namely,

$$\Omega earth = 2\pi(1 - \cos 8.7^{\circ}) = 0.0723 \text{ sr}$$

$$\Omega beam = (1.3 \text{ mr})^2 = 1.7 \times 10^{-6} \text{ sr at } 118 \text{ GHz}$$

$$t_d = 0.9 \times 6 \times 3600 \quad \frac{1.7 \times 10^{-6}}{0.0723} = 0.46 \text{ second}$$

$$R = \frac{16 \times 10}{0.46} = 350 \text{ bps}$$

These bit rates are likely to be even lower if the area coverage/unit time must be reduced to meet radiometric performance specifications. Preliminary MASR analog and digital telemetry requirements are indicated in Table 4-5.

4.2.3 MASR Command Requirements Interface

The basic issues involved in establishing the MASR command signal interface involve: 1) determination of command mode philosophy, and 2) implementation of that philosophy. For example, one instrument command philosophy will employ the MMS/C&DHM with a standard MASR remote decoder interface (the remote interface unit) to the C&DHM. All preprogrammed mode control required by the MASR would be accommodated by the general purpose computer in the C&DHM. An alternate mode would allow dedicated use of a microprocessor for mode control, operating on command data from the MMS/C&DHM. Conceivabl , a common microprocessor could accomplish mode control functions for both the AASIR and MASR. The approach chosen for the baseline STORMSAT payload command concept is that all commands, real time or stored, are provided to the MASR via the standardized RIU (remote decoder) interface with the MMS/C&DHM. No local command processing for the MASR is to be performed on the mission module.

4.2.4 MASR Signal Interface Hardware Configuration

Figure 4-8 illustrates the concept chosen for the physical location of the hardware providing the telemetry and command signal interface for the MASR with the MMS/C&DHM, particularly the physical distribution with respect to the MASR gimbal. The basic concept illustrated in this interface hardware configuration is that the size of the cable wrap brought across the MASR gimbal interface is to be minimized; that is, the minimum number of signal and prime power leads is to be used. Thus, the signal conditioning, multiplexing, and analog-to-digital signal conversion is to be performed on the instrument side of the gimbal, allowing only cable pairs for serial bit stream data to cross the gimbal. In particular, these cable pairs include redundant supervisory and reply multiplex data bus pairs for the MMS/C&DHM-RIU/EU link. Similar acquisition and reply cable pairs for the remote

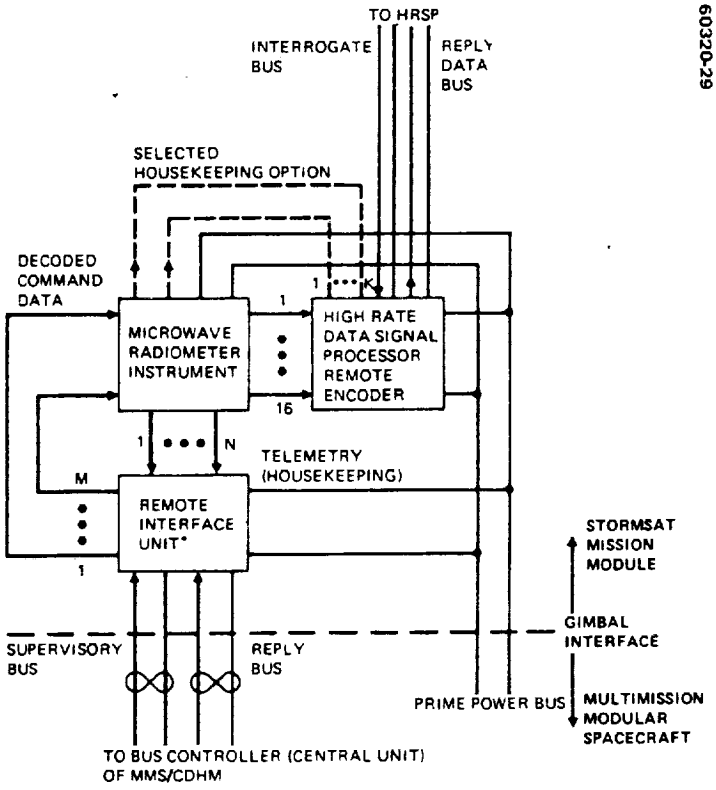

*PLUS AS MANY EXTENDER UNITS AS REQUIRED

FIGURE 4-8. BASELINE PHYSICAL DISTRIBUTION FOR MASR INTERFACE HARDWARE

TABLE 4-5. PRELIMINARY MASR TELEMETRY FUNCTIONS

ANALOG

1. + Low voltage signal power supply
* 2. + Low voltage auxiliary (telemetry reference) power supply
3. + Motor power supply
4. + Auxiliary motor power supply
* 5. Antenna temperature 1
* 6. Antenna temperature 2
* 7. Antenna temperature 3
* 8. Antenna temperature 4
* 9. Blackbody temperature 1
*10. Blackbody temperature 2
*11. Radiation cooler stage 1 temperature
*12. Electronics module temperature
*13. Infrared detector temperature control voltage
*14. Baffle tube forward end temperature
*15. Calibration mirror temperature
*16. 29 Vdc current level
17. Primary scan drive torque 1
18. Primary scan drive torque 2
19. Redundant scan drive torque 1
20. Redundant scan drive torque 2
*21. Radiation cooler sunshield temperature (earth shield)
*22. Radiation cooler ambient stage temperature
23. Local oscillator temperatures

Plus spares

DIGITAL

1. Primary power supply, ON/OFF
2. Redundant power supply, ON/OFF
3. Channel electronics, ON/OFF
4. IR channel 1 gain line
5. IR channel 2 gain line
6. IR channel 3 gain line
7. IR channel 4 gain line
8. IR channel 5 gain line
9. IR channel 6 gain line
10. IR channel 7 gain line
11. IR channel 8 gain line
12. IR channel 9 gain line
13. IR channel 10 gain line
14. IR channel 11 gain line
15. IR channel 12 gain line
16. IR channel 13 gain line
17. IR channel 14 gain line
18. IR channel 15 gain line
19. IR channel 16 gain line
20. IR radiation cooler heater 1, ON/OFF
21. IR radiation cooler heater 2, ON/OFF
22. Scan drive, PRIMARY/REDUNDANT 1
23. Scan drive, PRIMARY/REDUNDANT 2
24. Internal calibration command, ON/OFF
25. Antenna stow command, ON/OFF 1
26. Antenna stow command, ON/OFF 2
27. Scan ON/OFF 1
28. Scan ON/OFF 2
29. Processor, ON/OFF
30. Calibration shutter phase and amplitude lock
31. Blackbody heater ON/OFF
32. Frame size bit 1
33. Frame size bit 2
34. Frame size bit 3
35. Frame size bit 4
36. Frame size bit 5
37. Frame center bit 1
38. Frame center bit 2
39. Frame center bit 3
40. Frame center bit 4
41. Frame center bit 5
42. Frame center bit 6
43. Frame center bit 7

Plus spares

encoder-to-central unit portions of the high-rate signal data processor (HRSP) system on the mission module, and prime power/return for these units are provided.

4.3 REFERENCES

1. Dahl, P. R., "A Solid Friction Model," TOR-158 (3107-18), The Aerospace Corporation, El Segundo, CA, May 1968.

2. Kuo, B. C., Singh, G., and Seltzer, S. M., "Stability Study of the Large Space Telescope (LST) System with Nonlinear CMG Gimbal Friction," AIAA Mechanics and Control of Flight Conference, Anaheim, CA, August 1974.

5. ATTITUDE DETERMINATION AND CONTROL

This section describes the attitude control subsystem (ACS), fulfilling STORMSAT experimental mission pointing requirements described in Section 2.1. The ACS concept uses the Multimission Modular Spacecraft ACS (MACS) module and the on-board computer located in the communications and data handling (C&DH) module. Mission unique equipment is located on the mission module.

5.1 ACS REQUIREMENTS

Attitude pointing requirements for the ACS are summarized in Table 5-1; the rationale for these requirements is given in Section 2.1.3. The requirements define the alignment of the AASIR baseplate relative to the local vertical coordinate frame. This convention defines null attitude error with the yaw axis pointing to earth center and the pitch axis aligned with the negative orbit normal vector. The roll axis completes the triad and is aligned with the velocity vector when the orbit is exactly circular.

In this report no distinction is made between real time attitude determination and actual spacecraft pointing, as all absolute spacecraft pointing errors are well within the attitude determination requirement. Both short and long term stability errors are computed as the rms difference of line of sight errors over the indicated time interval.

5.2 DESIGN APPROACH

Figure 5-1 is a block diagram of the STORMSAT ACS components supplied as elements of the Multimission Modular Spacecraft (MMS). With the exception of the coarse sun sensor, the on-board computer, and the reaction control jets, all components are contained within the MACS module. The layout of this module is shown in Figure 5-2. The magnetometer and the magnetic torquer bars are not used because they cannot be reliably employed at synchronous altitude. The redundant gyro package has been omitted, since the primary inertial reference unit (IRU) contains three gyro units, each with two-axis output.

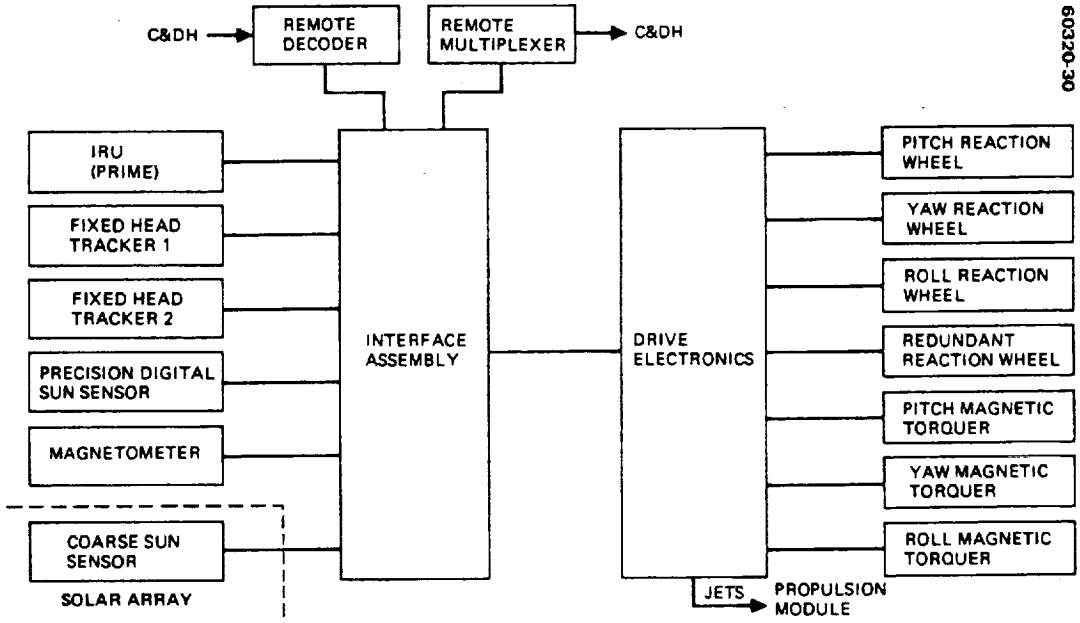

FIGURE 5-1. ATTITUDE CONTROL SYSTEM BLOCK DIAGRAM

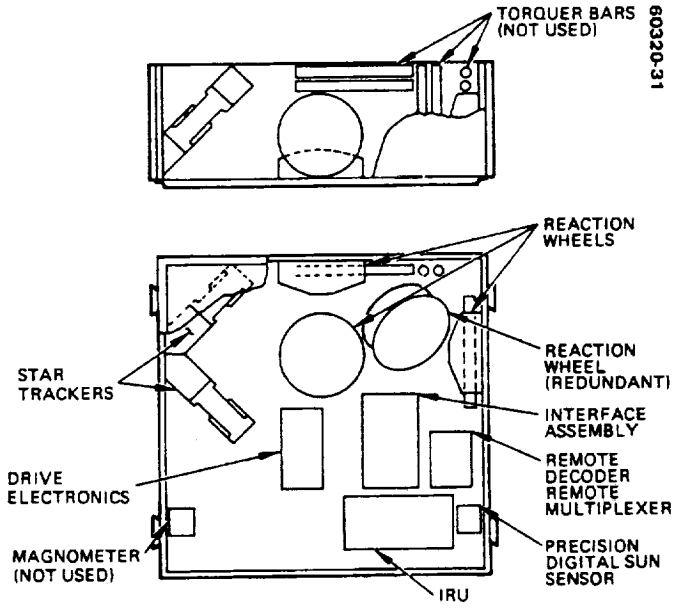

FIGURE 5-2. MACS MODULE COMPONENT LAYOUT

TABLE 5-1. ACS POINTING REQUIREMENTS

Requirement	Specification (1σ)
Real time attitude determination, deg	
Pitch	0.03
Roll	0.03
Yaw	0.18
Short term attitude stability (8 seconds), μrad	
Pitch	4.2
Roll	4.2
Yaw	25
Long term attitude stability (22 minutes), μrad	
Pitch	11
Roll	11
Yaw	87

On-orbit attitude reference is obtained from star sightings from fixed head trackers which update the short term attitude reference provided by the IRU. Star sensor outputs are provided to the on-board computer, which estimates spacecraft three-axis attitude and gyro drift rates using a six-state Kalman filter algorithm. The computer also accepts IRU angle increments and processes this information to generate momentum wheel commands for attitude error nulling. Initial acquisition utilizes the coarse sun sensor (CSS) and preliminary gyro drift calibration and attitude estimation are provided by a precision digital sun sensor (PDSS). These sensors are also available for failure mode attitude reference.

Spacecraft control torque and momentum storage are provided by the momentum wheels. These wheels are periodically unloaded via jets on the propulsion module coincident with solar array reorientation at 1 to 3 hour intervals. These functions are performed with the AASIR and MASR on standby.

5.2.1 Mission-Unique Attitude Sensor Trade Study

Simulation studies (described in Section 5.3) indicate that adequate STORMSAT pointing performance can be achieved by the MACS if both trackers are operating and if sensor performance is within specification. (IRU and tracker requirements for the STORMSAT mission are presented in Section 5.2.5). However, with single tracker failure, the frame-to-frame stability requirement is not achieved. Mission reliability may require the use of a mission-unique sensor for alternate reference with single tracker failure. Commonality considerations indicate that the alternate sensor should be a star tracker of the type used for MACS reference.

Several alternate sensors were also considered, and these are listed in Table 5-2, along with significant trade factors. Besides the fixed head

TABLE 5-2. MISSION-UNIQUE ACS SENSOR TRADE FACTORS

Sensor	Available Units	Performance Limitation	Mission Module Integration	Comments
Fixed head star tracker	CT-401 (BBRC) HEAO (HRC) OAO-III (Bendix)	Residual nonlinearities over field of view. Temperature, magnitude, and magnetic field errors	Not difficult	CT-401 on standard parts list. Commonality with MACS sensors
Star mapper	B5D (Honeywell)	False transits due to space-craft jitter	Not difficult	High reliability
Gimbaled star tracker	Skylab ATM (Bendix), OAO-23 (Kollsman)	Gimbal nonlinearities	Difficult	High weight, cost, power; low reliability
Earth horizon sensor	ATS-F (TRW) LSMC ESA (Lockheed)	Possible earth horizon variability	No problem	Requires synchronous orbit confirmation of anticipated performance. Potential relaxation of gyro drift requirements
Microwave interferometer	ATS-F (IBM)	Possible beacon line of sight variability. Payload multi-path interference	Difficult	Requires synchronous orbit confirmation of anticipated performance. Relaxation of gyro drift requirements.
Sun sensor	Not available	Nonlinearities over field of view	Field of view problems	Potential for reliable alternate sensor
Ultrastable rate integrating gyro	TGG (Northrop)	Long term drift stability	MACS integration acceptable	Performance levels classified.

tracker, two other stellar approaches were considered, the star mapper and two-gimbal star tracker. The star mapper detects star crossings of a solid state detector pattern in the image plane. The star field is scanned by the spacecraft orbital motion and comparison of measured and predicted crossing times is used as data for attitude determination. The mapper is highly susceptible to spacecraft jitter, which can produce multiple slit crossings. STORMSAT short term motion, in particular, the roll motion induced by the AASIR mirror, is not favorable for the star mapper. The gimbaled tracker appears to be unsuitable for STORMSAT, primarily because of its high cost, integration complexity, and low reliability.

Earth referenced sensors are attractive for synchronous orbit because the sensor target viewing geometry is virtually fixed in the sensor field of view. Thus, nonlinearity errors are greatly reduced. A concern for both the earth horizon sensor and the microwave interferometer is the influence of environmental effects on measured angle stability. For example, the CO_2 band horizon may be subject to shift due to high altitude clouds. It is expected that these effects are small relative to STORMSAT stability requirements. A definitive test from synchronous orbit is needed to verify the anticipated performance. Potential advantages of both types of earth reference sensors are due to low noise equivalent angle (NEA) which would permit relaxed gyro drift stability requirements. This is particularly true for systems using the interferometer reference, where relatively low performance gyros can provide satisfactory short term stability.

A sun sensor that meets the STORMSAT accuracy requirements over the full sun angle range is not presently developed. The potential for such a sensor should be recognized. It appears that a single axis sensor (sun azimuth) of suitable accuracy could provide the necessary independent measurement to meet STORMSAT pointing with single tracker failure.

Use of an ultrastable IRU was also considered. Single tracker simulation runs indicate that gyro drift stability somewhat better than 0.003 deg/hr over 24 hours would be required.

5.2.2 ACS Operation

5.2.2.1 Initial Sequence

The sequence of events for the initial operational mode is given in Table 5-3. It has been assumed that the IUS has placed the spacecraft on orbit with small (less than 45 fps) velocity residuals. The initial acquisition sequence further assumes a random initial orientation with small (less than 2 deg/sec) tumbling rates.

During transfer orbit, all ACS components are operated on standby. The ASSIR and MASR suspensions are locked by launch lock mechanisms to constrain motion. Immediately following separation from the IUS, the propulsion module is enabled to provide control torque for nulling spacecraft rates using the IRU as reference. When rates are stabilized, the solar cell array is deployed and the CSS is used for preliminary attitude determination.

TABLE 5-3. ACS SEQUENCE OF EVENTS

Function	Duration	Description	Attitude Sensor	Attitude Control	MACS Mode
Premission Phase					
Transfer orbit	1 to 2 days	Spacecraft on standby	Shuttle/interim upper stage (IUS)	Shuttle/IUS	-
IUS separation		Post apogee kick attitude with separation rates <2 deg/sec.	IUS	IUS	-
Inertial hold	$\leq$3 min	Reduce spacecraft spin to $<3 \times 10^{-4}$ deg/sec	IRU	Reaction control subsystem (RCS)	Inertial hold
Panel deployment	20 min	Deploy solar panels	IRU	RCS	Inertial hold
Sun acquisition	20 min	Propulsion module faces sun. Longitudinal axis along sun line	CSS/IRU/PDSS	RCS	Coarse/fine sun acquisition
Star acquisition	60 min	Spin (0.1 deg/sec) about sun line. Acquire reference stars	PDSS/IRU/ trackers	RCS/wheels	Slew/stellar acquisition
Orbit track	1 day	Trim IRU drift to <0.1 deg/hr during ground track	Tracker/IRU	Wheels	Stellar
Orbit trim orientation	$<$30 min	Align longitudinal axis along ΔV: (slew rate $\approx$ 0.1 deg/sec)	IRU	Wheels	Slew
Orbit trim	$<$4 min	ΔV $<$45 fps; F = 20 lb_f; W $\approx$ 3600 lb	IRU	RCS	Orbit adjust
Orbit trim, reorientation	$<$30 min	Align spacecraft to local vertical frame (slew rate = 0.1 deg/sec)	IRU/trackers	Wheels	Slew
AASIR and radiometer unlock/checkout	$\approx$ 8 hr	Verify AASIR and radiometer operation	IRU/trackers	Wheels/RCS	Earth pointing
System calibration	2 days	Calibrate ACS bias using AASIR	IRU/trackers	Wheels/RCS	Calibration
Mission	3 yrs	See below	IRU/trackers	Wheels/RCS	Normal operating modes
Mission Phase					
AASIR East-West scan/ retrace and radiometer sounding	1 to 3 hrs	Spacecraft fixed to local vertical reference frame	IRU/fixed head trackers	Wheels	Earth pointing
Solar panel orient/ momentum unload	1 to 3 min	Slew solar panel through 10 to 30° at 10 deg/min	IRU/fixed head trackers	Wheels/RCS	Earth pointing
		Pulse jets and counter torque wheels $\Delta H \approx 1$ ft-lb/sec			
Post-orientation settling	1 min	Reduce residual spacecraft motion			Earth pointing
Stationkeeping orientation	15 min	Align longitudinal axis along orbit normal vector (slew rate $\approx$ 0.1 deg/sec)	IRU	RCS	Slew
Stationkeeping maneuver	1 min	$\Delta V < 5.0$ fps/10 days	IRU	RCS	Orbit adjust
Stationkeeping reorientation	15 min	Align longitudinal axis along velocity vector (slew rate $\approx$ 0.1 deg/sec)	IRU	RCS	Slew
Post stationkeeping settling	1 to 2 hr	Re-establish state estimate	IRU/fixed head trackers	Wheels	Earth pointing
Spacecraft equinox inversion	30 min	Align spacecraft to local vertical reference frame with AASIR radiation cooler in cold hemisphere	Gyros	RCS	Slew
Post inversion settling	1 to 2 hr	Re-establish state estimate	IRU/fixed head trackers	Wheels/RCS	Earth pointing

The spacecraft is slewed to null the CSS output and bring the sun into the digital precision sun sensor field of view. After sun acquisition, the spacecraft is next maneuvered through a full rotation about the sun line and the tracker outputs are used by the computer to determine vehicle attitude about the sun line. The vehicle is then slewed about the sun line to a predetermined inertial attitude. When the predetermined star is acquired, the vehicle is maintained at a fixed attitude for gyro drift calibration. After gyro drift is nulled, alternate stars in the tracker field of view are tracked to verify and update the tracker ground calibration. During this time, the wheels are used for control.

The spacecraft orbital elements are determined by ground track during the orbit track interval and the initial velocity correction is computed. The orbit trim maneuver is initiated by slewing the spacecraft to the desired attitude. The longitudinal jets are fired for velocity correction. Following correction, the spacecraft is slewed to the operational attitude with the yaw axis aligned along local vertical and the pitch axis aligned along the orbit normal. Star crossing data are collected by the computer for final attitude and gyro drift estimation. During this interval, the AASIR and MASR are unlocked and payload checkout is begun. Finally, the overall system performance may be verified using the AASIR for precision attitude determination using earth landmark data.

5.2.2.2 Mission Sequence

During normal mission operations, the AASIR and MASR are used for picture generation and sounding. Disturbances due to payload motion are countered by wheel commands generated by ACS processing and initiated by event signals from payload processing. Residuals due to imperfect compensation are measured by the IRU and used to update the counter torque profile so that spacecraft motion is minimized. Under these conditions, the attitude control system maintains fixed attitude pointing in the local coordinate frame. Stars of opportunity are sighted by the trackers, which supply attitude information to the Kalman filter. This algorithm updates the attitude reference as maintained by the IRU. An event sequence for the mission phase is also given in Table 5-3.

During payload operation, the solar panels are maintained fixed relative to the spacecraft. Also, the wheels are used to store accumulated disturbance torque momentum. Spacecraft disturbances from solar panel rotation and the control jet firing are thereby avoided during intervals of AASIR and MASR operation. During intervals of opportunity (occurring roughly every 1 to 3 hours), the AASIR is placed on standby and the panel stepped to maintain nominal sun pointing. In addition, the attitude control jets are pulsed to unload the secular component of stored momentum. The wheels are simultaneously torqued to minimize the net attitude motion. After settling of the attitude motion (less than 1 minute following disturbance removal) normal mode operation of the AASIR may resume.

At approximately 10 day intervals, the spacecraft is oriented with the longitudinal axis perpendicular to the orbit plane for combined north-south

60320-32

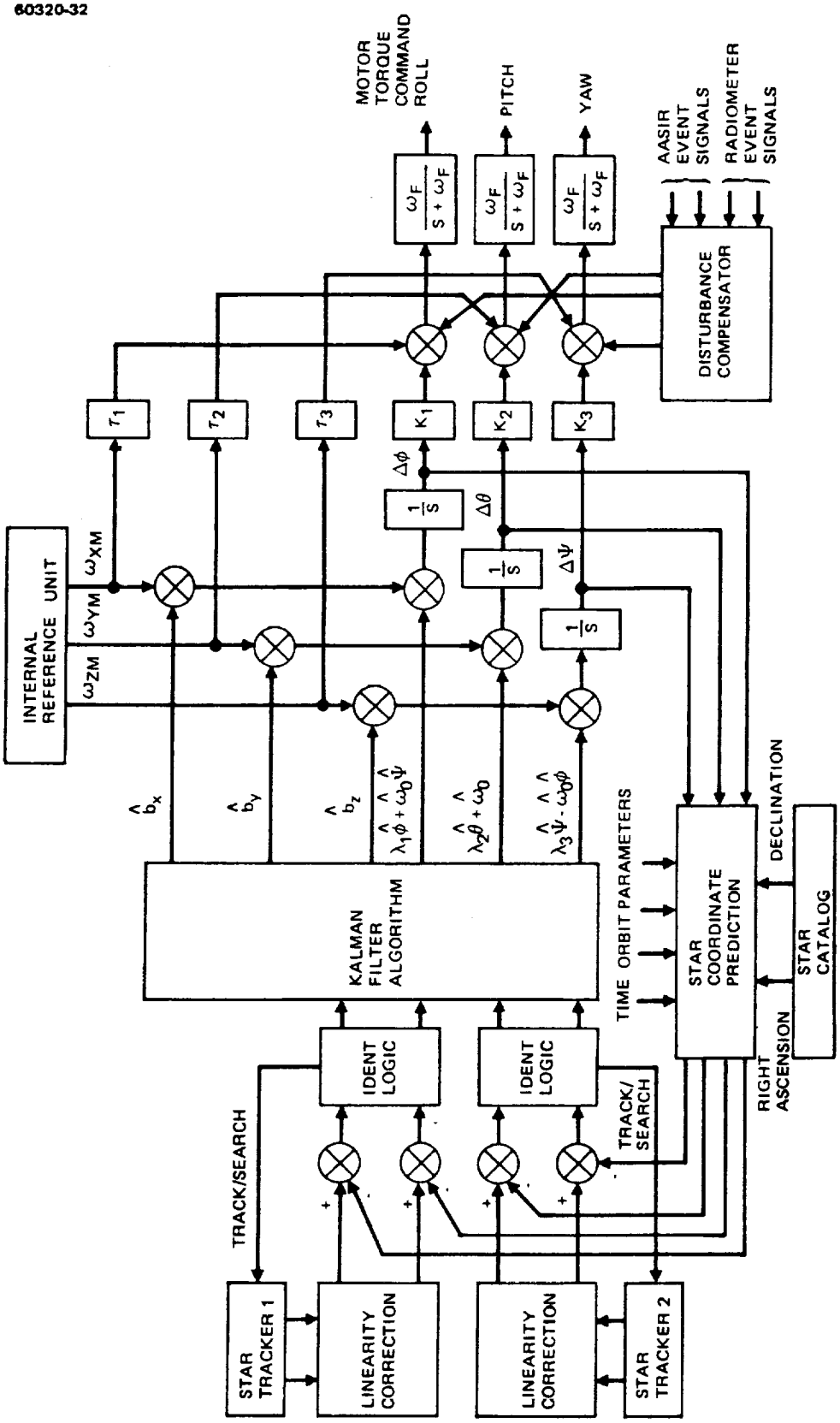

FIGURE 5-3. ACS-ON-ORBIT SIGNAL FLOW

and east-west stationkeeping. The maximum yearly east-west correction is 7.4 fps, while the north-south correction is approximately 170 fps. These velocity corrections may be performed periodically to maintain orbit inclination within $\pm 0.025^{\circ}$. During this maneuver the IRU is used for reference. Although the correction is relatively brief, the spacecraft slew rate is limited by the gyro input axis range (approximately 0.2 deg/sec) so that the 90° orientation will require 10 to 15 minutes. After the correction, the spacecraft is reoriented to local vertical and the stellar reference reestablished.

The spacecraft is normally oriented such that the AASIR cooler is in the cool celestial hemisphere (i.e., the cooler is pointed north during the winter and south during the summer). This is achieved by a 180° rotation about the yaw axis at the spring and autumnal equinox. After the spacecraft reorientation to its operational attitude, the stellar reference is reestablished using the star catalog appropriate for the cold hemisphere swath, and the gyro orbital rate parameters revised.

5.2.3 ACS On-Orbit Signal Flow

Signal flow during on-orbit operation is summarized in Figure 5-3. Based on time of day and the particular star tracker used, the appropriate star is selected from the catalog. Star data are stored in celestial coordinates. The on-board computer transforms these data into tracker coordinates based on spacecraft ephemeris data and corrects for satellite velocity aberration. Since the spacecraft is likely to have short period motion about the integrating gyro attitude null because of payload disturbances, the gyro output is used to correct the predicted star position. The tracker output signal is corrected for tracker nonlinearities as measured by preflight calibration. The resultant signal is compared with the predicted star position to generate the pointing error signal used by the Kalman filter to estimate vehicle attitude and gyro bias. The spacecraft attitude is estimated in local coordinates so that single-precision arithmetic is suitable for the limited state variable range. The candidate star is tracked for a significant interval (>16 seconds) to assure identity and average the random noise before the data are used by the control system. Alternate stars are tracked at a sample rate on the order of 2 to 20 minutes.

Although the gyro bias is immediately corrected following the update sample, the spacecraft attitude is not, since an immediate correction results in added frame-to-frame stability error. The spacecraft is therefore slowly slewed toward null and not immediately corrected. Although this results in increased absolute error, the error magnitude is quite acceptable relative to STORMSAT requirements. In roll and yaw an orbital coupling correction is also made. For noncircular orbits the local vertical varies slightly from uniform rotation in inertial coordinates and this correction is made prior to generation of pitch attitude error.

Wheel torque commands are generated to null the pointing errors $\Delta\phi$, $\Delta\theta$, and $\Delta\psi$. These commands are filtered to remove gyro sample noise and minimize wheel power. Although not shown in Figure 5-3, the body axis torque commands are converted into wheel coordinates, if required, by linear

transformation, using the on-board processor. Wheel torque commands are also generated to counter residual payload disturbances. These command profiles are initiated by signals from the processor. As the disturbance is repeatable, calibration is possible using telemetry signals from the gyros.

5.2.4 ACS Control Law

The control equations used to mechanize the stellar tracker/gyro attitude control system are given in Table 5-4. Parameter definition and preliminary values are also given. Since the mission phase requires the most critical pointing, only equations for this phase are included. These equations function to maintain vehicle attitude with the yaw axis aligned to the local vertical and the pitch axis aligned to the orbit normal. Although shown here in analog form, the equations will be computed within the on-board digital processor and so will be realized in discrete form. The Kalman filter equations that estimate spacecraft attitude and gyro drift are discussed in Section 5.2.5.

The dynamics given are for preliminary design and do not include cross-products of inertia or flexible body interaction effects. Coupling due to stored momentum has also been neglected. The attitude error integrator subtracts the gyro bias estimate from the gyro torquer pulse count to generate the integrated attitude error in roll, pitch, and yaw. As this error may be offset by an unknown initial value, the attitude estimate is also summed through a low gain path. The integrated attitude error is summed with the pulse count, weighted by the lead time constant, to obtain a shaped error signal. This error is multiplied by the torque gain constant and the resulting signal used to command the momentum wheels to null the integrated attitude error. These operations occur at a 5.0 Hz sample frequency. Loop gain selection gives a closed loop bandwidth of 0.25 rad/sec for all three attitude control loops.

5.2.5 Attitude Estimation System Model

A Kalman filter is used for spacecraft attitude estimation. The six state variables are the local coordinate frame Euler angles ϕ, θ, and ψ, and the gyro drift rates b_x, b_y, and b_z. The filter is based on the following system model:

$$\dot{\phi} = \omega_o \psi - b_x + w_1 + \hat{b}_x - \lambda \hat{\phi} - \omega_o \hat{\psi}$$

$$\dot{\theta} = \omega_o - b_y + w_2 + \hat{b}_y - \lambda \hat{\theta} - \hat{\omega}_o$$

$$\dot{\psi} = -\omega_o \phi - b_z + w_3 + \hat{b}_z - \lambda \hat{\psi} + \hat{\omega}_o \hat{\phi}$$

$$\dot{b}_x = w_4$$

$$\dot{b}_y = w_5$$

$$\dot{b}_z = w_6$$

TABLE 5-4. ATTITUDE CONTROL DYNAMICS

Equations of motion (rigid body)

Roll rate	$I_w\dot{\omega}_x = -\dot{H}_x + T_{xc} + T_{xD}$
Pitch rate	$I_y\dot{\omega}_y = -\dot{H}_y + T_{yc} + T_{yD}$
Yaw rate	$I_z\dot{\omega}_z = -\dot{H}_z + T_{zc} + T_{zD}$
Roll attitude	$\dot{\phi} = \omega_x + \omega_o\psi$
Pitch	$\dot{\theta} = \omega_y + \omega_o$
Yaw attitude	$\dot{\psi} = \omega_z - \omega_o\phi$

Attitude control law

Roll error	$\Delta\dot{\phi} = \omega_{xm} - \hat{b}_x + \lambda_1\hat{\phi} + \hat{\omega}_o\hat{\psi}$
Pitch error	$\Delta\dot{\theta} = \omega_{ym} - \hat{b}_y + \lambda_2\hat{\theta} + \hat{\omega}_o\theta$
Yaw error	$\Delta\dot{\psi} = \omega_{zm} - \hat{b}_z + \lambda_3\hat{\psi} - \hat{\omega}_o\hat{\phi}$
Roll torque command	$T_{xc} = K_1(\Delta\phi + \tau_1\omega_{xm}) + T_{xDC}$
Pitch torque command	$T_{yc} = K_2(\Delta\theta + \tau_2\omega_{ym}) + T_{yDC}$
Yaw torque command	$T_{zc} = K_3(\Delta\psi + \tau_3\omega_{zm}) + T_{zDC}$

Torque command filter

Roll command filter	$\dot{X}_1 = \omega_F(T_{xc} - X_1),\ \dot{H}_{xc} = X_1$
Pitch command filter	$\dot{X}_2 = \omega_F(T_{yc} - X_2),\ \dot{H}_{yc} = X_2$
Yaw command filter	$\dot{X}_3 = \omega_F(T_{zc} - X_3),\ \dot{H}_{zc} = X_3$

Dynamics state variables

$\omega_x, \omega_y, \omega_z$	Roll, pitch, and yaw inertial body rates
ϕ, θ, ψ	Roll, pitch, and yaw attitude angles in local coordinate frame
H_x, H_y, H_z	Roll, pitch, and yaw stored wheel momentum

Dynamics parameters

I_x, I_y, I_z	Roll, pitch, and yaw moments of inertia	1010, 2700, 2700 kg-m^2 (750, 2000, 2000 slug-ft^2)
ω_o	Orbit rate	7.27×10^{-5} rad/sec

Table 5-4 (continued)

Control state variables		
$\Delta\phi,\ \Delta\theta,\ \Delta\psi$	Roll, pitch, and yaw attitude errors	
$X_1,\ X_2,\ X_3$	Wheel torque command filter state variables	
Control input/output variables		
$\omega_{xm},\ \omega_{ym},\ \omega_{zm}$	Rate gyro angle increments per sample interval	
$\hat{b}_x,\ \hat{b}_y,\ \hat{b}_z$	Gyro bias estimate (from Kalman filter)	
$\hat{\phi},\ \hat{\theta},\ \hat{\psi}$	Attitude estimates (from Kalman filter)	
$\hat{\omega}_o$	Orbit rate prediction (from ephemeris)	
$T_{xDC},\ T_{yDC},\ T_{zDC}$	Compensation torques for residual payload disturbances	
$H_{xc},\ H_{yc},\ H_{zc}$	Torque commands in roll, pitch, and yaw to momentum wheels	
Controller parameters		
$\lambda_1,\ \lambda_2,\ \lambda_3$	Roll, pitch, and yaw attitude gain constants	10^{-4} rad/sec
$K_1,\ K_2,\ K_3$	Roll, pitch, and yaw torque gain constants	46, 125, 125 ft-lb/rad
$\tau_1,\ \tau_2,\ \tau_3$	Roll, pitch, and yaw lead shaping time constant	8.0 seconds
ω_F	Wheel command filter lag shaping frequency	2.5 rad/sec

This model approximates the long period dynamics obtained from the closed-loop response of the ACS control laws of the preceding section. Elimination of the short period gyro loop dynamics greatly reduces the filter computational requirements with no accuracy penalties. These equations may be expressed in standard matrix form as

$$\dot{x} = Fx + Gw + u,\quad w(t) \sim N(O,\ Q)$$

The star tracker measurements are nonlinear functions of the state variables, corrupted by noise. Measurements are made at discrete times t_k:

$$z_k = h[x(t_k)] + v_k\ ,\quad v_k \sim N(O,\ R)$$

Vectors and matrices in the above equations are defined in Table 5-5. The white noise terms $w_1,\ w_2,\ w_3$ in the system equations represent gyro random

TABLE 5-5. SYSTEM MODEL FOR ATTITUDE ESTIMATION

System model

$$\dot{x} = Fx + Gw + u \qquad w(t) \sim N(0, Q)$$

Measurement model

$$z_k = h[x(t_k)] + v_k \qquad v_k \sim N(0, R_k)$$

Nomenclature

- x = state vector
- u = vector of known inputs
- w = process noise vector (white)
- F = system dynamics matrix
- G = noise distribution matrix
- z_k = measurement vector at time t_k
- h = nonlinear vector function of state
- v_k = purely random measurement noise sequence
- Q = process noise power spectral density matrix (diagonal)
- R_k = measurement noise covariance matrix (diagonal)

$$x = \begin{bmatrix} \phi \\ \theta \\ \psi \\ b_x \\ b_y \\ b_z \end{bmatrix} \qquad w = \begin{bmatrix} w_1 \\ w_2 \\ w_3 \\ w_4 \\ w_5 \\ w_6 \end{bmatrix} \qquad u = \begin{bmatrix} \hat{b}_x - \lambda\hat{\phi} - \hat{\omega}_o\hat{\psi} \\ \hat{b}_y - \lambda\phi - \hat{\omega}_o + \omega_o \\ \hat{b}_z - \lambda\hat{\psi} + \hat{\omega}_o\hat{\phi} \\ 0 \\ 0 \\ 0 \end{bmatrix}$$

$$F = \left[\begin{array}{ccc:c} 0 & 0 & \omega_o & \\ 0 & 0 & f & -I_{3\times3} \\ -\omega_o & 0 & 0 & \\ \hdashline & C_{3\times3} & & 0_{3\times3} \end{array}\right], \quad G = I_{6\times6}$$

Table 5-5 (continued)

For tracker 1

$$H_1 = \begin{bmatrix} H_{11} & H_{12} & H_{13} & 0 & 0 & 0 \\ H_{21} & H_{22} & H_{23} & 0 & 0 & 0 \end{bmatrix}$$

For tracker 2

$$H_2 = \begin{bmatrix} H_{31} & H_{32} & H_{33} & 0 & 0 & 0 \\ H_{41} & H_{42} & H_{43} & 0 & 0 & 0 \end{bmatrix}$$

drift errors which result in random walk of the integrated rate signal. b_x, b_y and b_z represent gyro drift stability, which is also modeled as random walks. Inclusion of the white noise terms w_4, w_5 and w_6 also guarantees that the system is uniformly completely controllable, which helps to ensure stability of the filter equations.

The Kalman filter algorithm which is mechanized in the on-board computer is summarized in Table 5-6. The matrix Q_k used in the filter time updates is given by

$$Q_k = \int_0^{\Delta t_k} \Phi(\Delta t_k - \eta) Q \Phi^T(\Delta t_k - \eta)\, d\eta$$

The expression for Q_k given in Table 5-6 is a second-order Taylor series expansion of the above integral, which is far simpler to evaluate on-board than the integral itself.

5.2.6 ACS Sensor Specification

Table 5-7 summarizes the performance requirements for the ACS sensors used for reference during the STORMSAT mission phase. The IRU drift stability and random drift specifications are required to achieve the ACS frame-to-frame stability requirement assuming dual tracker operation. Tracker performance is based on the manufacturer's quoted specification for the CT-401 from Ball Brothers Research Center.

5.2.6.1 Star Availability

The sensor boresight declination and hour angle for the STORMSAT star trackers were determined using star ephemeris tables. Star data is derived from a computerized table of 6199 stars with positions circa 1950. The equivalent magnitude using the CT-401 S20 detector was determined by modifying the visual magnitude by an amount found by assuming the star is a blackbody radiator of a temperature determined by its type and class.

TABLE 5-6. KALMAN AND JOSEPH CONVENTION FILTER FORMULATIONS

Time update

$$\dot{\hat{x}} = F\hat{x} + u$$

$$P_{k+1}(-) = \Phi(\Delta t_k) P_k(+) \Phi^T(\Delta t_k) + Q_k$$

$$Q_k = Q\Delta t_k + (FQ + QF^T)\frac{(\Delta t_k)^2}{2}$$

$$\Delta t_k = t_{k+1} - t_k$$

Evaluation of state transition matrix

$$\Phi(\Delta t) = \left[\begin{array}{ccc|ccc} c\zeta & 0 & s\zeta & \frac{\Delta s}{\omega_o} & 0 & \frac{1-c\zeta}{\omega_o} \\ 0 & 1 & 0 & 0 & t & 0 \\ -s\zeta & 0 & c\zeta & \frac{c\zeta-1}{\omega_o} & 0 & \frac{s\zeta}{\omega_o} \\ \hline \multicolumn{3}{c|}{0_{3x3}} & \multicolumn{3}{c}{I_{3x3}} \end{array}\right]$$

where $\zeta = \omega_o \Delta t_k$

Measurement update

$$\hat{x}(t_k^+) = \hat{x}(t-) + K_k[z_k - h(\hat{x}(t_k-))]$$

$$K_k = P_k(-) H_k^T [H_k P_k(-) H_k^T + R_k]^{-1}$$

$$P_k(+) = (I - K_k H_k) P_k(-) \quad \text{(Kalman) or}$$

$$P_k(+) = (I - K_k H_k) P_k(-) (I - K_k H_k)^T + K_k R_k K_k^T \quad \text{(Joseph)}$$

TABLE 5-7. ACS SENSOR REQUIREMENTS

Inertial Reference Unit	
Input range	
Acquisition	± 2.0 deg/sec
Slew maneuver	± 0.2 deg/sec
Operating	± 0.005 deg/sec
Output pulse quantization	
Acquisition	5.0 arcsec
Operating	⩾ 0.5 arcsec
Bandwidth	> 10 Hz
Sample rate	5 Hz
Sample noise	
1σ sample average (0.2 second)	0.65 arcsec
Power spectral density (PSD) units	2.0 $\mu rad^2/Hz$
Random drift	
1σ rate units	0.02 deg/hr
PSD units	0.01 $(\mu rad/sec)^2/Hz$
Drift stability	
1σ 12 hour change	0.003 deg/hr
PSD units	5.0×10^{-9} $(\mu rad/sec^2)^2/Hz$
Scale factor stability, 1σ 12 hour change	50 ppm
Alignment stability, 1σ 12 hour change	25 μrad
Temperature range (baseplate)	20 to 30°C
Fixed Head Star Tracker	
Field of view	
Acquisition	8° square
Operating	8° diameter
Boresight declination (both trackers)	43.5°
Boresight hour angle	
Tracker 1	+60°
Tracker 2	-60°
Sun rejection angle	19°
Star magnitude (S-20)	6.0
Star crossing frequency (average each tracker)	4 stars/hr
Inertial scan rate	15 deg/hr
Absolute pointing accuracy, 1σ each axis over acquisition FOV	3 arc min
Calibration accuracy, 1σ each axis over operating FOV	10 arcsec
Noise equivalent angle, 1σ sample average (1 sec)	3 arcsec
Output bandwidth	0.16 Hz
Output quantization	7 arcsec
Temperature range (baseplate)	20 to 30°C

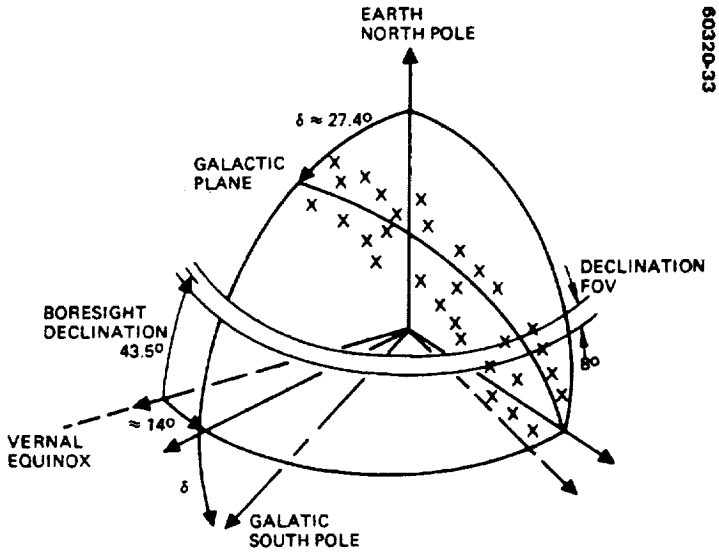

FIGURE 5-4. STORMSAT STAR SIGHTING GEOMETRY FOR 64PM-63 RATE SENSOR

The star sighting geometry for STORMSAT is illustrated in Figure 5-4. The majority of stars are located in the galactic plane (Milky Way), although useful stars are available at the galactic poles. Realistic boresight declinations are somewhat above (or below) the equatorial plane for sun avoidance during the ecliptic season and for moon and planet avoidance. Low latitudes are desirable however, both to maximize the solid angle which is scanned and to maintain high tracker angle sensitivity to pitch errors. These factors dictate declination angles between roughly 40 and 60°. As may be seen from Figure 5-4, this range of declinations implies sensor scan approximately through the sparse galactic pole region (north galactic pole during the winter and south galactic pole during the summer).

The results of a catalog search to determine boresight declination are given in Figure 5-5. Optimization of tracker boresight declination is based on the criteria of minimizing the maximum (single tracker) interval between sightings. Both northern and southern hemispheres are considered. In addition, the possibility of ± 1° of declination change was considered to avoid narrow minimums. Based on this search the nominal declination of 43.5° was selected. The maximum sighting intervals are 41 and 39 minutes for the northern and southern hemispheres, respectively.

5.3 PERFORMANCE ANALYSIS

In this section an error allocation for attitude pointing is developed. The starting point for these allocations is the STORMSAT ACS pointing requirements. In the pitch and roll channels these are 525, 11, and 4.2 μrad

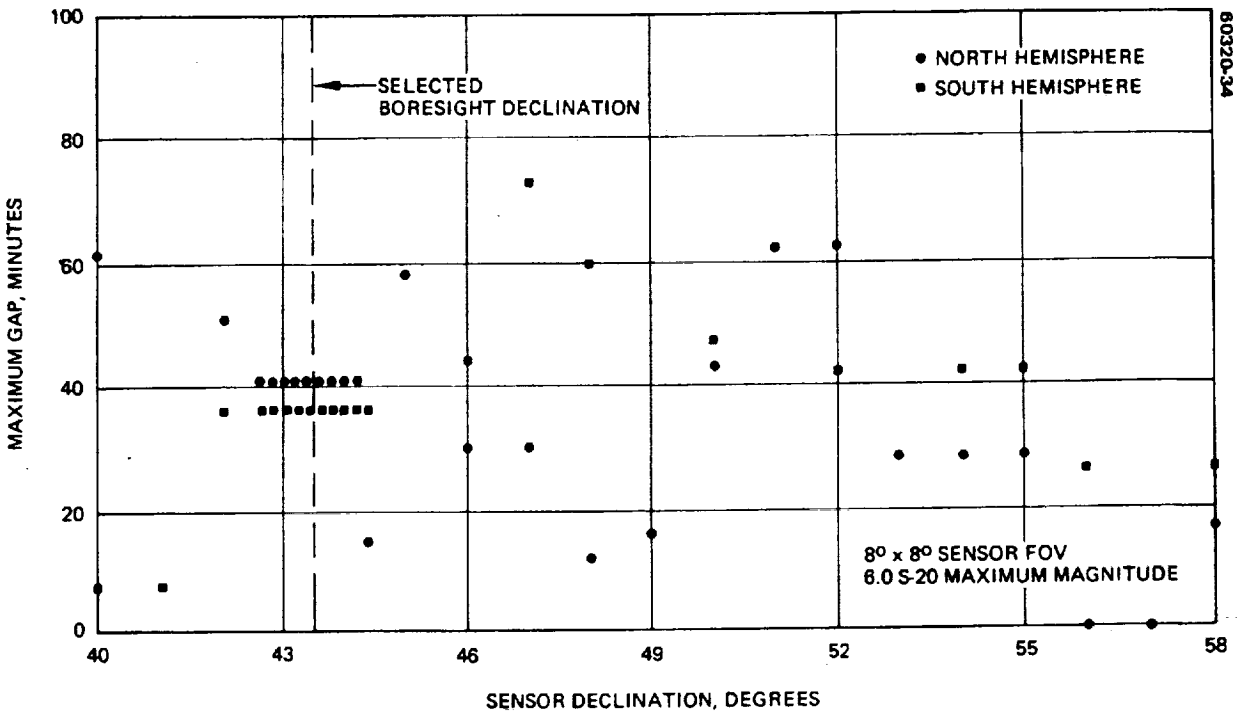

FIGURE 5-5. MAXIMUM GAPS IN STAR DATA VERSUS SENSOR DECLINATION FOR SYNCHRONOUS EQUATORIAL ORBIT

for the absolute pointing, 20 minute stability, and 8 second stability requirements, respectively. In the yaw channel these values are relaxed, as the AASIR line of sight errors are not as sensitive to spacecraft yaw motion as they are to pitch and roll motions.

Table 5-8 lists the contributions of all significant error sources influencing the attitude control pointing of the STORMSAT spacecraft. By the study contract ground rules, these errors relate only to the alignment between the local coordinate frame (i.e., local vertical, orbit normal) and the AASIR mounting plate. Errors contributed by the attitude sensors, processor, spacecraft structure, AASIR gimbal, and the spacecraft disturbances are included in the presented error allocation. Errors attributable to the AASIR assembly (exclusive of the gimbal) are not analyzed.

For budgetary purposes, attitude determination is defined as alignment error of the ACS module optical cube with respect to the local coordinate frame. Thus, the attitude determination allocation includes the alignment component between the ACS sensors and the optical cube. The alignment allocation between the ACS optical cube and the AASIR mount includes both structural/thermal alignment components and pitch bearing inaccuracies which contribute to position pointing errors.

TABLE 5-8. ATTITUDE CONTROL SYSTEM ERROR ALLOCATIONS

Error Source	ACS Pointing Error (1σ), μrad*								
	Roll			Pitch			Yaw		
	Absolute	20 min Stability	8 sec Stability	Absolute	20 min Stability	8 sec Stability	Absolute	20 min Stability	8 sec Stability
Attitude Determination Errors									
Fixed head tracker									
Random, N_S	10.9	3.7	–	12.2	3.9	–	8.9	3.8	–
Null alignment	100	0	0	100	0	0	100	0	0
Alignment stability	30	2.6	–	30	2.6	–	30	2.6	–
Processor									
Star ephemeris data	Combined with N_S			Combined with N_S			Combined with N_S		
Quantization	Combined with N_S			Combined with N_S			Combined with N_S		
Eccentricity residual	–	–	–	–	–	–	–	–	–
Inclination residual	–	–	–	–	–	–	–	–	–
Inertial reference unit									
Random drift, N_R	7.2	4.7	–	8.9	4.4	–	7.8	4.8	–
Drift stability N_A	18.0	4.0	–	31.0	4.5	–	23.2	4.9	–
Output noise, N_P	0.5	0.7	0.7	0.5	0.7	0.7	0.5	0.7	0.7
Scale factor stability	0	0	0	7.8	1.1	–	0	0	0
Alignment stability	2.2	0.5	–	0	0	0	2.9	0.6	–
RSS of attitude determination errors	107	7.7	0.7	110	8.0	0.7	108	8.3	0.7
AASIR Gimbal and Spacecraft Structural Errors									
Spacecraft structure									
Fixed alignment	126	0	0	126	0	0	126	0	0
Alignment stability	48.5	4.2	–	48.5	4.2	–	48.5	4.2	–
Gimbal structure									
Fixed alignment	50	0	0	50	0	0	50	0	0
Alignment stability	0	4.2	–	0	4.2	–	0	4.2	–
Gimbal servo									
Transducer accuracy/repeatability	0	0	–	20	4.0	0	0	0	0
Readout noise/quantization	0	0	0	0.6	0.8	0.8	0	0	0
Step settling time	–	–	–	–	–	–	–	–	–
Bearing									
Bearing friction	0	0	0	2.5	2.5	2.5	0	0	0
Bearing runout	2.0	2.0	–	0	0	0	2.0	2.0	–
RSS of gimbal and structural error	144	6.3	–	145	7.6	2.6	144	6.3	–

*Dash (–) indicates error of <0.5 μrad. Zero indicates no source influence.

TABLE 5-8 (continued)

Error Source	ACS Pointing Error (1σ), μrad*								
	Roll			Pitch			Yaw		
	Absolute	20 min Stability	8 sec Stability	Absolute	20 min Stability	8 sec Stability	Absolute	20 min Stability	8 sec Stability
Spacecraft Disturbances									
AASIR disturbance torques									
Steady state N-S scan	29	–	–	–	–	–	–	–	–
E-W AASIR step	–	–	–	–	–	–	–	–	–
Radiometer disturbance torques									
E-W step	–	–	–	2.0	2.0	2.0	–	–	–
N-S slew reversal	2.0	2.0	2.0	–	–	–	–	–	–
Solar panel disturbance									
Residual motion after reorient	–	–	–	–	–	–	–	–	–
Momentum wheel assembly									
Static unbalance	–	–	–	–	–	–	–	–	–
Dynamic unbalance	–	–	–	–	–	–	–	–	–
Solar torque disturbance	1.3	–	–	–	–	–	1.3	–	–
RSS of spacecraft disturbances	29.2	2.0	2.0	2.0	2.0	2.0	3.0	–	–
RSS of above	183	10.2	2.1	182	11.2	3.4	181	10.4	0.7
STORMSAT ACS budget allocation	525	11	4.2	525	11	4.2	3000	87	25

*Dash (–) indicates error of <0.5 μrad. Zero indicates no source influence.

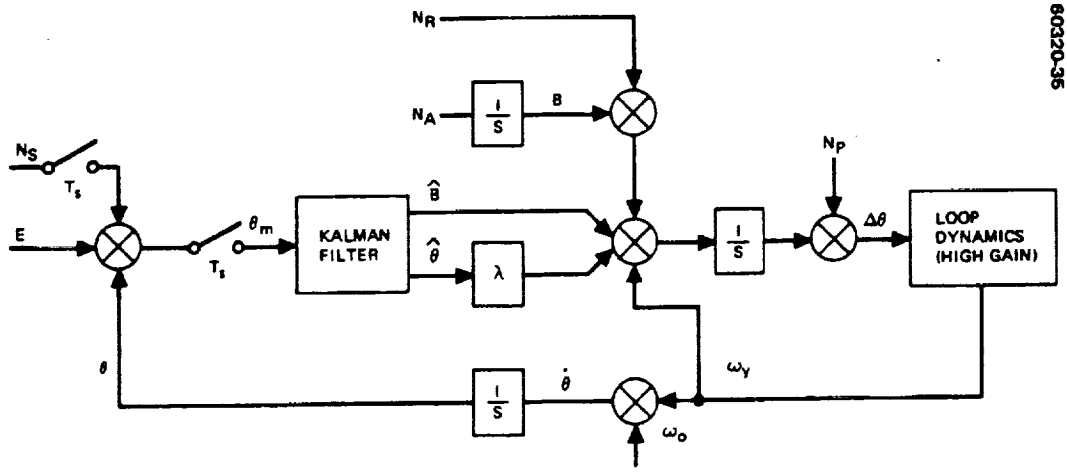

CONVARIANCE DEFINITION

$E\{N_R(t)\,N_R(t+\tau)\} = \delta(\tau)\,Q_R$
$E\{N_A(t)\,N_A(t+\tau)\} = \delta(\tau)\,Q_A$
$E\{N_P(t)\,N_P(t+\tau)\} = \delta(\tau)\,Q_P$
$E\{N_S(t+mT_s)\,N_S(t+nT_s)\} = \delta_{mn}\sigma_s^2$

FIGURE 5-6. ATTITUDE DETERMINATION PITCH ERROR MODEL

The remainder of this discussion treats the source contributions in detail. Two comments of a general nature are as follows:

1) Attitude determination errors and alignment drifts are the major contributors to frame-to-frame error. Contributions of roughly 6 to 8 μrad can be anticipated from each of these sources to the 20 minute stability error. The remainder is taken by dynamic errors due to payload motion; these short-period errors are bounded by the 4.2 μrad, 8 second stability requirement and, therefore, constitute only a minor component of the frame-to-frame requirement when included on an rms basis.

2) Satisfaction of absolute pointing requirements is not difficult, as component specifications meeting the stability requirements guarantees absolute performance well within ACS specification for all three channels. Yaw stability performance is likewise easily achievable for the same reason. Entries in Table 5-8 for absolute pointing and yaw stability reflect anticipated performance levels for the selected design point.

5.3.1 Attitude Determination Errors

The error model shown in Figure 5-6 describes the errors due to the attitude control sensors and attitude determination processing. Only the pitch loop is represented; the error effects in the roll and yaw channels are the same.

5.3.1.1 Fixed Head Tracker

A random error component for each star sighting is represented by the input N_S. This error is assumed to be uncorrelated from sample to sample (with standard deviation σ_s). The most significant component is due to sensor

TABLE 5-9. FIXED HEAD TRACKER ERRORS

Error Source	Source Variation	Error Variation,* arcsec	Calibration Technique	1σ Residual Error, arcsec
Nonlinearities over field of view (FOV)	8 by 8° FOV	500	10 term polynomial surface fit for each axis	±10
Ambient temperature	-10 to +50°C	120	1) Ambient temperature control $20 \leq T_A \leq 30°C$ 2) Calibrate for 2°C temperature increments	1.15
Star magnitude	+3 to +6	20	Calibrate for unit magnitude increments	1.44
Ambient magnetic field	±0.55 Gauss	40	Reduce ambient field to < 0.05 Gauss at tracker location	1.04
NEA and Quantization	NEA = 5 sec (1σ with 1 sec average)	–	Noise average for 16 seconds	1.25
RSS	–	–	–	10.3 (49.9 μrad)

*Absolute maximum variation over FOV with indicated source variation.

nonlinearities with star position over the field of view. Although the residual nonlinearity is repeatable, stars enter the field of view left edge at different latitudes, thereby randomizing the star-to-star error components in elevation and azimuth. Multiple sightings to average nonlinearities for a given star are possible if the star locations are widely separated in the tracker field of view so that samples are uncorrelated. A sighting separation of 2.5° (hour angle) is assumed so that three independent sightings may be made for each star as it passes through the field of view with sightings separated by 600 seconds. In general, more than one star will be in the field of view. Assuming an average of two stars, the average sample interval will be 300 seconds, and this value is assumed for each of the two trackers. The assumed error magnitude for σ_s is 50 μrad for each axis.

The foregoing assumptions are based on data supplied by Ball Brothers Research Center for a representative CT-401 tracker. Table 5-9 shows a breakdown of errors. Although the uncompensated errors far exceed the STORMSAT tracker requirements, these errors will be compensated using calibration data stored in the on-board computer. These calibration data will be stored as polynomial functions of star location in the tracker field of view with a surface fit for each axis of each tracker. A 10 term polynomial is used to reduce the residual error to less than 10 arcsec. Temperature and magnitude corrections will also be used. Baseplate temperature will be kept within 20° to 30°C, and observed star magnitudes will be between 2.0 and 6.0. Tracker errors are essentially linear between these limits and four calibrations will be supplied at the temperature and magnitude limits for on-board interpolation. These variables will be monitored with a temperature accuracy of ±1.0°C and a magnitude accuracy of ±0.5. For three trackers, each with two axes, and four calibrations for the temperature and magnitude end points, a total of 24 calibrations are required. On-board data storage of (24)(10) = 240 words of single precision will be required.

The star sighting assumptions are based on star catalog data which indicate that 100 to 200 stars (depending on hemisphere) per orbit will cross the field of view of each tracker at the design boresight declination of 43.5°. Assuming three uncorrelated sightings per star and the worst case (northern

hemisphere) availability, the average sighting frequency is 12 stars/hour. The possibility of three independent sightings is a judgemental assumption. Recognizing that a 10 coefficient surface fit is used to correct the calibrated error, the star track across the field of view is corrected by a third order polynomial which has a maximum of three zero crossings over the track line. The correlation angle along this track line may be scaled to the zero crossing interval, but with unknown scaling factor, which is of the order unity. The assumption of three independent sightings per star, therefore, cannot be fully defended, but appears reasonable. As discussed in Section 5.2.6, isolated intervals of roughly 40 minutes will occur when no stars will be available within the field of view of one of the trackers. With no star data available to either tracker, the attitude drift rate diverges as $0.003\sqrt{t}/(12)(3600)$, arcsec/sec. At t = 2400 seconds, when star sightings are resumed, the drift rate variation is 0.00071 arcsec/sec and the 20 minute drift is therefore less than one arcsec. These gap intervals occur only a few times per orbit and do not occur simultaneously for both trackers. The effect on frame-to-frame stability is therefore negligible.

Random noise and quantization effects will be averaged. With 12-bit quantization for each axis, the least significant bit (LSB) will be 7.03 arcsec and the 1σ error due to quantization will be 2.03 arcsec. Over several samples the quantization will be averaged by noise effects and so may be neglected. The rms noise error will be averaged as $1/\sqrt{t}$, and is reduced to low level after 16 second track interval.

The input E in Figure 5-6 is due to star sensor misalignment, both mechanical and electrical. This includes both a fixed component and a dynamic component that is assumed to be variable at orbit rate. For the absolute pointing error a fixed component of 100 μrad and a variable component of 30 μrad are allocated. The 20 minute stability error resulting from the variable components has a value of 2.6 μrad. Such an alignment stability is necessary to meet the attitude determination allocation in the presence of the sensor error sources due to the tracker and IRU.

5.3.1.2 Processor

ACS pointing errors similar to N_s may be attributed to the processor. Such errors result from star ephemeris errors and quantization. Each of these errors will be somewhat less than 1 arcsec and will be uncorrelated from star to star. Since calculations are made in local coordinates, the only significant processing error is due to quantization of the star celestial coordinates stored in the star catalog. The pointing contribution of each of these errors may be scaled to the tracker random contribution, as the influence is identical. For an upper bound of 5 μrad from these sources, the error contribution is less than 10 percent of that due to the 50 μrad tracker random error. These contributions may therefore be neglected.

The line of sight errors introduced by orbit eccentricity and inclination are not insignificant and require compensation by the processor. Spacecraft pointing is referenced to local coordinates, while the tracker and gyro measurements are inertially referenced and so satellite ephemeris must be provided. At geosynchronous orbit a spacecraft position error of 21 meters

results in a line of sight error of 0.5 μrad. As this positional accuracy is achievable, the residual error will be negligible.

5.3.1.3 Inertial Reference Unit

Three error sources are assumed for the IRU. Random drift of the integrated rate signal (i.e., random walk of measured attitude) is represented by the input N_R. This signal is characterized by a white noise power spectral density equal to Q_R in $(\mu rad/sec)^2/Hz$. It is often given in rate units (e.g., μrad/sec), and when so quoted is the integrated power spectral density below 0.5 Hz. For the random drift contribution to Table 5-8, the power spectral density for N_R is $Q_R = 0.01$ $(\mu rad/sec)^2/Hz$, corresponding to a random drift R_D, of 0.1 μrad/sec(≈0.02 deg/hr). The error contribution of N_R was determined by simulation which is described below.

Random drift of the gyro rate signal (i.e., random walk of drift rate) is represented by the input N_A. Physically, this represents a slow variation of bias torque about the output axis. As the spacecraft is rotating at orbit rate, pitch gyro scale factor variations will also contribute to N_A, as will roll and yaw gyro misalignment variation, given that such variations can be characterized as random walk. The assumed value for Q_A is 5.0×10^{-9} $(\mu rad/sec^2)^2/Hz$ corresponding to a random walk in drift rate of 0.003 deg/hr in 12 hours. The two gyro error contributions, as well as the contribution of the tracker random error, were determined by simulation as described below.

The input N_P represents IRU output noise due to internal effects (e.g., limit cycling, pickoff angle noise, and quantization) and is here represented by white noise with constant power spectral density, $Q_P = 2.0$ $\mu rad^2/Hz$. For an ACS closed loop bandwidth of 0.25 rad/sec this noise contributes 0.7 μrad to the 20 minute and 8 second budgets and 0.5 μrad to the absolute budget.

The errors introduced by gyro misalignments and scale factor variation of 25 μrad and 50 ppm, respectively, are modeled as random walks of 12 hour correlation period. Misalignments in roll and yaw couple with the 15 deg/hr orbit rate to produce 0.00037 deg/hr random walks in these axes. Scale factor variation couples with orbit rate to produce 0.00075 deg/hr random walk in this axis. These rates are one-eighth and one-fourth of the drift stability random walk and produce proportional errors.

DRIRU test data is shown in Figure 5-7. These data are supplied by the Singer Company-Kearfott Division. The STORMSAT required performance is also shown for comparison. For the three noise inputs modeled, the first difference curve is given by

$$\sigma_{\Delta\dot{\theta}} = (6 Q_P T_s^{-3} + 2 Q_R T_s^{-1} + \frac{2}{3} Q_R T_s)^{1/2}$$

which is asymptotic to $T_s^{-3/2}$, $T_s^{-1/2}$, and $T_s^{1/2}$ for short, intermediate, and long sample times, respectively. Thus, the first difference curve may be used for acceptance test given a suitable range of sample times.

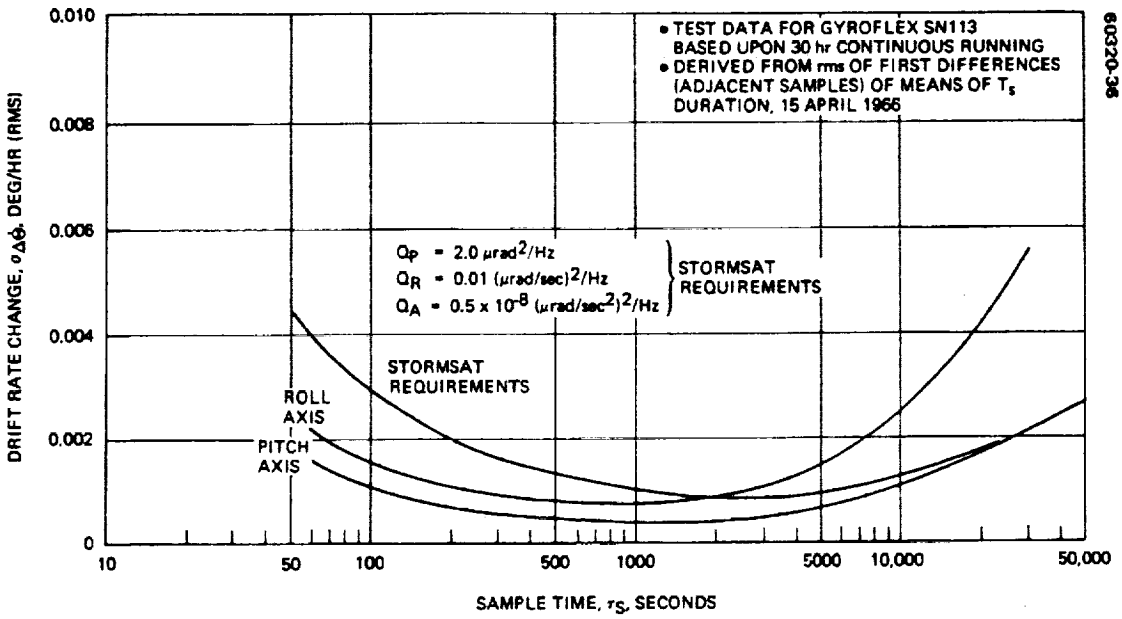

FIGURE 5-7. FIRST DIFFERENCE CURVE (DRIRU TEST DATA)

Comparison of STORMSAT IRU requirements with the test data demonstrates acceptable performance for the sample noise and random drift, represented by Q_P and Q_R, respectively. However, some difficulty is anticipated for acceptance of the drift stability requirement, represented by Q_A. This is indicated by violation of the STORMSAT requirement for long sample times. Although the pitch axis gyro would provide acceptable performance, the roll axis would be unacceptable. (These axes are test designations not necessarily coincident with spacecraft axes). Since the demonstrated long period performance is marginal it is recommended that suitable acceptance test procedures be adopted to eliminate units not meeting STORMSAT specification.

Three available floated inertial reference units could also be considered as candidates for the STORMSAT mission:

1) The Honeywell B5D PADS (with four Northrop G1K7G gyros) IRU designed for the Block 5D/Tiros-N would require improved random drift performance (by a factor of 3 to 4). This would be achieved either by an improved thermal design or by using the recently developed Honeywell Mod-Mig gyros.

2) The Honeywell GG2200 (three Honeywell GG334 gyros) IRU, which has flown on several classified missions, would satisfy all performance requirements for STORMSAT as demonstrated by test data made available by Honeywell.

3) The Bendix 64 PM RIG would also satisfy the STORMSAT IRU performance requirements as demonstrated by test data published by Bendix. This IRU is presently packaged in either a two gyro (HEAO) or a six gyro (IUE) configuration. Power spectral density

TABLE 5-10. SIMULATION RESULTS

No. Run	T_s	σ_S μrad	Q_R $(\mu r/sec^2)/Hz$	Q_A $(\mu r/sec^2)^2/Hz$	λ rad/sec	Covariance at t = 72 hours						Simulation rms for 72 hours					
						Attitude Estimate, σ_θ, μrad			Drift Estimate, σ_B, μrad			Absolute Accuracy σ_θ, μrad			20 Minute Stability, $\sigma_{\Delta\theta}$/20 minutes		
						R	P	Y	R	P	Y	R	P	Y	R	P	Y
Point Design	300	50	0.01	5×10^{-9}	10^{-4}	17.2	18.1	15.5	0.0052	0.0053	0.0051	23.5	37.5	26.0	7.2	7.6	7.0
1	300	50	0.01	2.5×10^{-9}	10^{-4}	15.8	16.6	14.2	0.0039	0.0040	0.0038	20	33	22	6.0	6.5	5.6
2	300	50	0.01	10^{-8}	10^{-4}	18.6	19.5	16.8	0.0065	0.0066	0.0063	27	42	30	8.4	8.8	8.4
3	300	50	0.01	6.25×10^{-10}	10^{-4}	13.5	14.2	12.3	0.0024	0.0024	0.0023	16	26	17	4.8	5.1	4.4
4	300	50	0.04	2.5×10^{-9}	10^{-4}	17.0	17.8	15.5	0.0042	0.0042	0.0041	22	37	26	9.0	9.1	8.2
5	300	50	0.0025	2.5×10^{-9}	10^{-4}	15.4	16.2	13.9	0.0038	0.0039	0.0037	19	32	21	4.9	5.7	5.0
6	1200	50	0.01	2.5×10^{-9}	10^{-4}	26.7	28.2	24.1	0.0047	0.0047	0.0046	30	45	32	7.3	8.0	7.7
7	300	10	0.01	2.5×10^{-9}	10^{-4}	5.3	5.5	4.9	0.0029	0.0029	0.0028	10	14	12	5.0	4.6	4.4
8(1)	300	50	0.01	2.5×10^{-9}	10^{-5}	67.7	67.3	37.6	0.0050	0.0054	0.0064	89	93	52	11.8	11.6	8.2
9(1)	300	50	0.0025	6.25×10^{-10}	10^{-4}	51.9	51.7	28.5	0.0030	0.0031	0.0042	72	73	40	7.8	7.6	5.3
10(2)	300	50	0.01	2.5×10^{-9}	10^{-4}	15.9	20.6	18.7	0.0038	0.0042	0.0041	20	37	25	6.1	6.8	5.9
11(3)	300	50	0.01	10^{-8}	10^{-4}	9.3	9.2	17.7	0.0034	0.0033	0.0041	13	20	25	5.4	5.4	5.9

Tracker boresights at ±60° hour angle (wrt zenith and 43.5° declination (wrt orbit plane).
T_s is star sample period per tracker.

NOTES: (1) Single tracker only, data for six orbits.
(2) Single MACS tracker plus payload tracker at zero hour angle.
(3) Single MACS tracker plus payload earth horizon sensor (NEA = 400 μrad at 1 second) for pitch and roll.

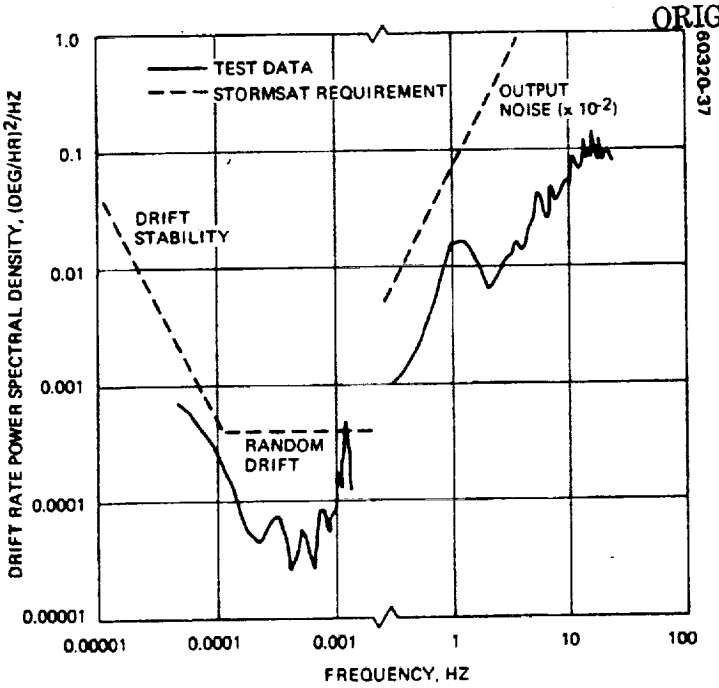

FIGURE 5-8. DRIFT RATE POWER SPECTRAL DENSITY

results are presented in Figure 5-8 for this gyro; also shown are STORMSAT power spectral density requirements. The output noise requirement is shown reduced by a factor of 100. The figure shows that the STORMSAT specification is met over virtually the entire spectrum.

5.3.1.4 Simulation Results

The major components of attitude determination error are due to tracker and IRU random errors. A three-axis digital simulation based on the equations given in Section 5.2.5 was used to determine the influence of these errors. The sensor noise model for this simulation includes the N_A, N_R, N_S noise inputs shown in Figure 5-6 and described previously. The results of several runs from this simulation are given in Table 5-10. The point design run is based on sensor requirements as specified in Table 5-7, and the results of this run are included in the error allocations of Table 5-8 for N_S, N_R, and N_A.

Runs 1 through 7 show sensitivity to the noise parameters. Taking run 1 as a nominal case for the parameters, the sensitivity to gyro drift stability is shown by runs 2 and 3, while runs 4 and 5 show sensitivity to gyro random drift. Run 6 shows influence of increased tracker sample period, while run 7 shows influence of improved tracker sample random error.

Single tracker performance is given by runs 8 and 9. The pitch and roll ACS stability performance for the nominal parameters violates the 11 rad allocated to all sources, while run 9 using a high performance gyro provides acceptable performance. It may be concluded from these two runs that

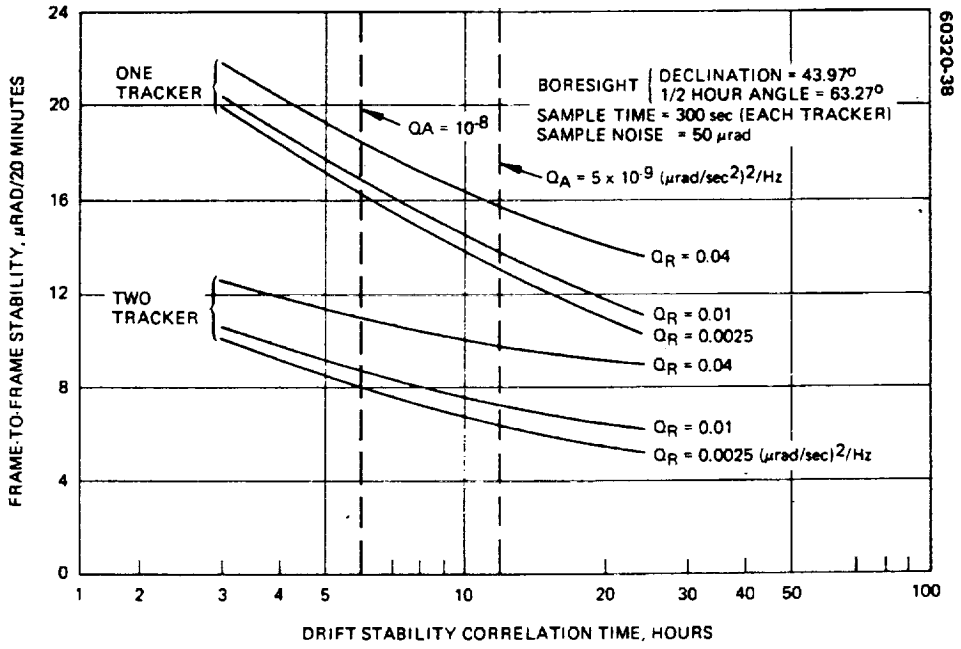

FIGURE 5-9. LONG TERM STABILITY VERSUS DRIFT STABILITY

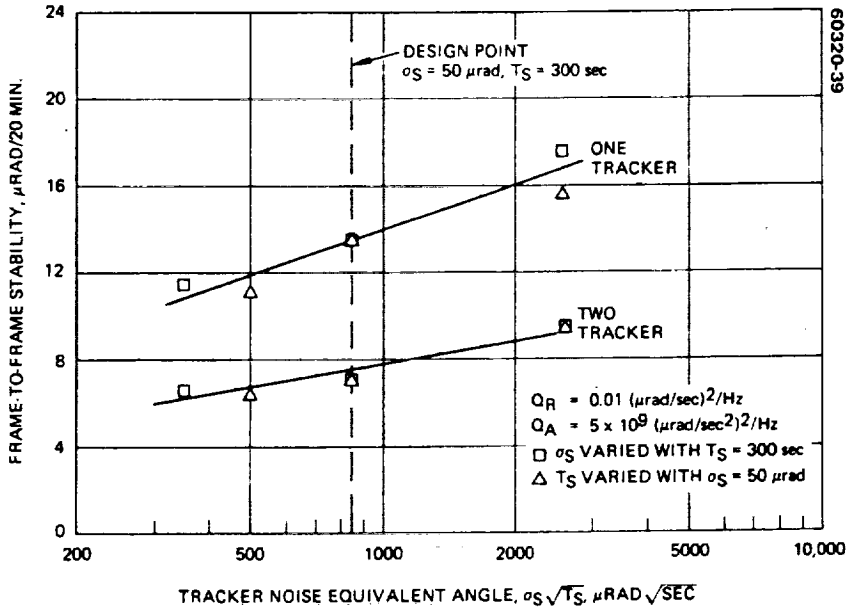

FIGURE 5-10. LONG TERM STABILITY VERSUS TRACKER NOISE

either a backup tracker or an improved IRU is needed to provide acceptable performance with single tracker failure. As shown by run 10, the backup tracker used with one of the primary trackers provides acceptable performance.

Figure 5-9 shows the frame-to-frame pointing stability as a function of IRU drift stability for several values of random drift error. In this figure, correlation time is defined as the time for the rms IRU drift rate to random walk to 0.003 deg/hr.

Figure 5-10 relates tracker errors to spacecraft pointing stability. The influence of star sighting interval is also included. The influence of sample noise and sample interval is combined in the parameter $\sigma_s\sqrt{T_s}$, which normalizes the sighting error to a sample interval of 1 second. This functional dependence is demonstrated for the simulated results shown.

An attractive STORMSAT option is an earth horizon sensor for pitch and roll reference. Performance capabilities with one tracker augmented by a horizon sensor are given in run 11. The effects of long-term horizon drift are not included. This run indicates the potential for satisfaction of STORMSAT requirements with relatively modest IRU drift requirements.

5.3.2 AASIR Bearing and Spacecraft Structural Errors

The following section describes errors occurring between the ACS optical cube and the AASIR mount. With the exception of short term gimbal servo errors which impact the 8 second short term stability, the dominant influence of errors in this class is on the frame-to-frame allocation.

5.3.2.1 Spacecraft Structure

The alignment path for these errors consists of: 1) MACS optical cube to the MACS module mounting reference, and 2) MACS module mounting reference to the payload module reference which will be taken as the AASIR bearing mount on the spacecraft side. Preliminary MACS specification for path (1) are as follows:

Absolute alignment	<200 arcsec
Actual alignment	to be measured
Uncertainty of measurement	<3 arcsec
Alignment stability - (12 hour)	<5 arcsec
- (continuous)	<10 arcsec

Fixed alignment will be measured and removed using the computer. The residual (worst case) 13 arcsec for path (1) is summed with an assumed equal error for path (2) to compute the absolute entries for fixed alignment of 126 μrad in Table 5-8. The alignment stability entry is based on 24-hour

TABLE 5-11. SPACECRAFT DISTURBANCE SOURCES

Assembly	Mass Properties	Gimbal Point Coordinates W rt S/C CM	Mass Center W rt Gimbal Point	Assembly Motion	Disturbance Interval, second	Spacecraft Motion Without ACS Compensation	ACS Wheel Torque Profile to Maintain Attitude Null for Disturbance			Spacecraft Residual Motion With ACS Compensation
							Profile Type	Peak Torque, ft-lb	Peak Momentum, ft-lb-sec	
AASIR Mirror	J_x = 0.26 kg-m^2 (0.20 slug-ft^2)		0	N-S sine scan at 0.387 Hz of ±6.35°	Continuous	Roll sine of ±29 μrad p-p	Sine at 0.387 Hz	0.13	0.05	Roll sine of ±29 rad peak
AASIR Assembly	J_y = 6.8 kg-m^2 (5.0 slug-ft^2)	x = 1650 mm (5 ft)	x = 0	E-W step of 4125 μrad amplitude	1.29	Pitch step $\Delta\theta$ = 10 μrad	Doublet over Δt = 1.29 sec	0.05	0.032	0.25 μrad
		y = 0 z = 0	y = 0 z = 0	E-W step of 375 μrad amplitude	0.5	Pitch step $\Delta\theta$ = 1.0 μrad	Doublet over Δt = 0.5 sec	0.003 0.03	0.008 0.008	0.025 μrad
MASR Assembly	m = 73 kg (5 slugs)	x = 3280 mm (10 ft)	x = 2 ft	E-W step = 0.8 mr	4.4	Pitch step $\Delta\theta$ = 80 μrad	Doublet over Δt = 4.4 sec	0.033	0.073	2.0 μrad peak
	J_x = 34 kg-m^2 (25 slug-ft^2) J_y = 135 kg-m^2 (100 slug-ft^2)	y = 0	y = 0	E-W step = 0.8 mr	2.75	Pitch step $\Delta\theta$ = 80 μrad	Doublet over Δt = 2.75 sec	0.084	0.117	2.0 μrad peak
	J_z = 34 kg-m^2 (25 slug-ft^2)	z = 0	z = 0	N-S slew reversal ±0.29 mr/sec	4.4	Roll ramp $\Delta\Phi$ = 20 μrad/sec	Impulse Δt = 4.4 sec	0.0033	0.015	2.0 μrad peak
				N-S slew reversal ±0.29 mr/sec	2.75	Roll ramp $\Delta\Phi$ = 20 μrad/sec	Impulse Δt = 2.75 sec	0.0053	0.015	2.0 μrad peak
Solar Panel	J_y = 68 kg-m^2 (50 slug-ft^2)	–	–	Panel slew from zero to 10 deg/min	10	Pitch ramp - 73 μrad/sec	Impulse Δt = 10 sec	0.015	0.15	

Spacecraft MOI: I_x = 1010 kg-m^2 (750 slug-ft^2), $I_y = I_z$ = 2700 kg-m^2 (2000 slug-ft^2)

sine 5 arcsec rms amplitude error over path (1) summed with an equal error over path (2). This results in 48.5 μrad absolute error and (48.50) $(2\pi)(20)/(60)(24) = 4.2$ μrad rms error over 20 minutes.

5.3.2.2 Bearing Support Structure

A 50 μrad allocation is given to fixed alignment between bearing mount and the AASIR mount. A 4.2 μrad allocation is given to the frame-to-frame variation. This is due to motor operation with varying duty cycle and other AASIR associated thermal gradient effects.

5.3.2.3 AASIR Positioner Servomechanism

Electrical and mechanical effects contributing to resolver readout absolute accuracy and repeatability, but not including electrical noise and quantization effects, have been measured as 20 μrad accuracy and 4 μrad repeatability for an available 72 speed resolver of 7 inch outside diameter manufactured by American Electronics. These values will be assumed as transducer contributions to the STORMSAT absolute and 20 minute budgets, respectively.

Sample noise due to quantization and random electrical noise will cause error due to high servo bandwidth. The contribution from this source to the stability budgets is calculated as $\sigma_p\sqrt{\omega_G T_p}$ where σ_p is the pickoff noise at the sample period, T_p, and ω_G is the closed-loop gimbal servo bandwidth. Assume sample noise of 3.0 μrad at 2000 Hz sample frequency. For dominant pole servo bandwidth of 140 μrad/sec. The stability error will equal $3.0\sqrt{140/2000} = 0.8$ μrad. This calculation assumes comparison of two measurements which are uncorrelated. The contribution to the absolute budget is the rms of the individual measurement and so is reduced by $1/\sqrt{2}$.

As the servo response time is small relative to the required step time of 0.5 second, the AASIR is well settled and so no contribution is given for this source. This is a result of the high gimbal bearing friction and resulting high servo bandwidth needed to meet the short-term stability requirement. Servo design is discussed in Section 4.1.1.5.

5.3.2.4 Bearing

If bearing friction is assumed to be less than 0.7 N-m (0.5 ft-lb) for dc torque gain equal to 0.27 MN-m/rad (200,000 ft-lb/rad) the maximum steady state pitch line of sight error due to friction will be 2.5 μrad. This value will be allocated for the 1σ pitch absolute and stability errors due to friction. Bearing runout due to ball eccentricity, Brinell spots, particulate contamination, race flatness, etc., will contribute to roll and yaw absolute pointing errors. In addition, a portion of this runout will be nonrepeatable and contribute to frame-to-frame errors. An allocation of 2 μrad is assumed for these errors.

5.3.3 Spacecraft Disturbance Errors

The major sources of spacecraft disturbance are summarized in Table 5-11. The rigid body model used to determine spacecraft motion is

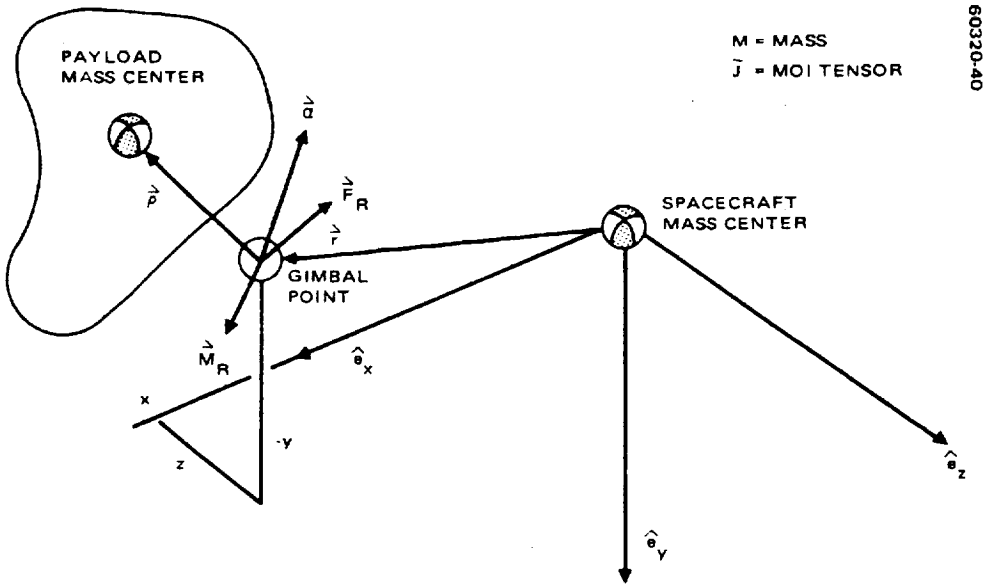

FIGURE 5-11. ARTICULATED STRUCTURE DISTURBANCE MODEL

shown in Figure 5-11. Disturbances due to payload or solar panel motion result from reaction torques and forces acting at the gimbal. Reaction torques are computed as $\vec{M}_R = -\tilde{J}\ \vec{\alpha}$, where $\vec{\alpha}$ is the inertial angular acceleration and $\tilde{J}$ is the moment of inertia tensor of the articulated structure about the gimbal point. In this equation, gyroscopic terms, which produce negligible added reaction torques, have been omitted to simplify the analysis. Because the spacecraft translational and rotational motions are small compared with motion of the gimbaled structure, the effect of such motion on disturbance torques may be neglected in a first order analysis. This is equivalent to assuming infinite spacecraft inertia properties. Reaction forces are computed as $\vec{F}_R = \vec{\rho}_m \times \vec{\alpha}$ where m is the mass of the structure and $\vec{\rho}_m$ is the structure mass center relative to the gimbal center of rotation. The translational spacecraft motion induced by these forces is negligible. However, if the force is not acting through the spacecraft mass center then significant attitude motion may result. The disturbance torque produced by the reaction force is equal to $\vec{r} \times \vec{F}_R$. where $\vec{r}$ is the gimbal station relative to the spacecraft mass center. The net disturbance may be summarized as

$$\vec{T}_D = -\tilde{J}\cdot\vec{\alpha} + \vec{r} \times (\vec{\rho}_m \times \vec{\alpha})$$

and this relation has been used to compute attitude response to articulated motion as summarized in Table 5-11. Spacecraft attitude residual motion without ACS compensation is shown. In all cases except for the north-south mirror scan, the ACS will remove the residual motion by open loop wheel speed control. Wheel torque and momentum magnitudes to null the residual motion are presented.

AASIR mirror scan for full earth coverage results in ±29 μrad of spacecraft roll motion. As this is repeatable from line-to-line and frame-to-frame no significant AASIR pointing errors result. This motion is also

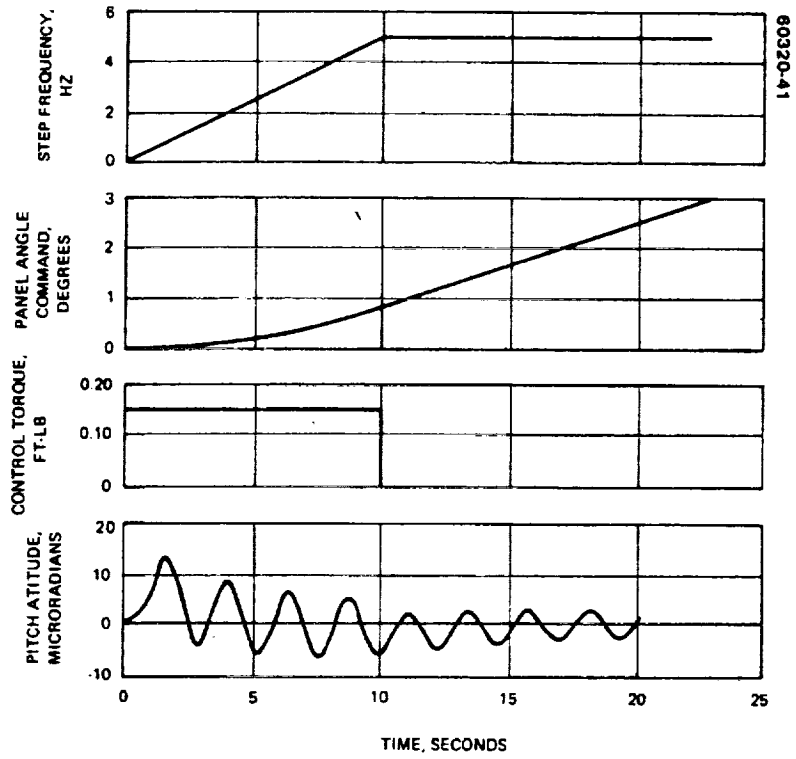

FIGURE 5-12. STORMSAT PANEL REORIENTATION ANALYSIS

small relative to MASR pointing requirements. The wheel torque level required for compensation would result in high continuous wheel power. Therefore, compensation is not used for this disturbance. With the exception of fast east-west radiometer steps (i.e., significantly less than 1.0 second) the remaining residual disturbances can be managed with the momentum wheels. This is true even without payload compensation, as wheel torque levels to directly compensate payload disturbances are within wheel motor torque limits. As the step or slew reversal interval becomes comparable to the modal period, the attitude motion at the flexible interaction frequency becomes comparable to the residual rigid body motion shown. The ACS cannot easily compensate these effects. In the present spacecraft configuration the first modal frequency is above 10 Hz and greater than 10:1 separation between the minimum disturbance interval, and the first mode period should preclude excessive flexible motion. Because of the large MASR inertia, it is not recommended that step or slew reversal intervals less than 2.0 seconds be employed.

Figure 5-12 shows spacecraft and solar panel motion in response to panel stepping at 5 Hz with step sizes of 1 arcmin. The corresponding slew rate of 5 deg/min is compatible with panel reorient during payload retrace intervals when disturbances are acceptable. Two techniques are employed to reduce the residual disturbance: First, the step frequency is ramped over a 10 second interval to the steady-state 5 Hz rate. This effectively limits the acceleration and, consequently, the spacecraft disturbance torque. Second, the pitch momentum wheel is torqued at a fixed value over the same

10 second interval to nominally counter the panel disturbance. Residual motion shown in Figure 5-12 is due to step quantization and the 0.5 Hz panel flexible mode. The startup motion shown is reversed at the end of the maneuver and residual motion would be on the order of that shown at 10 seconds with 0.5 percent damping. This motion is damped less than 3 μrad within 1 minute of maneuver conclusion, and less than 1 μrad within 2 minutes.

As may be seen, the uncompensated spacecraft motions due to payload and solar panel disturbances far exceed the pointing stability requirements. The largest error is due to MASR motion. East-west stepping results in a peak pitch error of 80 μrad. As the roll ACS bandwidth is 0.25 rad/sec, the peak roll error due to north-south slew reversal is (20 μrad/sec)/(0.25 rad/sec) = 80 μrad also. Reduction of these errors to less than 2.0 μrad requires torque compensation to less than 2.5 percent. With open loop compensation the largest error residual is due to wheel motor torque scale factor variations. To achieve the required residual accuracy, the error resulting from payload motion will be continuously monitored by observing the IRU output following the disturbance events. The IRU output noise of 0.65 arcsec requires averaging of only three disturbance profiles to reduce the residual to less than 2 μrad. Storage of motor torque profiles over a maximum interval of 2.75 seconds at 0.2 second sample rate requires only 4 storage locations. Thus compensation to 2.5 percent appears reasonable.

The solar panel will be reoriented during periods when the payload is not in use. The slew profile will be limited to a maximum acceleration of 0.0166 deg/sec^2 and a maximum rate of 0.166 deg/sec (10 deg/min). For a panel natural frequency of 2 radians/second, the panel motion will be approximately (0.0166 deg/sec^2)/(2 rad/sec)^2 = 0.0042°. The spacecraft motion will be reduced by the ratio of moments of inertia to 0.000105° (1. : μrad). Acceleration limiting is achieved by varying the panel stepper frequency from zero to maximum rate (or vice-versa) over a 10 second interval. Some panel excitation will result during this sweep. Simulation indicates a panel excitation of one half the step size. For a step size of 0.0333°, the spacecraft motion is 0.00042° (7.2 μrad). With a panel damping ratio of 0.01, the damping time constant will be 50 seconds. The residual spacecraft motion will be reduced to less than 1.0 μrad within 100 seconds of panel slew completion, and so does not contribute to pointing errors during steady-state AASIR operation.

Wheel static and dynamic mass unbalance can cause disturbance at wheel spin speed. Assume a dynamic mass unbalance of 1.0 oz-in^2 and spacecraft moment of inertia of 750 ft-lb-sec^2. The resulting vehicle motion assuming spin speed below the first mode resonance (≈ 10 Hz) will be roughly 0.06 μrad. Comparable vehicle motion will result from static unbalance (e.g., 0.05 oz-in with wheel mass center 20 inches from spacecraft mass center). These levels are negligible and have been so entered in the pointing budget.

The only significant external disturbance is due to solar torques. Based on a torque gain constant of 75 ft-lb/rad the steady state attitude error due to solar torques less than 10^{-4} ft-lb will be 1.3 μrad. The pointing variation over 20 minutes is entirely negligible as this torque varies at orbit rate.

5.4 INTERFACE REQUIREMENTS

5.4.1 Mechanical Interface

The STORMSAT mission requires stringent alignment stability between the ACS module and the payload module. Based on error allocations to meet the frame-to-frame pointing stability requirement, the 1σ angular alignment between the ACS module optical cube and the payload module shall be less than 1 arcsec over any 20 minute interval in all three axes.

5.4.2 Electrical Interfaces

5.4.2.1 C&DH Module

Tables 5-12, 5-13, and 5-14 summarize signal flow between the ACS module and the C&DH module. Magnetometer and magnetic torquer signals, as well as the redundant IRU are not used for the STORMSAT mission but shown for completeness.

5.4.2.2 Propulsion Module

The STORMSAT mission requires ACS interface to the propulsion module so that any of the 12 0.2 lbf desaturation thrusters can be fired by commands from the ACS.

5.4.2.3 Solar Array

The STORMSAT mission requires coarse sun sensor information for use during the backup survival model. The reference panel position will be such that the vehicle longitudinal axis will be parallel to the sun line with the propulsion module facing the sun.

5.4.2.4 Payload Module

No direct interface between the ACS module and the payload module is required for the STORMSAT mission. Event signals to the on-board computer in the C&DH module are required to counter disturbance events as follows:

1) AASIR step (375 μrad)
2) AASIR step (4125 μrad)
3) AASIR retrace (start to finish)
4) MASR step (positive E-W)
5) MASR step (negative E-W)
6) MASR slew reversal (positive N-S)

7) MASR slew reversal (negative N-S)

8) Solar panel slew (start to finish)

In addition the fixed head tracker will supply two axis data to the on-board computer for attitude control.

5.5 POTENTIAL PROBLEM AREAS

The analysis presented in Section 5.3 indicates that acceptable STORMSAT attitude control pointing can be achieved with the MMS. It is recommended that further study be conducted in the following areas to reinforce this conclusion:

5.5.1 Flexible Modes Analysis

The AASIR and MASR inertia properties are a significant fraction of other total spacecraft inertia. Repetitive and uncompensated payload motion can excite vibration modes causing pointing jitter potentially exceeding the 4.2 μrad short term stability allocation. A complete modal analysis should be conducted to determine compensation levels and payload motion constraints compatible with the disturbance allocations presented herein.

5.5.2 Control Loop Interaction

The stringent pointing stability required for the STORMSAT mission requires very high gains and closed-loop bandwidths for the AASIR and MASR pointing loops. The potential for unstable modes should be analyzed considering flexible interaction effects using the modal data produced by the flexible modes analysis. This analysis should assume a realistic model of bearing static and dynamic friction and should include simulation for performance verification.

5.5.3 Sensor Performance Verification

The STORMSAT mission requires stringent attitude control stability relative to other MMS missions. Due to the relatively large random component of star tracker measurements, a large number of sightings are needed to accurately update gyro drift. This results in a tight requirement on gyro drift stability so that drift rate changes during the update interval do not invalidate the update drift estimate. Drift rate stability of less than 0.003 deg/hr change in 12 hours is required to achieve the STORMSAT frame-to-frame stability requirement.

TABLE 5-12. INTERFACE REQUIREMENTS – ACS SENSORS (TO C&DH)

Unit	Unit Characteristics	Required Word Size	Minimum Required Word Rate to Computer	Total Bits Required for Interface
Star sensor (two per spacecraft – both operating at once)	8 by 8° field of view (FOV) 7 sec resolution 2 axis	2^{12} bits/axis	1 word/sec	2 sensors x 2 axes x 12 bits/axis = 48 bits
Inertial reference unit (two per spacecraft – one operating at one time	2/0.2 deg/sec rate 1/0.1 sec/bit resolution 3 – 2 axis gyros	2^{12} bits/axis	1 words/sec	3 gyros x 2 axes x 12 bits/axis = 72 bits
Precision digital sun sensor (one per spacecraft)	64° x 64° FOV 0.004° resolution 2 axis	2^{14} bits/axis	1 word/sec	1 sensor x 2 axes x 14 bits/axis = 28 bits
Coarse sun sensor (two per spacecraft – one operating at a time)	4 steradian FOV 1° resolution (assumed) 2 axis	2^8 bits axis/hemi-sphere	1 word/sec	2 sensors x 2 hemi-spheres x 2 axes x 8 bits/axis/hemisphere = 64 bits
Magnetometer (one per spacecraft) (not used for STORMSAT)	0.5 Gauss full scale 0.0005 Gauss resolution (assumed) 3 axis	2^{10} bits/axis	1 word/sec	1 sensor x 3 axes x 10 bits/axis = 30 bits
Reaction wheel absolute speed (four per spacecraft – all operating at once)	0 to ± 2500 rpm 1% of full scale resolution (assumed) 1/wheel	2^7 bits/axis	1 words/sec	4 wheels x 7 bits/wheel – 28 bits
			Total Sensors	270 bits

TABLE 5-13. INTERFACE REQUIREMENTS – ACS COMMANDS (FROM C&DH)

Command	Command Characteristics	Required Word Size	Minimum Required Word Rate For Computer	Command Type and Total Bits Required for Data Bus Interface
Reaction wheel torque command (four wheels per spacecraft)—all could be operating at once	0 to ± max. torque ± 0.2 percent F.S. resolution (assumed)	2^{10} $\frac{\text{bits}}{\text{Wheel}}$ (4 commands)	5 $\frac{\text{words}}{\text{sec}}$	Serial digital 4 wheels x 10 bits/wheel + 4 cmds x 4 address bits = 56 bits
Magnetic torquer command (not used for STORMSAT)	Zero or (+) full scale or (-) full scale (Ternary)	2 $\frac{\text{bits}}{\text{Torquer}}$ (1 command)	5 $\frac{\text{words}}{\text{sec}}$	Serial digital 3 torquers x 2 bits/torquer + 4 address bits = 10 bits
Star sensor control command	Bilevel control information	10 bits for both sensors	5 $\frac{\text{words}}{\text{sec}}$	Serial digital 10 bits + 4 address bits = 14 bits
Sensor control command	Bilevel control information	11 bits for IRU's and magneto-meters	5 $\frac{\text{words}}{\text{sec}}$	Serial digital 11 bits + 4 address bits = 15 bits
Electronic control command	Bilevel control information	10 bits total	5 $\frac{\text{words}}{\text{sec}}$	Serial digital 10 bits + 4 address bits = 14 bits
Unit power control	Bilevel control information	6 bits total	5 $\frac{\text{words}}{\text{sec}}$	Individual pulse commands = 6 bits
			Total Command	115 bits

TABLE 5-14. INTERFACE REQUIREMENTS – ACS TELEMETRY*

Telemetry	Telemetry Type	Required Number of Bits	Minimum Information Rate at Slowest Telemetry Bit Rate = 1 kbps	Total Bits Required for Data Bus Interface
Unit on-off status – (reaction wheels and magnetic torquers)	Individual bilevel status information	7 bits total (1 word)	once/second	7 bits
Sensor status	Individual bilevel status information	16 bits total (2 words)	once/second	16 bits
Electronics status	Individual bilevel status information	5 bits total	once/second	5 bits
Temperature sensors (25 sensors)	Thermistor analog (1 mA constant current)	8 bits/sensor	Subcommutated one readout/sec	None (A/D in remote unit)
Miscellaneous analog	0 to 5 V analog	8 bits/measurement	Subcommutated one readout/sec	None (A/D in remote unit)
			Total Telemetry	28
			Command	115
			Sensor	270
			Total	413

*Over and beyond what is already sent to computer from the sensors, or computed by the computer itself.

6. STORMSAT PAYLOAD, TELEMETRY, TRACKING, AND COMMAND DATA SYSTEM

The STORMSAT communications and data handling (C&DH) subsystem consists of the mission-unique high rate data transmission subsystem (HRDTS) and the communications and data handling module (C&DHM) of the Multimission Modular Spacecraft (MMS). The HRDTS is divided into signal processing and telecommunications equipment.

The high rate signal processor (HRSP) has signal conditioning, multiplexing, analog-to-digital conversion, buffer storage, formatting, and associated timing and control elements whose function is the on-board acquisition and processing of AASIR, and MASR data in a format suitable for the telecommunications group. In addition, the HRSP is to acquire and process selected payload housekeeping data necessary for ground based radiometric and geometric correction of the primary payload sensor data. The wideband RF telecommunications group has a quadraphase shift keyed (QPSK) modulator, local oscillator, upconverter, 30 watt S band transmitter, earth coverage antenna, RF coupling coax, waveguide, and optional RF switch. The digital bit stream data output from the HRSP provides appropriately formatted, differentially encoded pulse code modulation (PCM) input for this group. All of the HRDTS elements are located on the mission module.

The functions of the C&DHM are to acquire, process, and transmit spacecraft telemetry; receive, decode, and distribute command data on a realtime and stored basis; and transpond Goddard range and range rate (GRARR) tracking signals. It is a subsystem of the MMS. This subsystem is physically located in an MMS module, with the exception of: 1) its interfacing telemetry and command data units, the remote interface units (RIU), which are physically located on the STORMSAT mission module, 2) the two hemispherical coverage S band antennas, one or both of which may be boom-deployed from the mission module, and 3) the optional switchable RF interface with the high gain earth coverage HRDTS antenna located on the mission module. The elements of the MMS/C&DHM subsystem discussed briefly in Subsection 6.2.3 are: 1) central unit consisting of command decoder, format generator, spacecraft clock, bus controller, 2) premodulation processor, 3) multiplex data bus, 4) RIUs, 5) onboard computer (OBC), 6) standard computer interface, and 7) Spaceflight Tracking and Data Network (STDN) compatible transponder/demodulator. The overall STORMSAT data system functional flow and physical distribution relative to the mission adapter is shown in Figure 6-1.

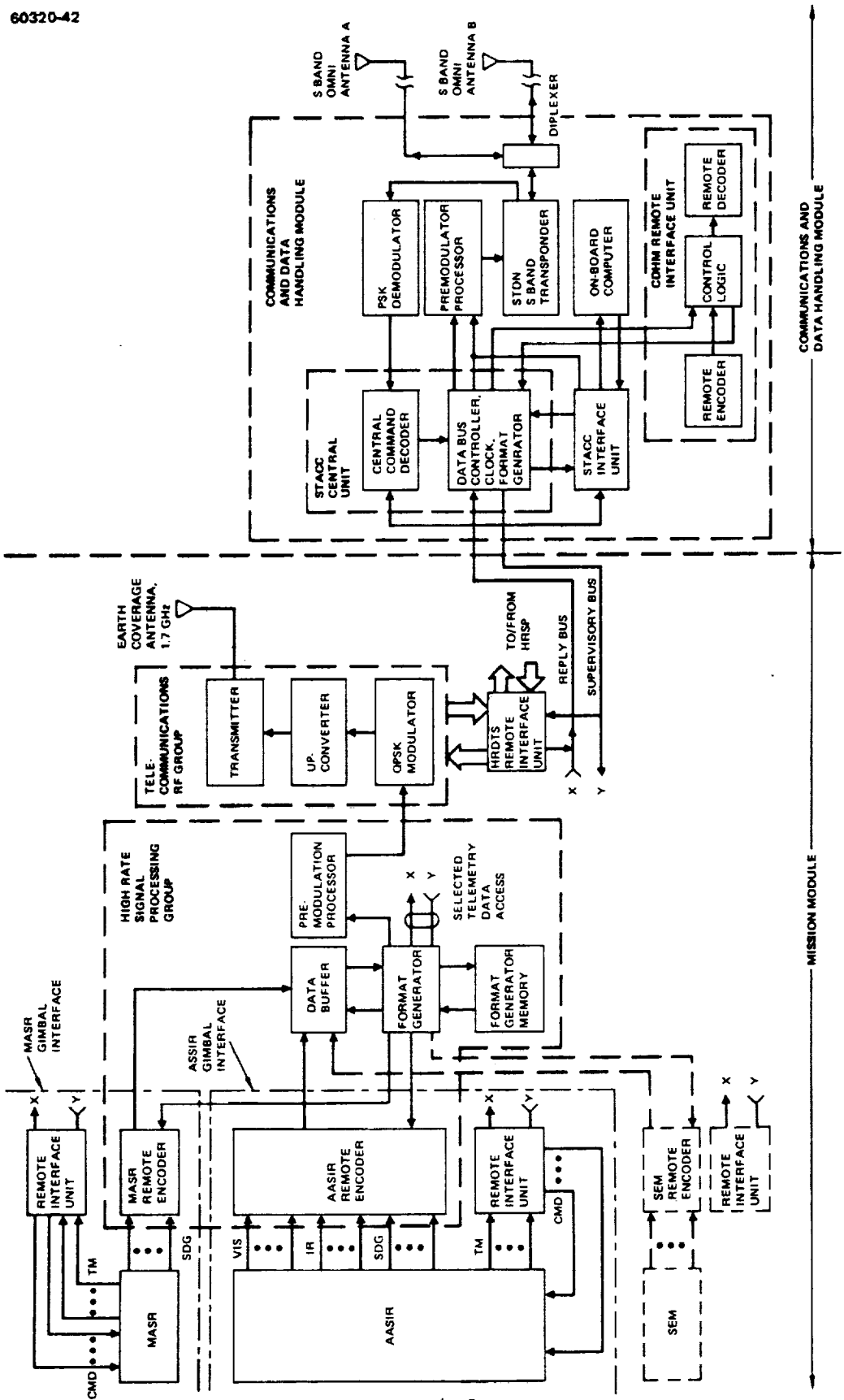

FIGURE 6-1. BASELINE STORMSAT PAYLOAD AND TT&C DATA SYSTEM BLOCK DIAGRAM

6.1 TELECOMMUNICATIONS SERVICE REQUIREMENTS

The STORMSAT data system must provide the following telecommunications services for a successful completion of the STORMSAT mission:

1) Initial Mission (Mission A)

- Process and transmit AASIR sensor and selected telemetry data to one or more receiving sites. The current synchronous meteorological satellite (SMS) stretched visible and infrared spin scan radiometer (VISSR) receiving facility at Federal Office Building No. 4 is typical of such a modest (G/T_s ~14.9 dB/°K) facility.

- Process and transmit MASR sensor and selected telemetry data to the same site as AASIR data.

- Process and transmit all STORMSAT spacecraft housekeeping (telemetry) data to the NASA STDN.

- Transpond GRARR tracking signals from the STDN to provide spacecraft orbital data.

- Receive and decode command signals from the STDN and one or more of the data acquisition sites for control of the spacecraft subsystems and payload.

These functions must be performed utilizing to the maximum the elements of the C&DHM in the MMS and providing all of the required signal interfaces to the C&DHM. Existing or currently available ground equipment and facilities of NASA and NOAA, particularly in their related environmental satellite programs, should also be used to the maximum extent possible. The characteristics of the telemetry tracking, and command signals must be compatible with NASA GSFC Aerospace Data Standards* (this is a ground rule for the MMS/C&DHM).

2) Follow-on Mission (Mission B)

- Provide a relay capability for the collection of data from a network of remote data collection platforms (DCP) currently used in the SMS/GOES program. The capability to relay DCP interrogation data as well as reporting data must be provided in appropriate frequency ranges (S band to UHF interrogation transponding; UHF to S band reporting transponding). Typical DCP locations visible from STORMSAT include Atlantic and Pacific waters and within CONUS.

*NASA/GSFC Document, X-560-63-2

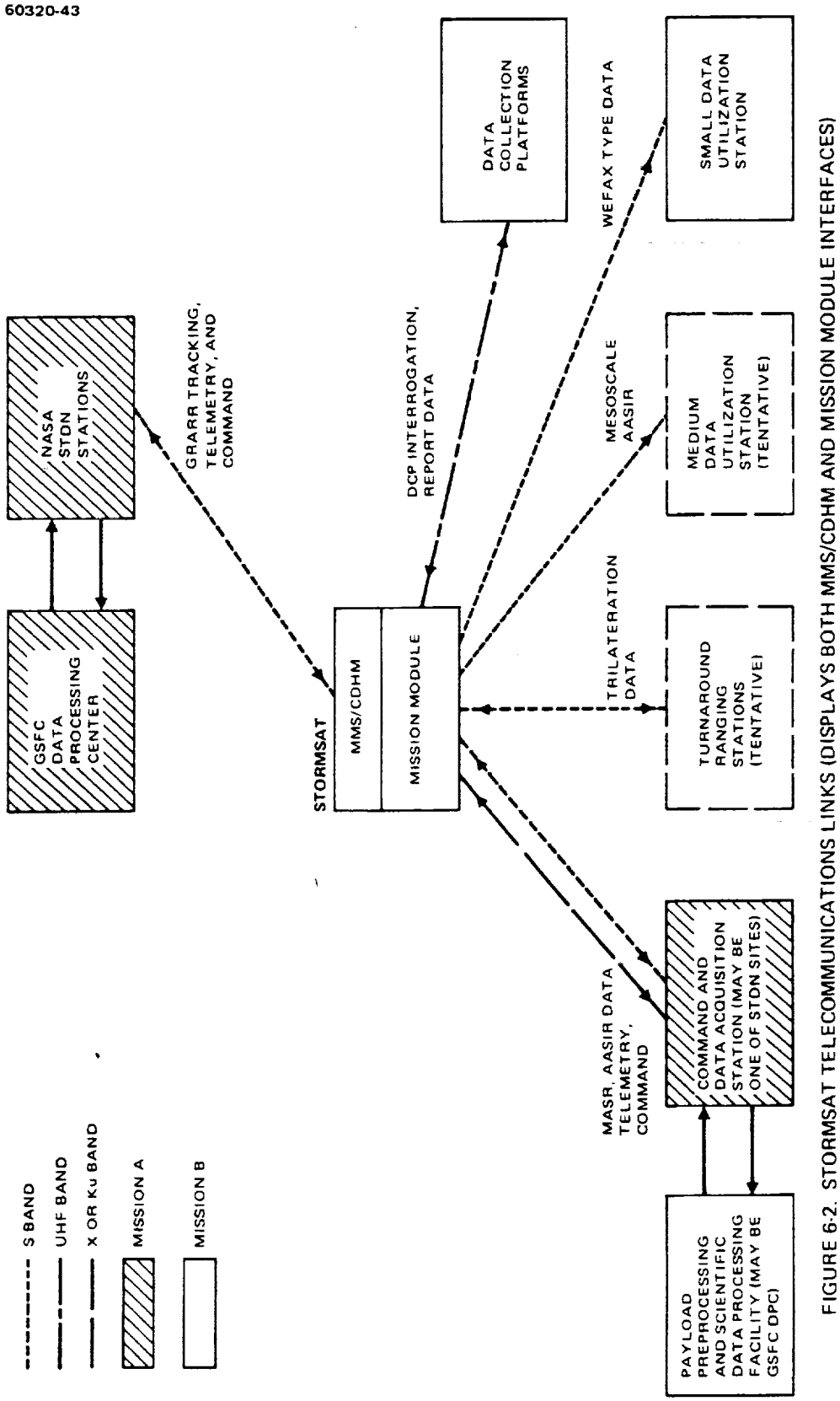

FIGURE 6-2. STORMSAT TELECOMMUNICATIONS LINKS (DISPLAYS BOTH MMS/CDHM AND MISSION MODULE INTERFACES)

- Provide a relay capability for low rate weather facsimile (WEFAX) and text data from one or more sites in CONUS to all receiving sites in view. The frequency band will be compatible with current SMS/GOES S band practice, to allow its WEFAX facilities to continue receiving this forecast product data.

- Process and transmit space environmental monitor (SEM) sensor and telemetry data to the site(s) which receive(s) AASIR data, and to the NOAA Environment Research Laboratory at Boulder, Colorado via an appropriate telemetry frequency.

- Provide the above services in a manner consistent with similar SMS/GOES services available in the STORMSAT launch period.

In addition, the STORMSAT system may be required to perform the following:

- Provide, if possible, mesoscale (less than global field of view) AASIR and all microwave radiometer data to any modest receiving facilities in view of the spacecraft. This will be accomplished at downlink bit rates much lower (≤500 kbps) than those associated with the global AASIR imaging/sounding data.

- Provide, if necessary, any other tracking data required for spacecraft orbit and attitude determination. A typical scheme to be considered in this regard is the trilateration concept, or a slight modification of it, as employed on the SMS/GOES program.

The major elements of the STORMSAT system telecommunications links for the primary and follow-on missions are shown in Figure 6-2.

6.1.1 Payload Data User Requirements

Several options exist for STORMSAT payload data distribution to users, which have a direct effect on the mechanization chosen for the baseline STORMSAT HRDTS. The user of AASIR imaging and sounding data may also require the real time acquisition of MASR data. Further, certain housekeeping data, such as instrument voltage, current, scan-angle, and temperature variables monitored for calibration of AASIR optical and sensor performance will be more useful if available at the AASIR imaging and sounding data processing center. Similar comments relative to MASR and certain other payload housekeeping data also apply. It appears desirable to transmit AASIR, MASR, and selected instrument/mission module telemetry data to a common site. In addition, generalized spacecraft (MMS plus MM)

telemetry data is transmitted to a mission operations facility (STDN/Spacecraft Operations Control Center (SOCC) for spacecraft health and status monitoring, attitude determination, and for other operational considerations. Clearly, these two data receiving sites may not be common either in a geographical or RF interface sense. The AASIR and related data acquisition facility may be a NOAA or dedicated NASA facility. Spacecraft telemetry will be received by the NASA STDN for the initial STORMSAT mission, with the addition of NOAA facilities for operational missions.

The baseline STORMSAT HRDTS concept has assumed that the payload data integration described above is desirable. This implies that the HRSP not only conditions, multiplexes, encodes, and formats AASIR imaging and sounding channel data, but also performs these functions for the MASR and selected instrument and MM telemetry functions. This data stream is then transmitted via the mission-unique wideband RF link from the mission module. This is defined to be a 1.7 GHz S band link for this study. Ku band may provide a more suitable allocation and should be considered for further missions. In parallel with this data acquisition, the AASIR, MASR, and all other MM telemetry data is also multiplexed and encoded by the MM/C&DHM RIUs and transmitted to the spacecraft telemetry data acquisition site via the 2.2 GHz MMS/STDN link.

The complete separation of AASIR imaging/sounding and MASR sounding data and their telemetry data, would simplify the requirements imposed on the HRSP, and the interaction between the HRSP and MMS/C&DHM. In this alternative approach, only AASIR imaging and sounding data is processed by the HRSP. All other data, including MASR sounding data and all MM telemetry data, would be processed and transmitted via the MMS/STDN link.

6.1.2 Telemetry and Command Requirements

The STORMSAT requirements for telemetry and command include:

1) Spacecraft telemetry data transmission to the SOCC via the STDN, and its associated NASCOM interface.

2) Selected spacecraft telemetry for inclusion in the composite high rate AASIR and other payload data stream. This specialized housekeeping data would typically include attitude control subsystem (ACS) attitude sensor error signals, payload calibration voltage, current, temperature, and any other data useful for radiometric and geometric correction of payload data.

3) Reception of command data for spacecraft and sensor control. Command data is transmitted from the SOCC via the STDN. The anticipated real time payload control requirements of STORMSAT may impose unique burdens on the STDN data interface with NASA central processing facilities, and the SOCC man/machine interface

(discussed in Section 11). The signal interface characteristics of the STORMSAT telemetry and command data systems are specified by STDN compatibility requirements. The MMS/C&DHM telemetry and command system is compatible with NASA data standards and the STDN interface.

6.1.3 Satellite Tracking Requirements

The requirements for satellite orbit and attitude state determination are currently provided by radio tracking from ground stations and on-board attitude reference sensors. For example, the SMS program uses a combination of radio tracking data (the GRARR system) available from the STDN and a NOAA trilateration scheme using RF sidetone ranging from a triad of ground sites, for orbit determination. Recent work* by NOAA and NASA personnel has shown that the VISSR imaging data available from the SMS can also be used to complement this radio tracking data. In this approach, landmark data extracted from VISSR images is used to provide combined orbit and attitude state estimation.

The STORMSAT mission has similar orbit and attitude estimation requirements which can also be addressed by a combination of radio tracking (and possibly landmark observations by the AASIR imagery) and on-board attitude sensors. The baseline STORMSAT design presumes that only GRARR radio tracking compatibility need be implemented, and that implementation is accomplished solely by the ranging capability of the MMS/C&DHM standard near earth transponder in the ranging mode. Thus, no compatibility with the NOAA trilateration system is required. The GRARR range determination accuracy (on the order of 0.5 km or better) and range rate resolution (on the order of cm/s), with observations updated at a rate compatible with STDN operational limitations is adequate to satisfy the STORMSAT orbit determination requirements.

6.2 DESIGN APPROACH

Spacecraft functions such as tracking, housekeeping, telemetry, and command can be handled by the standardized capabilities of the MMS/C&DHM and shall be assigned to it. Only those functions such as high rate AASIR sensor processing and transmission functions which appeared incompatible with MMS/C&DHM capabilities shall be accomplished by mission-unique equipment on the STORMSAT mission module. Though no ground facility has been firmly designated for AASIR data acquisition, an RF link using as a bounding case such as NOAA's FOB No. 4, Suitland, Maryland facility was designed. Link performance summaries for more capable alternate site characteristics are given later in this section.

---

*Fuchs, A. J.; Velez, C. E. and Good, C. C.; Orbit and Attitude State Resources from Landmark Data, AIAA Converence, Nassau, 1975.

TABLE 6-1. AASIR DATA AND MISSION MODULE SIGNAL PROCESSING AND RF TRANSMISSION CONCEPT TRADES

Concept	Advantages	Disadvantages
AASIR data plus MASR sensor data plus limited MM telemetry transmitted in single PCM bit stream, during active AASIR scan interval	• A single user can obtain AASIR imaging, sounding, plus MASR sounding data, plus limited MM telemetry • Single RF carrier, QPSK	• Additional number of channels for HRSP to process • Common data interface for HRSP and MMS/C&DHM • Limited or no storage of MASR and telemetry data required, more if MASR and limited MM telemetry desired during AASIR turnaround time
Time-shared AASIR sensor and all MM telemetry	• A single user can obtain AASIR/MASR imaging, sounding, and all MM telemetry data sounding • Single RF carrier, QPSK, with continuous PCM bit stream, even during turnaround	• Major impact on AASIR signal processor • Substantial storage of MASR plus telemetry data during active AASIR scan
AASIR data on MM wideband 1.7 GHz link, MASR and all MM telemetry on S band 2.2 GHz STDN link	• The AASIR data user cannot obtain MASR or MM telemetry data directly	• Minimum burden on the HRSP • All MM telemetry and MASR data processed by MMS/C&DHM • Little interface between the HRSP and the MMS/C&DHM
AASIR data and MASR data on MM link, all MM telemetry on S band STDN link	• The AASIR data user can obtain AASIR plus MASR sounding data, no MM telemetry	• Reduced burden on the HRSP (no telemetry) • Little interface between the HRSP and the MMS/C&DHM • Dual receive frequency capability required to obtain MM telemetry and AASIR data at AASIR user site
All data, including payload data transmitted via the MMS/C&DHM transponder link	• No mission unique RF equipments (except for an earth coverage antenna and related hardware) need be supplied • Single frequency capability at the STDN or equivalent, could receive all data	• The maximum data rate capability of the MMS/C&DHM transponder is on the order of 6 Mbps; onboard processing would be necessary to reduce the payload data rate to this value • Possible increases in AASIR image resolution or mechanization could quickly overburden this link • Excessive interaction between payload and MMS/C&DHM would exist

The STORMSAT payload and telemetry, tracking, and command (TT&C) data systems design process can be separated into several functional areas, such as acquisition and processing of: 1) AASIR sensor data, 2) MASR sensor data, 3) SEM data, 4) all payload status telemetry and command data, 5) RF transmission of mission sensor data, 6) transmission of spacecraft telemetry and command data, and 7) transponding of NASA GRARR tracking data. For the follow-on STORMSAT mission, additional areas include the RF relay of DCP and WEFAX data and addition of tracking via trilateration. These areas will be treated as additions to the primary Mission A STORMSAT data systems capability, as follows. A number of data system design trades have been considered. These trades are summarized in Table 6-1 and discussed in further detail below. The baseline STORMSAT data system and its interfaces are shown in the block diagram of Figure 6-3.

6.2.1 High Rate Signal Processor Design Trades

Several trades exist in the design of the HRSP, whose elements include payload instrument channel signal conditioning, multiplexer, analog-to-digital (A/D) converter, buffer storage, formatter, and timing and format control circuits. Some of these trades involve the choice of physical location of certain of the signal conditioning and multiplexing elements on either side of the AASIR/MM gimbal bearing and MASR gimbal interface, and are discussed in some detail in Subsections 4.1.2 and 4.1.3. To a first order, these placement trades are independent of the processing design philosophy. The major trades in the HRSP design involve: 1) AASIR imaging and sounding signal conditioning scheme; i.e., integrate and dump versus presample filter bandlimiting, or a combination of both, 2) selection of equal angle or equal time multiplexing and processing philosophy, 3) internal clocking rate and buffer stroage trades, 4) trades of RF link bit rate sizing versus onboard HRSP buffer storage, and 5) assignment of additional processing duties (i.e., microwave radiometer and other payload) to the HRSP. Each of these major trades will be discussed below, as well as lower level trades involved in the mechanization of the HRSP.

6.2.1.1 AASIR Signal Conditioning

No signal conditioning other than that buffering necessary to supply the AASIR imaging and sounding channel signals to the HRSP will be done within the AASIR instrument. Therefore, any conditioning which is required prior to sampling and digital encoding will be accomplished in the HRSP. Definitive trades for the particular form of conditioning to be used still remain to be done. Preliminary thinking indicates that an integrate-and-dump mechanization may prove optimum for at least the AASIR sounding channels; the mechanization for the visible and IR imaging channels is less obvious, since the quality measures are different than for the sounding signals. The requirements on registration error for sounding may disallow the memory characteristics of presample filtering (by active or passive means) for these channels. On the other hand, the noise suppression and allowable aliasing error requirements for image data may preclude the lack of selectivity in the amplitude versus frequency response of integrate-and-dump conditioning,

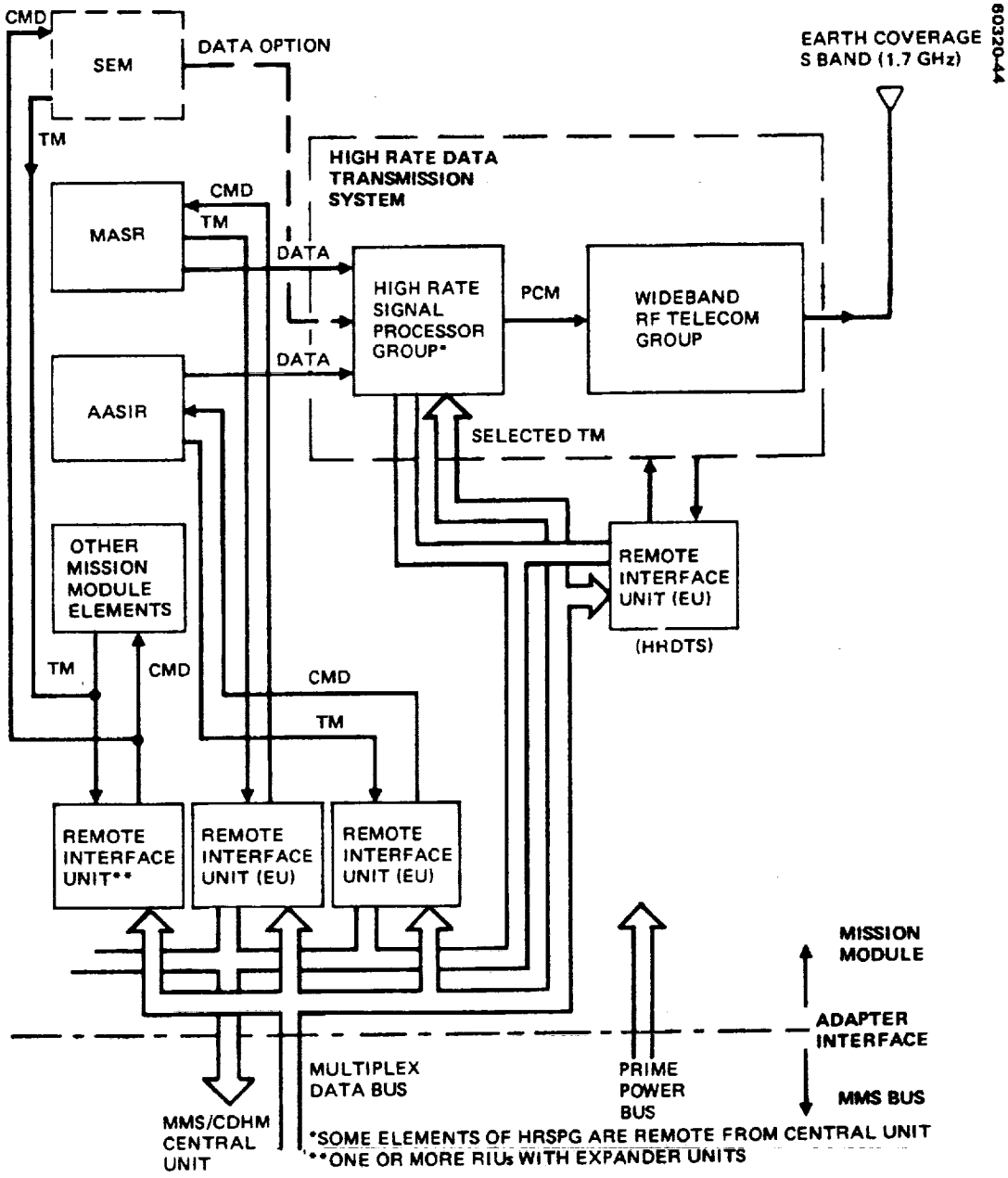

FIGURE 6-3. BASELINE STORMSAT PAYLOAD, TELEMETRY, AND COMMAND DATA HANDLING CONCEPT

and thus demand more selective presample filtering. In any event, whether an integrate-and-dump or presample filtering approach is taken, the variation in effective channel data baseband for the several field of view modes, i.e., global, 4°, and 1.2 by 1.2°, would call for a change in presample filter or integrate-and-dump circuit constants as a function of scanning mode. The HRSP configuration shown later in Figure 6-9 has neither mechanization specified, merely the generalized function of channel signal conditioning. It is understood that further analysis must be carried out in following study phases to finalize this channel conditioning aspect of the HRSP.

6.2.1.2 HRSP Data Rate/Buffer Storage Trades

The AASIR data processing requirements constitute the major influence on HRSP design, particularly those involved in buffer storage versus transmission rate trades. Recently proposed AASIR instrument focal plane arrangement changes can make substantial changes in AASIR data rates, relative to the baseline values shown earlier in Table 4-2, in Section 4. For the baseline focal plane arrangement, the maximum AASIR data rate occurs when all of the redundant data resulting from the proposed four-fold increase in imaging detector arrays scanned is transmitted. The maximum data rate can be as much as 40 Mbps. These bit rates are substantially beyond those assumed in the baseline concept of this report. If the four-fold (redundant) additional imaging data generated by the proposed focal plane arrangement in discarded by appropriate HRSP processing, then only the rate increase due to decreased scan dwell time will affect output AASIR data rate, namely 7 Mbps.

The AASIR instrument data generation rate for a given frame size is not constant, since the scan function is sinusoidal with time. By virtue of scan angle encoding the AASIR signal samples are available on an equal angle sampling basis, but not on an equal time sampling basis. At least two options exist for the subsequent AASIR signal processing. The first is that each AASIR sensor's output is conditioned, sampled at a nonuniform time rate based on strobe signals from the AASIR instrument scan angle encoder, and converted to a digital value essentially instantaneously by the HRSP and formatted into a composite PCM bit stream. As Table 4-2 indicated, the data rate variation over the entire scan sweep is almost a factor of two with no data during turnaround times. Thus, the ground equipment is faced with decoding burst PCM data of nonuniform rate. The second concept as employed in the baseline HRSP design multiplexes the channel data on a nonuniform time basis, performs the A/D conversion, and buffers and "packs" this along with the encoded MASR and selected housekeeping digital data into a composite data stream at a fixed maximum rate for subsequent RF modulation transmission. With this concept, the RF link must be sized to support the maximum composite payload data generation rate. Minimal on board data storage is required with the latter baseline scheme, since the processor is capable of digitally encoding maximum rate AASIR and all other payload data. The penalty paid is that fill data bits must be "stuffed" into the encoded data stream to maintain this constant maximum rate. If RF transmission at an intermediate rate were desired, then considerably more buffer storage would

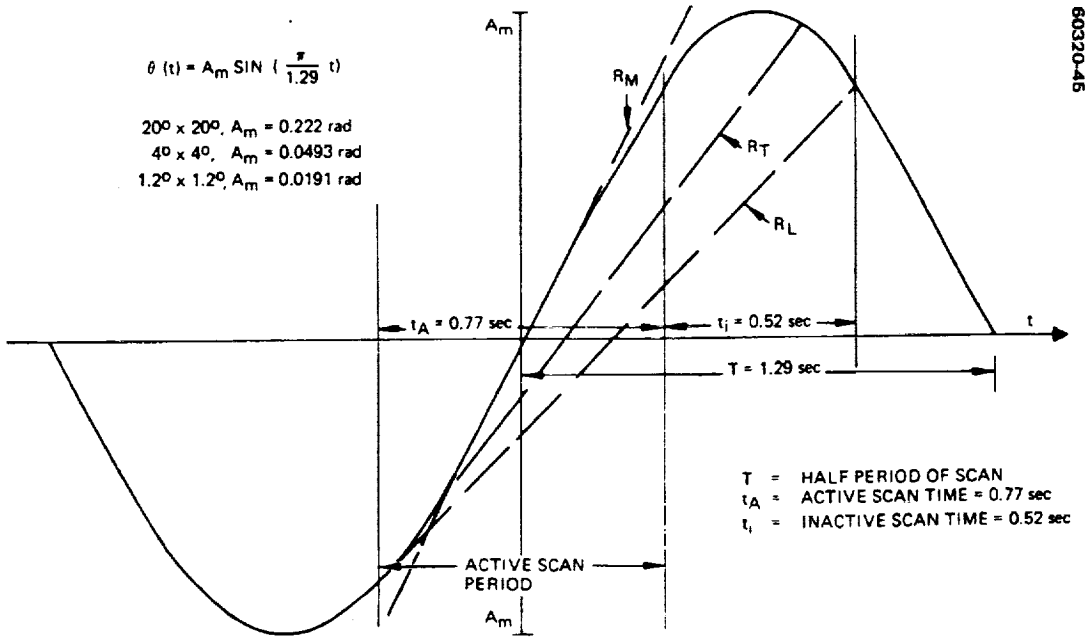

FIGURE 6-4. TYPICAL AASIR DATA BUFFERING/TRANSMISSION RATE OPTIONS

be required. In fact, the limits of such reduced (but constant) rate transmission can be understood by referring to Figure 6-4. If we choose to utilize all of the inactive scan time interval to transmit AASIR data we must store the maximum number of encoded AASIR data bits with the resulting minimum bit rate, R_L, for subsequent RF link modulation. The selection of the slope, R_T, will result in a considerably smaller number of bits to be buffered and a transmission rate, R_T, less than the maximum AASIR generation rate, R_M. The baseline approach results in the minimum data buffer storage, but at the cost of maximum rate RF transmission. Since prime power limits were not severe and RF bandwidth occupancy a secondary issue, adequate EIRP to support the maximum transmission rate was provided in the baseline design. Further analysis in the following study phases may modify this concept solution. For instance, the first option of allowing variable data rate transmission may not prove an insurmountable burden to the ground equipment. After all, the sinusoidal scan time function is known, a priori, and in fact, real time updating information is available from the AASIR scan angle encoder for variations in this function. An analog tracking loop could be mechanized in the ground bit synchronizer to account for this relatively slow data rate variation. The effects of reacquisition due to burst data will also require further study.

6.2.1.3 AASIR and Other Payload Data Multiplexing Options

Certain STORMSAT payload data other than the AASIR imaging and sounding data may prove of interest to the AASIR principal investigator or user. For example, MASR instrument outputs, spacecraft attitude and selected housekeeping data (i.e., calibration data) found in the MMS/C&DHM

telemetry data stream may prove of interest to the AASIR data user. Therefore, it is appropriate to consider techniques for transmitting AASIR sensor data, all other payload sensor data, and selected telemetry data to the AASIR data acquisition site. At least three techniques appear quite feasible for this purpose:

1) A composite serial digital bit stream, output by the HRSP, which includes all payload sensor and selected telemetry data. This is the baseline approach.

2) AASIR sensor and other MM payload/telemetry data are time-multiplexed by employing the inactive AASIR scan period (300 to 400 ms, depending on guard times allowed) for such non-AASIR sensor transmission. Since this low rate payload/telemetry data is being generated during the active AASIR scan interval, some form of data storage and reclocking at a rate consistent with AASIR RF link capability for turnaround time transmission will be necessary. This data buffering and formatting could be accomplished within the HRSP. The difficulties associated with reacquisition of high-rate data if the HRSP is inoperative during the inactive scan period (turnaround time) may require transmission of a continuous high-rate PCM bit stream in any event. Utilization of this period to transmit other MM payload/telemetry data at the nominal high-rate payload bit rate will thus serve two purposes: to deliver this data directly to the AASIR user (this low rate payload and telemetry data will continue to also be available at the MMS/C&DHM STDN receiving sites), and to ensure continuous high-rate PCM AASIR sensor data acquisition. Figure 6-5 illustrates this concept.

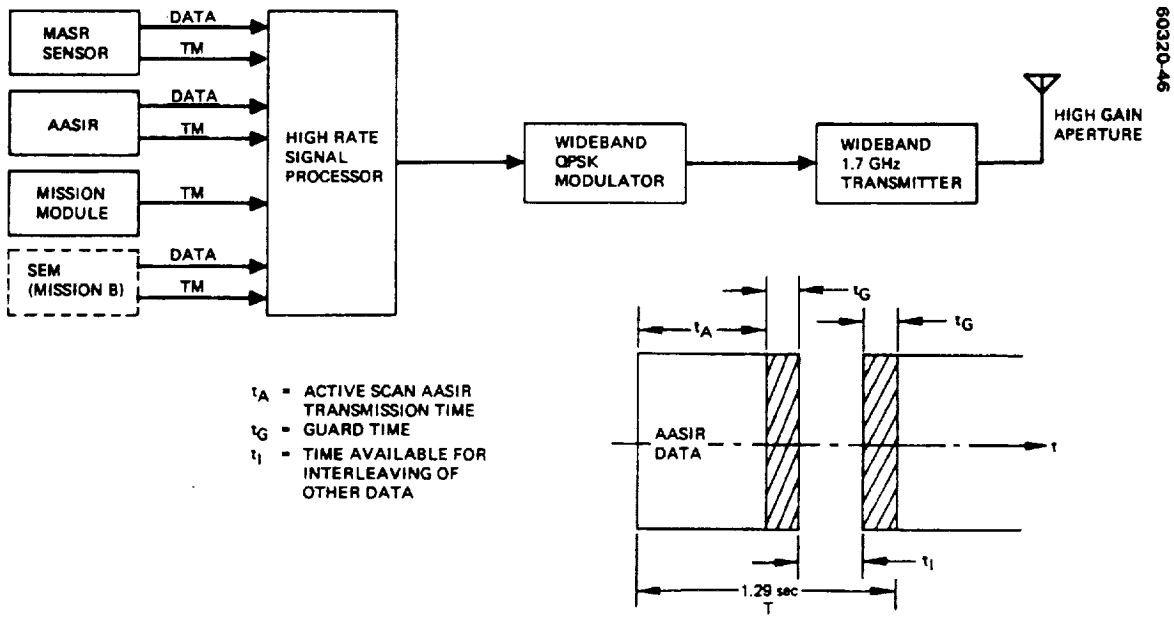

FIGURE 6-5. BOTH MASR AND AASIR DATA AND ALL MM TELEMETRY AVAILABLE AT SINGLE USER SITE ON A TIME SHARED BASIS

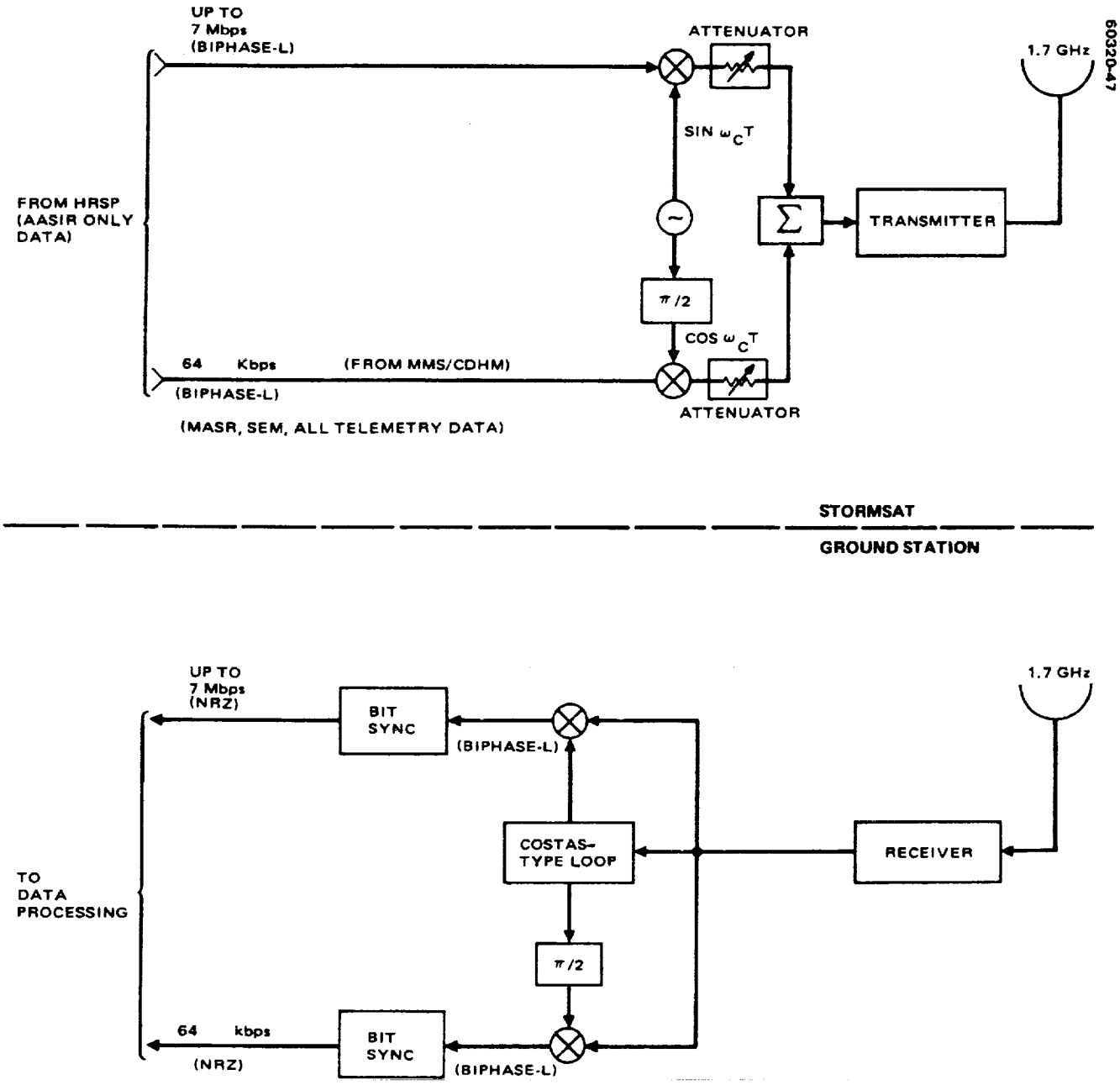

FIGURE 6-6. MODIFIED QPSK TRANSMISSION SCHEME FOR SIMULTANEOUS ASSIR/MASR AND MMS/CDHM TELEMETRY DATA ON WIDEBAND AASIR LINK

3) Frequency or phase multiplexing, wherein either multiple RF carriers or assymmetric QPSK phase modulation is used. For instance, the AASIR/imaging and sounding sensor data could be output from the HRSP for transmission on the 1.7 GHz (or Ku band) link, with all spacecraft telemetry and other payload data transmitted on the MMS/C&DHM 2.2 GHz link. The data acquisition site then could be provided with dual receive frequency capability, as well as appropriate equipment to recover the two independent data streams. Alternately, a modified form of QPSK could be used to transmit these two digital data streams via a single RF carrier. Figure 6-6 displays such a system concept. There are a number of technical considerations, such as tolerance to link mechanization which may make this approach less desirable. It is an interesting concept, currently used on the space shuttle, to combine two independent, rate-disparate signal bit streams.

6.2.1.4 HRDTS RF Group Trades

For purposes of illustration an S band (in particular, the space to earth frequency allocation of 1.7 GHz) RF link has been chosen for the STORMSAT baseline. Though several candidate payload acquisition sites exist, it is assumed the NOAA FOB No. 4 SMS/GOES stretched VISSR data acquisition site is representative of such a facility. As the link performance summary of Section 11 shows, other candidate sites, such as the NOAA command and data acquisition station (CDAS) at Wallops, or NASA STDN facilities, all produce larger link performance margins, since their receiving figure of merit (G/T_S) is greater than the FOB 4 facility.

It will be appropriate in the subsequent study phases to consider this RF acquisition facility in greater detail. In particular, the selection of downlink carrier frequency must take into account the availability of frequency spectrum based on other environmental satellite users, potential interface with radio astronomy bands, available site facilities, and hardware technology. For instance, it may prove desirable to abandon the S band allocation altogether (conversations with Elmer Carter, NASA/GSFC frequency allocation manager, indicate the S band allocation may prove overcrowded in the STORMSAT time frame) and implement a Ku band system. Appropriate Ku band hardware may be available from the tracking and data relay satellite system (TDRSS) program in the STORMSAT time frame. In this event, a new data acquisition site could be provided or necessary changes made at one or more STDN sites.

As has been mentioned previously, for the particular purposes of the STORMSAT primary mission it may even prove worthwhile to consider increasing the telemetry data rate capability of the MMS/C&DHM link to allow payload sensor data transmission or on-board processing of payload data to produce rates compatible with the current C&DHM transponder design.

The STDN-compatible standard near earth (S band) transponder in the MMS/C&DHM can currently transmit differentially encoded QPSK 6 Mbps data on the telemetry link. Thus, one of the two redundant MMS/C&DHM

transponders could be assigned to transmission of high-rate AASIR data, the other to transmission of routine STORMSAT telemetry data. Alternately, if both high-rate AASIR and MASR sensor data and spacecraft telemetry data are combined by signal processing into a single digital data stream, either MMS/C&DHM transponder could be used for transmission. Further study of the interactive trades of signal processing and RF transmission techniques will be necessary if such an integrated scheme is to be used. The approach chosen for the STORMSAT baseline minimizes this integration property by separating the high-rate payload data transmission from that of the spacecraft telemetry.

6.2.1.5 Ranging Technique Trades

The MMS C&DHM has an S band transponder which is designed to be STDN compatible. In particular, this standardized unit allows the transponding of the ranging tones of the GRARR system for range determination and two-way carrier doppler shift measurements for range rate determination concurrent with telemetry and command transmission. With current SMS GRARR tracking, data is obtained by NOAA on a one day per week basis from one or more STDN sites at which the ranging is done.

Typically, a three station data pass exhibits a range consistency of ±25 meters, with resultant computed spacecraft orbit residuals of 1 to 5 meters (1σ). The current delivery frequency of GRARR observations to NOAA for orbit determination is based on largely institutional limitations of scheduling, etc. The GRARR observations can be made without interference to the payload (AASIR) data transmission. For the STORMSAT situation, two conditions could be anticipated with respect to GRARR tracking. The first is that the multiple station ranging capability of the STDN is retained and GRARR tracking data is supplied on an as-required basis, particularly for the NASA mission. The other is that a combination of GRARR, trilateration, and landmarking techniques are required. The reasons for this may include a desire to obtain GRARR data more frequently than NASA can schedule it, simultaneity of GRARR or trilateration with landmark observations for AASIR line of sight calibration, or simply that the GRARR data is not adequate in its range resolution. Discussions with NOAA personnel indicate that either the GRARR or trilateration tracking data appears adequate for current SMS orbital determination and image gridding. Tests are currently proceeding at NOAA to compare these two RF techniques on a quantitative basis. If the combined RF/imaging navigation technique now being investigated by NOAA proves viable, then another STORMSAT option exists, i.e., determination of one range vector (using GRARR for example) in conjunction with AASIR landmark observations. If a single GRARR site is thus found adequate, then the update rate from the STDN may increase or GRARR compatible equipment may be installed at an AASIR data acquisition site (not in the STDN).

If the current SMS concept of transponding S band ranging tones from three sites (including the master command and data acquisition station at Wallops) is used, then a major change in the baseline STORMSAT telecommunications capability is required. Its baseline transmit only capability

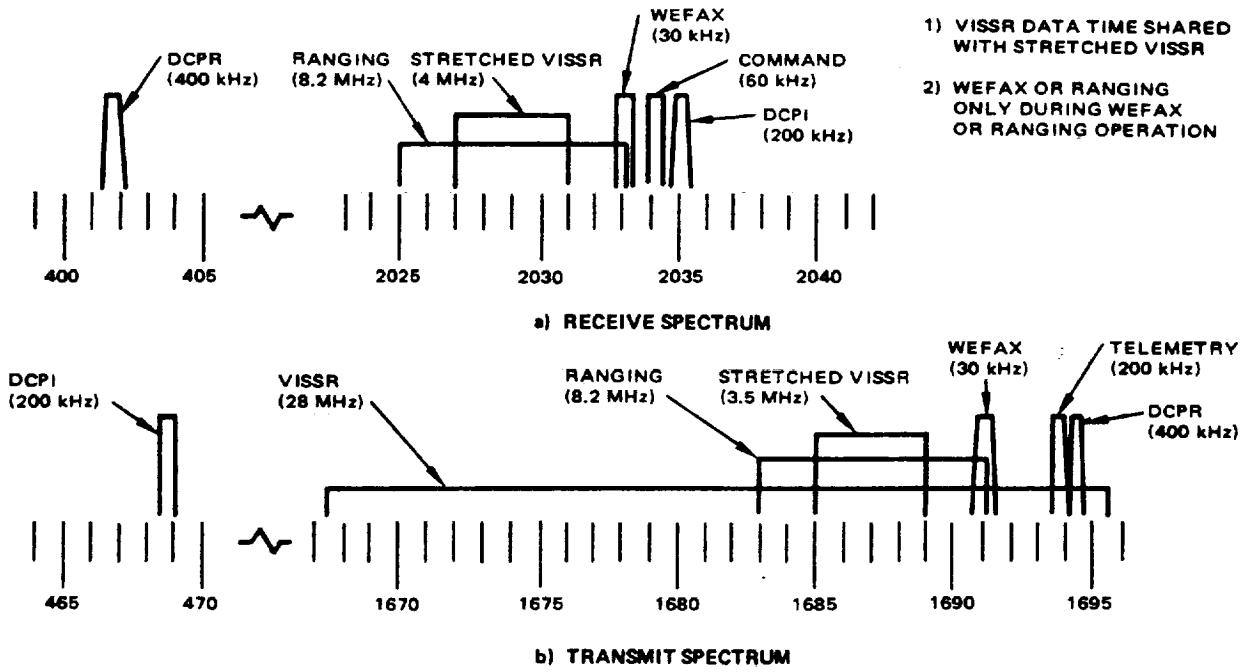

FIGURE 6-7. SMS RF SPECTRUM UTILIZATION

would require the addition of an S band receive capability and channelized repeater. If complete frequency compatibility with the current SMS/GOES trilateration turnaround ranging stations (TARS) were necessary, tight control of these satellite repeater specifications to minimize intermodulation, group delay variation, and spurious output would be necessary, particularly if compatibility with current WEFAX and DCP SMS data systems were also to be implemented.

6.2.1.6 Mission B Growth

If payload data transmissions could be located in an appropriate frequency band such as Ku band, an S band trilateration scheme using the current SMS/GOES interface could be implemented which would allow simultaneous payload data transmission and trilateration. If such an S band repeater function were mechanized for the NOAA trilateration scheme, then the Mission B WEFAX and DCP relay functions could utilize elements of this repeater, plus additional elements. Figure 6-7 shows the current SMS/GOES trilateration and other service frequency assignments, and Figure 6-8 illustrates a typical spacecraft repeater configuration to realize the telecommunications services anticipated for Mission B.

6.2.2 Mission-Unique Baseline System Description

6.2.2.1 High-Rate Signal Processor

Functional Description

The HRSP accepts analog sensor data from the AASIR, MASR, SEM (for mission B), and selected digital telemetry; conditions, multiplexes,

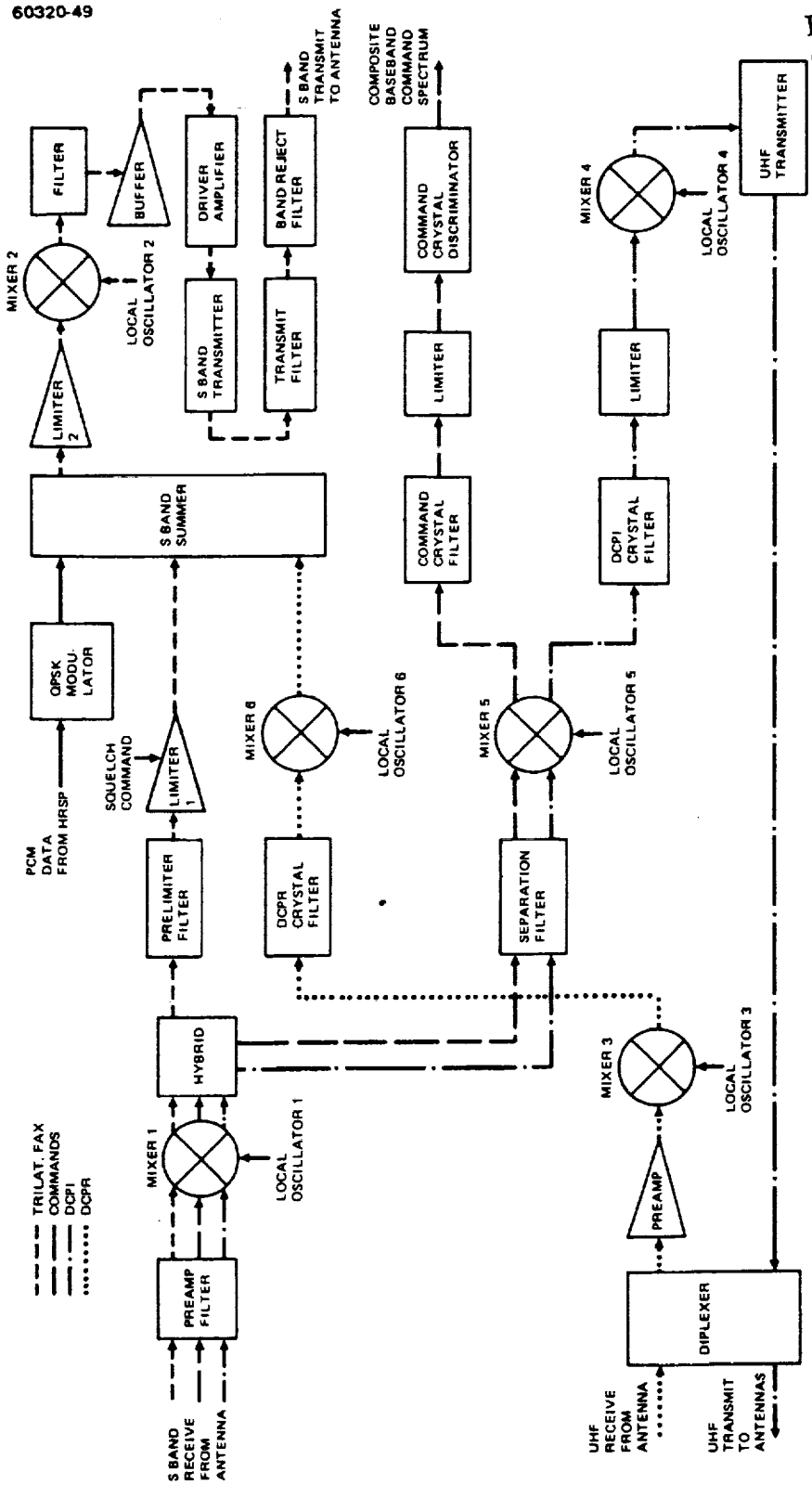

FIGURE 6-8. TYPICAL COMBINED S BAND, UHF TRANSPONDER SYSTEM BLOCK DIAGRAM

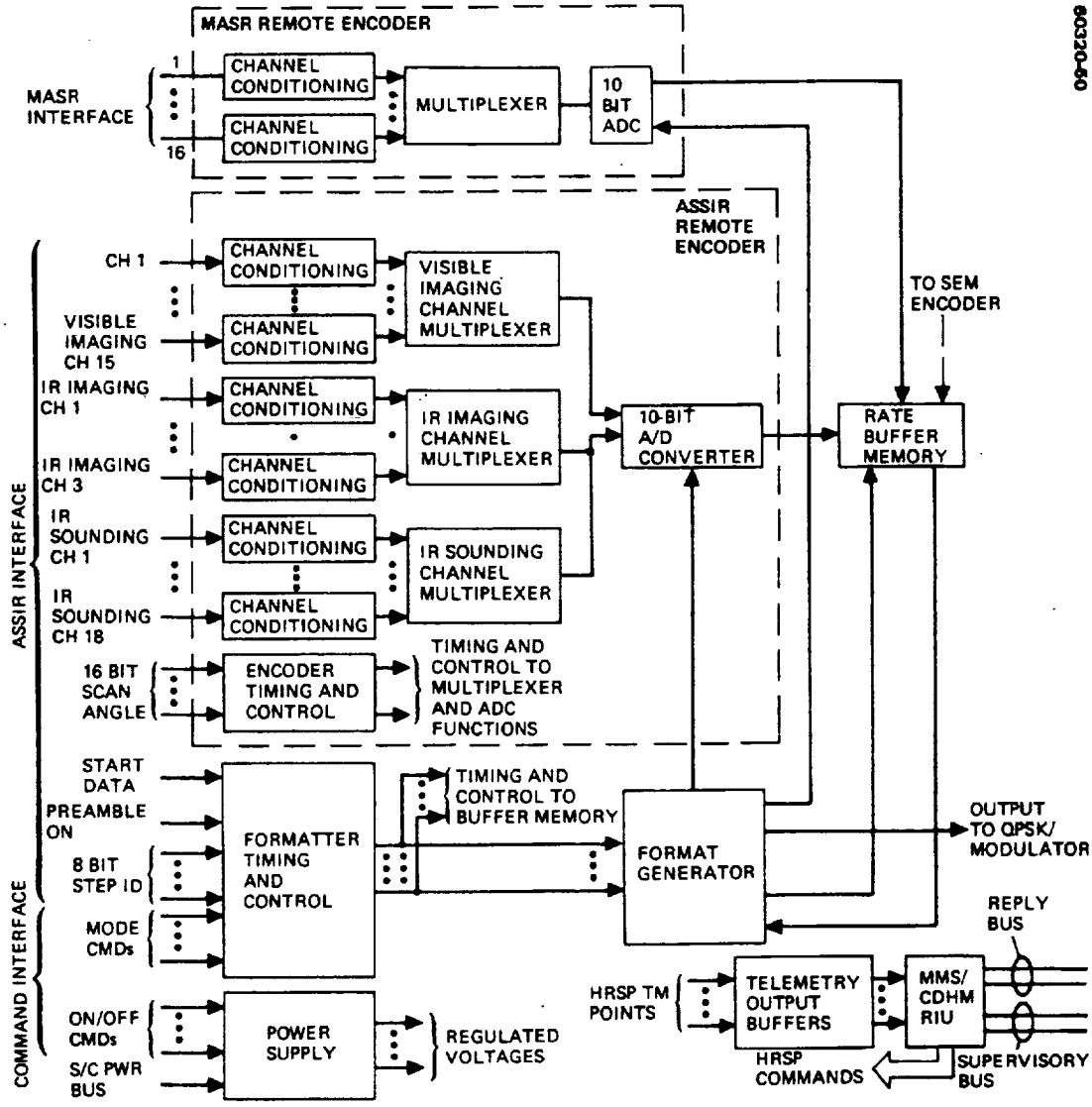

FIGURE 6-9. HIGH RATE SIGNAL PROCESSOR BLOCK DIAGRAM

encodes, and formats the data into two differentially encoded half-rate PCM data streams for QPSK modulation of the RF carrier. The mechanization chosen for these functions consists of remote encoder units for the AASIR and MASR (and SEM, if needed) data digitizing located on the instrument package, and a centralized portion of the HRSP, located within the mission module, which combines this digital data, as well as selected digital telemetry data obtained from the MMS/C&DHM, by rate buffering and formatting into a composite data stream for RF transmission, as shown in Figure 6-9. This approach has been taken to minimize cable wrap across both the AASIR and MASR gimbals. Encoding by remote units physically placed on the instrument case allows small cable sets of HRSP data bus, RIU multiplex data bus for the MMS/C&DHM, and prime power. Note that an alternate scheme of

TABLE 6-2. HRSP PERFORMANCE CHARACTERISTICS

	HRSP Scan Angle Modes, deg		
	20 by 20	4 by 4	1.2 by 1.2
AASIR, data channels			
Visible	15	15	15
IR	3	3	3
Sounding	18	18	18
MASR	16	NA	NA
SEM			
Selected	TBD	NA	NA
Telemetry	TBD	NA	NA
Format			
Typical AASIR presampling filter bandwidths (-3 dB)			
Visible, kHz	19.2	3.9	1.2
Sampling period			
Visible, μrad	10	10	10
IR, μrad	60	60	60
Sounding, μrad	180	180	180
Quantization AASIR			
Visible, bits, linear	8	8	8
IR, bits, linear	10	10	10
Sounding, bits, linear	10	10	10
MASR, bits, linear	10	10	10
Composite bit rate, Mbps	6.95	1.55	0.60
Encoding	NRZ-S	NRZ-S	NRZ-S
Modulation	QPSK	QPSK	QPSK
Bit rate stability			
0.5 sec	1×10^{-9}	1×10^{-9}	1×10^{-9}
1 year	5×10^{-6}	5×10^{-6}	5×10^{-6}
Mirror cycle period, sec	2.58	2.58	2.58
Transmission duty cycle, percent	60 (overscan of 0.573° included)	60	60

obtaining MASR data exists, whereby all MASR sensor data, plus its housekeeping is encoded by the MMS/C&DHM RIU servicing this unit, and that the MASR sensor as well as selected telemetry data is obtained from the MMS/C&DHM, via either its multiplex data bus (as shown in Figure 6-9) or directly from the C&DHM/OBC.

The HRSP accepts 15 visible sensor channel, 3 IR channel, and 18 sounding channel data from the AASIR. Before sampling and multiplexing, the visible channels may be filtered to limit aliasing error and provide noise suppression. All sensor data are sampled at equal-angle intervals, corresponding to twice the Nyquist rate (i.e., four times the maximum spatial frequency as determined from the sensor instantaneous field of view (IFOV). Equal-angle sampling allows picture alignment from scan to scan. The IR and sounding channels are processed typically by integrate, hold, and dump circuits, prior to multiplexing and encoding. This, together with equal-angle sampling, addresses the repeatability requirement for sample alignment from scan to scan at each east-west step position. Using a 10 bit analog-to-digital converter (ADC), the visible channel samples are encoded into 8 bit words and the IR and sounding samples are encoded into 10 bit words. Similarly, the HRSP conditions, multiplexes, and encodes the 16 channel sensor data from the MASR, rate buffers and formats this digital data stream into the composite PCM bit stream, as shown in Figure 6-9.

The HRSP has three bit rate modes of operation, the three scan angle modes of the AASIR: 1) 20 by 20°, 2) 4 by 4°, and 3) 1.2 by 1.2°. In these three modes, the HRSP output bit rates are approximately 6.95, 1.55, and 0.60 Mbps, respectively (if the bit stuffing approach previously discussed is used).

The HRSP performance characteristics are summarized in Table 6-2. The physical characteristics of the HRSP are estimated to be as follows:

1) Peak prime power = 22.5 watts

2) Weight = 9.8 kg (21.5 lb); this unit mass is distributed between the central unit and remote encoder units

3) Volume ~ 9800 cm^3 (600 in^3)

AASIR Data Format

As shown in Figure 6-10, the AASIR data frame format, representing either a complete north-south or south-north scan, consists of preamble bits, sync words, and minor frames of AASIR data. The preamble bits are transmitted to maintain bit synchronization on the ground and possibly for word synchronization.

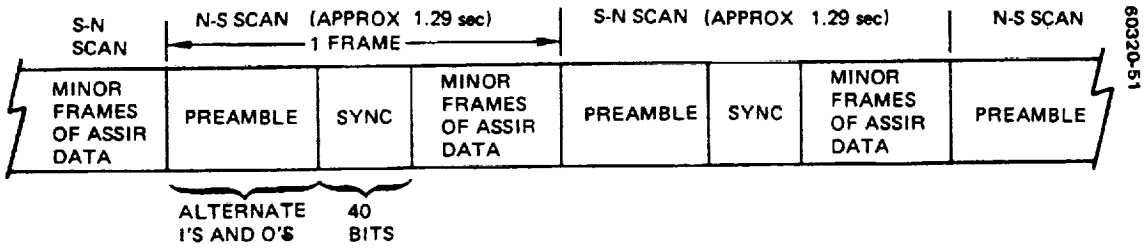

NOTE: BIT RATE CHANGES WITH EACH COMMAND SELECTED SCAN MODE
$20^0 \times 20^0$ MODE → 6.95 Mbps
$4^0 \times 4^0$ MODE → 1.55 Mbps
$1.2^0 \times 1.2^0$ MODE → 0.60 Mbps

a) FRAME FORMAT

DECOM SYNC	STEP ID	SCAN ANGLE
16 BITS	8 BITS	16 BITS

b) AASIR SYNC FORMAT

	ROW ID							
ROW	1		MNFS	S1	V1	V2	V14	V15
	2		(FILL)	S2	V1	V2	V14	V15
	3		(FILL)	S3	V1	V2	V14	V15
	4		IR 1	S4	V1	V2	V14	V15
	5		IR 2	S5	V1	V2	V14	V15
	6		IR 3	S6	V1	V2	V14	V15
	7		(FILL)	S7	V1	V2	V14	V15
	8		(FILL)	S8	V1	V2	V14	V15
	9		(FILL)	S9	V1	V2	V14	V15
	10		IR 1	S10	V1	V2	V14	V15
	11		IR 2	S11	V1	V2	V14	V15
	12		IR 3	S12	V1	V2	V14	V15
	13		(FILL)	S13	V1	V2	V14	V15
	14		(FILL)	S14	V1	V2	V14	V15
	15		(FILL)	S15	V1	V2	V14	V15
	16		IR 1	S16	V1	V2	V14	V15
	17		IR 2	S17	V1	V2	V14	V15
ROW	18		IR 3	S18	V1	V2	V14	V15
		2 BITS	10 BITS	10 BITS	8 BITS	8 BITS	8 BITS	8 BITS

142 BITS PER ROW 18 ROWS PER MINOR FRAME

c) AASIR MINOR FRAME FORMAT

FIGURE 6-10. TYPICAL HRSP DATA FORMATS

AASIR Sync Word Format

The sync words consist of a 16 bit decommutated sync word, 8 bit step ID word, and 16 bit scan angle. The decommutated sync word is a unique Barker code to allow for frame synchronization on the ground. The step ID indicates the east-west position of each scan. The scan angle indicates the start of scan, hence allowing scans at the same east-west position to be aligned.

AASIR Minor Frame Format

The minor format consists of 18 rows of 142 bits each, where each row is transmitted sequentially (one row after another, serially). The first 2 bits of each row are the 2 least significant bits of the row counter. As will be discussed later, the row ID identifies an invalid row of data on the ground. Bits 3 through 12 of row 1 are the minor frame sync word, which indicates the start of a minor frame on the ground; these 10 bits in rows 4, 5, 6, 10, 11, and 12 are supercommutated IR data words. Bits 13 through 22 in each row are the commutated sounding data words. The next 15 8-bit words in each row are the supercommutated visible data words. The supercommutation of the visible and IR words are consistent with their sample period.

Other Payload Data Format

The MASR, (SEM), and selected telemetry data formats would typically consists of a sync word followed by frame data, as shown in Figure 6-10.

Operational Description

AASIR Data Encoding. The remote encoder portion of the HRSP conditions,* samples, multiplexes, and digitizes the AASIR and other data. Since the three scan angle modes of the AASIR present three discrete maximum scan angle rates, four circuit constants are command selectable for each conditioning circuit.

The AASIR encoder timing is asynchronous with the output format timing, since equal-angle sampling is performed on all sensor data. The encoder timing and control logic accepts and decodes the 16 bit scan angle of ~100 μrad resolution from the AASIR and generates required timing and control signals to sample, multiplex, and digitize sensor data at their required sample angle intervals. The sample angle intervals for visible, IR, and sounding sensor data are 10, 60, and 180 μrad. The timing and control signals are generated every 10 μrad to sequentially sample, multiplex, and digitize the sensor data in each row of the format as defined in Figure 6-10. The bit rate clock from which the timing and control signal burst is derived is approximately 15 MHz, which assures that the encoding process for a row of sensor data is complete before the next 10 μrad increments are processed.

The AASIR visible, IR, and sounding multiplexers time multiplex the sensor data, after appropriate channel conditioning according to the row format defined in Figure 6-10. A common 10 bit ADC within the remote AASIR encoder digitizes the multiplexed sensor samples. These digitized samples are written into the rate buffer memory where they are read out according to the minor frame format. Similarly, the remote encoder for

*Either presample filtering or integrate-and-dump, for instance.

the MASR (SEM) conditions and time multiplexes the 16 MASR channels, then digitizes to a 10 bit word. These digitized samples are also read into the central rate buffer memory in a burst mode, for subsequent formatting into the composite PCM bit stream.

Formatting. The formatter under control of the format timing and control logic forms the composite bit stream as defined by the frame format in Figure 6-10. The preamble ON signal causes the formatter to insert the preamble code. The START DATA signal causes the formatter to insert the decommutated sync, step ID, and scan angle words. After inserting the AASIR data sync word, the formatter accepts the digitized sensor data from the buffer memory, inserting minor frame sync codes in the AASIR data stream and unique sync words into the MASR, SEM, and the selected housekeeping data streams.

The output bit rate in each mode was selected to be consistent with the maximum scan angle rate of change and row period of 10 μrad. This means that the formatter timing and control will request AASIR data readout from the rate buffer at least as fast as data is written into the AASIR data portion of the buffer memory. This, in turn, minimizes the required buffer memory capacity (currently estimated to be several hundred bits). Since the read-in rate to the AASIR data portion of the buffer memory can be as low as ~0.6 of the readout rate, data in the buffer memory may not be ready at the time of a request. In this case, filler bits are inserted into a row of AASIR data with a row ID identical with the previous row ID. This will enable the ground user to identify the filler bits and hence to ignore them. Minor frames of AASIR data are sequentially transmitted in this manner until the next preamble ON signal occurrence. In the case of MASR and SEM data, data is read into their portion of the buffer memory, then read out as a data burst as shown in Figure 6-9.

6.2.2.2 Mission Data Transmitter Group Description

The baseline STORMSAT mission module RF group concept has only S band transmit capability. The tracking data functions are assumed to be satisfied by the GRARR compatibility of the MMS/C&DHM; therefore, no ranging data transponding compatibility with the trilateration system of SMS/GOES is provided on the mission module. The allowable HRDTS transmit aperture for on-station use is ~0.6 meter (2 feet) in diameter. There is room on the earth viewing face of the MM for another antenna for dedicated receiving purposes, approximately 2 feet in aperture diameter, if diplexing a single antenna is not desirable. Incorporation of redundant command, WEFAX relay, and data collection services for the STORMSAT follow-on mission may require this antenna, as well as one or more UHF antennas. Since high rate payload data transmission is anticipated only on-station after synchronous orbit insertion, the high-gain, earth-coverage S band antenna will be used for payload data transmission. The two hemispherical coverage antennas will be used in a switched or combined mode for MMS/C&DHM telemetry and command links at orbit injection and thereafter. The capability to utilize the earth-coverage antenna for TT&C may also be provided.

S band Transmitter

This unit consists of redundant solid state driver and paired output amplifiers, cross-strapped such that either output pair can be driven by either preamplifier. RF output will be 30 watts maximum, with an intermediate 7 watt RF output level from the driver stage. Additional output capacity can be added for Mission B, in addition to other elements required for providing Mission B services.

Wideband Modulator/Upconverter

This redundant unit will provide quadraphase shift keyed (QPSK) carrier modulation by the differentially-encoded 7 Mbps PCM baseband data from the HRSP. The total prime power requirements and per unit mechanical characteristics of these RF elements are:

	Watts	Mass	Volume
QPSK modulator/upconverter/ transmitter	95	3.1 kg (6.7 lb)	11,200 cm^3 (680 in^3)

S Band Antenna

The S band transmit antenna is a prime focus, cup dipole-fed parabolic reflector design as used on the GMS program. The antenna design is shown in Figure 6-11. This antenna design was chosen on the basis of mechanical simplicity, high aperture efficiency, and compatibility with available space. If a single antenna structure is used, separation of transmit and receive signals is accomplished with a diplexer mounted directly behind the parabolic reflectors; otherwise separate antennas would be used for Mission B requirements. The characteristics of this antenna are summarized below:

Electrical Characteristics

	Transmit	Receive (Mission B)
• Frequency, MHz	1670 to 1695	2024 to 2036
• Transmit power capability, watts	25	N/A
• Gain		
• Beam peak, dB	18.0	18.2
• Off axis, dB	14.2 (±9.2°)	13.7 (±9.2°)

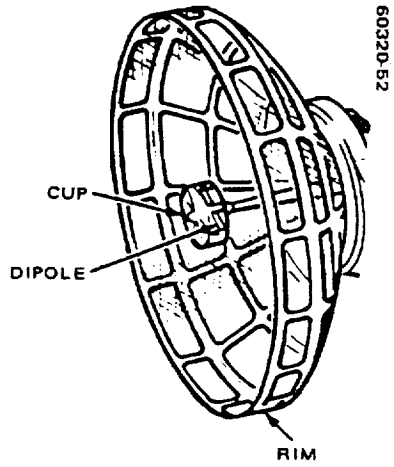

FIGURE 6-11. TYPICAL S BAND
EARTH COVERAGE ANTENNA (GMS)

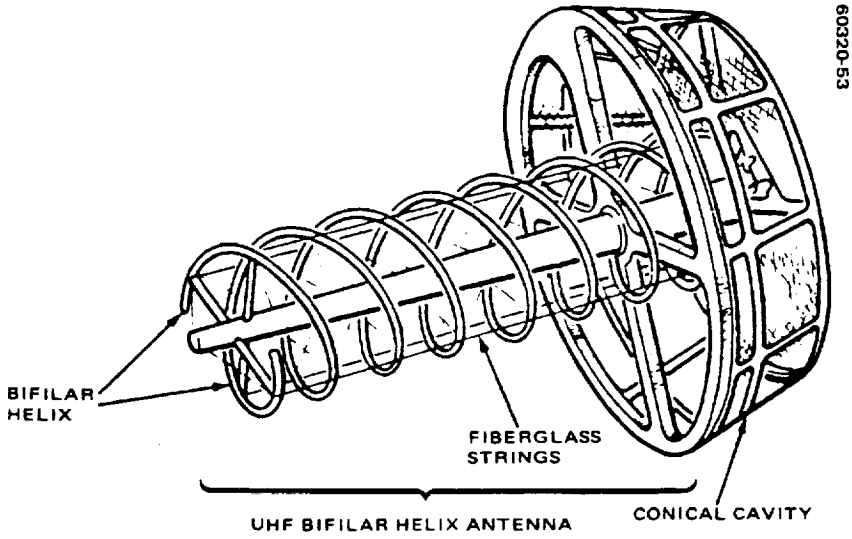

FIGURE 6-12. TYPICAL UHF ANTENNA (TRANSMIT/RECEIVE)
CONSTRUCTION (GMS)

Dimensions

	mm	Inches
• Reflector diameter	610	24
• Reflector height	220	8.5

UHF Antenna (Mission B Requirement)

The UHF antenna is a bifilar, cavity backed helix as used on the GMS program. This type of antenna provides broadband circularly polarized coverage. The design is shown in Figure 6-12. The characteristics of the UHF antenna are listed below:

Electrical Characteristics

	Transmit	Receive
• Frequency, MHz	469 ±1.0	402 ±1.0
• Power level, watts	10 maximum	N/A
• Gain peak, dB	10.5	9.0
• Gain at ±9.2°, dB	10.0	8.5

Helix Dimensions

	mm	Inches
• Helix length	790	31
• Helix diameter	250	10

Conical Cavity Dimensions

• Base diameter	410	16
• Front face diameter	470	18.5
• Cavity depth	130	5

6.2.3 Payload Data (HRDTS) Performance Analysis

The detailed mission-unique RF link budget analysis summary is given in Section 11, Ground System Studies. The estimated payload transmission link performance margins for several candidate data acquisition sites are given in Table 6-3. (For purposes of illustration, and worst-case sizing, the current NOAA FOB No. 4 facility is assumed for the baseline design.)

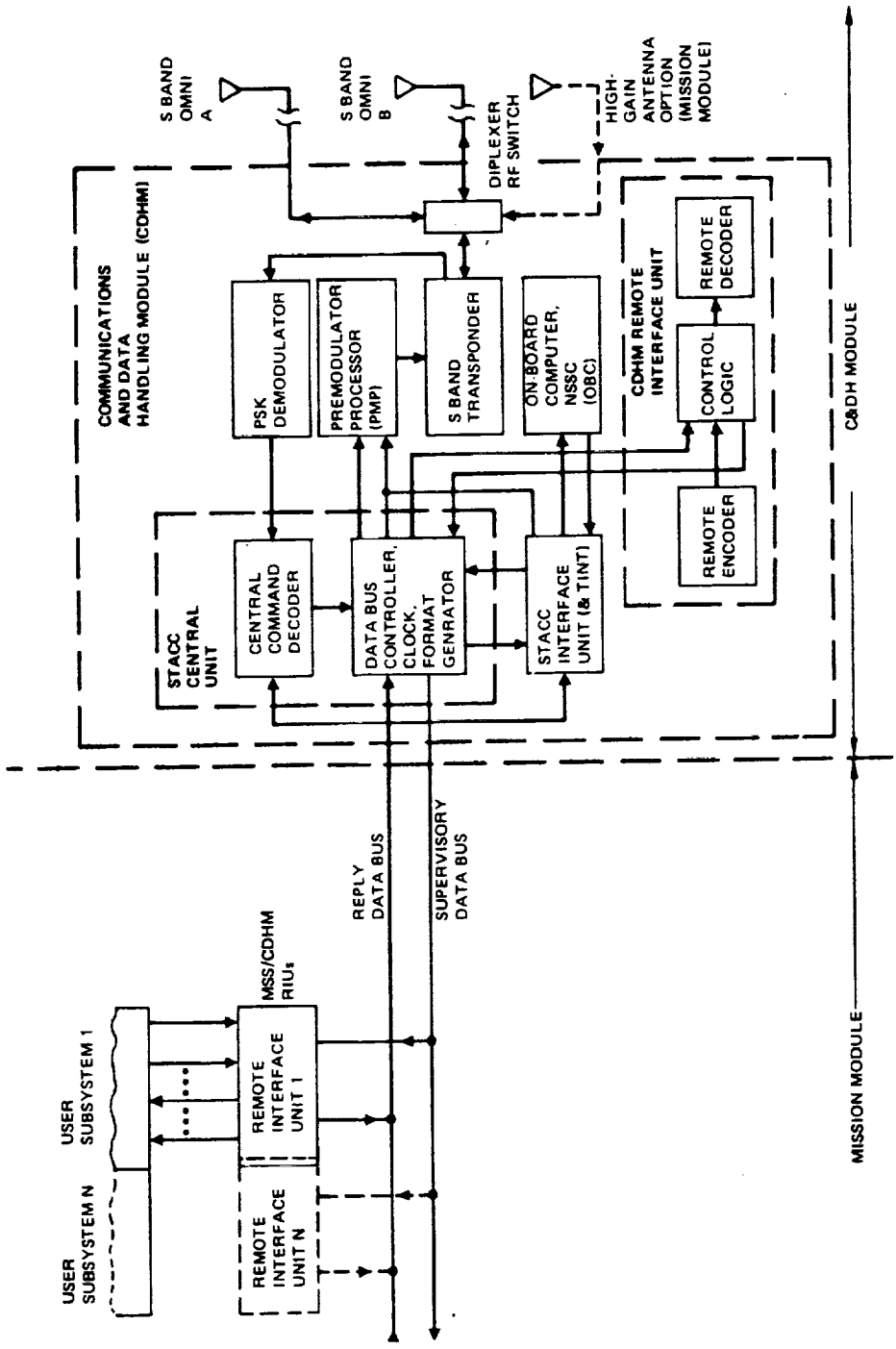

FIGURE 6-13. SIMPLIFIED BLOCK DIAGRAM OF MMS/CDHM SUBSYSTEM AND ITS SPACECRAFT DATA INTERFACES

TABLE 6-3. SUMMARY OF HIGH-RATE PAYLOAD TRANSMISSION LINK (1.7 GHz) PERFORMANCE MARGINS

Data Acquisition Facility	Nominal Link Margin, dB*
NOAA FOB 4	+4.0
STDN (ETC/GSFC) 30 ft reflector	8.7
NOAA SMS CDAS	13.4

*For 7.0 Mbps PCM payload data rate, including AASIR global frame (20 by 20°) data.

6.2.3.1 MMS/C&DHM Subsystem Block Diagram and Top Level Description

The following discussion will highlight the MMS/C&DHM subsystem, using information from NASA/GSFC. The discussion below will merely define the elements of this subsystem and its STORMSAT interfaces; namely, 1) telemetry (housekeeping) and command signal processing interface with the mission module payload, and 2) RF interface with the NASA STDN, providing TT&C links. This mission-independent TT&C subsystem on the MMS bus has standard RF and data interface formats and is compatible with the STDN system.

Figure 6-13 displays the major elements of the MMS/C&DHM. The MMS/C&DHM subsystem as described will consist of: 1) S band transponder (STDN-compatible); 2) command detector; 3) standard telemetry and command components (STACC); 4) STACC interface unit (STINT); 5) on-board computer (OBC); 6) premodulation processor; 7) multiplex data bus; and 8) RIUs. Though the MMS/C&DHM is only to provide spacecraft TT&C functions, Figure 6-14 displays the external data interface with the premodulation processor (PMP) which would be used if mission module payload data of any sort were to be transmitted via the transponder links.

Since the only data interface in the baseline concept between the STORMSAT mission module (MM) and the MMS bus is via the RIUs and their capacity-increasing expander units (EU), the salient features of these elements are given below. One or more RIUs (and necessary EU) will be physically mounted on the MM. There will be physical RF interface between the MMS/C&DHM and STORMSAT MM, since one of the two hemispherical omni antennas may be mounted on the MM; further, it may be desirable to allow a high command/telemetry data rate option wherein the MM earth-coverage antenna is switched to the MMS/C&DHM transponder input/output port.

6.2.3.2 Remote Interface Unit Description

This MMS/C&DHM element provides a standard interface between the various MMS and payload user subsystems and the STACC central unit (STACC-CU). The RIU communicates with the STACC by means of a "party

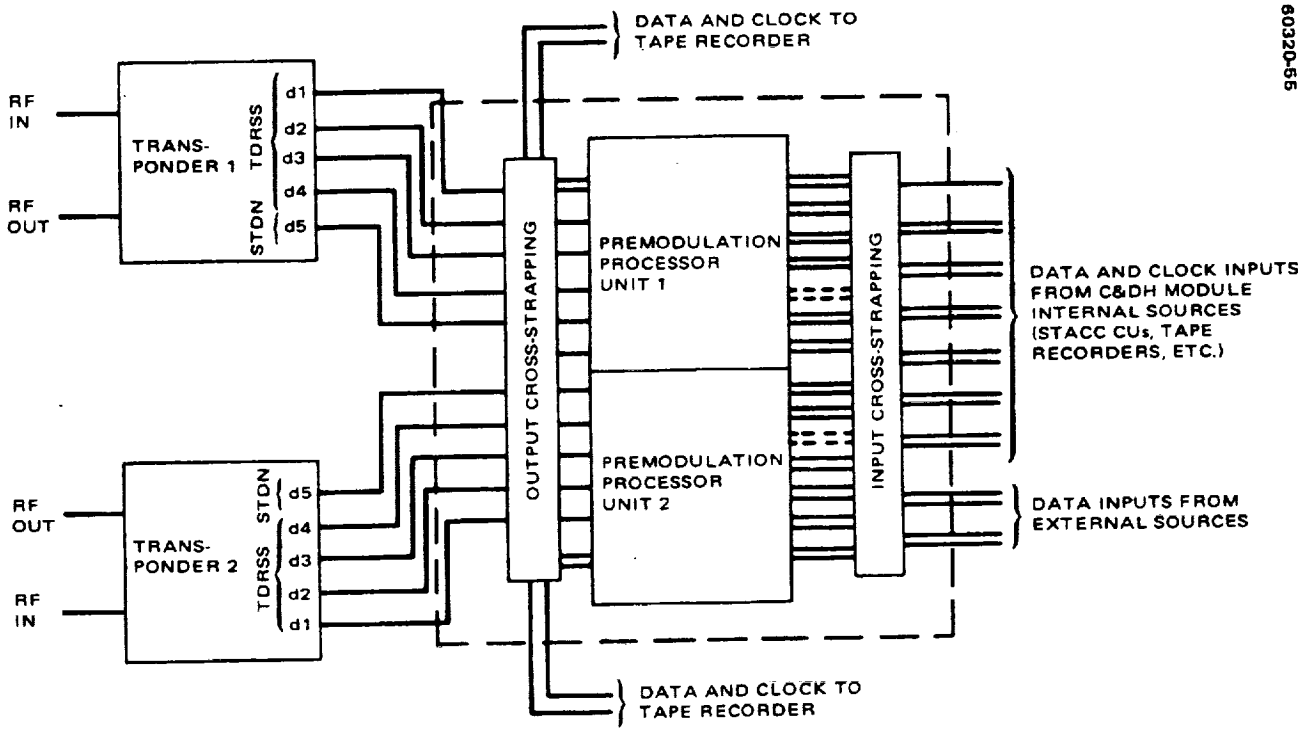

FIGURE 6-14. PMP INTERFACES WITH DATA SOURCES AND SINKS

line" called the multiplex data bus. The CU transmits instruction messages to the RIUs over a redundant supervisory line. The RIUs transmit data return messages to the CU over redundant reply lines. The RIU shall be designed to accept 32-bit instruction messages from the CU, recognize its own unique address, and respond appropriately to the instruction by performing one of the following functions:

1) Decode and distribute commands to the users

2) Decode and distribute selected clock signals to the users

3) Accept, condition, format, and transmit user's telemetry data. This includes supplying all necessary control and conditioning signals to the user to effect data transfer.

Figure 6-15 illustrates a typical RIU interface for the STORMSAT mission. It should be observed that a single RIU, with several EUs, could service the AASIR, MASR, and other payload TT&C; or, multiple RIUs could be used for this purpose. The salient characteristics of the RIU are given below.

RIU Characteristics

- Outputs — 63 discrete commands; outputs
  16 telemetry request signals for digital data,
  16 1 mA constant current pulses for
  analog data

- Inputs: 64 input channels for analog, bilevel, and digital data
- Mechanical: 7.0 by 8.0 inches (footprint); volume of 140 in^3; unit weight ≤ 2.5 pounds
- Prime power requirements

Operating Mode	Dissipation, +28 Volt Bus, Watts
Off	0.55
Standby	0.6
Active (analog)	3.0
(digital	1.4

6.2.3.3 RIU Expander Unit Functional Description

The purpose of the EU is to increase the RIU multiplexer capability by 64 telemetry channels. Up to seven EUs may be attached to an RIU. Thus, with a full complement of EUs the RIU capacity is 512 telemetry channels. The salient characteristics of the EU are given below.

EU Characteristics

- Inputs: 64 telemetry channels
- Outputs: 16 enable outputs for serial digital data
- Size: 175 x 200 mm (7 x 8 inches)
- Mass: 1.1 kg (2.5 pounds)
- Prime power requirements

Operating Mode	Dissipation, +28 Volt Bus, watts
Standby	0.075
Active	0.175

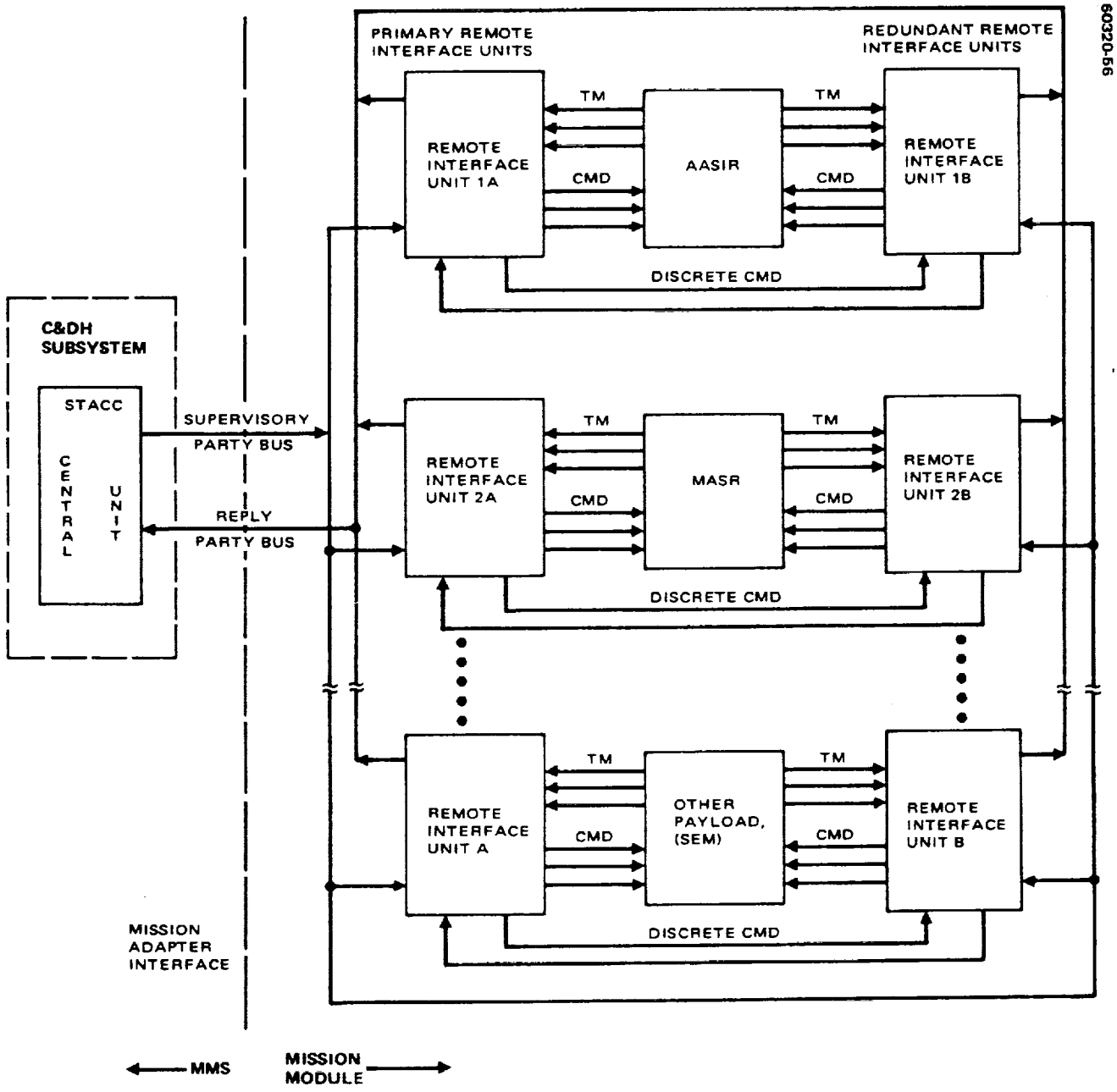

NOTE: A SINGLE REMOTE INTERFACE UNIT, WITH SEVERAL EXPANDER UNITS, COULD SERVICE BOTH THE AASIR, MASR, AND PAYLOAD T&C, OR MULTIPLE REMOTE INTERFACE UNITS COULD BE USED.

FIGURE 6-15. TYPICAL INTERFACE BETWEEN RIUs LOCATED ON STORMSAT MM AND MMS/CDHM

7. ELECTRICAL POWER

A modular power subsystem (MPS) is included in the Multimission Modular Spacecraft (MMS). The MPS design can support various types of missions and payloads in low earth and geosynchronous orbits. The solar cell array is tailored to the mission requirements, and batteries are selected from a choice of either 20 or 50 A-hr sizes to meet mission power requirements.

7.1 POWER REQUIREMENTS

STORMSAT estimated power requirements are listed in Table 7-1. Periodic peak power is required by the payload sensors and their electromechanical positioning drives and by the attitude control subsystem (ACS) during orbit adjustment maneuvers and for momentum wheel angular momentum control. Peak loads are not expected to occur simultaneously, but the solar cell array should support expected transient loads to avoid frequent voltage swings.

During boost and prior to separation the Space Shuttle will supply power to the spacecraft through the interim upper stage (IUS). The IUS will have the capability of supplying some power to its payload after separation from the orbiter. As the IUS is not currently designed, it is conservatively assumed that the spacecraft will not be dependent on the IUS for its electrical power needs. The electrical power subsystem is designed to support the transfer orbit loads while it is attached to the IUS.

7.2 DESIGN APPROACH

The electrical power subsystem design consists of power control units of the power subsystem module of MMS, batteries selected from the standard sizes available for the MMS program, and a mission-unique solar cell array with its drive and deployment mechanisms. The MPS supplies 22 to 35 volts dc power to the spacecraft and payload subsystem. All equipment requiring close voltage control will be connected to a separate regulated power supply which is external to the MPS. The solar array connected to the MPS was designed to operate at a minimum voltage of 39 volts dc, and it will have an open circuit voltage well below the permissible 150 volts dc maximum. The power regulator unit (PRU) in the MPS will transform the power received from the higher solar array voltage level to the load bus voltage and will control the battery charge currents.

TABLE 7-1. POWER REQUIREMENTS FOR STORMSAT

Item	Normal Mode, W	ACS Maximum Mode, W	Eclipse Mode, W	Reference
AASIR	100	50	100	SBRC
AASIR bearing driver	30	5	30	Estimate
Multiplexer	21	21	21	Estimate
MASR	50	50	50	GSFC
Gimbal driver	35	10	35	Estimate
Mission data transmitter	90	90	90	Estimate
Payload voltage regulator	20	20	20	Estimate
Communications and data handling module	115	115	115	MMS specification
Attitude control module	170	340	170	MMS specification
Propulsion valve drivers	10	130	10	MMS specification
Solar cell array drive	5	30	5	Estimate
Thermal control	100	100	100	Allocation
Power subsystem fixed loads	50	50	50	MMS specification
Battery charge (c/15)	233	–	–	Allocation
Contingency (10 percent)	103	101	80	Allocation
Bus load	1132	1112	876	–
Power regulator (η = 90 percent)	125	123	–	Estimate
Power source load	1257	1235	876	–

7.2.1 Battery Selection

The MPS batteries must support the mission for 5 years or longer. The standard nickel-cadmium spacecraft battery consists of 22 cells connected in series. The MPS can have two or three identical batteries in parallel, and the batteries can have either 20 or 50 A-hr capacity. Based on the estimated maximum eclipse power, and a 1.2 hour eclipse in synchronous orbit at a maximum 60 percent of discharge, 72 A-hr total battery capacity is required. Two 50 A-hr standard batteries are selected for the STORMSAT mission.

7.2.2 Solar Cell Array Selection

Rigid folding solar cell array panels and the flexible rolled up solar array (FRUSA) were considered for this mission. The FRUSA is easier to integrate into the spacecraft, as it occupies a compact cylindrical envelope when stowed as shown in Figure 7-1. Rigid solar cell array panels require at least four tiedowns during launch to provide for launch survival. This results in a more complex structural arrangement than required for FRUSA launch support. The FRUSA for STORMSAT is

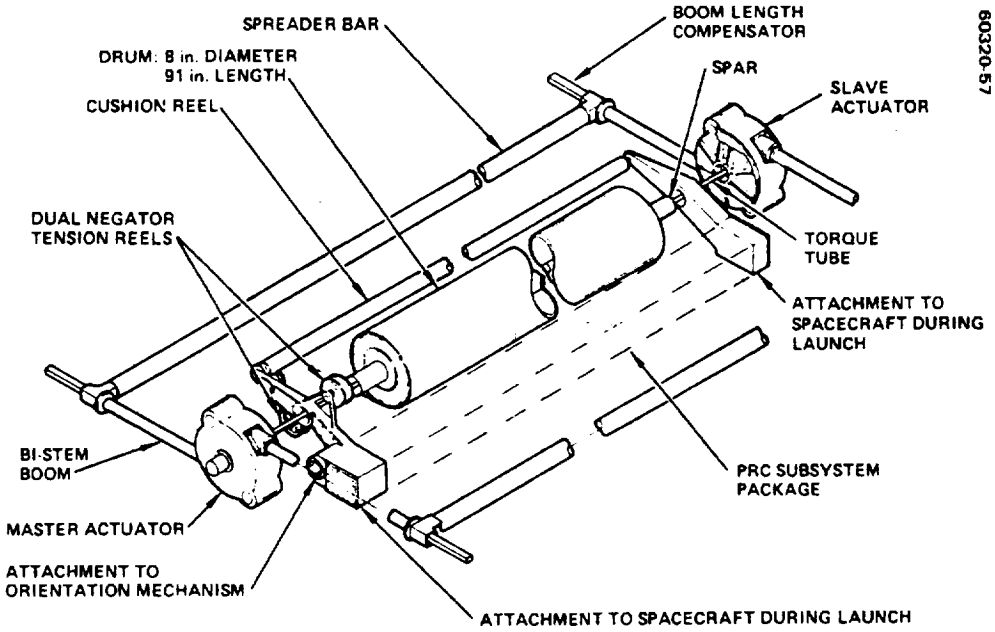

FIGURE 7-1. FRUSA STOWAGE AND DEPLOYMENT MECHANISM

essentially identical to the space qualified configuration flow successfully in 1972 (Figures 7-2 and 7-3) with the exception of the solar cell type and the length and width of the panels. The STORMSAT solar panels are shorter and wider, resulting in increased structural rigidity.

In launch configuration the array can be partially rolled out to power the spacecraft in transfer orbit and recharge the batteries. The solar array will be retracted before firing the rocket motors of the IUS. Deployment of the solar array will occur after the IUS separation in synchronous orbit. It is located in the opposite side of the spacecraft that is reserved for the AASIR radiation cooler field of view. The deployment link is connected to the solar cell array positioner and is free to rotate to secure full solar illumination.

The FRUSA consists of two flexible solar cell array panels attached to a storage drum. The solar cell panels are supported by deployed booms and spreader bars as indicated in Figure 7-4. Before launch, the panel support booms are retracted within the boom actuator housing. Both panels are rolled tightly around the drum to form a compact cylindrical shape. The 200 mm (8 inches) storage drum is a thin wall magnesium cylinder with end plates of sandwich-type aluminum titanium honeycomb construction. The STORMSAT drum differs from the original FRUSA drum, being 300 mm (12 inches) longer. The panel boom diameter is 22 mm (0.86 inch), the same as on the earlier FRUSA designs. It will ensure that the first mode frequency in bending would be at least 0.18 Hz, found acceptable on the FRUSA flight experiment.

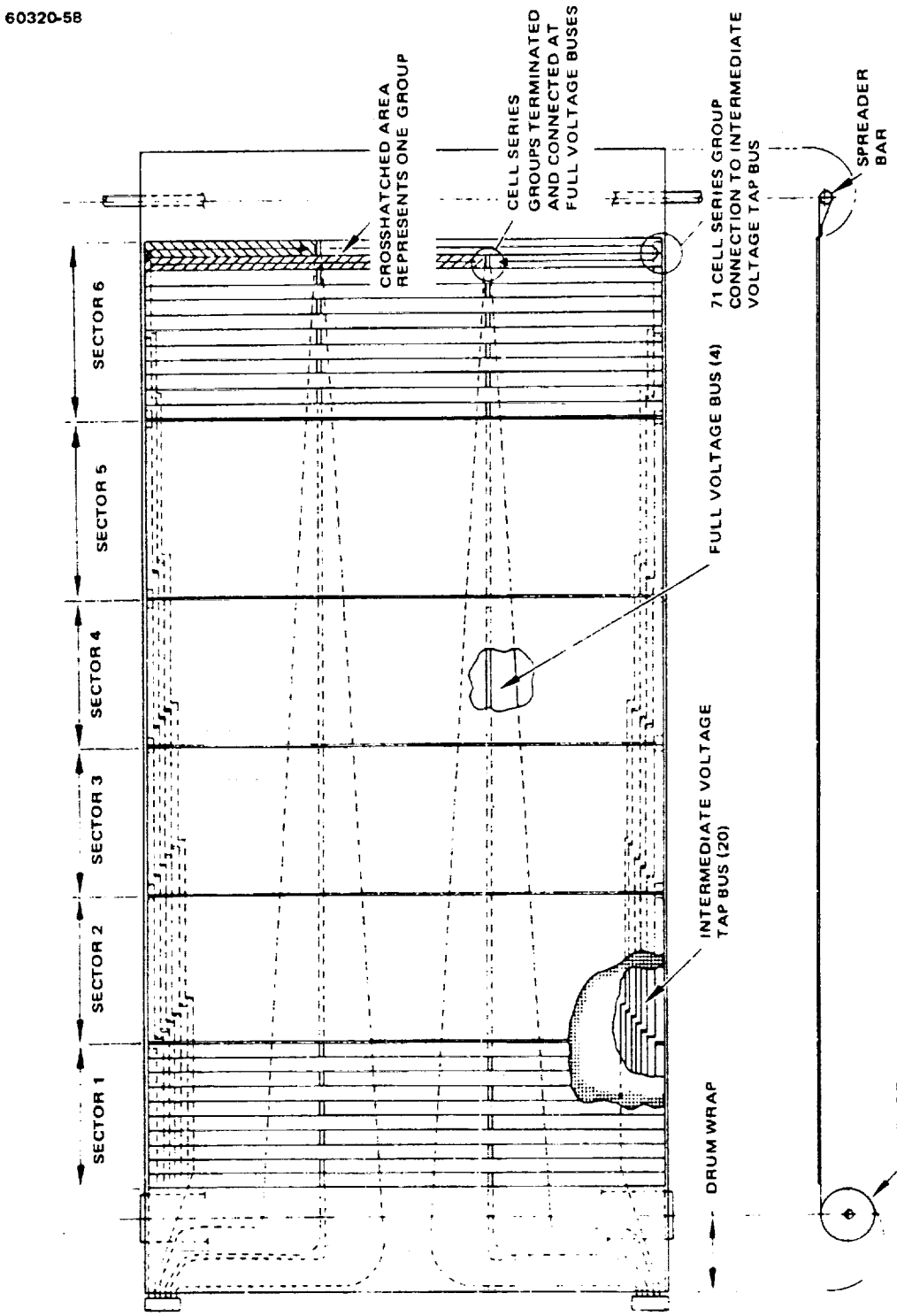

FIGURE 7-2. TYPICAL PANEL LAYOUT

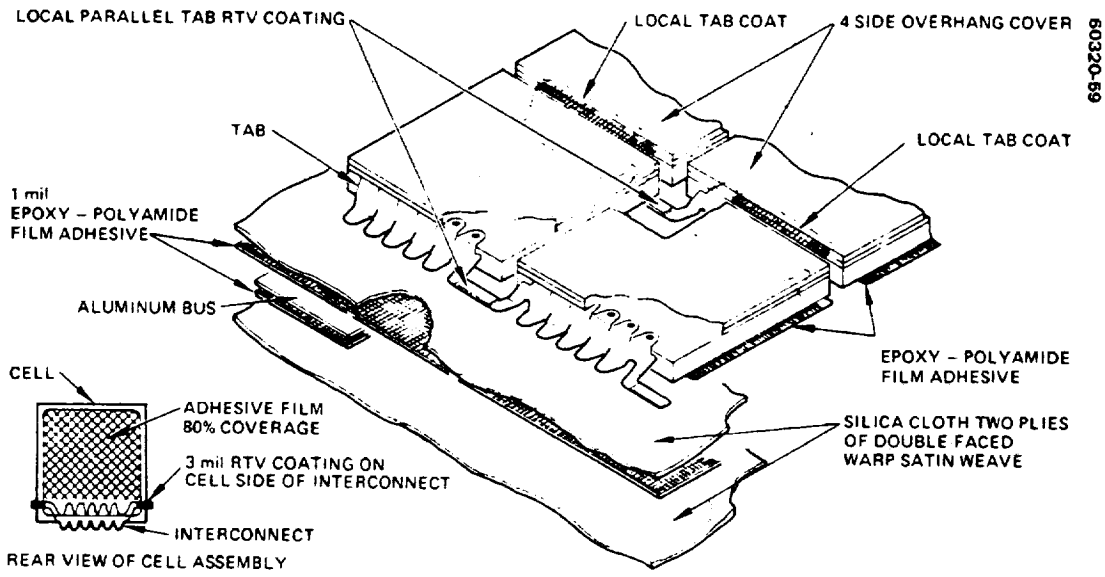

FIGURE 7-3. PANEL DETAIL DESIGN

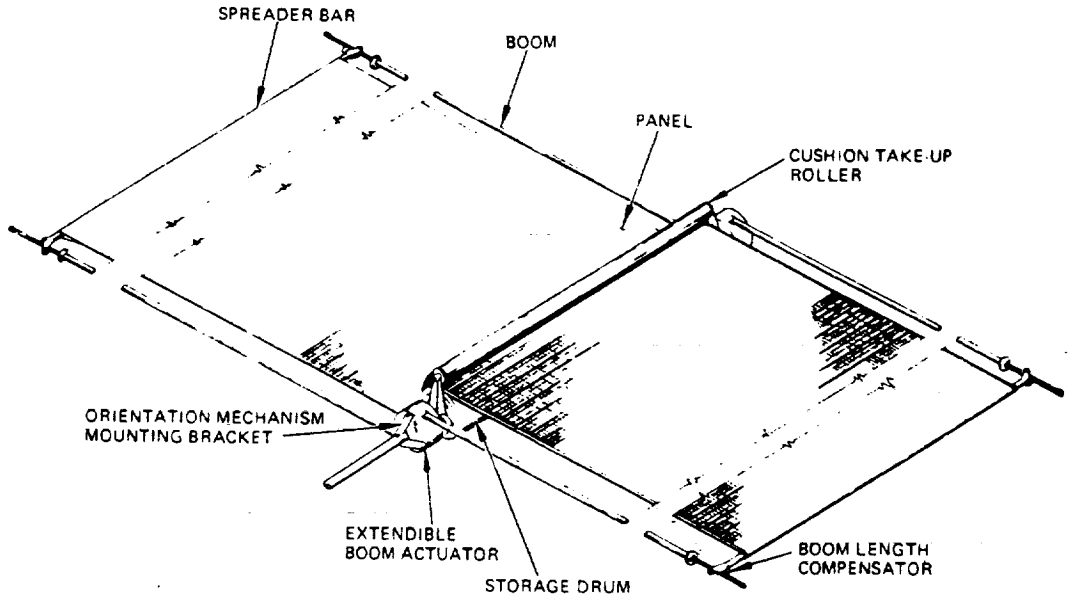

FIGURE 7-4. STORAGE AND DEPLOYMENT MECHANISMS WITH SOLAR PANELS

Protection of the solar cells during launch vibration consists of a cushion and panel roll-up tension. The cushion is an embossed 25 μm (1 mil) Kapton film interleaved between the solar cell layers of the dual panel that are lying over each other when rolled on the storage drum. Its primary task is to provide a means of distributing cell-to-cell stress. The flexible substrate chosen for this design combines the qualities of two materials. It uses a DuPont Kapton H-film bonded to Type 108 fiberglass. Electrical buses are placed on the back side of the solar panel to allow as high a packing factor for the solar cells as possible. All sectors of the array operate at the same voltage so that the longest buses are the widest, in order to maintain a uniform voltage drop between the sectors and the drum, regardless of bus strength. Negative and positive buses are alternated to provide minimum electromagnetic induction.

The solar cells selected for STORMSAT are high efficiency cells which are commercially available from Spectrolab. The cells have the designation K-7 (essentially the same as Helios cells with sculptured surface finish), and have a beginning-of-life power conversion efficiency of 13.6 percent. The cells are 2 by 2 cm N/P silicon with a P+ back surface, 250 to 300 μm (10 to 12 mils). They have fused silica covers over the active cell area. To protect the cell areas around the bar contact, organic radiation shield will be applied locally. Electrically, the selected cells provide 163 mA at 490 mV under standard conditions at 25°C and nominal sunlight in space.

The solar cell array design data are listed in Table 7-2. The voltage drop in the solar array buses are calculated with the standard 15 milliohms maximum line resistance. There is an additional voltage drop in the slip rings and diodes connected in series with the cell groups. The solar cell degradation in the synchronous orbit environment is higher for FRUSA type panels than rigid panels due to the reduced shielding effect on the back side of the cells. The solar panel design is based on power demand in eclipse season because the battery charge requirements are substantial. Each group of solar cells will consist of three parallel strings of 116 series connected cells which are terminated into panel mounted redundant diodes.

7.2.3 Solar Cell Array Drive

A solar cell array drive is expected to be available as a standard spacecraft component. The drive must step the solar cell array one revolution per day. In the spring and summer the solar cell array is located on the north side of the spacecraft, and the array is moved clockwise with respect to the body. In fall and winter the spacecraft is inverted and the array is moved counterclockwise. The drive assembly must also provide adequate structural stiffness for supporting the solar cell array and transfer power access slip rings and brushes to the spacecraft body.

A drive unit currently under development employs two stepper motors geared to the output shaft. Each motor drives a pinion through a normally engaged clutch. Electrical failures are countered by switching to the redundant motor. The clutch on either motor can be disengaged to clear a mechanical fault such as a stuck bearing.

TABLE 7-2. SOLAR ARRAY DESIGN DATA

Power requirements, eclipse season		1257 W
Solar array voltage at maximum power		39 V
Mission duration		5 years
Solar array temperature		60°C
Solar Cell Characteristics		
Solar cell type		K-7
Solar cell size		2 by 2 cm
Cell current at 25°C		163 mA
Cell voltage at 25°C		490 mV
Voltage Losses		
Line drop, solar panel		1.9 V
15 milliohm/lead	0.71 V	
Slip ring and connector drop	0.39 V	
Diode drop	0.80 V	
Radiation damage (includes backside) contribution in COMSAT Exhibit E, INTELSAT V environment)		-13%
Current Losses		
Fabrication losses		-3%
Cover darkening		-2%
Radiation damage		-12%
Number of cells in series		116
Number of parallel cell strings		238
Total number of cells		27,608

7.2.4 Power Subsystem Mass

The power subsystem weight estimate is based on the performance requirements for the MPS and on actual FRUSA weight data. The full capacity MPS weight is specified to be 583 pounds or less, which includes three 50 A-hr batteries. The selected MPS with two 50 A-hr batteries is estimated to weigh 270 kg (476 pounds). The estimated power subsystem mass is listed in Table 7-3.

7.3 PERFORMANCE ANALYSIS

The solar array design is based on experimentally and analytically developed data correlated with actual in space performance measurements. The solar cell degradation due to space radiation damage was calculated for both the geomagnetically trapped and solar flare radiation with the COMSAT Exhibit E environment as defined for INTELSAT V for the 1978 to 1985 time

TABLE 7-3. POWER SUBSYSTEM ESTIMATED MASS

Item	Mass, kg	Mass, lb
Module with two 50 A-hr batteries	216	476
FRUSA	38	85
Deployment mechanism	7	15
FRUSA drive mechanism	7	15
Drive electronics	2	4
Total Mass	270	595

period. The fabrication losses listed in Table 7-2 are due to slight performance variation between series connected solar cells. The cover darkening is a well characterized degradation in space environment.

The solar array output is maximum during equinox when the panels are oriented normal to incident sun. This coincides with the eclipse seasons when battery recharging increases the load requirements on the solar panels. Between eclipse seasons both the solar array output and the power requirements are reduced. The solar array output is approximately 10 percent less at summer solstice. This is more than sufficient to charge the batteries at low rate.

Battery augmentation of the solar array may be needed during ACS maximum operating mode between eclipse seasons. This will result in very shallow battery discharges which will be replenished during subsequent low rate charge periods.

7.4 PROBLEM AREAS

The power subsystem for MMS utilizes a series regulator for control of bus voltage to primarily control battery charge current. This results in a bus voltage varying with time, and ancilliary voltage regulators are required for payload sensors and electronics. A second impact on system design is the power loss in the series connected power regulator unit. It is specified to be at least 90 percent efficient. This power loss requires a larger solar cell array (by approximately 10 percent) than if a shunt type regulator were selected for battery control. It is suggested that a power subsystem design utilizing shunt type solar cell array voltage limiting and independent battery charge control with sequential charging be considered for synchronous missions. The solar cell array power requirements could thereby be reduced approximately 20 percent relative to the present MMS power subsystem configuration.

8. PROPULSION

The conceptual designs for the MMS propulsion are not compatible with respect to interfacing with the IUS nor are they configured to minimize overall IUS/spacecraft length. Accordingly, a mission unique propulsion module design is described for STORMSAT. It is sized for a spacecraft of 1546 kg (3400 pounds) mass at separation from the IUS with a design lifetime of 5 years. If full IUS payload of 2273 kg (5000 pounds) is utilized for STORMSAT, the module may provide the required service lifetime by using a larger tank. Some reconfiguration of the MMS structural brackets and wire harness connectors may be required to accommodate a tank larger than the 560 x 1420 mm (22 x 56 inches) tank currently selected for STORMSAT. Preliminary review of the MMS structure indicates that a tank 660 mm (26 inches) in diameter could be accommodated within the basic structural constraints. A 660 x 1420 mm (26 x 56 inches) tank would contain 286 kg (630 pounds) of hydrazine, which would be sufficient propellant for a 5 year mission.

8.1 REQUIREMENTS

Propulsion for STORMSAT is required for initial station acquisition, station change maneuvers, stationkeeping, orbit inclination control, and angular momentum control for the attitude control subsystem (ACS). The IUS is assumed capable of delivering the spacecraft payload to the synchronous equatorial orbit with essentially no velocity error.

Propellant budgets are presented for the spacecraft for both 3 and 5 years, corresponding to the experimental and operational mission. Propellant budgets are based on one initial spacecraft mass following separation from the IUS of 1546 kg (3400 pounds). Propulsion requirements and propellant budgets are listed in Table 8-1. These requirements translate into a propellant load of 129.5 kg (285.4 pounds) for the 3 year mission and 204.7 kg (450.3 pounds) for the 5 year missions. Although inclination is not necessarily required for the STORMSAT mission, this function is included to minimize the ground system data processing functions.

8.2 DESIGN APPROACH

The design approach utilized during this study was to maximize the usage of the MMS concept. Four versions of the propulsion module are given for use on a large class of spacecraft missions. As far as propulsion

TABLE 8-1. MISSION REQUIREMENTS AND PROPELLANT BUDGET

	3 Year Mission				5 Year Mission			
	Requirement		Propellant Required		Requirement		Propellant Required	
	m/sec	fps	kg	lb	m/sec	fps	kg	lb
Station acquisition	14.3	47	10.2	22.5	14.3	47	10.2	22.5
Stationkeeping	6.4	21	6.7	14.7	10.7	35	11.1	24.4
Inclination control	155.5	510	106.3	233.8	259.1	850	172.4	379.4
Attitude control	12,800 N-m/sec	9450 ft-lb-sec	6.5	14.4	21,400 N-m/sec	15,750 ft-lb-sec	20.9	24.0
Total		–	129.7	285.4		–	204.6	450.3

NOTE: Injection error corrections are assumed to be performed by the IUS.

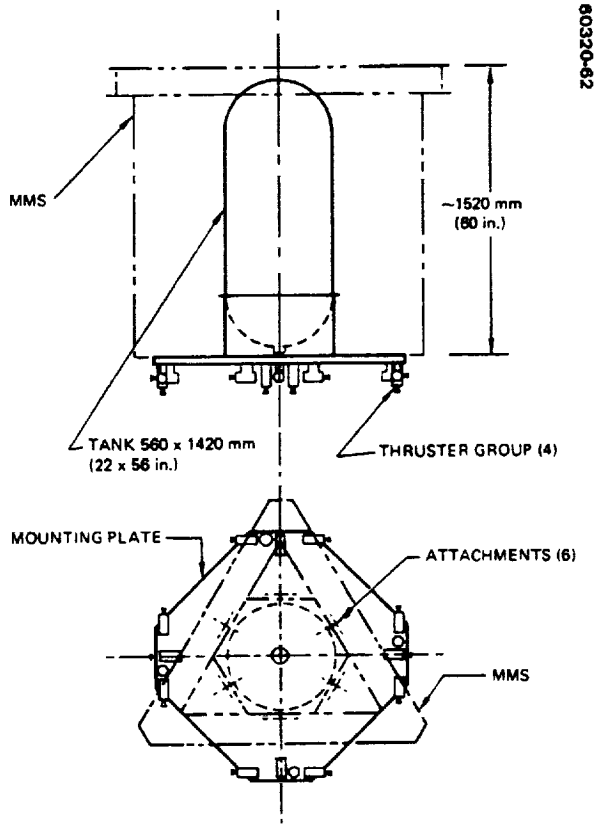

FIGURE 8-1. MISSION UNIQUE PROPULSION MODULE FOR STORMSAT

capability is concerned there are only two distinct propulsion subsystem designs. Only the large propulsion module (SPS-II) provides adequate propellant capacity to perform the STORMSAT mission. This module is 192 mm (75.5 inches) long and is not mechanically compatible with either the MMS or the IUS. As detail design is not being performed on the propulsion modules, it is suggested that a mission-unique propulsion module be selected for the STORMSAT mission.

A preliminary mission-unique propulsion module design for STORMSAT is shown in Figure 8-1. It consists of a 560 x 1420 mm (22 x 56 inches) cylindrical tank with hemispherical end closures, a fill and drain valve assembly, a propellant control assembly, and four rocket engine modules, each containing three 1 N (0.2 lbf) thrusters (Figure 8-2) and one 22 N (5 lbf) thruster (Figure 8-3). The propulsion equipment is integrated on a structural plate which attaches to the MMS structure at its base. The propellant tank occupies the available space within the MMS. This approach is desirable for the STORMSAT mission because the overall length of the spacecraft is minimized. This tank would not be a new design, since Fansteel has the forging dies available. The 560 mm (22 inches) diameter tank was used on the Gemini program, the Minuteman boost propulsion system, and as a helium sphere on the Aerobee missile. Use is made of other propulsion components which are being developed by the NASA Low Cost Systems Office. Propulsion equipment and estimated mass is listed in Table 8-2.

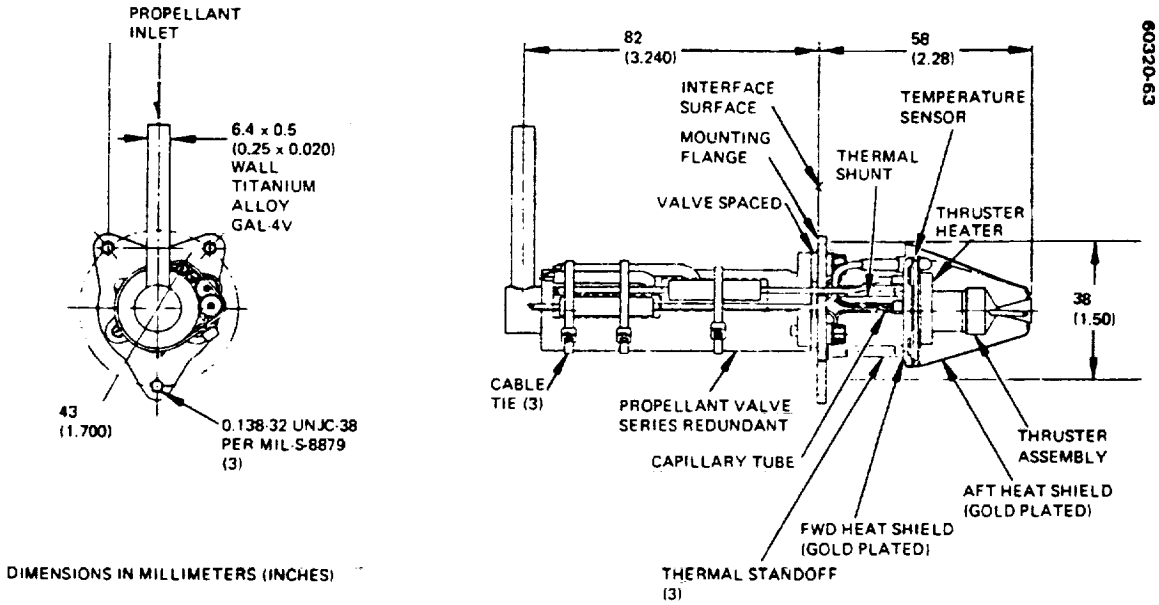

FIGURE 8-2. 0.2 LBF THRUSTER ASSEMBLY

TABLE 8-2. PROPULSION MODULE COMPONENT MASSES

		Mass	
Item	Quantity	kg	lb
Tank	1	20.4	45.0
Thruster, 1 N (0.2 lbf)	12	3.3	7.2
Thruster, 22 N (5 lbf)	4	2.2	4.8
Filter	1	0.2	0.4
Latching valve	4	1.8	2.0
Fill and drain valve	4	1.8	2.0
Pressure transducers	1	0.1	0.3
Structure and integration	1	41.2	90.0
Total		68.0	150.0

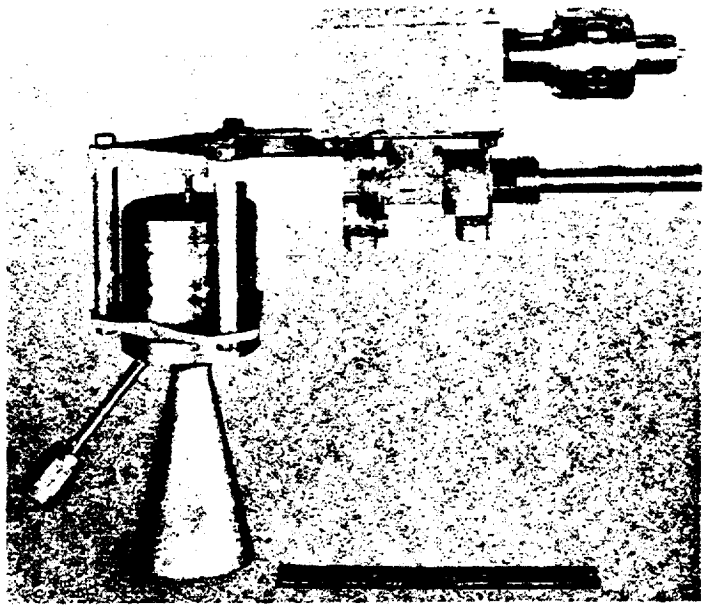

FIGURE 8-3. 22N (5 LBF) THRUST CHAMBER AND VALVE ASSEMBLY (PHOTO 74-26274)

8.3 PERFORMANCE ANALYSIS

Performance curves for typical 1 and 22 N (0.2 and 5 lbf) thrusters are provided in the MMS report dated May 1975. Unfortunately, the full range of thruster operation is not presented for the 1 N (0.2 lbf) thruster. Because of this lack of definitive information regarding performance versus tank pressure, it was assumed that all pulsing operation would have a mission average specific impulse of 150 seconds. The mission average specific impulse for steady state thrusting modes was estimated to be 220 seconds. These average values should be approximately the actual performance, but until a mission profile is defined in greater detail, more realistic predictions cannot be developed.

8.4 INTERFACE REQUIREMENTS

Special consideration must be given to the propellant tank installation in the center of the mission module, and to the detail interface between this mission-unique propulsion module and the MMS structure.

8.5 POTENTIAL PROBLEM AREAS

One potential problem area with the current configuration of STORMSAT and its propulsion module is the need to reorient the spacecraft to perform orbit inclination control maneuvers. This maneuver is expected to require approximately 1 hour to execute and it must be performed at the proper orbital phase to be efficient. This can result in loss of service for STORMSAT on the average of every 10 days. Alternative design approaches are: 1) to align the MMS longitudinal axis normal to the orbital plane, or 2) to place the orbit inclination control thrusters near to the spacecraft center of mass.

A second potential problem area may arise if STORMSAT grows to the full IUS payload capability. In this event, a larger diameter propellant tank may be required to be integrated within the MMS structural frame. A review of the MMS structural design is suggested for this configuration.

9. STRUCTURE

Spacecraft structure consists of the IUS/spacecraft adapter, MMS structure, and mission-unique structural elements. The MMS structure consists of a module support structure and a transition adapter. Mission-unique structure elements consist of the AASIR bearing support structure, the MASR gimbal support structure, and a truss structure which supports the mission-unique electronic equipment compartments, the FRUSA, and the MASR gimbal support structure. All structural elements must interface properly and support the spacecraft as an integrated entity during boost, transfer orbit, and operational orbit. The approach taken for the spacecraft structural design is to configure and size the mission unique structure and to establish requirements for those structural elements to be supplied as Government-furnished equipment. A spacecraft/IUS load and stress analysis must be performed to qualify the spacecraft for flight on the Space Shuttle System. This analysis will consider the dynamic interactions between the spacecraft, the IUS, and the Space Shuttle Orbiter. Preliminary design levels are provided in the IUS system specification.

9.1 REQUIREMENTS

The STORMSAT structure must support the spacecraft elements during launch and in orbit. The structure must also withstand Orbiter atmospheric entry, landing, and crash loads in the event of an aborted launch attempt. Spacecraft acceleration limit load factors for IUS payloads are listed in Table 9-1. Coordinate axis are defined in Figure 9-1. It is observed that the most severe loading condition is for Orbiter landing loads. These will be used for preliminary structural analysis.

Spacecraft orbital operations require ultrastable structural mounting for the ACS module and the mission meteorological sensors. A structural distortion of 4 μrad in 20 minutes between the AASIR and the ACS module has been allocated for the STORMSAT mission. This, in turn, will impose temperature control requirements on aluminum structural members. Pointing and stability requirements for the MASR are more relaxed than for the AASIR. A drift rate of 40 μrad in 30 minutes has been allocated for thermal structural distortion effects.

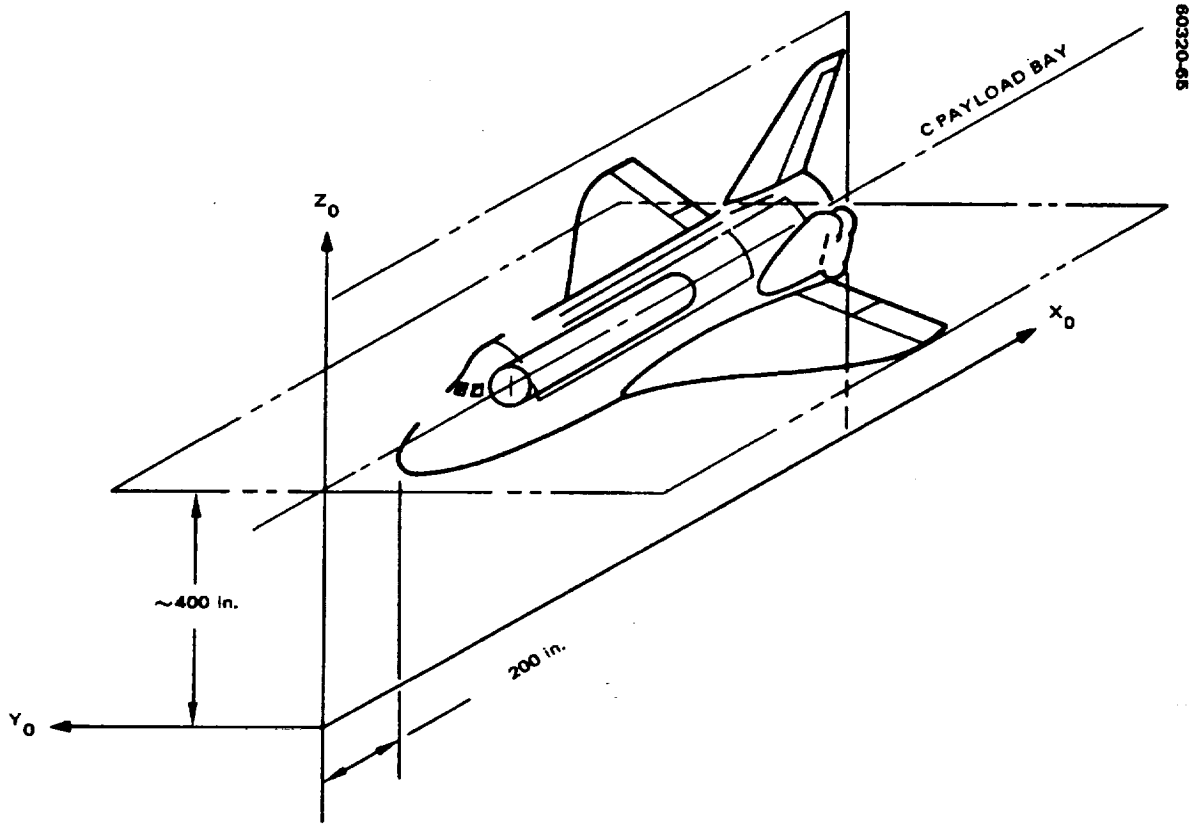

TYPE: ROTATING, ORBITER REFERENCED

ORIGIN: APPROXIMATELY 200 in. AHEAD OF NOISE AND APPROXIMATELY 400 in. BELOW CENTERLINE OF PAYLOAD BAY

ORIENTATION AND LABELING:

X AXIS IS PARALLEL TO CENTERLINE OF PAYLOAD BAY, NEGATIVE IN DIRECTION OF LAUNCH

Z AXIS IS POSITIVE UPWARD IN LANDING ATTITUDE

Y COMPLETES RIGHT-HANDED SYSTEM

STANDARD SUBSCRIPT IS 0

REFERENCE: SPACE SHUTTLE SYSTEM PAYLOAD ACCOMMODATIONS; JSC-07700, VOL. XIV, DATED JULY 3, 1974.

FIGURE 9-1. ORBITER COORDINATE SYSTEM

TABLE 9-1. CARGO LIMIT DESIGN ACCELERATIONS FOR 65 KLB UP AND 32 KLB DOWN

Condition	Linear, g			Angular, rad/sec^2		
	X	Y	Z	X-X	Y-Y	Z-Z
Liftoff	+1.5 -4.5	+2.0 -2.0	+4.5 -4.5	+0.10 -0.10	+0.15 -0.15	+0.15 -0.15
High Q boost	-1.6 -2.0	+0.5 -0.5	+0.6 -0.6	+0.10 -0.10	+0.15 -0.15	+0.15 -0.15
Boost maximum LF (stack)	-2.7 -3.3	+0.2 -0.2	-0.3 -0.3	+0.20 -0.20	+0.25 -0.25	+0.25 -0.25
Boost maximum LF (orbit alone)	-2.7 -3.3	+0.2 -0.2	-0.75 -0.75	+0.20 -0.20	+0.25 -0.25	+0.25 -0.25
Entry and deceleration pitch up	+1.06 -0.02	0 0	+2.5 -1.0	+0.25 -0.25	+0.75 -0.75	+0.30 -0.30
Entry and deceleration yaw	+0.75 +0.75	+1.25 -1.25	+1.0 +1.0	+0.25 -0.25	+0.30 -0.30	+0.75 -0.75
Landing	+4.5 -4.5	+4.0 -4.0	+10.0 -8.0	+0.25 -0.25	+1.25 -0.75	+0.30 -0.30
Crash	+9.00 -1.5	+1.50 -1.50	+4.5 -2.0			
Crash (crew compartment interior)	+20.0 -3.3	+3.3 -3.3	+10.0 -4.4			

NOTES:
1) Sign convention follows that of the Orbiter coordinate system in Figure 9-1. Angular accelerations follow the right hand rule.
2) Crash accelerations are ultimate. The longitudinal accelerations are directed in all aftward azimuths within a cone of 20° half-angle. The specified accelerations shall operate separately.
3) Liftoff and landing loads are from IUS System Specification, SS-STS-100, Vol. 3, dated January 5, 1976.
4) All other loads from Space Shuttle System Payload Accommodations, JSC-07700, Vol. XIV, dated July 3, 1974.

9.2 DESIGN APPROACH

Mission-unique payload structure is designed to interface with the transition adaptor of the MMS. The MMS utilizes aluminum structures and this study of STORMSAT also utilizes aluminum in the construction of the mission-unique structural elements. A truss is provided for the support of the MASR, mission-unique electronic equipment compartments, and for launch support of the solar cell array. The main truss assembly, shown in Figure 3-1 (Refer to Section 3) consists of a triangular frame supported off the transition adapter by three tripods. Auxiliary members provide support for equipment items. The MASR gimbal is supported by a tripod attached to the corners of the triangular truss frame. Auxiliary struts provide support for the electronic equipment compartments and the stowed FRUSA. The AASIR is mounted in a bearing assembly which in turn is supported directly off the transition adapter by an aluminum frame structure. Both the truss and frame structures are welded assemblies which are pinned and bolted to the transition adaptor.

A mission-unique propulsion module is installed at the aft end of the MMS structure. Propulsion equipment is attached to a plate which is then bolted to the MMS aft frame structure. A cylindrical adapter extends from the plate to the cylindrical section of the propellant tank and is secured by a marman type band. The plate structure is an aluminum honeycomb sandwich. The cylindrical adapter is of monocoque aluminum construction.

An adapter provides the structural interface between the MMS structural frame, and the IUS payloads for the IUS are attached on a 111.77 inch diameter bolt circle at eight points. The MMS is designed with three longitudinal load members. A conical adapter provides the transition from the three bolt interface with the MMS to the eight bolt interface with the IUS. Separation nut assemblies are installed on both sides of the MMS/adapter inteface to effect separation from the IUS. Preliminary limit bending moment is estimated to be 2.9×10^6 in-lb at the adapter/IUS interface and 2.0×10^6 in-lb at the adapter/MMS interface. Corresponding limit vertical shear loads are 34,000 and 32,000 pounds, respectively, and limit axial loads are 16,000 and 15,000 pounds, respectively.

9.3 PRELIMINARY ANALYSIS

Preliminary design loads are computed for the MMS longitudinal numbers and separation nut and bolt assemblies.

$$P_x = \left(\frac{2 M_y}{\sqrt{3}\, b} + \frac{L_x}{3} \right) \cdot (FS)$$

when P_x is axial load in member

b is spacing of longitudinal members of MMS

M_y is moment due to vertical acceleration loads on spacecraft

L_x is force due to axial acceleration loads on spacecraft

FS is factor of safety.

$$P_x = \left(\frac{2 \times 2.0 \times 10^6}{\sqrt{3} \times 53} + \frac{32,000}{3} \right) \quad 1.65$$

$$= (43,500 + 10,700) \times 1.65 = 90,000 \text{ pounds}$$

$$= 0.40 \text{ MN}$$

This will require a 25 mm (1.0 inch) diameter bolt and separation nut with an ultimate tensile stress value of 160,000 psi (MIL-S-7742, Class T-6) or a 19 mm (0.75 inch) diameter bolt and separation nut with an ultimate tensile stress of 260,000 psi (MIL-S-8879, Class T-10). The MMS structure must also withstand the axial design load of 0.40 MN (90,000 pounds) applied at any vertex of the structure without yielding to avoid changes in alignment between the mission sensors and the ACS module.

Thermo-structural distortion is limited to 4.2 μrad in any 20 minute period for AASIR to ACS module alignment. An analysis considering simple beam deflection is presented. It is noted that other distortions may occur within the ACS module but are not considered in this analysis. Angular distortion between the AASIR support and the ACS module support is calculated by the beam deflection formula:

$$\delta\theta = \frac{L}{D} \cdot \alpha \cdot \delta T$$

where $\delta\theta$ is incremental angular distortion

L is length of structure

D is depth of structure

δT is incremental temperature difference

Rearranging:

$$\delta T = \frac{D \cdot \delta\theta}{L \cdot \alpha}$$

For the structural path between the center of the ACS module and the center of the AASIR mount,

$$\delta T = \frac{46 \times 4.2 \times 10^{-6}}{60 \times 1.3 \times 10^{-5}} = 0.25°F$$

$$= 0.14°C$$

If the variation in structural temperature is due to solar heating, the maximum allowable temperature gradient across the structure is approximately 1.6°C (2.8°F) in a 24 hour period. This result is, of course, only an order of magnitude estimate to provide guidance for this STORMSAT preliminary design effort. More detailed analysis are expected to be performed during the development phase of STORMSAT to provide a well defined thermo-structural distortion design criteria.

9.4 PROBLEM AREAS

The MMS structure design is constrained by the Delta launch vehicle envelope to a spacing between longerons of 1350 mm (53 inches). Design loads for the Space Shuttle System are much greater than for the Delta launch vehicle, as emergency landing loads must be considered in the design for reasons of flight safety. The orbiter payload compartment is 15 feet in diameter, and a more efficient structure would be allowed for Space Shuttle operations save for the requirement of common MMS structures for Delta and Space Shuttle payloads. The transition between three MMS attachment points and eight IUS attachment points presents problems of load distribution within the spacecraft/IUS adapter structure. A further consideration is the installation of a propellant tank within the MMS structure. A 22 inch tank is the largest diameter that can be accommodated within the current structure design. All these factors suggest that a more appropriate structural arrangement would be achieved by increasing the spacing or the number of longitudinal members in the MMS structure. Consideration should be given to a semi-monocoque spacecraft structure for Space Shuttle/IUS spacecraft payloads. This would permit the use of a band type separation clamp at the spacecraft/adapter interface and avoid the large concentrated loads associated with the frangible nut and bolt separation devices used in the current MMS spacecraft design. Graphite fiber reinforced plastic structures are suggested for applications requiring ultrastable spacecraft structures. This material is currently utilized in precision antenna structures and for optical assemblies that experience transient temperature changes.

10. THERMAL DESIGN

Thermal design requirements and design approaches are considered for the integration of mission-unique payload equipment onto the MMS. Government-furnished mission payload sensors and spacecraft modules are provided with adequate thermal control. Thermal control of aluminum spacecraft structure is required, as it provides the mechanical interface between the attitude control module, and the mission sensors and pointing accuracy is dependent on its relative stability. Preliminary requirements and design approaches are also presented for new equipment items for the STORMSAT mission.

10.1 REQUIREMENTS

10.1.1 AASIR Thermal Control

The AASIR is designed to be a thermally independent subsystem. The AASIR limit operating temperatures are 0 to 35°C (32 to 95°F). Nonoperating temperature limits are 0 to 45°C (32 to 113°F). The AASIR is mounted on a bearing assembly which provides the east-west scan degree of freedom. The bearing assembly is mounted to a support structure which is attached to the transition adapter of the MMS. The operating temperature of the bearing assembly is required to be in the AASIR operating temperature range of 0 to 35°C (32 to 95°F) to minimize heat transfer between the AASIR and the bearing assembly

Structural temperature differences from one side of the spacecraft to the other are required to be stable with a maximum rate of change of the order of 0.1°C (0.2°F) in any 20 minute period. This requirement is imposed to provide an acceptably low alignment drift error between the attitude control reference and AASIR line of sight pointing.

10.1.2 MASR Thermal Control

The MASR is a thermally independent subsystem. Principal design requirements are to minimize temperature changes in the antenna and receiver which will affect calibration and to maintain low temperature gradients in the antenna structure which could result in geometric distortions that spoil the beam.

The MASR is mounted on a gimbal attached to the mission module structure. It is desirable to minimize heat transfer across the mounting interface between the MASR and its gimbal. This will in turn minimize temperature gradients in the MASR structure and subsequent structural distortion. The temperature limits of the antenna are unknown at this time, but it is reasonable to assume that they could be controlled locally at the gimbal interface to the range of 0 to 35°C (32 to 95°F). The gimbal should also be controlled to this range. Pointing requirements for the MASR are more relaxed than for the AASIR. It is estimated that the rate of change of the temperature gradient in the MASR support structure should not exceed 1°C (1.8°F) in any 30 minute period.

10.1.3 Mission-Unique Electronic Equipment Thermal Control

Electronic equipment associated with payload sensor operation and mission sensor data transmission is mounted in equipment modules attached to the mission module structure. Temperature control requirements for this equipment is similar to that provided by the MMS for its equipment modules. Bulk operating temperature range is 0 to 40°C (32 to 104°F).

10.2 THERMAL DESIGN APPROACH

The general approach to thermal control is to isolate the spacecraft and its equipment from the environment by means of multilayer insulation blankets except for those surfaces required for radiation of internally generated heat.

10.2.1 AASIR Thermal Control

Thermal control of the AASIR is accomplished by radiating heat from the entrance aperture and from the thermal detector radiation cooler and by isolating the remainder of the AASIR from the space and spacecraft thermal environments. This can be accomplished by enclosing the AASIR in an insulation blanket and by providing low conductance paths to the interface structure mounting points.

The AASIR and its supporting bearing assembly will further be isolated from the spacecraft by additional multilayer insulation blankets. AASIR thermal control will be accomplished by rejection of internally generated heat through the optical aperture and radiation cooler. The allowable temperature gradient along the optical axis of the AASIR is determined by the focus adjustment range of the active focusing mechanism. Minimization of the AASIR focusing activities is a design goal. This is to be accomplished within the temperature range by using fused silica-invar construction of the AASIR optics.

10.2.2 MASR Thermal Control

Thermal control of the microwave radiometer involves the use of thermal insulation blankets and thermal control coatings to minimize temperature

gradients in the antenna structure. The use of thermal control surfaces on the antenna to minimize the effect of sunlight on radiometer thermal performance, and the use of insulation blankets, thermal control surfaces, and heaters to maintain the MASR and associated data handling equipment within their design temperature limits. An insulation blanket placed on the back of the antenna reflector will block heat transfer from one side to the other, thereby minimizing temperature gradients in the antenna structure. The cantilever feed support and gimbal attachment should be blanketed on all sides to minimize temperature gradients and avoid antenna boresight shifts.

The receiver and antenna feed assembly will be installed in a thermally controlled compartment at the focus of the antenna reflector. This is accomplished by techniques similar to those used for the MMS equipment modules. Radiator surfaces are provided on the north and south facing surfaces of the compartment and are coated with a low α/ϵ material such as silverized teflon or quartz. The remaining sides of the compartment are insulated except for cutouts for the antenna feeds. The feeds may be covered with a low α material which is transparent at microwave frequencies to minimize thermal loading due to sunlight. The detail design of this compartment must be undertaken as a part of the MASR development.

The gimbal should be maintained at approximately the same temperature as the antenna feed support. This may be accomplished by designing the interconnection structure between the antenna and gimbal with a low conductance material and by providing radiators and heaters for temperature control of the gimbal drive motors. Structure supporting the gimbal may be insulated by blankets. This is expected to result in acceptable temperature gradient control for operation of the microwave radiometer.

10.2.3 Electronic Equipment Thermal Control

Mission-unique electronic equipment are mounted in compartments with north or south facing radiators and with a high degree of isolation from the space environment on all other surfaces. This arrangement minimizes temperature variations due to daily rotation of the run about the body. These equipment platforms are oriented in the same direction as the AASIR radiation cooler to minimize solar heating. A combination of insulation blankets, radiators, louvers, and heaters may be required to effect temperature control over the mission lifetime. One approach to consider is to provide half size equipment modules similar in design to the MMS equipment modules for mounting mission-unique equipment. This would permit flexibility in the design process for achieving the required mounting area without using more payload mass than necessary for equipment mounting.

10.2.4 Solar Cell Array Thermal Control

Solar cell array temperatures are typical of high performance, lightweight, oriented solar arrays. Good thermal coupling from cell side to a high emittance back side is required in order to achieve minimum solar cell temperatures. High back surface emittance is achieved for minimum weight by carbon black impregnation of the face sheet. Peak operating temperature

is 60°C (140°F) with normal sunlight. Temperatures drop sharply during eclipse due to the large area-to-mass ratio to a minimum of -150°C (-238°F). The posteclipse voltage transient is directly influenced by the minimum temperature experienced, but is controlled by the power regulator unit. The low temperature and high rate of change of temperature are critical design conditions for the solar cell array.

11. GROUND SYSTEM STUDIES

The processing requirements and associated definition of ground system facilities required for the STORMSAT project are currently in process of formulation and discussion of a STORMSAT ground system must necessarily be generalized. However, some of the unique elements of the anticipated ground system can be identified, and their functional characteristics described. The selection of specific facilities or operational constraints is not possible at this time.

The traditional elements of any meteorological satellite system include

1) A spacecraft operational control center (SOCC) for spacecraft monitoring and control,

2) Facilities for operational data acquisition, transmission, and processing, such as the telemetry, tracking and command (TT& C) data functions, and

3) Mission sensor data acquisition and processing facilities.

Figure 11-1 illustrates these conventional ground system functions. A major difference between previous meteorological satellite and the STORMSAT mission lies in the real time requirements for STORMSAT mission sensor control, based on at least payload image data display at a SOCC man-machine interface, and possibly large scale computer processing of payload data (vertical temperature profiles derived from sounding data, wind fields extracted from successive image frames). The current payload data processing concept, as employed by SMS and other satellite programs, of transferring payload data in magnetic tape medium from acquisition to processing sites, and subsequent off-line processing is simply not appropriate for the anticipated real time STORMSAT requirements. High-speed data transfer facilities employing terrestrial microwave and/or communications relay, with appropriate interface electronics and computing facilities with adequate throughput rates will be necessary. Alternately, the requirements of high-rate real time data acquisition, processing, display, and payload control function may require collocation of the ground system facilities performing these functions.

60320-67

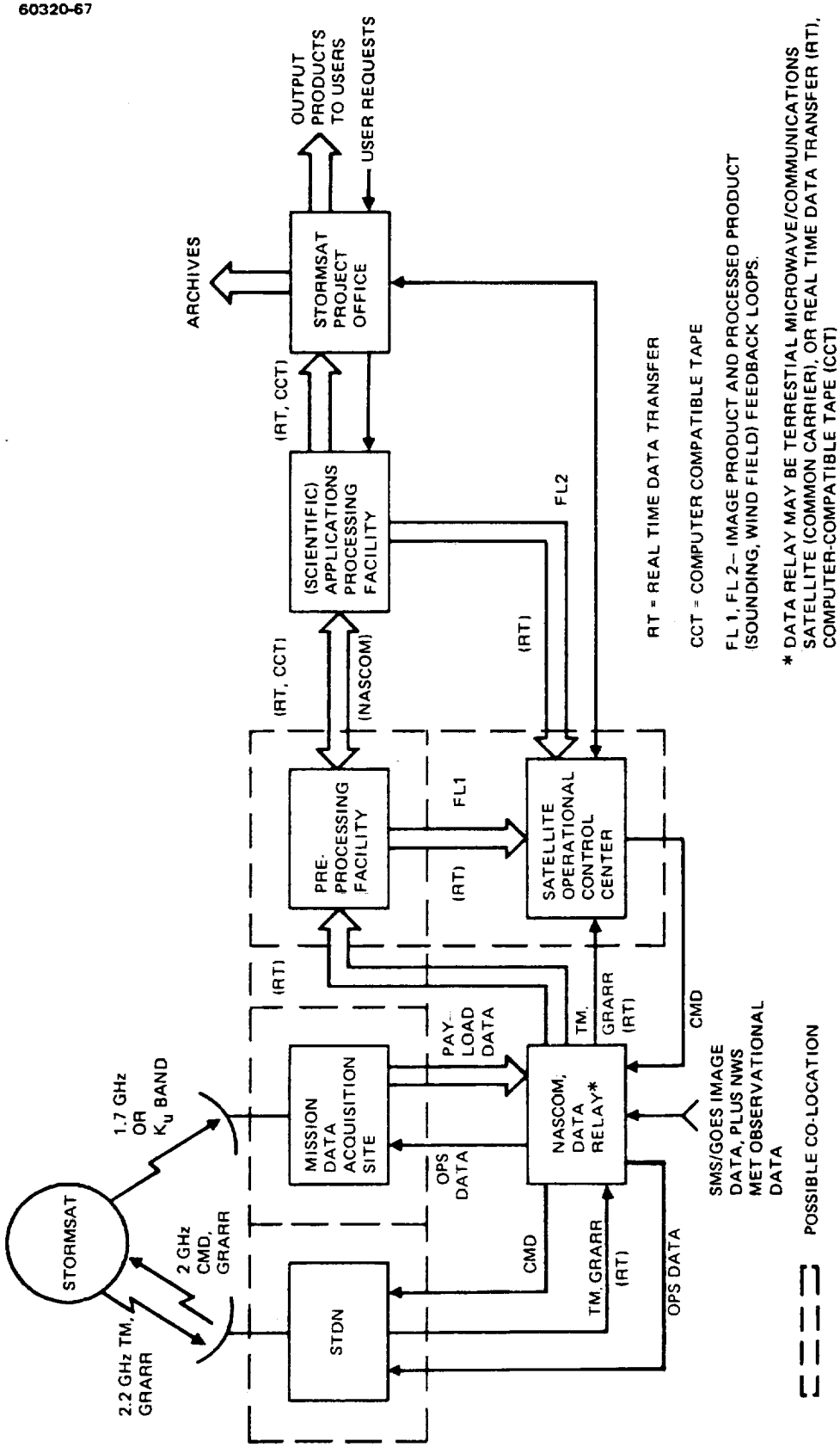

FIGURE 11-1. TYPICAL STORMSAT GROUND SYSTEM DATA FLOW

The data processing function has two major components. The first component is largely mission-dependent and consists of: 1) preprocessing telemetry and mission sensor data in a convenient format, and 2) presentation and display at a spacecraft operational control facility (SOCC). The second component is largely mission-independent, such as a large-scale scientific computing facility which receives the preprocessed mission data. The latter function is mission-independent to the degree that it satisfies the computational needs of many users in terms of computational speed, capacity, and variety of input/output peripherals. Most third or fourth generation facilities of the type encountered currently or planned at GSFC or NOAA's central processing facility in Suitland, Maryland may be large enough to provide STORMSAT mission computational capability. However, real time data transfer interfaces do not currently exist. The interactive man-machine interface necessary to provide real time AASIR line of sight and mode control depends on display of certain data products, such as AASIR imagery, atmospheric temperature profiles extracted from sounding data, or wind fields extracted from visible and infrared imagery by frame-to-frame correlation techniques. Data interface networks capable of transmitting mission sensor and associated telemetry data in real time will be necessary to interconnect the SOCC, STDN, and central data processing facilities. The current (or near-term projected) NASCOM ground data transmission capabilities of 52 kbps and eventual 1 Mbps+ data rates will be totally inadequate for the required real time payload baseband data transmission rates (7 Mbps) if any of STDN sites not collocated with the data processing facility are used to acquire RF data. Thus, real time data acquisition, transfer, and processing requirements will strongly influence the selection of sites, and collocation of facilities, as well as the characteristics of the preprocessing, display, and central data processing facilities.

11.1 COMMAND, TRACKING AND DATA ACQUISITION REQUIREMENTS

11.1.1 Command Requirements

The primary interface for transmission of commands to STORMSAT will be the NASA/STDN. This will certainly be true for initial orbital insertion and in-orbit checkout procedures, and unless replaced by a dedicated Command and Data Acquisition Station (CDAS), such as the Wallops Island facility for SMS/GOES, will hold for on-station operations. The baseline STORMSAT concept has command uplink interface only with the MMS/C&DHM, at S band, and with signal formats compatible with NASA Aerospace Standards. In summary, this RF interface is characterized by:

RF uplink frequency range: 2015 to 2025 MHz

Typical ground station EIRP: +112.0 dBm STDN

(+85.2 dBm NOAA CDAS)

Command rate: See MMS specification

The on-board computational and storage capability of the MMS computer subsystem will allow generation of command sequences for AASIR and other payload instrumentation mode control. The degree to which this is possible is dependent on the available on-board resources of the C&DHM and detailed payload mode control requirements. A limiting case would be a real time ground command concept. The interactive nature of AASIR and MASR line of sight and scanning mode control as based on ground interpretation of payload data will make the design of on-board versus ground command distribution critical, since the MMS/C&DHM command distribution capability is rate limited.

11.1.2 Tracking Requirements

The baseline STORMSAT MMS approach requires radio tracking for orbit determination using the Goddard Range and Range Rate (GRARR) system of the STDN. Ranging from two or more STDN sites should provide sufficient accuracy to control orbit inclination to 0.025°, and orbital longitudinal position to 0.01°, using the MMS transponder. The nominal in-orbit tracking data acquisition flow characteristic of the SMS/GOES could also be employed for STORMSAT. At scheduled intervals, the tracking data will be relayed in near real time to GSFC, where orbital trajectories are computed (Tracking and Data System Directorate). Spacecraft attitude data, as derived from onboard telemetry data, could also be furnished to GSFC DSD.

11.1.3 Data Acquisition Requirements

The requirements for STORMSAT data acquisition can be considered for two types of data, the first being spacecraft telemetry data, the second being mission sensor data. Mission sensor data is defined here as AASIR and MASR data, plus selected mission module telemetry. The SEM instrument data on the operational spacecraft could also be included with this payload data and also output as part of the spacecraft telemetry data stream.

11.1.3.1 Spacecraft Telemetry Data Acquisition Requirements

As in the current GOES application, it is assumed that a combination of digitized PCM and real time event telemetry data will be transmitted to the STDN and/or CDAS via the MMS/C&DHM S band link. In particular, the nominal housekeeping data which monitors the ACS status will need to be supplemented by appropriate ACS calibration and sensor/control element output signals for enhanced attitude state vector estimation. Real time event data, such as star tracker target time crossings, may be telemetered by multiplexed transmission to a central processing facility from the CDAS. At the processing facility, the raw data values will be transformed into proper physical units and presented in formats appropriate for operator display, parameter alarming, and subsequent processing and archiving. The various display and computer processed outputs will be presented to the SOCC for overall spacecraft and sensor evaluation and control.

The conventional SOCC functions and capabilities are:

1) Operational control — issue and maintain schedule via satellite communications, teletype and voice conference links with CDAS, GSFC, NASCOM/STDN, central processing facility.

2) Monitor spacecraft health, diagnose and correct anomalies via CRT display of commands, events, telemetry; plus hard copy and tape records of commands, events, and telemetry; CRT and strip chart display of real time telemetry.

3) Monitor payload data for quality.

The physical location of these generic ground system modes must be compatible with planned NASA/GSFC facility planning for the STORMSAT time-frame, and will, in fact, help determine site selection based on facility availability, and high speed data interface capability. The SOCC function for STORMSAT is unique only in its high speed interactive interface with central data processing facilities. The interactive processing/display/command/capability of the Atmospheric and Oceanographic Information Processing System will be typical of this interactive SOCC interface.

11.1.3.2 Telemetry Data Transmission

The SOCC will receive data simultaneously from any one of several STDN ground stations. The data will be multiplexed by the digital data formatter at the STDN sites and continuously transmitted to the SOCC over a high speed data circuit. As an example, the data stream will be inputted directly into the SOCC computers where the data will be demultiplexed, processed, and displayed in an appropriate media.

11.1.3.3 Payload Data Acquisition Requirements

The distribution of AASIR and MASR sensor and selected telemetry data chosen for the baseline HRDTS STORMSAT concept requires that one or more sites must be capable of RF reception in the metsat S band (~ 1.7 GHz), baseband data demodulation and decoding at digital data rates at the order of 7 Mbps, and subsequent preprocessing of this recovered data for transmission to scientific data processing facilities. The medium by which this recovered digital data is made available at the data processing facility will be determined by the extent to which processed data of various levels is required for real time STORMSAT command and control. Current SMS/GOES data transmission techniques allow the relay of slowed payload (stretched VISSR) digital data via the satellite repeater from its RF acquisition site at Wallops Island to the NOAA central processing facility at Suitland, Maryland, Worst case requirements for STORMSAT in terms of real time processing will demand ground network solutions which include: 1) collocation of RF acquisition and data processing facilities which can be hard-wired with adequate multimegahertz bandwidth signal interface units and transmission lines, or 2) location of one or more RF acquisition and baseband

recovery facilities (Rosman, N. C., for instance) remote from a selected data processing facility (GSFC, for instance) with appropriate interconnecting wideband satellite and/or terrestrial microwave radio links, or 3) a combination of the two concepts, wherein an SOCC facility is collocated with the RF acquisition facility, providing high data rate image display equipments, but with no large-scale data processing capability. In this concept, it is assumed that only relatively low-rate data, such as AASIR sounding and MASR sounding data need be supplied to a remotely located central processing facility for real time processing and subsequent SOCC command action. Conventional computer-compatible tape media would allow full scale processing of any payload data desired, at the central scientific data processing facility, on an off-line basis, for archival and/or scientific analysis purposes.

11.1.4 Equipment Description

The RF acquisition site(s) for the MMS/C&DHM telemetry data is the NASA STDN. At least two STDN facilities are also candidates for STORMSAT payload data acquisition: the Engineering Training Center (ETC) and Rosman (ROS). The existent capability of any of the STDN sites, with respect to TT&C data via the MMS/C&DHM, is adequate for the STORMSAT mission. However, the metsat RF receive frequency capability may not be available at all STDN sites which might also be considered at STORMSAT CDAS. Clearly, the NOAA Suitland facility (FOB 4) does have this receive capability. The QPSK demodulation and digital baseband processing equipment suitable for STORMSAT will, in general, not be available at either current STDN or NOAA facilities. However, no new technology is required, and in fact, modifications of existent hardware such as demodulators, bit synchronizers, demultiplexer equipments will be adequate.

11.1.5 RF Link Budgets

Table 11-1 summarizes the expected performance for: 1) the high-rate payload data link from the STORMSAT mission module to a minimum candidate data acquisition site (FOB 4), 2) a MMS/C&DHM telemetry link to an acquisition site typical of the STDN (30 foot reflector), 3) NOAA SMS CDAS at Wallops Island, based on the detailed link budget of Table 11-2 and the major characteristics of these acquisition facilities.

TABLE 11-1. NOMINAL G/Ts FIGURES OF MERIT FOR CANDIDATE RF DATA ACQUISITION SITES (AT 1.7 GHz)

Data Acquisition Facility	Nominal G/Ts, dB/°K	On-Axis Receive Gain, dB	Parabolic Reflector Diameter, ft	System Noise Temperature, °K	Receiving Circuit Loss, dB	Nominal Link Margin,* dB
NOAA, FOB 4, Suitland	+14.9	39.7	24	300	Included in gain	+ 4.0
STDN (ETC/GSFC) 30 foot Reflector	+19.6	41.6	30	160	-0.5	+ 8.7
NOAA, CDAS (Wallops)	+24.3	47.2	60	195	-0.6	+13.4

*For a 7 Mbps downlink data rate; RF power = 30 W

TABLE 11-2. CIRCUIT MARGIN SUMMARY FOR STORMSAT-TO-GROUND STATION AASIR DATA TRANSMISSION CHANNEL

Item	Parameter	Value	Typical Tolerances	
			Favorable	Adverse
1	STORMSAT transmit power, dBm	P_T	+0.0	-1.0
2	STORMSAT transmit loss, dB	-0.5	+0.1	-0.3
3	STORMSAT transmit antenna gain (2.0 ft dia), dB	18.0	+0.2	-0.6
4	STORMSAT antenna pointing loss, dB	-0.1	+0.0	-0.1
5	STORMSAT EIRP, dBm (sum 1 through 4)	P_T + 17.4	+0.3	-2.0
6	Space loss (1.7 GHz), dB	-189.2	+0.0	-0.3
7	Polarization loss, dB	-0.1	+0.0	-0.1
8	Ground receive antenna gain,* dB	$+G_R$	+0.1	-0.5
9	Total received power, dBm (sum 5 through 8)	$P_T + G_R$ -171.9	+0.4	-2.9
10	Ground system noise temperature, ^oK	T_s	-0.3	+0.4
11	Receiving figure-of-merit, G_R/T_S dB/^oK	(G_R/T_S)	+0.4	-0.9
12	Boltzmann's constant (10 Log 1.38×10^{-19}), dBm/^oK-Hz	-198.6	+0.0	-0.0
13	Ground noise spectral density, dBm/Hz (sum 10 and 12)	T_s - 198.6	+0.3	-0.4
14	Received power/noise spectral density (P_c/N_o), dB-Hz (9 minus 13)	$P_T + (G_R/T_S)$ + 26.7	+0.7	-3.3
15	Bit-rate bandwidth (10 Log B_t Mbps) dB-Hz	B_t	+0.0	-0.0
16	Signal-to-noise ratio in bit-rate bandwidth (E_b/N_o), dB (14 minus 15)	$P_T + (G/T_s)$ - B_t + 26.7	+0.7	-3.3
17	Theoretical E_b/N_o for bit-error probability 10^{-5}, dB	9.6	+0.0	-0.0
18	Data link degradation, dB QPSK degradation -2.5 dB Bit sync loss -1.5 dB Miscellaneous losses -0.3 dB	-4.3	-1.0	+0.5
19	Required E_b/N_o dB (17 minus 18)	13.9	-1.0	+0.5
20	Data circuit margin, dB (16 minus 19)	$P_T + (G/T_s)$ - B_t + 12.8	+1.7	-3.8

*Referenced to antenna output port.

Note that other contemplated AASIR focal plane and scan rate changes, with their attendent higher composite payload PCM data STORMSAT transmission rates (36 Mbps), will demand a higher capability RF data acquisition facility than FOB 4. Typical STDN or SMS CDAS capability is more appropriate in this instance.

12. NEW TECHNOLOGY

This study involved the conceptual design of a satellite system utilizing, under the guidelines of the study, developed subsystems and payload instruments. Mission-unique equipment and subsystems were identified and, for the most part, do not involve new technology.

Some of the mission-unique subsystems will subsequently require a detailed design analysis and it is expected that, at that time, this equipment development may involve new technology. Since this study merely provides as an output the identification of the mission-unique equipment, this study does not have any new technology to report.